



**LiGO**  
SYSTEM



**Boston**  
Electronics

# IR DETECTOR AND MODULE CATALOG

## Table of contents

	TABLE OF CONTENTS.....	2
	<b>INFRARED DETECTORS AND DETECTION MODULES – STANDARD.....</b>	<b>4</b>
	STANDARD INFRARED DETECTORS.....	5
	STANDARD INFRARED DETECTION MODULES.....	5
<b>DETECTORS</b>	PVI-4-1×1-TO39-NW-36.....	6
	PVI-5-1×1-TO39-NW-36.....	8
	PVI-2TE-4-1×1-TO8-WAL <sub>2</sub> O <sub>3</sub> -36.....	10
	PVI-2TE-5-1×1-TO8-WAL <sub>2</sub> O <sub>3</sub> -36.....	12
	PVI-2TE-6-1×1-TO8-WZNS <sub>SEAR</sub> -36.....	14
	PVI-4TE-6-1×1-TO8-WZNS <sub>SEAR</sub> -36.....	16
	PVM-10.6-1×1-TO39-NW-90.....	18
	PVM-2TE-10.6-1×1-TO8-WZNS <sub>SEAR</sub> -70.....	20
	PVMI-2TE-10.6-1×1-TO8-WZNS <sub>SEAR</sub> -36.....	22
	PVMI-4TE-10.6-1×1-TO8-WZNS <sub>SEAR</sub> -36.....	24
	PEM-10.6-2×2-PEM-SMA-WZNS <sub>SEAR</sub> -48.....	26
	PCI-3TE-12-1×1-TO8-WZNS <sub>SEAR</sub> -36.....	28
<b>MODULES</b>	UM-I-6.....	30
	UM-10.6.....	32
	UM-I-10.6.....	34
	MICROM-10.6.....	36
	LABM-I-6.....	38
	LABM-I-10.6.....	40
	UHSM-10.6.....	42
	UHSM-I-10.6.....	44
	<b>INFRARED DETECTORS AND MODULES – OPTIONAL.....</b>	<b>46</b>
	HOW TO CHOOSE AND INFRARED DETECTOR?.....	47
	HOW TO CHOOSE A PREAMPLIFIER?.....	48
<b>DETECTORS</b>	PC SERIES.....	49
	PC-2TE SERIES.....	51
	PC-3TE SERIES.....	53
	PC-4TE SERIES.....	55
	PCI SERIES.....	57
	PCI-2TE SERIES.....	59
	PCI-3TE SERIES.....	61
	PCI-4TE SERIES.....	63
	PV SERIES.....	65
	PV-2TE SERIES.....	67
	PV-3TE SERIES.....	69
	PV-4TE SERIES.....	71
	PVI SERIES.....	73
	PVI-2TE SERIES.....	75
	PVI-3TE SERIES.....	77
	PVI-4TE SERIES.....	79
	PVM SERIES.....	81
	PVM-2TE SERIES.....	83
	PVMI SERIES.....	85
	PVMI-2TE SERIES.....	87
	PVMI-3TE SERIES.....	89
	PVMI-4TE SERIES.....	91
	PEM SERIES.....	93
	PEMI SERIES.....	95

	PVA SERIES .....	97
	PVA-2TE SERIES .....	99
	PVIA SERIES .....	101
	PVIA-2TE SERIES .....	103
	PCQ .....	105
	PVMQ.....	107
<b>PREAMPS</b>	AIP SERIES .....	109
	PIP SERIES.....	111
	MIP SERIES .....	113
	FIP SERIES .....	115
	SIP SERIES .....	117
	<b>ACCESSORIES .....</b>	<b>119</b>
	PTCC-01 SERIES .....	120
	PPS-03 SERIES.....	123
	AC ADAPTOR AND CABLES .....	124
	DRB-2 BASE MOUNTING SYSTEM.....	125
	MHS-2 HEATSINK.....	126
	DH-2 DETECTOR HOLDER .....	127
	MH-1 MODULE HOLDER .....	127
	OTA OPTICAL THREADED ADAPTER .....	128
	<b>GLOSSARY AND TECHNICAL INFORMATION.....</b>	<b>129</b>
	GLOSSARY .....	130
	DETECTOR'S PACKAGES AND INFRARED WINDOWS .....	133
	THERMOELECTRIC COOLING .....	134
	TEMPERATURE CONTROL .....	134
	HEAT SINKING .....	135
	OPTICAL IMMERSION TECHNOLOGY .....	136
	PRECAUTIONS FOR USE .....	137
	<b>CONTACT AND DISTRIBUTORS.....</b>	<b>138</b>
	VIGO SYSTEM S.A.....	139
	OUR DISTRIBUTORS .....	139

---

# INFRARED DETECTORS AND DETECTION MODULES – STANDARD

We present VIGO most popular [infrared detectors](#) and [integrated detection modules](#). These devices are suitable for both laboratory research as well as tests, prototyping, R&D stage and in a variety of MWIR and LWIR industrial applications.

## Main features

- High performance and reliability
- Very good repeatability in mass production
- Cost-effective solutions
- Fast delivery

## Standard infrared detectors

Photo	Detector type	Photo	Detector type
	<a href="#">PVI-4-1x1-TO39-NW-36</a>		<a href="#">PVM-10.6-1x1-TO39-NW-90</a>
	<a href="#">PVI-5-1x1-TO39-NW-36</a>		<a href="#">PVM-2TE-10.6-1x1-TO8-wZnSeAR-70</a>
	<a href="#">PVI-2TE-4-1x1-TO8-wAl<sub>2</sub>O<sub>3</sub>-36</a>		<a href="#">PVMI-2TE-10.6-1x1-TO8-wZnSeAR-36</a>
	<a href="#">PVI-2TE-5-1x1-TO39-wAl<sub>2</sub>O<sub>3</sub>-36</a>		<a href="#">PVMI-4TE-10.6-1x1-TO8-wZnSeAR-36</a>
	<a href="#">PVI-2TE-6-1x1-TO39-wZnSeAR-36</a>		<a href="#">PEM-10.6-2x2-PEM-SMA-wZnSeAR-48</a>
	<a href="#">PVI-4TE-6-1x1-TO39-wZnSeAR-36</a>		<a href="#">PCI-3TE-12-1x1-TO8-wZnSeAR-36</a>

## Standard infrared detection modules

	Photo	Detection module type		Photo	Detection module type
UM series – universal		3.0 – 6.7 μm and DC – 1 MHz HgCdTe universal module with optically immersed photovoltaic detector <a href="#">UM-I-6</a>	LabM series – laboratory, programmable		3.0 – 7.5 μm and over 200 MHz HgCdTe programmable, laboratory module with optically immersed photovoltaic detector <a href="#">LabM-I-6</a>
		2 – 12 μm and DC – 70 MHz HgCdTe universal IR detection module with photovoltaic multiple junction detector <a href="#">UM-10.6</a>			2 – 12 μm and DC – 100 MHz HgCdTe programmable, laboratory module with optically immersed photovoltaic detector <a href="#">LabM-I-10.6</a>
micro-size		2 – 12 μm and DC – 100 MHz HgCdTe universal module with optically immersed photovoltaic multiple junction detector <a href="#">UM-I-10.6</a>	UHSM series – ultra high-speed		3 – 12 μm and over 1GHz HgCdTe ultra high speed (>700 MHz) module with photovoltaic detector <a href="#">UHSM-10.6</a>
		2 – 12 μm and DC – 10 MHz HgCdTe micro-size module with photovoltaic multiple junction detector <a href="#">microM-10.6</a>			3 – 12 μm and over 700 MHz HgCdTe ultra high speed module with optically immersed photovoltaic detector <a href="#">UHSM-I-10.6</a>

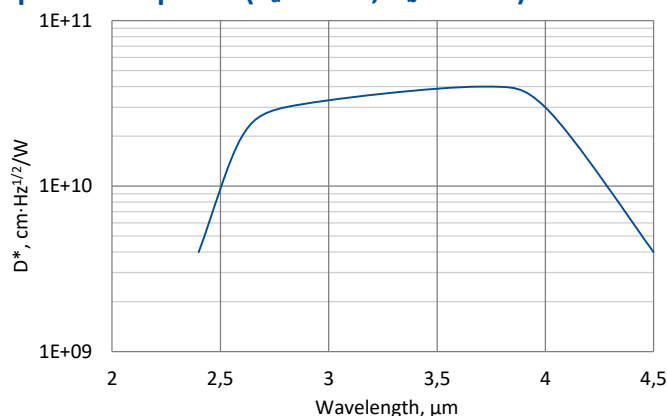
To get the information about specific parameters and applications of each detector and detection module type please see particular datasheets.

## PVI-4-1x1-TO39-NW-36

### 2.4 – 4.5 $\mu\text{m}$ HgCdTe ambient temperature, optically immersed photovoltaic detector

**PVI-4-1x1-TO39-NW-36** is uncooled IR photovoltaic detector based on sophisticated HgCdTe heterostructure for the best performance and stability. The device is optimized for the maximum performance at 4  $\mu\text{m}$ . Detector element is monolithically integrated with hyperhemispherical GaAs microlens in order to improve performance of the device. Reverse bias may significantly increase response speed and dynamic range. It also results in improved performance at high frequencies, but 1/f noise that appears in biased devices may reduce performance at low frequencies

#### Spectral response ( $T_a = 20^\circ\text{C}$ , $V_b = 0\text{ mV}$ )



Exemplary spectral detectivity, the spectral response of delivered devices may differ.



#### Specification ( $T_a = 20^\circ\text{C}$ , $V_b = 0\text{ mV}$ )

Parameter	Detector type
	PVI-4-1x1-TO39-NW-36
Active element material	epitaxial HgCdTe heterostructure
Cut-on wavelength $\lambda_{\text{cut-on}}$ (10%), $\mu\text{m}$	$2.4 \pm 0.5$
Peak wavelength $\lambda_{\text{peak}}$ , $\mu\text{m}$	$3.4 \pm 0.5$
Optimum wavelength $\lambda_{\text{opt}}$ , $\mu\text{m}$	4.0
Cut-off wavelength $\lambda_{\text{cut-off}}$ (10%), $\mu\text{m}$	$4.5 \pm 0.3$
Detectivity $D^*(\lambda_{\text{peak}})$ , $\text{cm}\cdot\text{Hz}^{1/2}/\text{W}$	$\geq 4.0 \times 10^{10}$
Detectivity $D^*(\lambda_{\text{opt}})$ , $\text{cm}\cdot\text{Hz}^{1/2}/\text{W}$	$\geq 3.0 \times 10^{10}$
Current responsivity $R_i(\lambda_{\text{peak}})$ , A/W	$\geq 2.0$
Current responsivity $R_i(\lambda_{\text{opt}})$ , A/W	$\geq 1.0$
Time constant $\tau$ , ns	$\leq 150$
Resistance R, $\Omega$	$\geq 600$
Optical area $A_o$ , $\text{mm}\times\text{mm}$	1x1
Package	TO39
Acceptance angle $\Phi$	$\sim 36^\circ$
Window	none

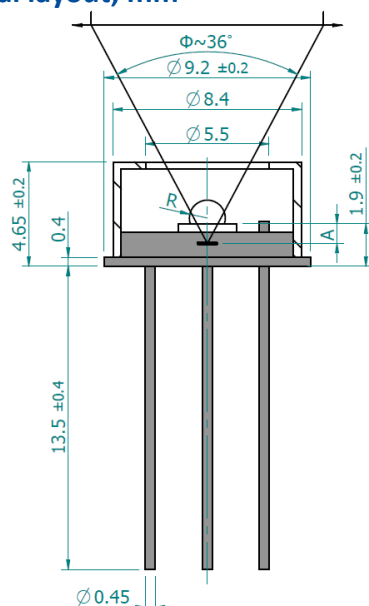
#### Features

- Wide dynamic range
- Convenient to use
- Very small size
- Cost-effective solution
- Quantity discounted price
- Fast delivery

#### Applications

- Gas detection, monitoring and analysis ( $\text{CH}_4$ ,  $\text{C}_2\text{H}_2$ ,  $\text{CH}_2\text{O}$ ,  $\text{HCl}$ ,  $\text{NH}_3$ ,  $\text{SO}_2$ ,  $\text{C}_2\text{H}_6$ )
- Breath analysis
- Explosion prevention
- Flue gas denitrification
- Emission control (exhaust fumes, greenhouse gases)

## Mechanical layout, mm

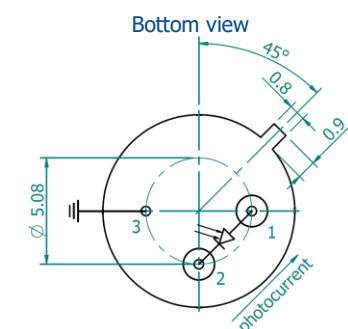


Parameter	Value
Immersion microlens shape	hyperhemisphere
Optical area $A_o$ , mm×mm	1×1
R, mm	0.8
A, mm	2.4±0.2

$\Phi$  – acceptance angle

R – hyperhemisphere microlens radius

A – distance from the bottom of hyperhemisphere microlens to the focal plane



Function	Pin number
Detector	1, 2
Reverse bias (optional)	1(-), 2(+)
Chassis ground	3

## Precautions for use and storage

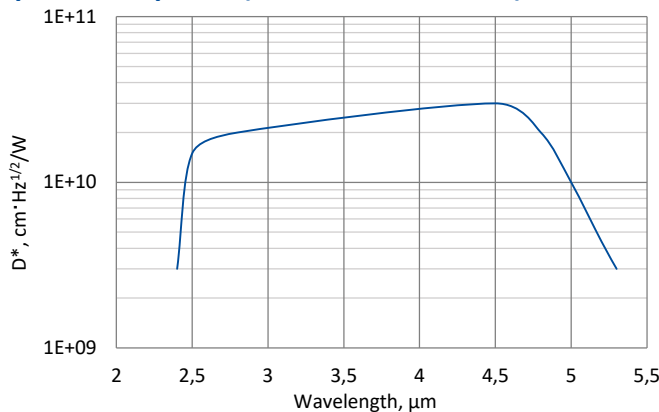
- Standard ohmmeter may overbias and damage the detector. Bias of 10 mV can be used for resistance measurements.
- Operation in 10% to 80% humidity and -20°C to 30°C ambient temperature.
- Beam power limitations for optically immersed detector:
  - irradiance with CW or single pulse longer than 1  $\mu$ s irradiance on the apparent optical active area must not exceed 2.5 W/cm<sup>2</sup>,
  - irradiance of the pulse shorter than 1  $\mu$ s must not exceed 10 kW/cm<sup>2</sup>.
- Storage in dark place with 10% to 90% humidity and -20°C to 50°C ambient temperature.

## PVI-5-1x1-TO39-NW-36

### 2.4 – 5.5 $\mu\text{m}$ HgCdTe ambient temperature, optically immersed photovoltaic detector

**PVI-5-1x1-TO39-NW-36** is uncooled IR photovoltaic detector based on sophisticated HgCdTe heterostructure for the best performance and stability. The device is optimized for the maximum performance at 5  $\mu\text{m}$ . Detector element is monolithically integrated with hyperhemispherical GaAs microlens in order to improve performance of the device. Reverse bias may significantly increase response speed and dynamic range. It also results in improved performance at high frequencies, but  $1/f$  noise that appears in biased devices may reduce performance at low frequencies

#### Spectral response ( $T_a = 20^\circ\text{C}$ , $V_b = 0\text{ mV}$ )



Exemplary spectral detectivity, the spectral response of delivered devices may differ.



#### Specification ( $T_a = 20^\circ\text{C}$ , $V_b = 0\text{ mV}$ )

Parameter	Detector type
	PVI-5-1x1-TO39-NW-36
Active element material	epitaxial HgCdTe heterostructure
Cut-on wavelength $\lambda_{\text{cut-on}}$ (10%), $\mu\text{m}$	$2.4 \pm 0.5$
Peak wavelength $\lambda_{\text{peak}}$ , $\mu\text{m}$	$4.2 \pm 0.5$
Optimum wavelength $\lambda_{\text{opt}}$ , $\mu\text{m}$	5.0
Cut-off wavelength $\lambda_{\text{cut-off}}$ (10%), $\mu\text{m}$	$5.5 \pm 0.3$
Detectivity $D^*(\lambda_{\text{peak}})$ , $\text{cm} \cdot \text{Hz}^{1/2} / \text{W}$	$\geq 3.0 \times 10^{10}$
Detectivity $D^*(\lambda_{\text{opt}})$ , $\text{cm} \cdot \text{Hz}^{1/2} / \text{W}$	$\geq 1.0 \times 10^{10}$
Current responsivity $R_i(\lambda_{\text{peak}})$ , A/W	$\geq 2.0$
Current responsivity $R_i(\lambda_{\text{opt}})$ , A/W	$\geq 1.0$
Time constant $\tau$ , ns	$\leq 150$
Resistance R, $\Omega$	$\geq 100$
Optical area $A_o$ , mm $\times$ mm	1 $\times$ 1
Package	TO39
Acceptance angle $\Phi$	$\sim 36^\circ$
Window	none

#### Features

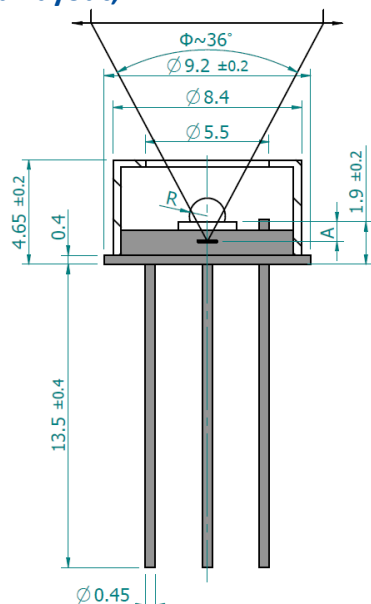
- Wide dynamic range
- Convenient to use
- Very small size
- Cost-effective solution
- Quantity discounted price
- Fast delivery

#### Applications

- Contactless temperature measurements (railway transport, industrial and laboratory processes monitoring)
- Flame and explosion detection
- Threat warning systems
- Gas detection, monitoring and analysis ( $\text{CO}$ ,  $\text{CO}_2$ ,  $\text{NO}_x$ )
- Breath analysis
- Solids analysis
- Leakage control in gas pipelines
- Combustion process control

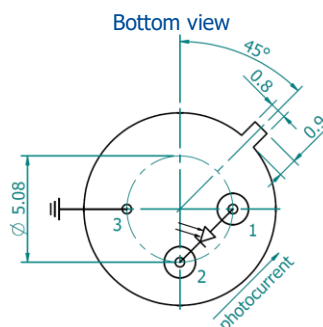


### Mechanical layout, mm



Parameter	Value
Immersion microlens shape	hyperhemisphere
Optical area $A_o$ , mm×mm	1×1
R, mm	0.8
A, mm	2.4±0.2

Φ – acceptance angle  
 R – hyperhemisphere microlens radius  
 A – distance from the bottom of hyperhemisphere microlens to the focal plane



Function	Pin number
Detector	1, 2
Reverse bias (optional)	1(-), 2(+)
Chassis ground	3

### Precautions for use and storage

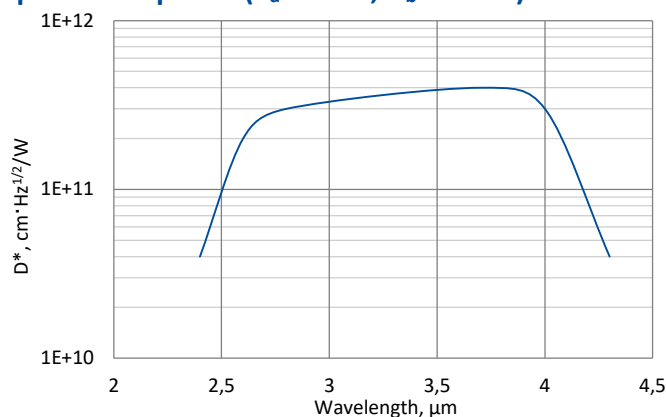
- Standard ohmmeter may overbias and damage the detector. Bias of 10 mV can be used for resistance measurements.
- Operation in 10% to 80% humidity and -20°C to 30°C ambient temperature.
- Beam power limitations for optically immersed detector:
  - irradiance with CW or single pulse longer than 1 μs irradiance on the apparent optical active area must not exceed 2.5 W/cm<sup>2</sup>,
  - irradiance of the pulse shorter than 1 μs must not exceed 10 kW/cm<sup>2</sup>.
- Storage in dark place with 10% to 90% humidity and -20°C to 50°C ambient temperature.

## PVI-2TE-4-1x1-TO8-wAl<sub>2</sub>O<sub>3</sub>-36

### 2.4 – 4.3 μm HgCdTe two-stage thermoelectrically cooled, optically immersed photovoltaic detector

**PVI-2TE-4-1x1-TO8-wAl<sub>2</sub>O<sub>3</sub>-36** is two-stage thermoelectrically cooled IR photovoltaic detector based on sophisticated HgCdTe heterostructure for the best performance and stability. The device is optimized for the maximum performance at 4 μm. Detector element is monolithically integrated with hyperhemispherical GaAs microlens in order to improve performance of the device. Reverse bias may significantly increase response speed and dynamic range. It also results in improved performance at high frequencies, but 1/f noise that appears in biased devices may reduce performance at low frequencies. 3° wedged sapphire (wAl<sub>2</sub>O<sub>3</sub>) window prevents unwanted interference effects.

#### Spectral response ( $T_a = 20^\circ\text{C}$ , $V_b = 0\text{ mV}$ )



Exemplary spectral detectivity, the spectral response of delivered devices may differ.

#### Specification ( $T_a = 20^\circ\text{C}$ , $V_b = 0\text{ mV}$ )

Parameter	Detector type
	PVI-2TE-4-1x1-TO8-wAl <sub>2</sub> O <sub>3</sub> -36
Active element material	epitaxial HgCdTe heterostructure
Cut-on wavelength $\lambda_{\text{cut-on}}$ (10%), μm	2.4±0.5
Peak wavelength $\lambda_{\text{peak}}$ , μm	3.5±0.5
Optimum wavelength $\lambda_{\text{opt}}$ , μm	4.0
Cut-off wavelength $\lambda_{\text{cut-off}}$ (10%), μm	4.3±0.3
Detectivity $D^*(\lambda_{\text{peak}})$ , cm·Hz <sup>1/2</sup> /W	≥4.0×10 <sup>11</sup>
Detectivity $D^*(\lambda_{\text{opt}})$ , cm·Hz <sup>1/2</sup> /W	≥3.0×10 <sup>11</sup>
Current responsivity $R_i(\lambda_{\text{peak}})$ , A/W	≥2.0
Current responsivity $R_i(\lambda_{\text{opt}})$ , A/W	≥1.3
Time constant $\tau$ , ns	≤100
Resistance $R$ , Ω	≥20000
Active element temperature $T_{\text{det}}$ , K	~230
Optical area $A_o$ , mm×mm	1×1
Package	TO8
Acceptance angle $\Phi$	~36°
Window	wAl <sub>2</sub> O <sub>3</sub>

#### Features

- High performance
- D\* better by one order of magnitude compared with the same type uncooled detector
- Wide dynamic range
- Quantity discounted price
- Fast delivery

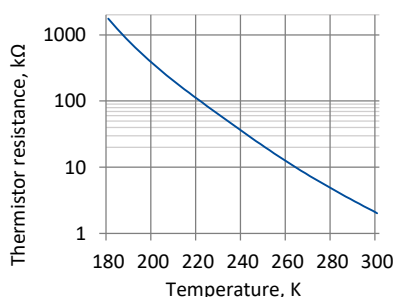
#### Applications

- Gas detection, monitoring and analysis (CH<sub>4</sub>, C<sub>2</sub>H<sub>2</sub>, CH<sub>2</sub>O, HCl, NH<sub>3</sub>, SO<sub>2</sub>, C<sub>2</sub>H<sub>6</sub>)
- Breath analysis
- Explosion prevention
- Flue gas denitrification
- Emission control (exhaust fumes, greenhouse gases)

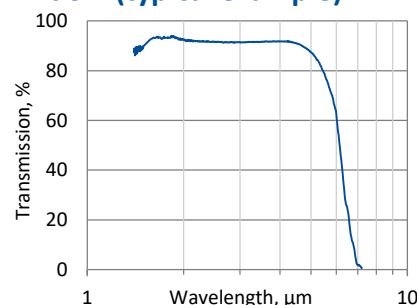
#### Two-stage thermoelectric cooler parameters

Parameter	Value
$T_{\text{det}}$ , K	~230
$V_{\text{max}}$ , V	1.3
$I_{\text{max}}$ , A	1.2
$Q_{\text{max}}$ , W	0.36

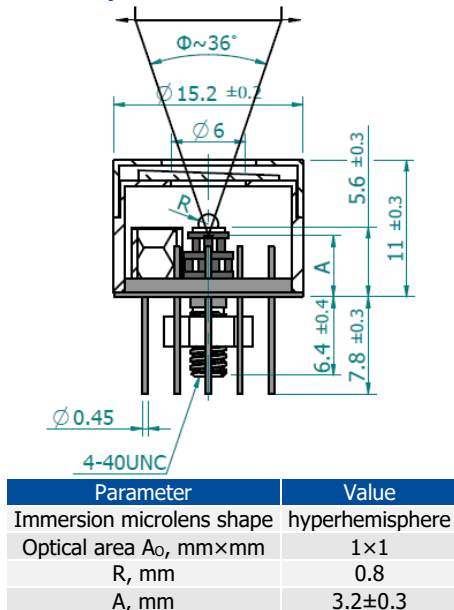
#### Thermistor characteristics



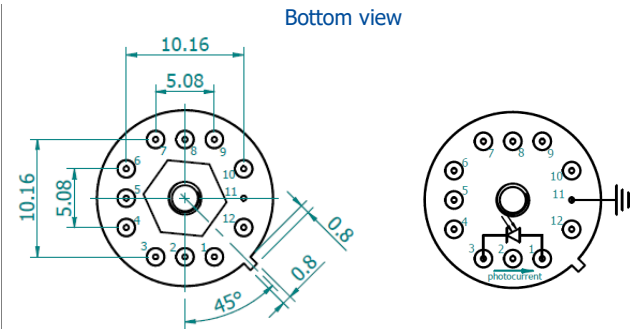
#### Spectral transmission of wAl<sub>2</sub>O<sub>3</sub> window (typical example)



### Mechanical layout, mm



Φ – acceptance angle  
 R – hyperhemisphere microlens radius  
 A – distance from the bottom of the 2TE-TO8 header to the focal plane



Function	Pin number
Detector	1, 3
Reverse bias (optional)	1(-), 3(+)
Thermistor	7, 9
TE cooler supply	2(+), 8(-)
Chassis ground	11
Not used	4, 5, 6, 10, 12

### Precautions for use and storage

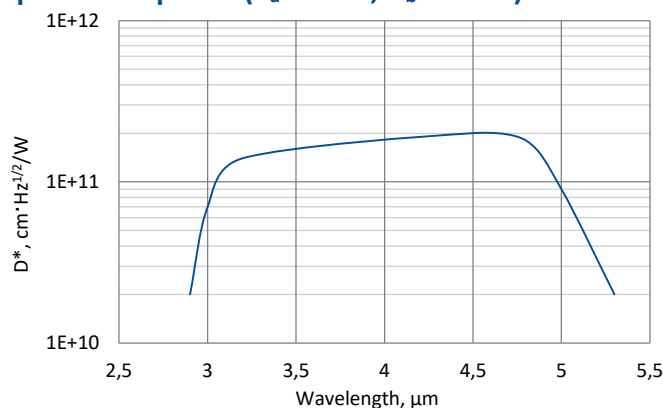
- Standard ohmmeter may overbias and damage the detector. Bias of 10 mV can be used for resistance measurements.
- Heatsink with thermal resistance of ~2 K/W is necessary to dissipate heat generated by 2TE cooler.
- Operation in 10% to 80% humidity and -20°C to 30°C ambient temperature.
- Beam power limitations for optically immersed detector:
  - irradiance with CW or single pulse longer than 1 μs irradiance on the apparent optical active area must not exceed 2.5 W/cm<sup>2</sup>,
  - irradiance of the pulse shorter than 1 μs must not exceed 10 kW/cm<sup>2</sup>.
- Storage in dark place with 10% to 90% humidity and -20°C to 50°C ambient temperature.

## PVI-2TE-5-1x1-TO8-wAl<sub>2</sub>O<sub>3</sub>-36

### 2.9 – 5.5 μm HgCdTe two-stage thermoelectrically cooled, optically immersed photovoltaic detector

**PVI-2TE-5-1x1-TO8-wAl<sub>2</sub>O<sub>3</sub>-36** is two-stage thermoelectrically cooled IR photovoltaic detector based on sophisticated HgCdTe heterostructure for the best performance and stability. The device is optimized for the maximum performance at 5 μm. Detector element is monolithically integrated with hyperhemispherical GaAs microlens in order to improve performance of the device. Reverse bias may significantly increase response speed and dynamic range. It also results in improved performance at high frequencies, but 1/f noise that appears in biased devices may reduce performance at low frequencies. 3° wedged sapphire (wAl<sub>2</sub>O<sub>3</sub>) window prevents unwanted interference effects.

#### Spectral response ( $T_a = 20^\circ\text{C}$ , $V_b = 0\text{ mV}$ )



Exemplary spectral detectivity, the spectral response of delivered devices may differ.



#### Specification ( $T_a = 20^\circ\text{C}$ , $V_b = 0\text{ mV}$ )

Parameter	Detector type
	PVI-2TE-5-1x1-TO8-wAl <sub>2</sub> O <sub>3</sub> -36
Active element material	epitaxial HgCdTe heterostructure
Cut-on wavelength $\lambda_{\text{cut-on}}$ (10%), μm	2.9±1.0
Peak wavelength $\lambda_{\text{peak}}$ , μm	4.2±0.5
Optimum wavelength $\lambda_{\text{opt}}$ , μm	5.0
Cut-off wavelength $\lambda_{\text{cut-off}}$ (10%), μm	5.5±0.3
Detectivity $D^*(\lambda_{\text{peak}})$ , cm·Hz <sup>1/2</sup> /W	≥2.0×10 <sup>11</sup>
Detectivity $D^*(\lambda_{\text{opt}})$ , cm·Hz <sup>1/2</sup> /W	≥9.0×10 <sup>10</sup>
Current responsivity $R_i(\lambda_{\text{peak}})$ , A/W	≥2.0
Current responsivity $R_i(\lambda_{\text{opt}})$ , A/W	≥1.3
Time constant $\tau$ , ns	≤80
Resistance $R$ , Ω	≥1000
Active element temperature $T_{\text{det}}$ , K	~230
Optical area $A_O$ , mm×mm	1×1
Package	TO8
Acceptance angle $\Phi$	~36°
Window	wAl <sub>2</sub> O <sub>3</sub>

#### Features

- High performance
- $D^*$  better by one order of magnitude compared with the same type uncooled detector
- Wide dynamic range
- Quantity discounted price
- Fast delivery

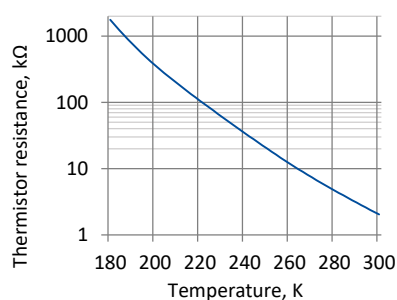
#### Applications

- Contactless temperature measurements (railway transport, industrial and laboratory processes monitoring)
- Flame and explosion detection
- Threat warning systems
- Gas detection, monitoring and analysis (CO, CO<sub>2</sub>, NO<sub>x</sub>)
- In-vivo alcohol detection
- Breath analysis
- Solids analysis
- Leakage control in gas pipelines
- Combustion process control

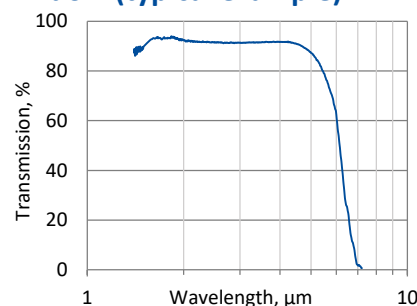
#### Two-stage thermoelectric cooler parameters

Parameter	Value
$T_{\text{det}}$ , K	~230
$V_{\text{max}}$ , V	1.3
$I_{\text{max}}$ , A	1.2
$Q_{\text{max}}$ , W	0.36

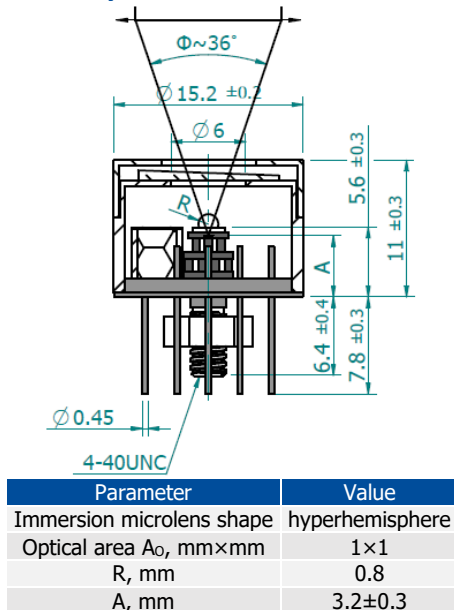
#### Thermistor characteristics



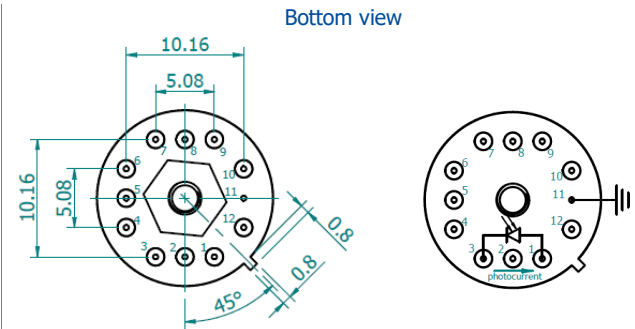
#### Spectral transmission of wAl<sub>2</sub>O<sub>3</sub> window (typical example)



### Mechanical layout, mm



Φ – acceptance angle  
 A – distance from the bottom of the 2TE-TO8 header to the focal plane  
 R – hyperhemisphere microlens radius



Function	Pin number
Detector	1, 3
Reverse bias (optional)	1(-), 3(+)
Thermistor	7, 9
TE cooler supply	2(+), 8(-)
Chassis ground	11
Not used	4, 5, 6, 10, 12

### Precautions for use and storage

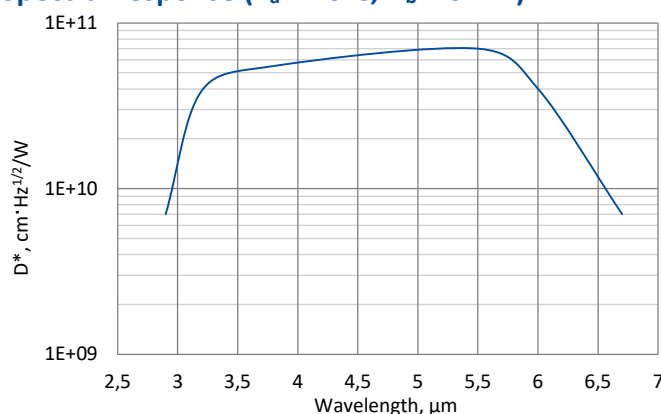
- Standard ohmmeter may overbias and damage the detector. Bias of 10 mV can be used for resistance measurements.
- Heatsink with thermal resistance of ~2 K/W is necessary to dissipate heat generated by 2TE cooler.
- Operation in 10% to 80% humidity and -20°C to 30°C ambient temperature.
- Beam power limitations for optically immersed detector:
  - irradiance with CW or single pulse longer than 1 μs irradiance on the apparent optical active area must not exceed 2.5 W/cm<sup>2</sup>,
  - irradiance of the pulse shorter than 1 μs must not exceed 10 kW/cm<sup>2</sup>.
- Storage in dark place with 10% to 90% humidity and -20°C to 50°C ambient temperature.

## PVI-2TE-6-1x1-TO8-wZnSeAR-36

### 3.0 – 6.7 μm HgCdTe two-stage thermoelectrically cooled, optically immersed photovoltaic detector

**PVI-2TE-6-1x1-TO8-wZnSeAR-36** is two-stage thermoelectrically cooled IR photovoltaic detector based on sophisticated HgCdTe heterostructure for the best performance and stability. The device is optimized for the maximum performance at 6 μm. Detector element is monolithically integrated with hyperhemispherical GaAs microlens in order to improve performance of the device. Reverse bias may significantly increase response speed and dynamic range. 3° wedged zinc selenide anti-reflection coated (wZnSeAR) window prevents unwanted interference effects.

#### Spectral response ( $T_a = 20^\circ\text{C}$ , $V_b = 0\text{ mV}$ )



Exemplary spectral detectivity, the spectral response of delivered devices may differ.

#### Specification ( $T_a = 20^\circ\text{C}$ , $V_b = 0\text{ mV}$ )

Parameter	Detector type
	PVI-2TE-6-1x1-TO8-wZnSeAR-36
Active element material	epitaxial HgCdTe heterostructure
Cut-on wavelength $\lambda_{\text{cut-on}}$ (10%), μm	3.0±1.0
Peak wavelength $\lambda_{\text{peak}}$ , μm	5.2±0.5
Optimum wavelength $\lambda_{\text{opt}}$ , μm	6.0
Cut-off wavelength $\lambda_{\text{cut-off}}$ (10%), μm	6.7±0.3
Detectivity $D^*(\lambda_{\text{peak}})$ , cm·Hz <sup>1/2</sup> /W	≥7.0×10 <sup>10</sup>
Detectivity $D^*(\lambda_{\text{opt}})$ , cm·Hz <sup>1/2</sup> /W	≥4.0×10 <sup>10</sup>
Current responsivity $R_i(\lambda_{\text{peak}})$ , A/W	≥2.7
Current responsivity $R_i(\lambda_{\text{opt}})$ , A/W	≥1.5
Time constant $\tau$ , ns	≤50
Resistance $R$ , Ω	≥200
Active element temperature $T_{\text{det}}$ , K	~230
Optical area $A_o$ , mm×mm	1×1
Package	TO8
Acceptance angle $\Phi$	~36°
Window	wZnSeAR

#### Features

- High performance
- Wide dynamic range
- Versatility
- Quantity discounted price
- Fast delivery

#### Applications

- Gas detection, monitoring and analysis (CO, CO<sub>2</sub>, NH<sub>3</sub>, NO<sub>x</sub>)
- Flue gas denitrification
- Fuel combustion monitoring at power plants and other industrial facilities
- Contactless temperature measurements

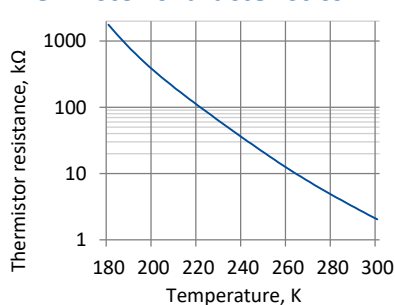
#### Related product

- [UM-I-6 detection module](#)

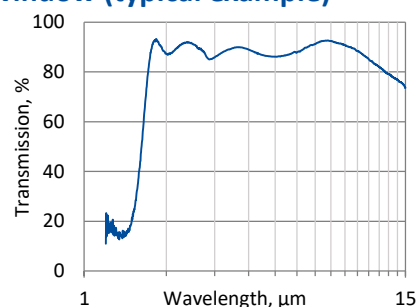
#### Two-stage thermoelectric cooler parameters

Parameter	Value
$T_{\text{det}}$ , K	~230
$V_{\text{max}}$ , V	1.3
$I_{\text{max}}$ , A	1.2
$Q_{\text{max}}$ , W	0.36

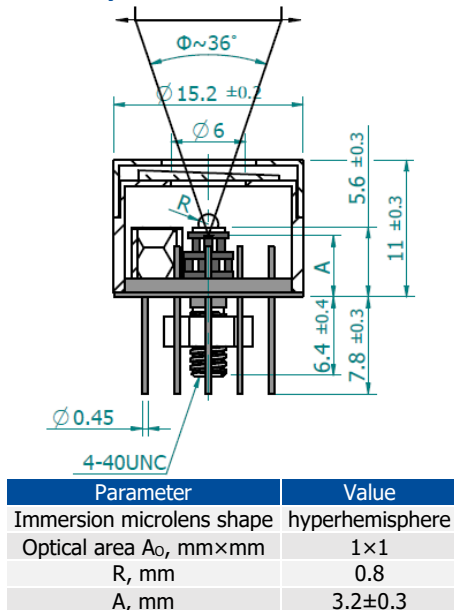
#### Thermistor characteristics



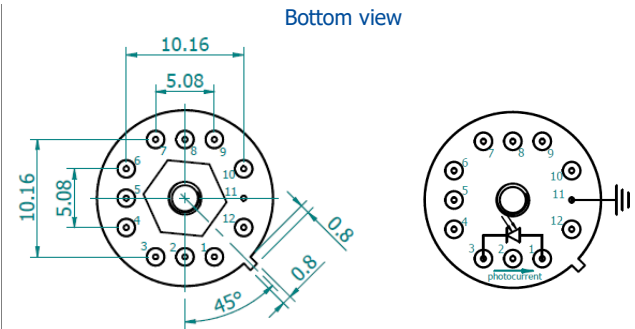
#### Spectral transmission of wZnSeAR window (typical example)



### Mechanical layout, mm



Φ – acceptance angle  
 R – hyperhemisphere microlens radius  
 A – distance from the bottom of the 2TE-TO8 header to the focal plane



Function	Pin number
Detector	1, 3
Reverse bias (optional)	1(-), 3(+)
Thermistor	7, 9
TE cooler supply	2(+), 8(-)
Chassis ground	11
Not used	4, 5, 6, 10, 12

### Precautions for use and storage

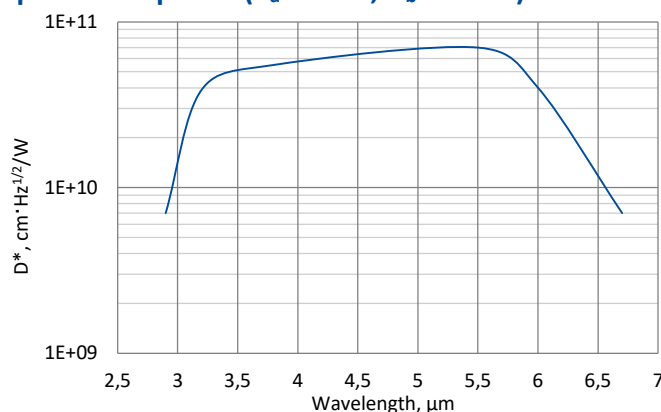
- Standard ohmmeter may overbias and damage the detector. Bias of 10 mV can be used for resistance measurements.
- Heatsink with thermal resistance of ~2 K/W is necessary to dissipate heat generated by 2TE cooler.
- Operation in 10% to 80% humidity and -20°C to 30°C ambient temperature.
- Beam power limitations for optically immersed detector:
  - irradiance with CW or single pulse longer than 1 μs irradiance on the apparent optical active area must not exceed 2.5 W/cm<sup>2</sup>,
  - irradiance of the pulse shorter than 1 μs must not exceed 10 kW/cm<sup>2</sup>.
- Storage in dark place with 10% to 90% humidity and -20°C to 50°C ambient temperature.

## PVI-4TE-6-1x1-TO8-wZnSeAR-36

### 3.0 – 6.9 μm HgCdTe four-stage thermoelectrically cooled, optically immersed photovoltaic detector

**PVI-4TE-6-1x1-TO8-wZnSeAR-36** is four-stage thermoelectrically cooled IR photovoltaic detector based on sophisticated HgCdTe heterostructure for the best performance and stability. The device is optimized for the maximum performance at 6 μm. Detector element is monolithically integrated with hyperhemispherical GaAs microlens in order to improve performance of the device. Reverse bias may significantly increase response speed and dynamic range. It also results in improved performance at high frequencies, but 1/f noise that appears in biased devices may reduce performance at low frequencies. 3° wedged zinc selenide anti-reflection coated (wZnSeAR) window prevents unwanted interference effects.

#### Spectral response ( $T_a = 20^\circ\text{C}$ , $V_b = 0\text{ mV}$ )



Exemplary spectral detectivity, the spectral response of delivered devices may differ.

#### Specification ( $T_a = 20^\circ\text{C}$ , $V_b = 0\text{ mV}$ )

Parameter	Detector type
	PVI-4TE-6-1x1-TO8-wZnSeAR-36
Active element material	epitaxial HgCdTe heterostructure
Cut-on wavelength $\lambda_{\text{cut-on}}$ (10%), μm	3.0±1.0
Peak wavelength $\lambda_{\text{peak}}$ , μm	5.5±0.5
Optimum wavelength $\lambda_{\text{opt}}$ , μm	6.0
Cut-off wavelength $\lambda_{\text{cut-off}}$ (10%), μm	6.9±0.3
Detectivity $D^*(\lambda_{\text{peak}})$ , $\text{cm}\cdot\text{Hz}^{1/2}/\text{W}$	$\geq 8.0 \times 10^{10}$
Detectivity $D^*(\lambda_{\text{opt}})$ , $\text{cm}\cdot\text{Hz}^{1/2}/\text{W}$	$\geq 6.0 \times 10^{10}$
Current responsivity $R_i(\lambda_{\text{peak}})$ , A/W	$\geq 2.7$
Current responsivity $R_i(\lambda_{\text{opt}})$ , A/W	$\geq 1.5$
Time constant $\tau$ , ns	$\leq 50$
Resistance R, Ω	$\geq 300$
Active element temperature $T_{\text{det}}$ , K	~195
Optical area $A_o$ , mm×mm	1×1
Package	TO8
Acceptance angle $\Phi$	~36°
Window	wZnSeAR

#### Features

- Very high performance
- Wide dynamic range
- Versatility
- Quantity discounted price
- Fast delivery

#### Applications

- Gas detection, monitoring and analysis (CO, CO<sub>2</sub>, NH<sub>3</sub>, NO<sub>x</sub>)
- Flue gas denitrification
- Fuel combustion monitoring at power plants and other industrial facilities
- Contactless temperature measurements

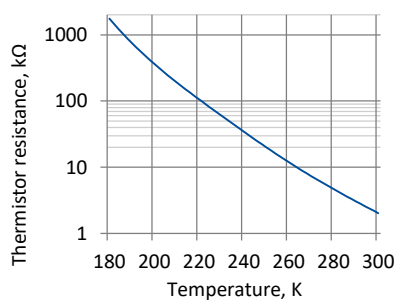
#### Related product

- [LabM-I-6 detection module](#)

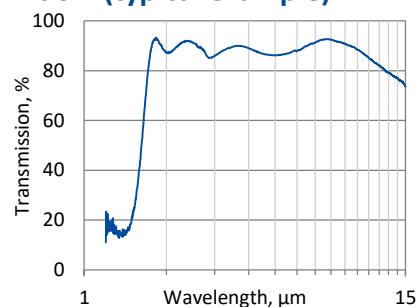
#### Four-stage thermoelectric cooler parameters

Parameter	Value
$T_{\text{det}}$ , K	~195
$V_{\text{max}}$ , V	8.3
$I_{\text{max}}$ , A	0.4
$Q_{\text{max}}$ , W	0.28

#### Thermistor characteristics

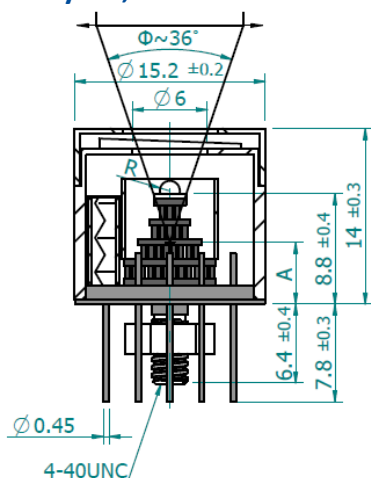


#### Spectral transmission of wZnSeAR window (typical example)



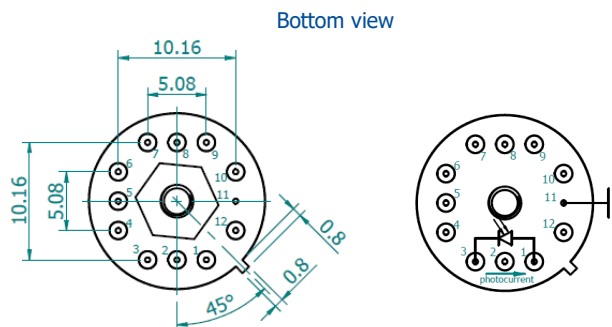


### Mechanical layout, mm



Parameter	Value
Immersion microlens shape	hyperhemisphere
Optical area $A_o$ , mm×mm	1×1
R, mm	0.8
A, mm	6.4±0.4

$\Phi$  – acceptance angle  
 R – hyperhemisphere microlens radius  
 A – distance from the bottom of the 4TE-TO8 header to the focal plane



Function	Pin number
Detector	1, 3
Reverse bias (optional)	1(-), 3(+)
Thermistor	7, 9
TE cooler supply	2(+), 8(-)
Chassis ground	11
Not used	4, 5, 6, 10, 12

### Precautions for use and storage

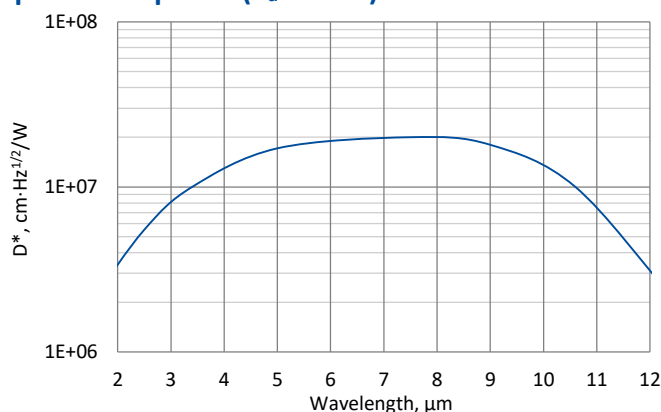
- Standard ohmmeter may overbias and damage the detector. Bias of 10 mV can be used for resistance measurements.
- Heatsink with thermal resistance of ~1 K/W is necessary to dissipate heat generated by 4TE cooler.
- Operation in 10% to 80% humidity and -20°C to 30°C ambient temperature.
- Beam power limitations for optically immersed detector:
  - irradiance with CW or single pulse longer than 1  $\mu$ s irradiance on the apparent optical active area must not exceed 2.5 W/cm<sup>2</sup>;
  - irradiance of the pulse shorter than 1  $\mu$ s must not exceed 10 kW/cm<sup>2</sup>.
- Storage in dark place with 10% to 90% humidity and -20°C to 50°C ambient temperature.

## PVM-10.6-1x1-TO39-NW-90

### 2 – 12 μm HgCdTe ambient temperature photovoltaic multiple junction detector

**PVM-10.6-1x1-TO39-NW-90** is uncooled IR photovoltaic multiple junction detector based on sophisticated HgCdTe heterostructure for the best performance and stability. The device is designed for the maximum performance at 10.6 μm and especially useful as a large active area detector to detect CW and low frequency modulated radiation.

#### Spectral response ( $T_a = 20^\circ\text{C}$ )



Exemplary spectral detectivity, the spectral response of delivered devices may differ.

#### Specification ( $T_a = 20^\circ\text{C}$ )

Parameter	Detector type
	PVM-10.6-1x1-TO39-NW-90
Active element material	epitaxial HgCdTe heterostructure
Cut-on wavelength $\lambda_{\text{cut-on}}$ (10%), μm	≤2.0
Peak wavelength $\lambda_{\text{peak}}$ , μm	8.5±1.5
Optimum wavelength $\lambda_{\text{opt}}$ , μm	10.6
Cut-off wavelength $\lambda_{\text{cut-off}}$ (10%), μm	≥12.0
Detectivity $D^*(\lambda_{\text{peak}})$ , $\text{cm}\cdot\text{Hz}^{1/2}/\text{W}$	≥2.0×10 <sup>7</sup>
Detectivity $D^*(\lambda_{\text{opt}})$ , $\text{cm}\cdot\text{Hz}^{1/2}/\text{W}$	≥1.0×10 <sup>7</sup>
Current responsivity $R_i(\lambda_{\text{peak}})$ , A/W	≥0.004
Current responsivity $R_i(\lambda_{\text{opt}})$ , A/W	≥0.002
Time constant $\tau$ , ns	≤1.5
Resistance R, Ω	≥30
Active area A, mm×mm	1×1
Package	TO39
Acceptance angle $\Phi$	~90°
Window	none

#### Features

- Wide spectral range from 2 to 12 μm
- Large active area 1×1 mm<sup>2</sup>
- No bias required
- No flicker noise
- Short time constant ≤ 1.5 ns
- Operation from DC to high frequency
- Sensitive to IR radiation polarisation
- Very small size
- Convenient to use
- Versatility
- Cost-effective solution
- Quantity discounted price
- Fast delivery

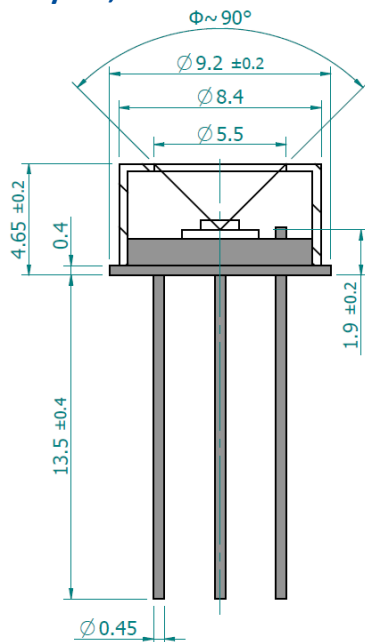
#### Applications

- CO<sub>2</sub> laser (10.6 μm) measurements
- Laser power monitoring and control
- Laser beam profiling and positioning
- Laser calibration
- Dentistry

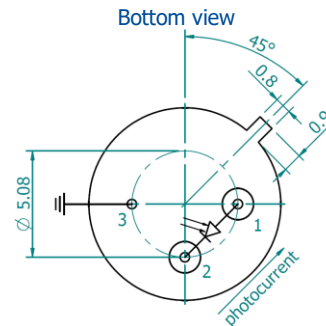
#### Related product

- [microM-10.6 detection module](#)

### Mechanical layout, mm



Φ – acceptance angle



Function	Pin number
Detector	1, 2
Chassis ground	3

### Precautions for use and storage

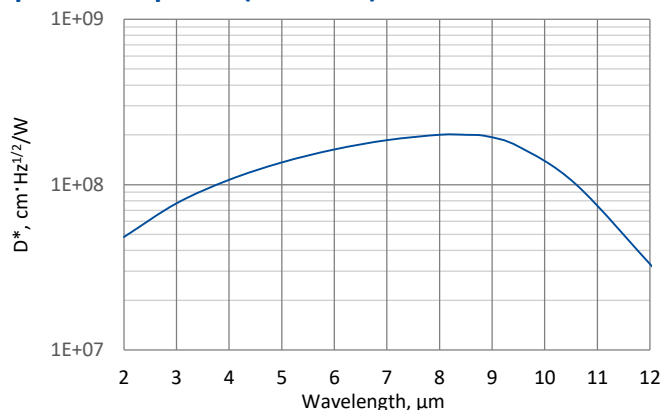
- Operation in 10% to 80% humidity and -20°C to 30°C ambient temperature.
- Beam power limitations:
  - irradiance with CW or single pulse longer than 1 μs irradiance on the apparent optical active area must not exceed 100 W/cm<sup>2</sup>,
  - irradiance of the pulse shorter than 1 μs must not exceed 1 MW/cm<sup>2</sup>.
- Storage in dark place with 10% to 90% humidity and -20°C to 50°C ambient temperature.

## PVM-2TE-10.6-1x1-TO8-wZnSeAR-70

### 2 – 12 μm HgCdTe two-stage thermoelectrically cooled photovoltaic multiple junction detector

**PVM-2TE-10.6-1x1-TO8-wZnSeAR-70** is two-stage thermoelectrically cooled IR photovoltaic multiple junction detector based on sophisticated HgCdTe heterostructure for the best performance and stability. The device is designed for the maximum performance at 10.6 μm and especially useful as a large active area detector to detect CW and low frequency modulated radiation. 3° wedged zinc selenide anti-reflection coated (wZnSeAR) window prevents unwanted interference effects.

#### Spectral response ( $T_a = 20^\circ\text{C}$ )



Exemplary spectral detectivity, the spectral response of delivered devices may differ.

#### Specification ( $T_a = 20^\circ\text{C}$ )

Parameter	Detector type
	PVM-2TE-10.6-1x1-TO8-wZnSeAR-70
Active element material	epitaxial HgCdTe heterostructure
Cut-on wavelength $\lambda_{\text{cut-on}}$ (10%), μm	≤2.0
Peak wavelength $\lambda_{\text{peak}}$ , μm	8.5±2.0
Optimum wavelength $\lambda_{\text{opt}}$ , μm	10.6
Cut-off wavelength $\lambda_{\text{cut-off}}$ (10%), μm	≥12.0
Detectivity $D^*(\lambda_{\text{peak}})$ , $\text{cm}\cdot\text{Hz}^{1/2}/\text{W}$	≥2.0×10 <sup>8</sup>
Detectivity $D^*(\lambda_{\text{opt}})$ , $\text{cm}\cdot\text{Hz}^{1/2}/\text{W}$	≥1.0×10 <sup>8</sup>
Current responsivity $R_i(\lambda_{\text{peak}})$ , A/W	≥0.015
Current responsivity $R_i(\lambda_{\text{opt}})$ , A/W	≥0.01
Time constant $\tau$ , ns	≤4
Resistance R, Ω	≥90
Active element temperature $T_{\text{det}}$ , K	~230
Active area A, mm×mm	1×1
Package	TO8
Acceptance angle $\Phi$	~70°
Window	wZnSeAR

#### Features

- Wide spectral range from 2 to 12 μm
- Large active area 1×1 mm<sup>2</sup>
- No bias required
- No flicker noise
- Operation from DC to high frequency
- Sensitive to IR radiation polarisation
- Versatility
- Quantity discounted price
- Fast delivery

#### Applications

- CO<sub>2</sub> laser (10.6 μm) measurements
- Laser power monitoring and control
- Laser beam profiling and positioning
- Laser calibration
- Dentistry

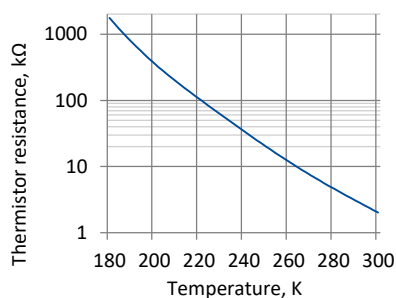
#### Related product

- [UM-10.6 detection module](#)

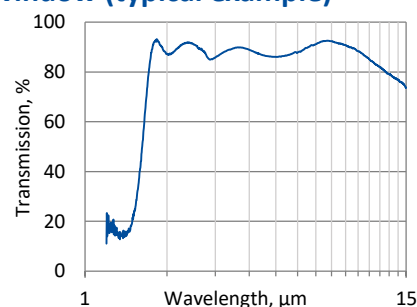
#### Two-stage thermoelectric cooler parameters

Parameter	Value
$T_{\text{det}}$ , K	~230
$V_{\text{max}}$ , V	1.3
$I_{\text{max}}$ , A	1.2
$Q_{\text{max}}$ , W	0.36

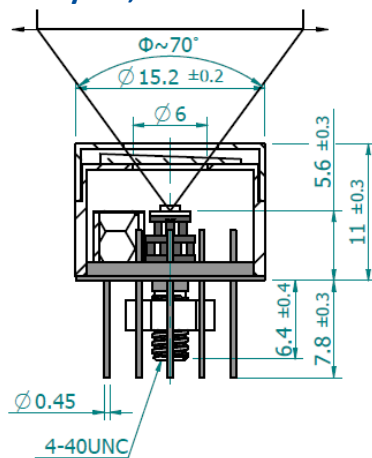
#### Thermistor characteristics



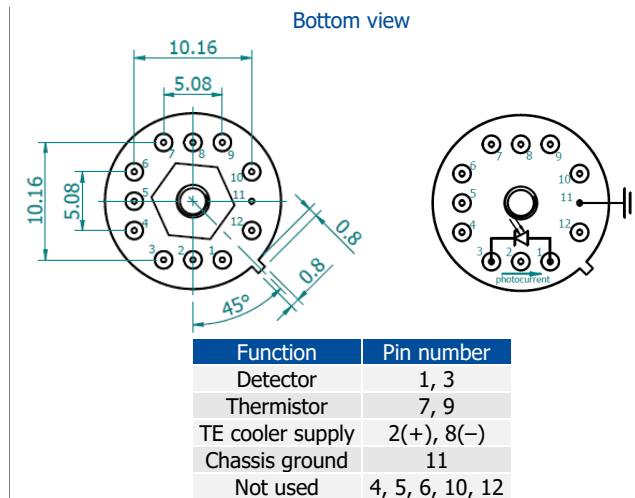
#### Spectral transmission of wZnSeAR window (typical example)



### Mechanical layout, mm



Φ – acceptance angle



### Precautions for use and storage

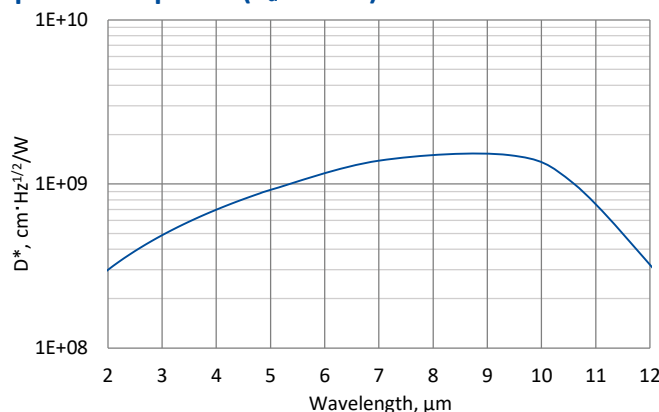
- Heatsink with thermal resistance of ~2 K/W is necessary to dissipate heat generated by 2TE cooler.
- Operation in 10% to 80% humidity and -20°C to 30°C ambient temperature.
- Beam power limitations:
  - irradiance with CW or single pulse longer than 1 μs irradiance on the apparent optical active area must not exceed 100 W/cm<sup>2</sup>,
  - irradiance of the pulse shorter than 1 μs must not exceed 1 MW/cm<sup>2</sup>.
- Storage in dark place with 10% to 90% humidity and -20°C to 50°C ambient temperature.

## PVMI-2TE-10.6-1x1-TO8-wZnSeAR-36

### 2 – 12 μm HgCdTe two-stage thermoelectrically cooled, optically immersed photovoltaic multiple junction detector

**PVMI-2TE-10.6-1x1-TO8-wZnSeAR-36** is two-stage thermoelectrically cooled IR photovoltaic multiple junction detector based on sophisticated HgCdTe heterostructure for the best performance and stability. The device is designed for the maximum performance at 10.6 μm. Detector element is monolithically integrated with hyperhemispherical GaAs microlens in order to improve performance of the device. 3° wedged zinc selenide anti-reflection coated (wZnSeAR) window prevents unwanted interference effects.

#### Spectral response ( $T_a = 20^\circ\text{C}$ )



Exemplary spectral detectivity, the spectral response of delivered devices may differ.

#### Specification ( $T_a = 20^\circ\text{C}$ )

Parameter	Detector type
	PVMI-2TE-10.6-1x1-TO8-wZnSeAR-36
Active element material	epitaxial HgCdTe heterostructure
Cut-on wavelength $\lambda_{\text{cut-on}}$ (10%), μm	≤2.0
Peak wavelength $\lambda_{\text{peak}}$ , μm	8.5±1.5
Optimum wavelength $\lambda_{\text{opt}}$ , μm	10.6
Cut-off wavelength $\lambda_{\text{cut-off}}$ (10%), μm	≥12.0
Detectivity $D^*(\lambda_{\text{peak}})$ , $\text{cm}\cdot\text{Hz}^{1/2}/\text{W}$	≥1.5×10 <sup>9</sup>
Detectivity $D^*(\lambda_{\text{opt}})$ , $\text{cm}\cdot\text{Hz}^{1/2}/\text{W}$	≥1.0×10 <sup>9</sup>
Current responsivity $R_i(\lambda_{\text{peak}})$ , A/W	≥0.15
Current responsivity $R_i(\lambda_{\text{opt}})$ , A/W	≥0.1
Time constant $\tau$ , ns	≤3
Resistance $R$ , Ω	≥90
Active element temperature $T_{\text{det}}$ , K	~230
Optical area $A_o$ , mm×mm	1×1
Package	TO8
Acceptance angle $\Phi$	~36°
Window	wZnSeAR

#### Features

- Wide spectral range from 2 to 12 μm
- No bias required
- No flicker noise
- Operation from DC to high frequency
- Sensitive to IR radiation polarisation
- Versatility
- Quantity discounted price
- Fast delivery

#### Applications

- CO<sub>2</sub> laser (10.6 μm) measurements
- Laser power monitoring and control
- Laser beam profiling and positioning
- Laser calibration
- Dentistry

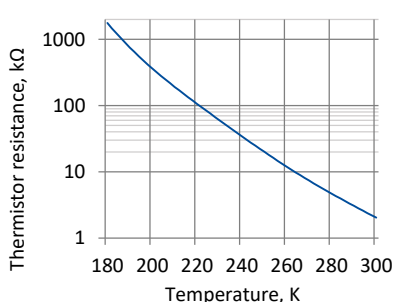
#### Related product

- [UM-I-10.6 detection module](#)

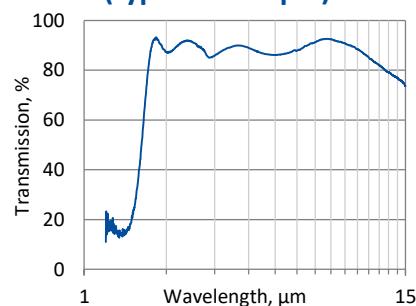
#### Two-stage thermoelectric cooler parameters

Parameter	Value
$T_{\text{det}}$ , K	~230
$V_{\text{max}}$ , V	1.3
$I_{\text{max}}$ , A	1.2
$Q_{\text{max}}$ , W	0.36

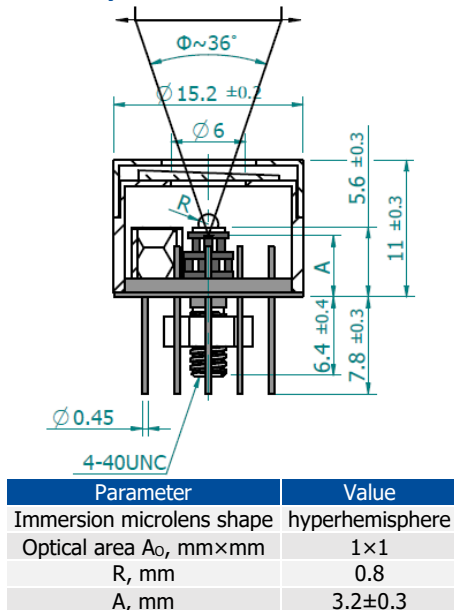
#### Thermistor characteristics



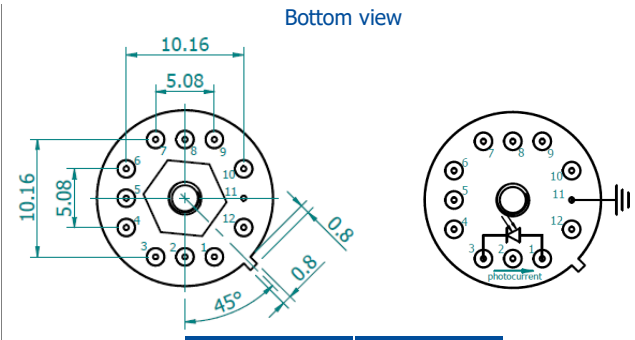
#### Spectral transmission of wZnSeAR window (typical example)



### Mechanical layout, mm



Φ – acceptance angle  
 A – distance from the bottom of the 2TE-TO8 header to the focal plane  
 R – hyperhemisphere microlens radius



Function	Pin number
Detector	1, 3
Thermistor	7, 9
TE cooler supply	2(+), 8(-)
Chassis ground	11
Not used	4, 5, 6, 10, 12

### Precautions for use and storage

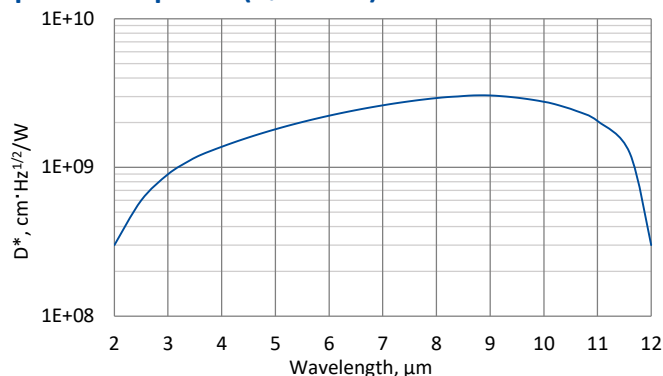
- Heatsink with thermal resistance of ~2 K/W is necessary to dissipate heat generated by 2TE cooler.
- Operation in 10% to 80% humidity and -20°C to 30°C ambient temperature.
- Beam power limitations for optically immersed detector:
  - irradiance with CW or single pulse longer than 1 μs irradiance on the apparent optical active area must not exceed 2.5 W/cm<sup>2</sup>,
  - irradiance of the pulse shorter than 1 μs must not exceed 10 kW/cm<sup>2</sup>.
- Storage in dark place with 10% to 90% humidity and -20°C to 50°C ambient temperature.

## PVMI-4TE-10.6-1x1-TO8-wZnSeAR-36

### 2 – 12 μm HgCdTe four-stage thermoelectrically cooled, optically immersed photovoltaic multiple junction detector

**PVMI-4TE-10.6-1x1-TO8-wZnSeAR-36** is four-stage thermoelectrically cooled IR photovoltaic multiple junction detector based on sophisticated HgCdTe heterostructure for the best performance and stability. The device is designed for the maximum performance at 10.6 μm. Detector element is monolithically integrated with hyperhemispherical GaAs microlens in order to improve performance of the device. 3° wedged zinc selenide anti-reflection coated (wZnSeAR) window prevents unwanted interference effects.

#### Spectral response ( $T_a = 20^\circ\text{C}$ )



Exemplary spectral detectivity, the spectral response of delivered devices may differ.



#### Specification ( $T_a = 20^\circ\text{C}$ )

Parameter	Detector type
	PVMI-4TE-10.6-1x1-TO8-wZnSeAR-36
Active element material	epitaxial HgCdTe heterostructure
Cut-on wavelength $\lambda_{\text{cut-on}}$ (10%), μm	$\leq 2.0$
Peak wavelength $\lambda_{\text{peak}}$ , μm	$8.5 \pm 2.0$
Optimum wavelength $\lambda_{\text{opt}}$ , μm	10.6
Cut-off wavelength $\lambda_{\text{cut-off}}$ (10%), μm	$\geq 12.0$
Detectivity $D^*(\lambda_{\text{peak}})$ , $\text{cm}\cdot\text{Hz}^{1/2}/\text{W}$	$\geq 3.0 \times 10^9$
Detectivity $D^*(\lambda_{\text{opt}})$ , $\text{cm}\cdot\text{Hz}^{1/2}/\text{W}$	$\geq 2.5 \times 10^9$
Current responsivity $R_i(\lambda_{\text{peak}})$ , A/W	$\geq 0.25$
Current responsivity $R_i(\lambda_{\text{opt}})$ , A/W	$\geq 0.18$
Time constant $\tau$ , ns	$\leq 3$
Resistance R, Ω	$\geq 120$
Active element temperature $T_{\text{det}}$ , K	$\sim 195$
Optical area $A_o$ , mm×mm	1×1
Package	TO8
Acceptance angle $\Phi$	$\sim 36^\circ$
Window	wZnSeAR

#### Features

- High performance
- Wide spectral range from 2 to 12 μm
- No bias required
- No flicker noise
- Operation from DC to high frequency
- Sensitive to IR radiation polarisation
- Versatility
- Quantity discounted price
- Fast delivery

#### Applications

- CO<sub>2</sub> laser (10.6 μm) measurements
- Laser power monitoring and control
- Laser beam profiling and positioning
- Laser calibration
- Semiconductor manufacturing
- Glucose monitoring
- Detection of hazardous chemicals (i.e. ammonia) in the air

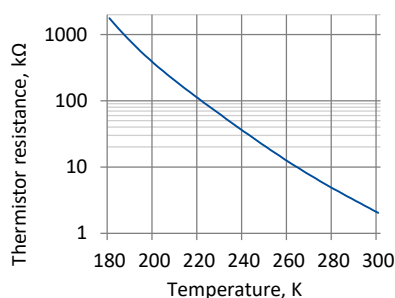
#### Related product

- [LabM-I-10.6 detection module](#)

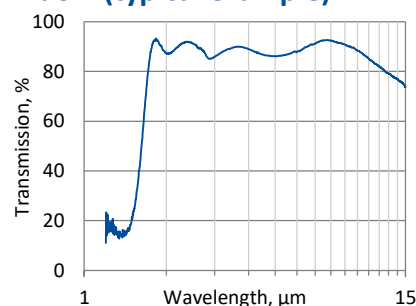
#### Four-stage thermoelectric cooler parameters

Parameter	Value
$T_{\text{det}}$ , K	$\sim 195$
$V_{\text{max}}$ , V	8.3
$I_{\text{max}}$ , A	0.4
$Q_{\text{max}}$ , W	0.28

#### Thermistor characteristics

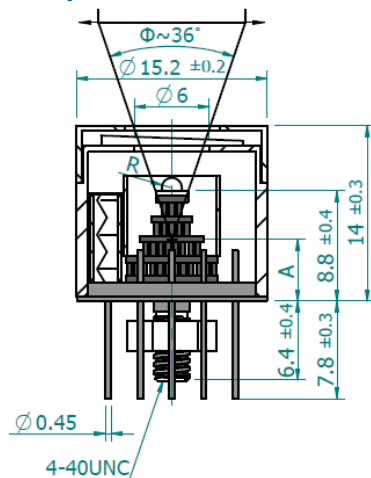


#### Spectral transmission of wZnSeAR window (typical example)



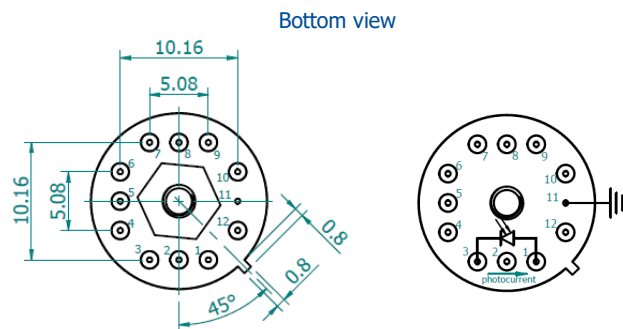


### Mechanical layout, mm



Parameter	Value
Immersion microlens shape	hyperhemisphere
Optical area $A_o$ , mm×mm	1×1
R, mm	0.8
A, mm	6.4±0.4

$\Phi$  – acceptance angle  
 A – distance from the bottom of the 4TE-TO8 header to the focal plane  
 R – hyperhemisphere microlens radius



Function	Pin number
Detector	1, 3
Thermistor	7, 9
TE cooler supply	2(+), 8(-)
Chassis ground	11
Not used	4, 5, 6, 10, 12

### Precautions for use and storage

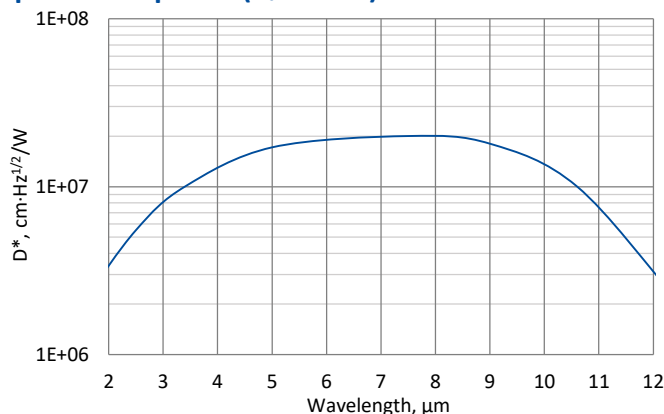
- Heatsink with thermal resistance of  $\sim 1$  K/W is necessary to dissipate heat generated by 4TE cooler.
- Operation in 10% to 80% humidity and  $-20^{\circ}\text{C}$  to  $30^{\circ}\text{C}$  ambient temperature.
- Beam power limitations for optically immersed detector:
  - irradiance with CW or single pulse longer than  $1 \mu\text{s}$  irradiance on the apparent optical active area must not exceed  $2.5 \text{ W/cm}^2$ ,
  - irradiance of the pulse shorter than  $1 \mu\text{s}$  must not exceed  $10 \text{ kW/cm}^2$ .
- Storage in dark place with 10% to 90% humidity and  $-20^{\circ}\text{C}$  to  $50^{\circ}\text{C}$  ambient temperature.

## PEM-10.6-2x2-PEM-SMA-wZnSeAR-48

### 2 – 12 $\mu\text{m}$ HgCdTe ambient temperature photoelectromagnetic detector

**PEM-10.6-2x2-PEM-SMA-wZnSeAR-48** is uncooled IR photovoltaic multiple junction HgCdTe detector based on photoelectromagnetic effect in the semiconductor – spatial separation of optically generated electrons and holes in the magnetic field. This device is designed for the maximum performance at 10.6  $\mu\text{m}$  and especially useful as a large active area detector to detect CW and low frequency modulated radiation. This device is mounted in specialized package with incorporated magnetic circuit inside and SMA signal output connector. 3° wedged zinc selenide anti-reflection coated window prevents unwanted interference effects and protects against pollution.

#### Spectral response ( $T_a = 20^\circ\text{C}$ )



Exemplary spectral detectivity, the spectral response of delivered devices may differ.

#### Specification ( $T_a = 20^\circ\text{C}$ )

Parameter	Detector type
	PEM-10.6-2x2-PEM-SMA-wZnSeAR-48
Active element material	epitaxial HgCdTe heterostructure
Cut-on wavelength $\lambda_{\text{cut-on}}$ (10%), $\mu\text{m}$	$\leq 2.0$
Peak wavelength $\lambda_{\text{peak}}$ , $\mu\text{m}$	$8.5 \pm 1.5$
Optimum wavelength $\lambda_{\text{opt}}$ , $\mu\text{m}$	10.6
Cut-off wavelength $\lambda_{\text{cut-off}}$ (10%), $\mu\text{m}$	$\geq 12.0$
Detectivity $D^*(\lambda_{\text{peak}})$ , $\text{cm}\cdot\text{Hz}^{1/2}/\text{W}$	$\geq 2.0 \times 10^7$
Detectivity $D^*(\lambda_{\text{opt}})$ , $\text{cm}\cdot\text{Hz}^{1/2}/\text{W}$	$\geq 1.0 \times 10^7$
Current responsivity $R_i(\lambda_{\text{peak}})$ , A/W	$\geq 0.002$
Current responsivity $R_i(\lambda_{\text{opt}})$ , A/W	$\geq 0.001$
Time constant $\tau$ , ns	$\leq 1.2$
Resistance $R$ , $\Omega$	$\geq 40$
Active area $A$ , mm $\times$ mm	2x2
Package	PEM with SMA connector
Acceptance angle $\Phi$	$\sim 48^\circ$
Window	wedged zinc selenide AR coated (wZnSeAR)

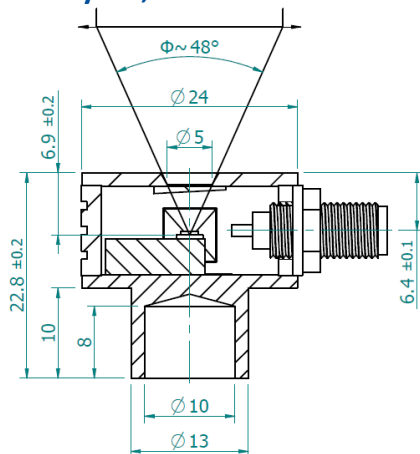
#### Features

- Wide spectral range from 2 to 12  $\mu\text{m}$
- Large active area 2x2 mm<sup>2</sup>
- Wide dynamic range
- No bias required
- No flicker noise
- Short time constant  $\leq 1.2$  ns
- Radiation polarisation sensitive
- Convenient to use
- Quantity discounted price
- Fast delivery

#### Applications

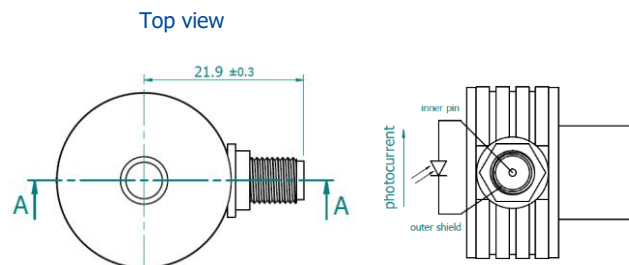
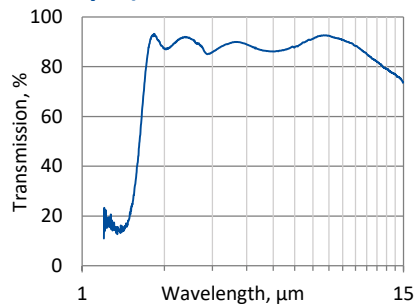
- CO<sub>2</sub> laser (10.6  $\mu\text{m}$ ) measurements
- Laser power monitoring and control
- Laser beam profiling and positioning
- Laser calibration

### Mechanical layout, mm



$\Phi$  – acceptance angle

### Spectral transmission of wZnSeAR window (typical example)



### Included accessories

- SMA-BNC cable

### Precautions for use and storage

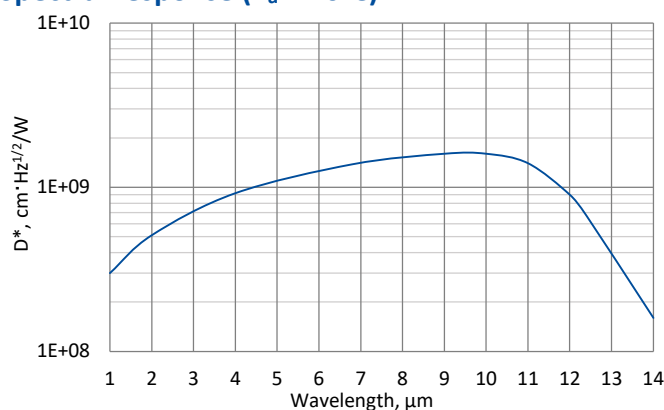
- Operation in 10% to 80% humidity and -20°C to 30°C ambient temperature.
- Beam power limitations:
  - irradiance with CW or single pulse longer than 1  $\mu$ s irradiance on the apparent optical active area must not exceed 100 W/cm<sup>2</sup>,
  - irradiance of the pulse shorter than 1  $\mu$ s must not exceed 1 MW/cm<sup>2</sup>.
- Storage in dark place with 10% to 90% humidity and -20°C to 50°C ambient temperature.

## PCI-3TE-12-1x1-TO8-wZnSeAR-36

### 2 – 14 μm HgCdTe three-stage thermoelectrically cooled, optically immersed photoconductive detector

**PCI-3TE-12-1x1-TO8-wZnSeAR-36** is a three-stage thermoelectrically cooled IR photoconductor, based on sophisticated HgCdTe heterostructure for the best performance and stability. The device is optimized for the maximum performance at 12 μm. Detector element is monolithically integrated with hyperhemispherical GaAs microlens in order to improve performance of the device. Photoconductive detector should operate in optimum bias voltage and current readout mode. Performance at low frequencies is reduced due to 1/f noise. 3° wedged zinc selenide anti-reflection coated (wZnSeAR) window prevents unwanted interference effects.

#### Spectral response ( $T_a = 20^\circ\text{C}$ )



Exemplary spectral detectivity, the spectral response of delivered devices may differ.

#### Specification ( $T_a = 20^\circ\text{C}$ )

Parameter	Detector type
	PCI-3TE-12-1x1-TO8-wZnSeAR-36
Active element material	epitaxial HgCdTe heterostructure
Cut-on wavelength $\lambda_{\text{cut-on}}$ (10%), μm	$\leq 2.0$
Peak wavelength $\lambda_{\text{peak}}$ , μm	$10.0 \pm 0.2$
Optimum wavelength $\lambda_{\text{opt}}$ , μm	12.0
Cut-off wavelength $\lambda_{\text{cut-off}}$ (10%), μm	$14.0 \pm 0.2$
Detectivity $D^*(\lambda_{\text{peak}})$ , $\text{cm}\cdot\text{Hz}^{1/2}/\text{W}$	$\geq 1.6 \times 10^9$
Detectivity $D^*(\lambda_{\text{opt}})$ , $\text{cm}\cdot\text{Hz}^{1/2}/\text{W}$	$\geq 9.0 \times 10^8$
Current responsivity $R_i(\lambda_{\text{peak}})$ , A/W	$\geq 0.11$
Current responsivity $R_i(\lambda_{\text{opt}})$ , A/W	$\geq 0.07$
Time constant $\tau$ , ns	$\leq 5$
Resistance $R$ , Ω	$\leq 300$
Bias voltage $V_b$ , V	$\leq 1.8$
1/f noise corner frequency $f_c$ , kHz	$\leq 20$
Active element temperature $T_{\text{det}}$ , K	$\sim 210$
Optical area $A_o$ , mm×mm	1×1
Package	TO8
Acceptance angle $\Phi$	$\sim 36^\circ$
Window	wZnSeAR

#### Features

- Wide spectral range from 1 to 14 μm
- High responsivity
- Large dynamic range
- Excellent long term stability and reliability
- Quantity discounted price
- Fast delivery

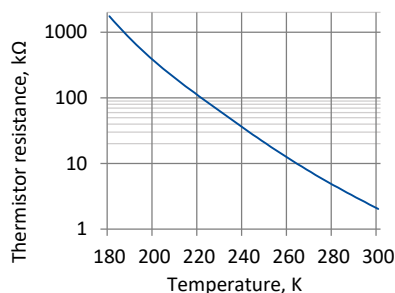
#### Applications

- FTIR spectroscopy and spectrometry

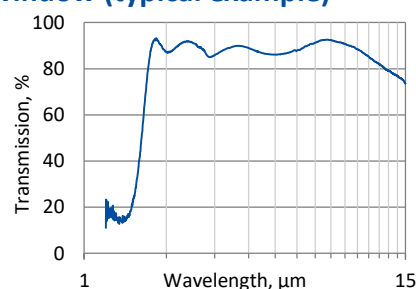
#### Three-stage thermoelectric cooler parameters

Parameter	Value
$T_{\text{det}}$ , K	$\sim 210$
$V_{\text{max}}$ , V	3.6
$I_{\text{max}}$ , A	0.45
$Q_{\text{max}}$ , W	0.27

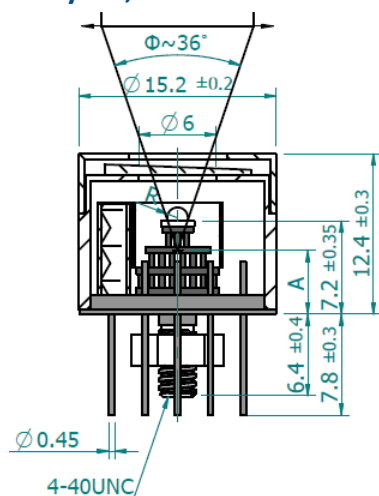
#### Thermistor characteristics



#### Spectral transmission of wZnSeAR window (typical example)

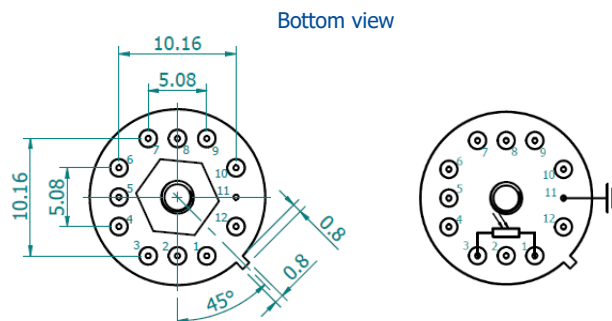


### Mechanical layout, mm



Parameter	Value
Immersion microlens shape	hyperhemisphere
Optical area $A_o$ , mm×mm	1×1
R, mm	0.8
A, mm	4.8±0.35

$\Phi$  – acceptance angle  
 R – hyperhemisphere microlens radius  
 A – distance from the bottom of the 3TE-TO8 header to the focal plane



Function	Pin number
Detector	1, 3
Thermistor	7, 9
TE cooler supply	2(+), 8(-)
Chassis ground	11
Not used	4, 5, 6, 10, 12

### Precautions for use and storage

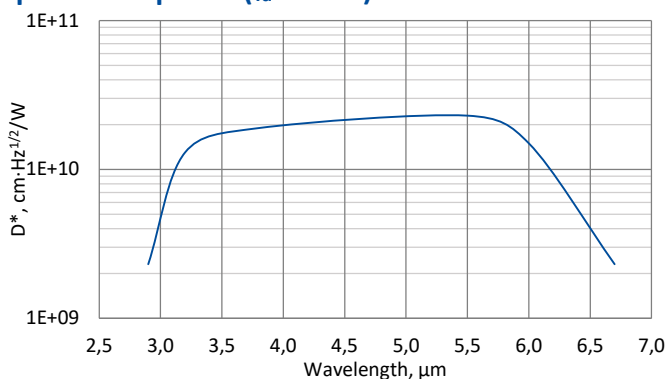
- Heatsink with thermal resistance of ~2 K/W is necessary to dissipate heat generated by 3TE cooler.
- Operation in 10% to 80% humidity and -20°C to 30°C ambient temperature.
- Beam power limitations for optically immersed detector:
  - irradiance with CW or single pulse longer than 1  $\mu$ s irradiance on the apparent optical active area must not exceed 2.5 W/cm<sup>2</sup>,
  - irradiance of the pulse shorter than 1  $\mu$ s must not exceed 10 kW/cm<sup>2</sup>.
- Storage in dark place with 10% to 90% humidity and -20°C to 50°C ambient temperature.

## UM-I-6

### 3.0 – 6.7 $\mu\text{m}$ and DC – 1 MHz HgCdTe universal IR detection module with optically immersed photovoltaic detector

**UM-I-6** is universal „all-in-one“ IR detection module. Thermoelectrically cooled, optically immersed photovoltaic detector, based on HgCdTe heterostructure, is integrated with transimpedance, DC coupled preamplifier, a fan and a thermoelectric cooler controller in a compact housing. 3° wedged zinc selenide anti-reflection coated window prevents unwanted interference effects. UM-I-6 detection module is very convenient and user-friendly device, thus can be easily used in a variety of MWIR applications.

#### Spectral response ( $T_a = 20^\circ\text{C}$ )



Exemplary spectral detectivity, the spectral response of delivered devices may differ.



#### Specification ( $T_a = 20^\circ\text{C}$ )

Parameter	Typical value
<b>Optical parameters</b>	
Cut-on wavelength $\lambda_{\text{cut-on}}$ (10%), $\mu\text{m}$	3.0 $\pm$ 1.0
Peak wavelength $\lambda_{\text{peak}}$ , $\mu\text{m}$	5.2 $\pm$ 0.5
Optimum wavelength $\lambda_{\text{opt}}$ , $\mu\text{m}$	6.0
Cut-off wavelength $\lambda_{\text{cut-off}}$ (10%), $\mu\text{m}$	6.7 $\pm$ 0.3
Detectivity $D^*(\lambda_{\text{peak}})$ , $\text{cm}\cdot\text{Hz}^{1/2}/\text{W}$	$\geq 2.3 \times 10^{10}$
Detectivity $D^*(\lambda_{\text{opt}})$ , $\text{cm}\cdot\text{Hz}^{1/2}/\text{W}$	$\geq 1.5 \times 10^{10}$
Output noise density $v_n$ (100 kHz), $\text{nV}/\text{Hz}^{1/2}$	$\leq 350$
<b>Electrical parameters</b>	
Voltage responsivity $R_v(\lambda_{\text{peak}})$ , $\text{V}/\text{W}$	$\geq 6.5 \times 10^4$
Voltage responsivity $R_v(\lambda_{\text{opt}})$ , $\text{V}/\text{W}$	$\geq 3.6 \times 10^4$
Low cut-off frequency $f_{\text{lo}}$ , $\text{Hz}$	DC
High cut-off frequency $f_{\text{hi}}$ , $\text{Hz}$	$\geq 1\text{M}$
Output impedance $R_{\text{out}}$ , $\Omega$	50
Output voltage swing $V_{\text{out}}$ , $\text{V}$	$\pm 2$ ( $R_L = 1 \text{ M}\Omega^*$ ) $\pm 1$ ( $R_L = 50 \Omega^*$ )
Output voltage offset $V_{\text{off}}$ , $\text{mV}$	max $\pm 20$
Power supply voltage $V_{\text{sup}}$ , $\text{V}$	+5
<b>DC monitor (approx. 0 V offset)</b>	
Voltage responsivity $R_v(\lambda_{\text{peak}})$ , $\text{V}/\text{W}$	$\geq 6.5 \times 10^3$
Voltage responsivity $R_v(\lambda_{\text{opt}})$ , $\text{V}/\text{W}$	$\geq 3.6 \times 10^3$
Low cut-off frequency $f_{\text{lo}}$ , $\text{Hz}$	DC
High cut-off frequency $f_{\text{hi}}$ , $\text{Hz}$	150k
<b>Other information</b>	
Active element material	epitaxial HgCdTe heterostructure
Optical area $A_o$ , $\text{mm}\times\text{mm}$	1 $\times$ 1
Window	wedged zinc selenide AR coated (wZnSeAR)
Acceptance angle $\Phi$	$\sim 36^\circ$
Ambient operating temperature $T_a$ , $^\circ\text{C}$	10 to 30
Signal output socket	SMA
DC monitor socket	SMA
Power supply socket	DC 2.5/5.5
Mounting hole	M4
Fan	yes

#### Features

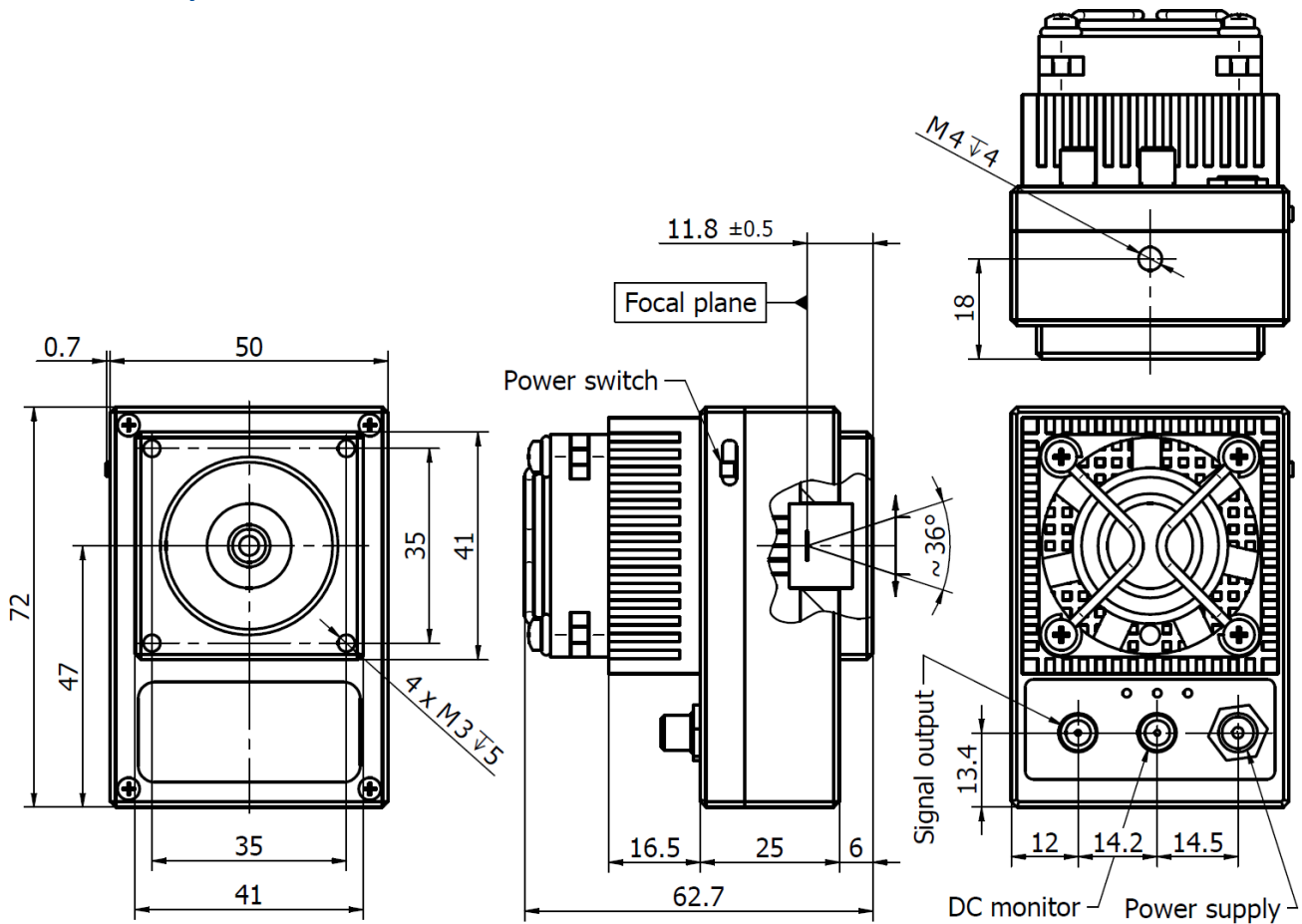
- Integrated TEC controller and fan
- Single power supply
- DC monitor
- Optimised for effective heat dissipation
- Compatible with optical accessories
- Cost effective OEM version available
- Universal and flexible
- Quantity discounted price
- Fast delivery

#### Applications

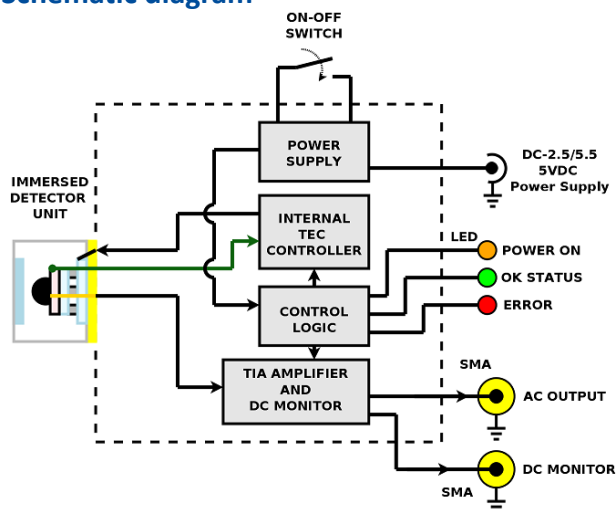
- Gas detection, monitoring and analysis ( $\text{CO}$ ,  $\text{CO}_2$ ,  $\text{NH}_3$ ,  $\text{NO}_x$ )
- Flue gas denitrification
- Fuel combustion monitoring at power plants and other industrial facilities
- Contactless temperature measurements

<sup>\*)</sup>  $R_L$  – load resistance

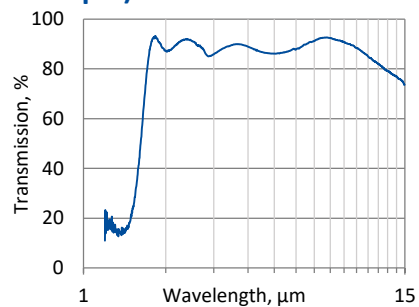
**Mechanical layout, mm**



**Schematic diagram**



**Spectral transmission of wZnSeAR window (typical example)**



**Included accessories**

- 2x SMA-BNC cables + AC adaptor

**Dedicated accessories**

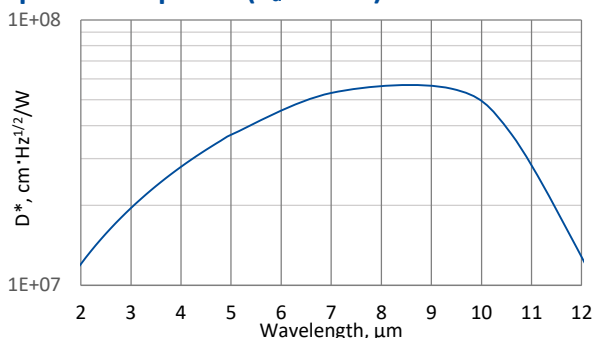
- [OTA](#) optical threaded adapter
- [DRB-2](#) base mounting system

## UM-10.6

### 2 – 12 μm and DC – 70 MHz HgCdTe universal IR detection module with photovoltaic multiple junction detector

**UM-10.6** is an universal „all-in-one“ IR detection module. Thermoelectrically cooled photovoltaic detector, based on HgCdTe heterostructure, is integrated with transimpedance, DC coupled preamplifier, a fan and a thermoelectric cooler controller in a compact housing. 3° wedged zinc selenide anti-reflection coated window prevents unwanted interference effects. UM-10.6 detection module is very convenient and user-friendly device, thus can be easily used in a variety of LWIR applications.

#### Spectral response ( $T_a = 20^\circ\text{C}$ )



Exemplary spectral detectivity, the spectral response of delivered devices may differ.



#### Specification ( $T_a = 20^\circ\text{C}$ )

Parameter	Typical value
<b>Optical parameters</b>	
Cut-on wavelength $\lambda_{\text{cut-on}}$ (10%), μm	≤2.0
Peak wavelength $\lambda_{\text{peak}}$ , μm	9.3±2.0
Optimum wavelength $\lambda_{\text{opt}}$ , μm	10.6
Cut-off wavelength $\lambda_{\text{cut-off}}$ (10%), μm	≥12.0
Detectivity $D^*(\lambda_{\text{peak}})$ , cm·Hz <sup>1/2</sup> /W	≥5.0×10 <sup>7</sup>
Detectivity $D^*(\lambda_{\text{opt}})$ , cm·Hz <sup>1/2</sup> /W	≥4.0×10 <sup>7</sup>
Output noise density $v_n$ (averaged over 1 MHz to $f_{\text{hi}}$ ), nV/Hz <sup>1/2</sup>	≤380
<b>Electrical parameters</b>	
Voltage responsivity $R_v(\lambda_{\text{peak}})$ , V/W	≥1.6×10 <sup>2</sup>
Voltage responsivity $R_v(\lambda_{\text{opt}})$ , V/W	≥1.0×10 <sup>2</sup>
Low cut-off frequency $f_{\text{lo}}$ , Hz	DC
High cut-off frequency $f_{\text{hi}}$ , Hz	≥70M
Output impedance $R_{\text{out}}$ , Ω	50
Output voltage swing $V_{\text{out}}$ , V	±2 ( $R_L = 1 \text{ M}\Omega^*)$ )
Output voltage offset $V_{\text{off}}$ , mV	max ±20
Power supply voltage $V_{\text{sup}}$ , V	+5
<b>DC monitor (approx. 0 V offset)</b>	
Voltage responsivity $R_v(\lambda_{\text{peak}})$ , V/W	≥3.6×10 <sup>1</sup>
Voltage responsivity $R_v(\lambda_{\text{opt}})$ , V/W	≥2.4×10 <sup>1</sup>
Low cut-off frequency $f_{\text{lo}}$ , Hz	DC
High cut-off frequency $f_{\text{hi}}$ , Hz	150k
<b>Other information</b>	
Active element material	epitaxial HgCdTe heterostructure
Active area $A$ , mm×mm	1×1
Window	wedged zinc selenide AR coated (wZnSeAR)
Acceptance angle $\Phi$	~70°
Ambient operating temperature $T_a$ , °C	10 to 30
Signal output socket	SMA
DC monitor socket	SMA
Power supply socket	DC 2.5/5.5
Mounting hole	M4
Fan	yes

\*<sup>1</sup>)  $R_L$  – load resistance

#### Features

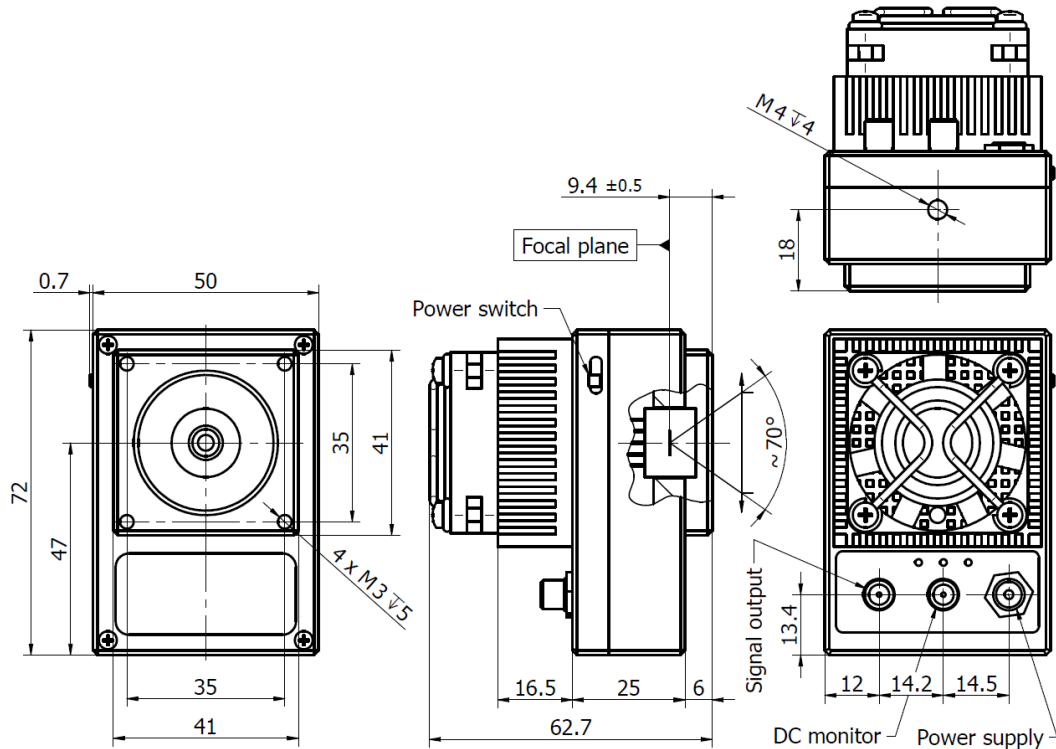
- Integrated TEC controller and fan
- Single power supply
- DC monitor
- Sensitive to IR radiation polarisation
- Optimised for effective heat dissipation
- Compatible with optical accessories
- Cost effective OEM version available
- Universal and flexible
- Quantity discounted price
- Fast delivery

#### Applications

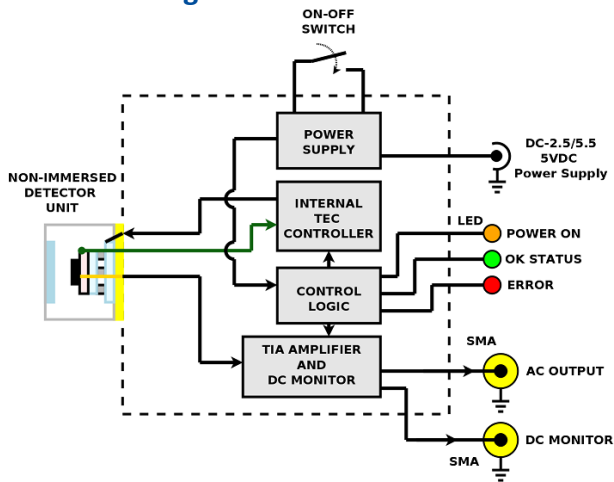
- Gas detection, monitoring and analysis
- CO<sub>2</sub> laser (10.6 μm) measurements
- Laser power monitoring and control
- Laser beam profiling and positioning
- Laser calibration



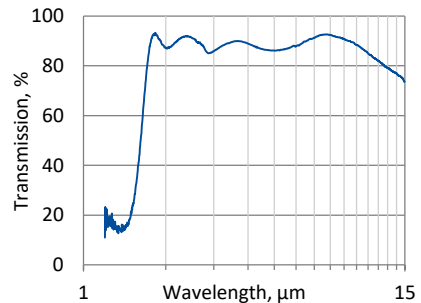
**Mechanical layout, mm**



**Schematic diagram**



**Spectral transmission of wZnSeAR window (typical example)**



**Included accessories**

- 2x SMA-BNC cables + AC adaptor

**Dedicated accessories**

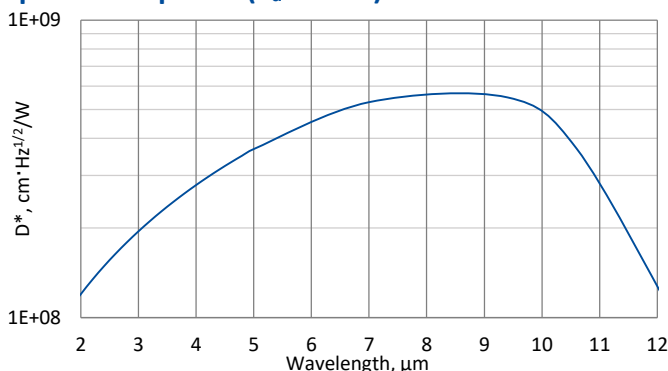
- [OTA](#) optical threaded adapter
- [DRB-2](#) base mounting system

## UM-I-10.6

### 2 – 12 μm and DC – 100 MHz HgCdTe universal IR detection module with optically immersed photovoltaic multiple junction detector

**UM-I-10.6** is universal „all-in-one“ IR detection module. Thermoelectrically cooled, optically immersed photovoltaic detector, based on HgCdTe heterostructure, is integrated with transimpedance, DC coupled preamplifier, a fan and a thermoelectric cooler controller in a compact housing. 3° wedged zinc selenide anti-reflection coated window prevents unwanted interference effects. UM-I-10.6 detection module is very convenient and user-friendly device, thus can be easily used in a variety of LWIR applications.

#### Spectral response ( $T_a = 20^\circ\text{C}$ )



Exemplary spectral detectivity, the spectral response of delivered devices may differ.



#### Specification ( $T_a = 20^\circ\text{C}$ )

Parameter	Typical value
<b>Optical characteristics</b>	
Cut-on wavelength $\lambda_{\text{cut-on}}$ (10%), μm	≤2.0
Peak wavelength $\lambda_{\text{peak}}$ , μm	8.5±1.5
Optimum wavelength $\lambda_{\text{opt}}$ , μm	10.6
Cut-off wavelength $\lambda_{\text{cut-off}}$ (10%), μm	≥12.0
Detectivity $D^*(\lambda_{\text{peak}})$ , $\text{cm}\cdot\text{Hz}^{1/2}/\text{W}$	≥5.5×10 <sup>8</sup>
Detectivity $D^*(\lambda_{\text{opt}})$ , $\text{cm}\cdot\text{Hz}^{1/2}/\text{W}$	≥3.7×10 <sup>8</sup>
Output noise density $v_n$ (averaged over 1 MHz to $f_{\text{hi}}$ ), $\text{nV}/\text{Hz}^{1/2}$	≤330
<b>Electrical parameters</b>	
Voltage responsivity $R_v(\lambda_{\text{peak}})$ , V/W	≥9.7×10 <sup>2</sup>
Voltage responsivity $R_v(\lambda_{\text{opt}})$ , V/W	≥6.5×10 <sup>2</sup>
Low cut-off frequency $f_{\text{lo}}$ , Hz	DC
High cut-off frequency $f_{\text{hi}}$ , Hz	≥100M
Output impedance $R_{\text{out}}$ , Ω	50
Output voltage swing $V_{\text{out}}$ , V	±1 ( $R_L = 50 \Omega^*$ )
Output voltage offset $V_{\text{off}}$ , mV	max ±20
Power supply voltage $V_{\text{sup}}$ , V	+5
<b>DC monitor (approx. 0 V offset)</b>	
Voltage responsivity $R_v(\lambda_{\text{peak}})$ , V/W	≥2.2×10 <sup>2</sup>
Voltage responsivity $R_v(\lambda_{\text{opt}})$ , V/W	≥1.5×10 <sup>2</sup>
Low cut-off frequency $f_{\text{lo}}$ , Hz	DC
High cut-off frequency $f_{\text{hi}}$ , Hz	150k
<b>Other information</b>	
Active element material	epitaxial HgCdTe heterostructure
Optical area $A_o$ , mm×mm	1×1
Window	wedged zinc selenide AR coated (wZnSeAR)
Acceptance angle $\Phi$	~36°
Ambient operating temperature $T_a$ , °C	10 to 30
Signal output socket	SMA
DC monitor socket	SMA
Power supply socket	DC 2.5/5.5
Mounting hole	M4
Fan	yes

#### Features

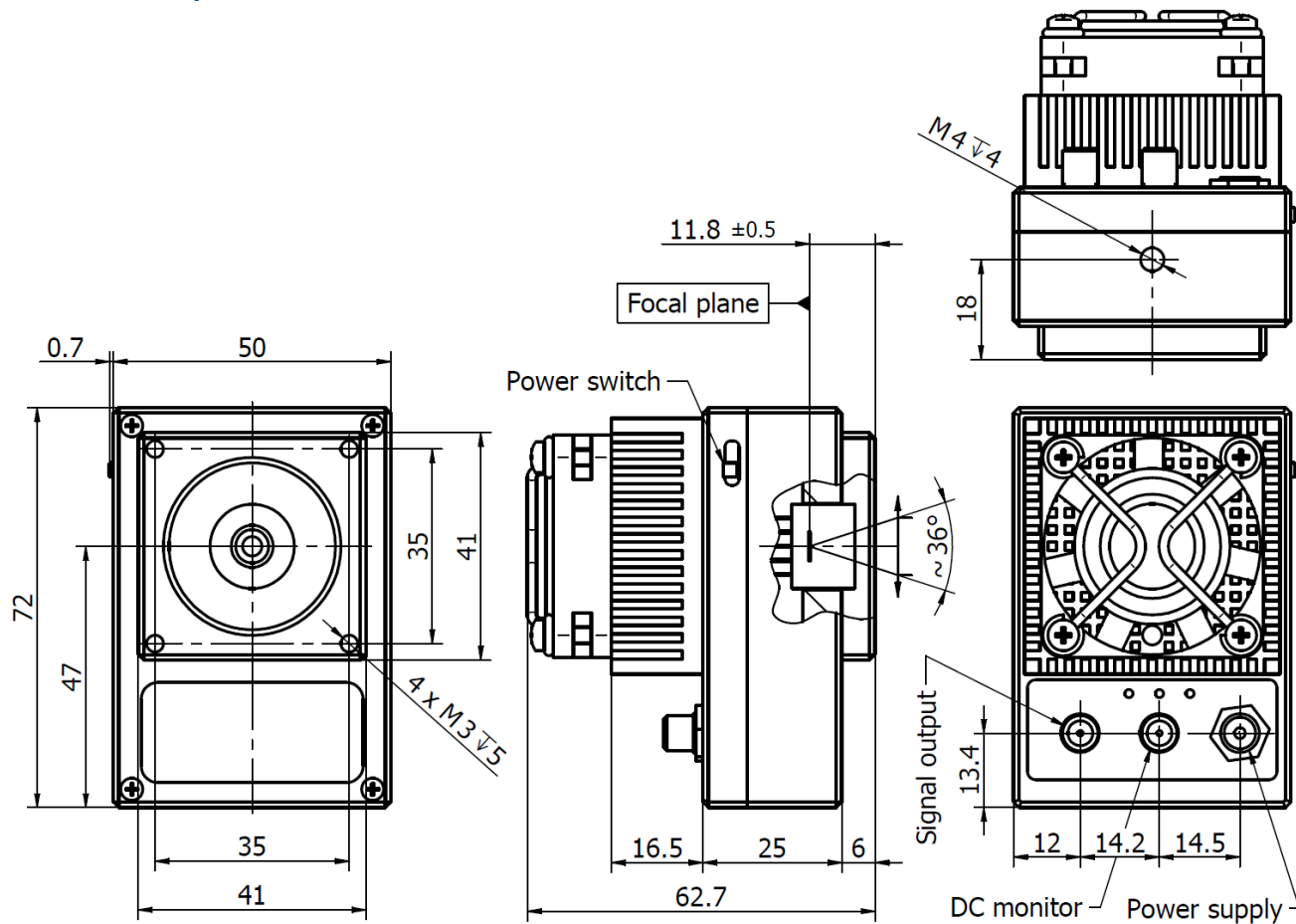
- Integrated TEC controller and fan
- Single power supply
- DC monitor
- Sensitive to IR radiation polarisation
- Optimised for effective heat dissipation
- Compatible with optical accessories
- Cost effective OEM version available
- Universal and flexible
- Quantity discounted price
- Fast delivery

#### Applications

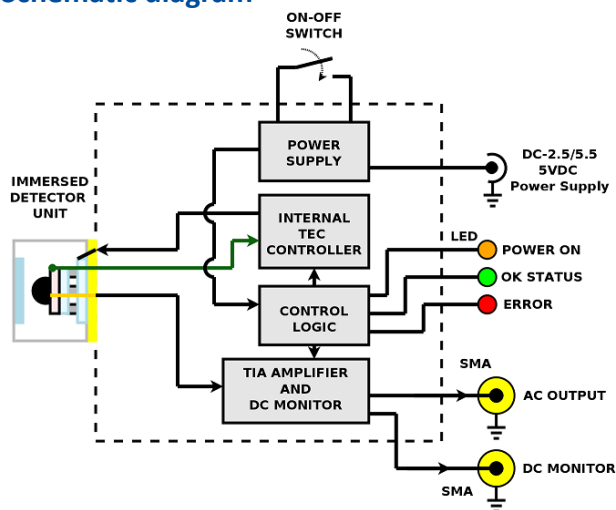
- Gas detection, monitoring and analysis
- CO<sub>2</sub> laser (10.6 μm) measurements
- Laser power monitoring and control
- Laser beam profiling and positioning
- Laser calibration

\* )  $R_L$  – load resistance

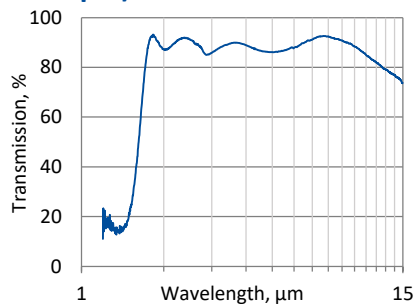
**Mechanical layout, mm**



**Schematic diagram**



**Spectral transmission of wZnSeAR window (typical example)**



**Included accessories**

- 2x SMA-BNC cables + AC adaptor

**Dedicated accessories**

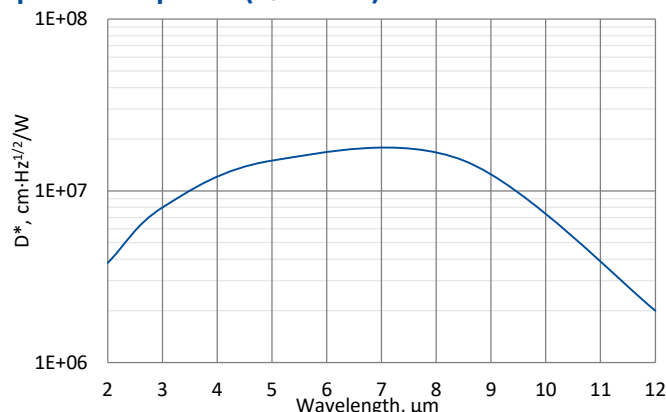
- [OTA](#) optical threaded adapter
- [DRB-2](#) base mounting system

## microM-10.6

### 2 – 12 μm and DC – 10 MHz HgCdTe micro-size IR detection module with photovoltaic multiple junction detector

**microM-10.6** is a micro-size IR detection module. Uncooled photovoltaic multiple junction detector, based on HgCdTe heterostructure, is integrated with transimpedance, DC coupled preamplifier. It is easy to assembly in space limited measuring systems of LWIR applications.

#### Spectral response ( $T_a = 20^\circ\text{C}$ )



Exemplary spectral detectivity, the spectral response of delivered devices may differ.

#### Specification ( $T_a = 20^\circ\text{C}$ )

Parameter	Typical value
<b>Optical parameters</b>	
Cut-on wavelength $\lambda_{\text{cut-on}}$ (10%), μm	≤2.0
Peak wavelength $\lambda_{\text{peak}}$ , μm	8.0±1.5
Optimum wavelength $\lambda_{\text{opt}}$ , μm	10.6
Cut-off wavelength $\lambda_{\text{cut-off}}$ (10%), μm	≥12.0
Detectivity $D^*(\lambda_{\text{peak}})$ , cm·Hz <sup>1/2</sup> /W	≥1.5×10 <sup>7</sup>
Detectivity $D^*(\lambda_{\text{opt}})$ , cm·Hz <sup>1/2</sup> /W	≥5.0×10 <sup>6</sup>
Output noise density $v_n$ (100 kHz), μV/Hz <sup>1/2</sup>	≤1
<b>Electrical parameters</b>	
Voltage responsivity $R_v$ ( $\lambda_{\text{peak}}$ ), V/W	≥1.2×10 <sup>2</sup>
Voltage responsivity $R_v$ ( $\lambda_{\text{opt}}$ ), V/W	≥5.0×10 <sup>1</sup>
Low cut-off frequency $f_{\text{lo}}$ , Hz	DC
High cut-off frequency $f_{\text{hi}}$ , Hz	≥10M
Output impedance $R_{\text{out}}$ , Ω	50
Output voltage swing $V_{\text{out}}$ , V	±1 ( $R_L = 50 \Omega^*$ )
Output voltage offset $V_{\text{off}}$ , mV	max ±20
Power supply voltage $V_{\text{sup}}$ , V	+9
<b>Other information</b>	
Active element material	epitaxial HgCdTe heterostructure
Active area A, mm×mm	1×1
Window	none
Acceptance angle $\Phi$	~85°
Ambient operating temperature $T_a$ , °C	10 to 30
Signal output plug	SMA
Power supply plug	03T-JWPF-VSLE-S (male)
Mounting hole	none
Fan	none

\*<sup>1</sup>)  $R_L$  – load resistance

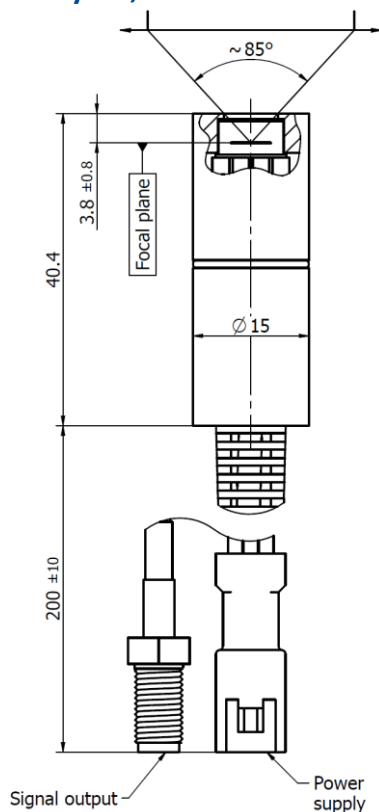
#### Features

- Very small size
- Convenient to use
- Versatility
- Sensitive to IR radiation polarisation
- Cost effective OEM version available
- Quantity discounted price
- Fast delivery

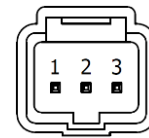
#### Applications

- Gas detection, monitoring and analysis
- CO<sub>2</sub> laser (10.6 μm) measurements
- Laser power monitoring and control
- Laser beam profiling and positioning
- Laser calibration

### Mechanical layout, mm

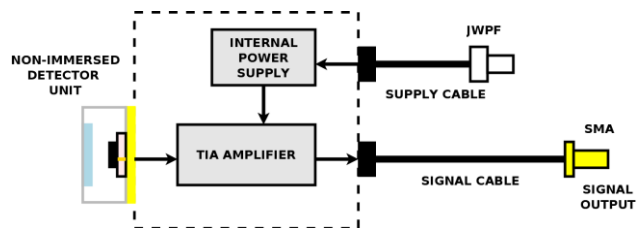


### Power supply plug 03T-JWPF-VSLE-S (male)



Function	Symbol	Pin number
Power supply input (-)	$-V_{sup}$	1
Ground	GND	2
Power supply input (+)	$+V_{sup}$	3

### Schematic diagram



### Included accessories

- SMA-BNC, JWPF-DB9 cables

### Dedicated accessories

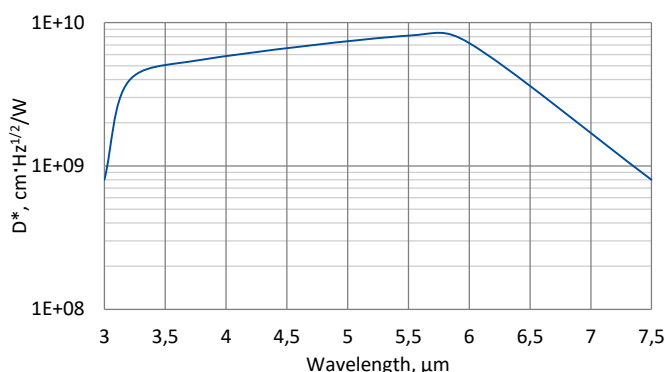
- [PPS-03](#) preamplifier power supply + AC adaptor
- [MH-1](#) module's holder
- [DRB-2](#) base mounting system

## LabM-I-6

### 3.0 – 7.5 $\mu\text{m}$ and over 200 MHz HgCdTe programmable, laboratory IR detection module with optically immersed photovoltaic detector

**LabM-I-6** is a laboratory IR detection module with optically immersed photovoltaic detector based on HgCdTe heterostructure, integrated with transimpedance, programmable preamplifier. 3° wedged zinc selenide anti-reflection coated window prevents unwanted interference effects. For proper operation programmable „smart“ VIGO thermoelectric cooler controller PTCC-01 (sold separately) and Smart Manager Software (freeware) are required. LabM-I-6 module comes complete with PTCC-01 and Smart Manager is the best solution for prototyping and R&D stage in a variety of MWIR applications. This set provides flexible approach to different needs of system designers.

#### Spectral response ( $T_a = 20^\circ\text{C}$ )



Exemplary spectral detectivity, the spectral response of delivered devices may differ.



#### Specification ( $T_a = 20^\circ\text{C}$ , default module settings)

Parameter	Typical value
<b>Optical parameters</b>	
Cut-on wavelength $\lambda_{\text{cut-on}}$ (10%), $\mu\text{m}$	$3.0 \pm 1.0$
Peak wavelength $\lambda_{\text{peak}}$ , $\mu\text{m}$	$5.5 \pm 0.5$
Optimum wavelength $\lambda_{\text{opt}}$ , $\mu\text{m}$	6.0
Cut-off wavelength $\lambda_{\text{cut-off}}$ (10%), $\mu\text{m}$	$7.5 \pm 0.5$
Detectivity $D^*(\lambda_{\text{peak}})$ , $\text{cm}\cdot\text{Hz}^{1/2}/\text{W}$	$\geq 8.1 \times 10^9$
Detectivity $D^*(\lambda_{\text{opt}})$ , $\text{cm}\cdot\text{Hz}^{1/2}/\text{W}$	$\geq 7.2 \times 10^9$
Output noise density $v_n$ (10 MHz), $\text{nV}/\text{Hz}^{1/2}$	$\leq 350$
<b>Electrical parameters</b>	
Voltage responsivity $R_v(\lambda_{\text{peak}})$ , $\text{V}/\text{W}$	$\geq 2.3 \times 10^4$
Voltage responsivity $R_v(\lambda_{\text{opt}})$ , $\text{V}/\text{W}$	$\geq 2.0 \times 10^4$
Low cut-off frequency $f_{\text{lo}}$ , Hz	10
High cut-off frequency $f_{\text{hi}}$ , Hz	$\geq 200\text{M}$ (adjustable)
Output impedance $R_{\text{out}}$ , $\Omega$	50
Output voltage swing $V_{\text{out}}$ , V	$\pm 1$ ( $R_L = 1 \text{ M}\Omega^*)$ )
Output voltage offset $V_{\text{off}}$ , mV	max $\pm 20$
<b>Other information</b>	
Active element material	epitaxial HgCdTe heterostructure
Optical area $A_o$ , $\text{mm}\times\text{mm}$	1x1
Window	wedged zinc selenide AR coated (wZnSeAR)
Acceptance angle $\Phi$	$\sim 36^\circ$
Ambient operating temperature $T_a$ , $^\circ\text{C}$	10 to 30
Signal output socket	SMA
Power supply and TEC control socket	LEMO (female) ECG.0B.309.CLN
Mounting hole	M4
Fan	yes

<sup>\*)</sup>  $R_L$  – load resistance

#### Features

- Very high performance and reliability
- DC offset compensation
- Compatible with optical accessories
- Versatility and flexibility
- Quantity discounted price
- Fast delivery

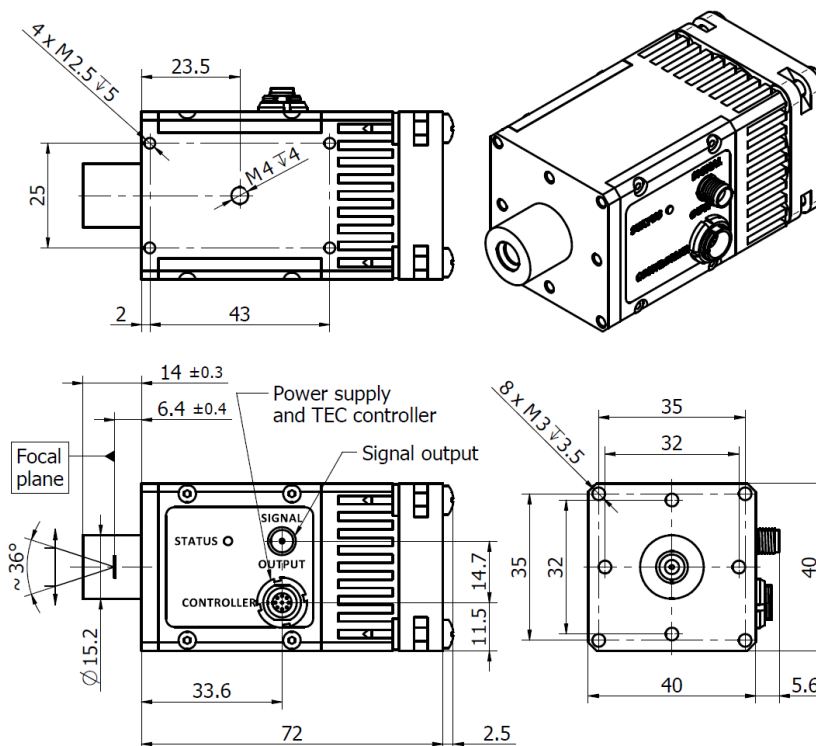
#### Parameters configurable by the user

- Output voltage offset
- Gain (in 40 dB range)
- Bandwidth (1.5 MHz/15 MHz/200 MHz)
- Coupling AC/DC
- Detector's parameters (temperature, reverse bias etc.)

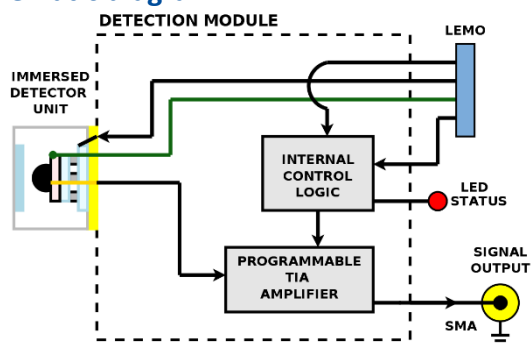
#### Applications

- MWIR gas detection, monitoring and analysis
- Flue gas denitrification
- Fuel combustion monitoring at power plants and other industrial facilities
- Breath analysis
- Explosion prevention
- Emission control (exhaust fumes, greenhouse gases)
- Contactless temperature measurements

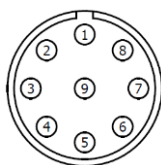
### Mechanical layout, mm



### Schematic diagram

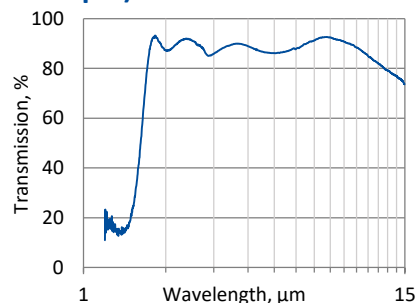


### Power supply and TEC control socket LEMO (female) ECG.0B.309.CLN



Function	Symbol	Pin number
Fan and programmable preamp internal logic auxiliary supply	FAN+	1
Thermistor output (2)	TH2	2
TEC supply input (-)	TEC-	3
Power supply input (-)	-V <sub>sup</sub>	4
Ground	GND	5
Power supply input (+)	+V <sub>sup</sub>	6
TEC supply input (+)	TEC+	7
Thermistor output (1)	TH1	8
Bidirectional data pin	DATA	9

### Spectral transmission of wZnSeAR window (typical example)



### Included accessories

- SMA-BNC, LEMO-DB9 cables

### Dedicated accessories

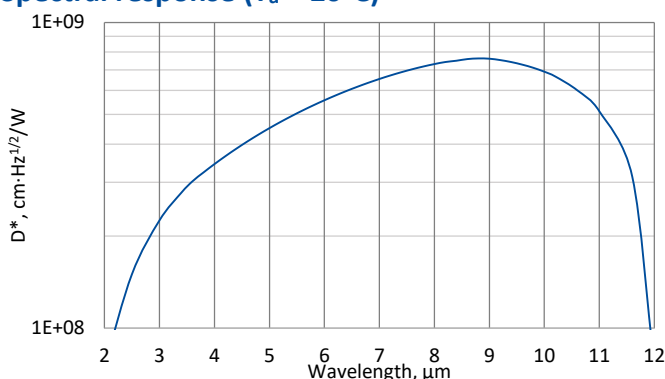
- [PTCC-01-BAS](#) TEC controller + **USB: TypeA-MicroB** cable + **AC adaptor**
- [PTCC-01-ADV](#) TEC controller + **USB: TypeA-MicroB** cable + **AC adaptor**
- [PTCC-01-OEM](#) TEC controller + **USB: TypeA-MicroB**, **KK2-POWER** cables
- [OTA](#) optical threaded adapter
- [DRB-2](#) base mounting system

## LabM-I-10.6

### 2 – 12 $\mu\text{m}$ and DC – 100 MHz HgCdTe programmable, laboratory IR detection module with optically immersed photovoltaic detector

**LabM-I-10.6** is a laboratory IR detection module with optically immersed photovoltaic detector based on HgCdTe heterostructure, integrated with transimpedance, programmable preamplifier. 3° wedged zinc selenide anti-reflection coated window prevents unwanted interference effects. For proper operation programmable „smart“ VIGO thermoelectric cooler controller PTCC-01 (sold separately) and Smart Manager Software (freeware) are required. LabM-I-10.6 module comes complete with PTCC-01 and Smart Manager is the best solution for prototyping and R&D stage in a variety of LWIR applications. This set provides flexible approach to different needs of system designers.

#### Spectral response ( $T_a = 20^\circ\text{C}$ )



Exemplary spectral detectivity, the spectral response of delivered devices may differ.



#### Specification ( $T_a = 20^\circ\text{C}$ , default module settings)

Parameter	Typical value
<b>Optical parameters</b>	
Cut-on wavelength $\lambda_{\text{cut-on}}$ (10%), $\mu\text{m}$	$\leq 2.0$
Peak wavelength $\lambda_{\text{peak}}$ , $\mu\text{m}$	$9.5 \pm 0.5$
Optimum wavelength $\lambda_{\text{opt}}$ , $\mu\text{m}$	10.6
Cut-off wavelength $\lambda_{\text{cut-off}}$ (10%), $\mu\text{m}$	$\geq 12.0$
Detectivity $D^*(\lambda_{\text{peak}})$ , $\text{cm}\cdot\text{Hz}^{1/2}/\text{W}$	$\geq 7.2 \times 10^8$
Detectivity $D^*(\lambda_{\text{opt}})$ , $\text{cm}\cdot\text{Hz}^{1/2}/\text{W}$	$\geq 6.0 \times 10^8$
Output noise density $v_n(10 \text{ MHz})$ , $\text{nV}/\text{Hz}^{1/2}$	$\leq 400$
<b>Electrical parameters</b>	
Voltage responsivity $R_v(\lambda_{\text{peak}})$ , $\text{V}/\text{W}$	$\geq 2.4 \times 10^3$
Voltage responsivity $R_v(\lambda_{\text{opt}})$ , $\text{V}/\text{W}$	$\geq 2.0 \times 10^3$
Low cut-off frequency $f_{\text{lo}}$ , $\text{Hz}$	DC
High cut-off frequency $f_{\text{hi}}$ , $\text{Hz}$	$\geq 100\text{M}$ (adjustable)
Output impedance $R_{\text{out}}$ , $\Omega$	50
Output voltage swing $V_{\text{out}}$ , $\text{V}$	$\pm 1$ ( $R_L = 1 \text{ M}\Omega^*)$ )
Output voltage offset $V_{\text{off}}$ , $\text{mV}$	max $\pm 20$
<b>Other information</b>	
Active element material	epitaxial HgCdTe heterostructure
Optical area $A_o$ , $\text{mm}\times\text{mm}$	1x1
Window	wedged zinc selenide AR coated (wZnSeAR)
Acceptance angle $\Phi$	$\sim 36^\circ$
Ambient operating temperature $T_a$ , $^\circ\text{C}$	10 to 30
Signal output socket	SMA
Power supply and TEC control socket	LEMO (female) ECG.0B.309.CLN
Mounting hole	M4
Fan	yes

\* $\text{)} R_L$  – load resistance

#### Features

- Very high performance and reliability
- DC offset compensation
- Sensitive to IR radiation polarisation
- Compatible with optical accessories
- Versatility and flexibility
- Quantity discounted price
- Fast delivery

#### Parameters configurable by the user

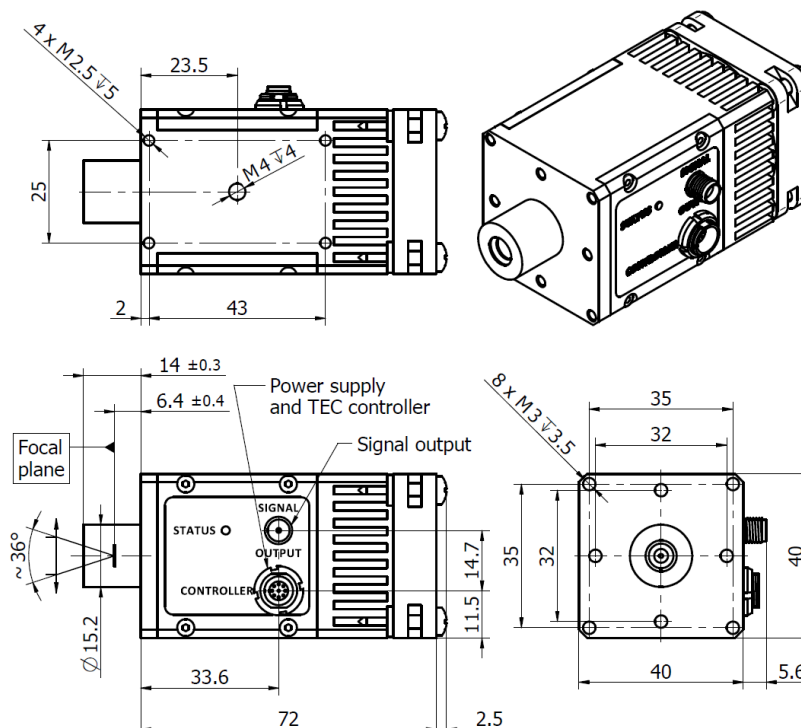
- Output voltage offset
- Gain (in 40 dB range)
- Bandwidth (1.5 MHz/15 MHz/100 MHz)
- Coupling AC/DC
- Detector's parameters (temperature, reverse bias etc.)

#### Applications

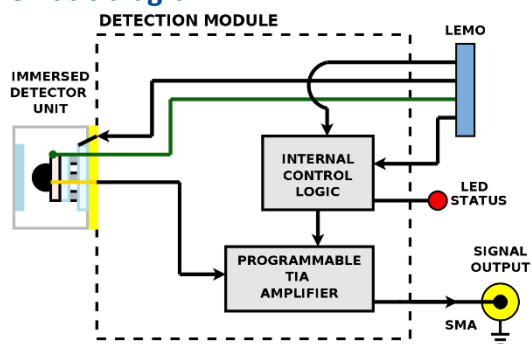
- Gas detection, monitoring and analysis
- $\text{CO}_2$  laser (10.6  $\mu\text{m}$ ) measurements
- Laser power monitoring and control
- Laser beam profiling and positioning
- Laser calibration
- Semiconductor manufacturing
- Glucose monitoring
- Dentistry



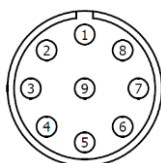
### Mechanical layout, mm



### Schematic diagram

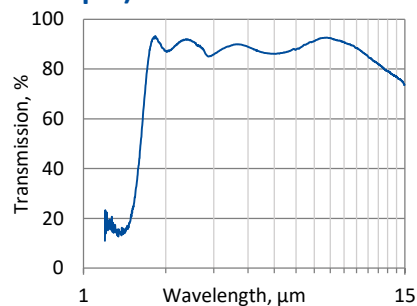


### Power supply and TEC control socket LEMO (female) ECG.0B.309.CLN



Function	Symbol	Pin number
Fan and programmable preamp internal logic auxiliary supply	FAN+	1
Thermistor output (2)	TH2	2
TEC supply input (-)	TEC-	3
Power supply input (-)	-V <sub>sup</sub>	4
Ground	GND	5
Power supply input (+)	+V <sub>sup</sub>	6
TEC supply input (+)	TEC+	7
Thermistor output (1)	TH1	8
Bidirectional data pin	DATA	9

### Spectral transmission of wZnSeAR window (typical example)



### Included accessories

- SMA-BNC, LEMO-DB9 cables

### Dedicated accessories

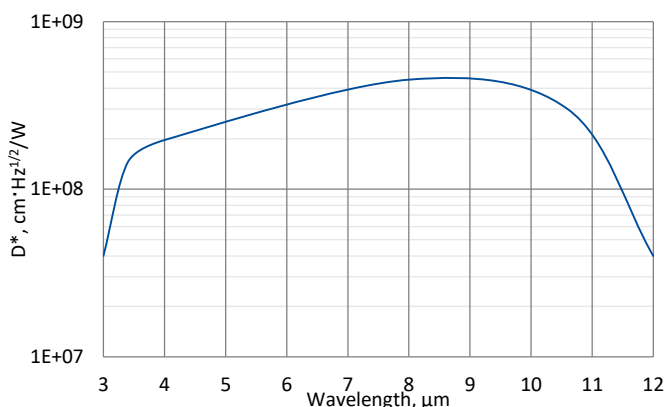
- **PTCC-01-BAS** TEC controller + **USB: TypeA-MicroB** cable + **AC adaptor**
- **PTCC-01-ADV** TEC controller + **USB: TypeA-MicroB** cable + **AC adaptor**
- **PTCC-01-OEM** TEC controller + **USB: TypeA-MicroB**, **KK2-POWER** cables
- **OTA** optical threaded adapter
- **DRB-2** base mounting system

## UHSM-10.6

### 3 – 12 $\mu\text{m}$ and over 1GHz HgCdTe ultra high speed IR detection module with photovoltaic detector

**UHSM-10.6** is ultra high speed „all-in-one“ IR detection module. Thermoelectrically cooled, photovoltaic detector, based on HgCdTe heterostructure, is integrated with transimpedance, AC coupled preamplifier, a fan and a thermoelectric cooler controller in a compact housing.  $3^\circ$  wedged zinc selenide anti-reflection coated (wZnSeAR) window prevents unwanted interference effects. UHSM-10.6 detection module is very convenient and user-friendly device, thus can be easily used in a variety of LWIR applications requiring wide frequency bandwidth.

#### Spectral response ( $T_a = 20^\circ\text{C}$ )



Exemplary spectral detectivity, the spectral response of delivered devices may differ.



#### Specification ( $T_a = 20^\circ\text{C}$ )

Parameter	Typical value
<b>Optical parameters</b>	
Cut-on wavelength $\lambda_{\text{cut-on}}$ (10%), $\mu\text{m}$	$\leq 3.0$
Peak wavelength $\lambda_{\text{peak}}$ , $\mu\text{m}$	$8.0 \pm 1.0$
Optimum wavelength $\lambda_{\text{opt}}$ , $\mu\text{m}$	10.6
Cut-off wavelength $\lambda_{\text{cut-off}}$ (10%), $\mu\text{m}$	$\geq 12.0$
Detectivity $D^*(\lambda_{\text{peak}}, 100 \text{ MHz})$ , $\text{cm}\cdot\text{Hz}^{1/2}/\text{W}$	$\geq 4.5 \times 10^8$
Detectivity $D^*(\lambda_{\text{opt}}, 100 \text{ MHz})$ , $\text{cm}\cdot\text{Hz}^{1/2}/\text{W}$	$\geq 3.0 \times 10^8$
Output noise density $v_n(100 \text{ MHz})$ , $\text{nV}/\text{Hz}^{1/2}$	$\leq 70$
<b>Electrical parameters (<math>R_L = 50 \Omega^*)</math></b>	
Voltage responsivity $R_v(\lambda_{\text{peak}})$ , $\text{V}/\text{W}$	$\geq 4.5 \times 10^3$
Voltage responsivity $R_v(\lambda_{\text{opt}})$ , $\text{V}/\text{W}$	$\geq 3.0 \times 10^3$
Low cut-off frequency $f_{\text{lo}}$ , $\text{Hz}$	300
High cut-off frequency $f_{\text{hi}}$ , $\text{Hz}$	$\geq 1.0\text{G}$
Output voltage swing $V_{\text{out}}$ , $\text{V}$	$\pm 1$
1/f noise corner frequency $f_c$ , $\text{Hz}$	$\leq 10\text{M}$
Power supply voltage $V_{\text{sup}}$ , $\text{V}$	+9
<b>DC monitor (approx. 1 V offset, <math>R_L = 100 \text{ k}\Omega^*)</math></b>	
Voltage responsivity $R_v(\lambda_{\text{peak}})$ , $\text{V}/\text{W}$	$\geq 1.7 \times 10^3$
Voltage responsivity $R_v(\lambda_{\text{opt}})$ , $\text{V}/\text{W}$	$\geq 1.1 \times 10^3$
Low cut-off frequency $f_{\text{lo}}$ , $\text{Hz}$	DC
High cut-off frequency $f_{\text{hi}}$ , $\text{Hz}$	260
<b>Other information</b>	
Active element material	epitaxial HgCdTe heterostructure
Active area $A$ , $\text{mm}\times\text{mm}$	0.05 $\times$ 0.05
Window	wZnSeAR
Acceptance angle $\Phi$	$\sim 80^\circ$
Ambient operating temperature $T_a$ , $^\circ\text{C}$	10 to 30
Signal output socket (RF output)	SMA
DC monitor socket	SMA
Power supply socket	DC 2.1/5.5
Mounting hole	M4
Fan	yes

<sup>\*)</sup>  $R_L$  – load resistance

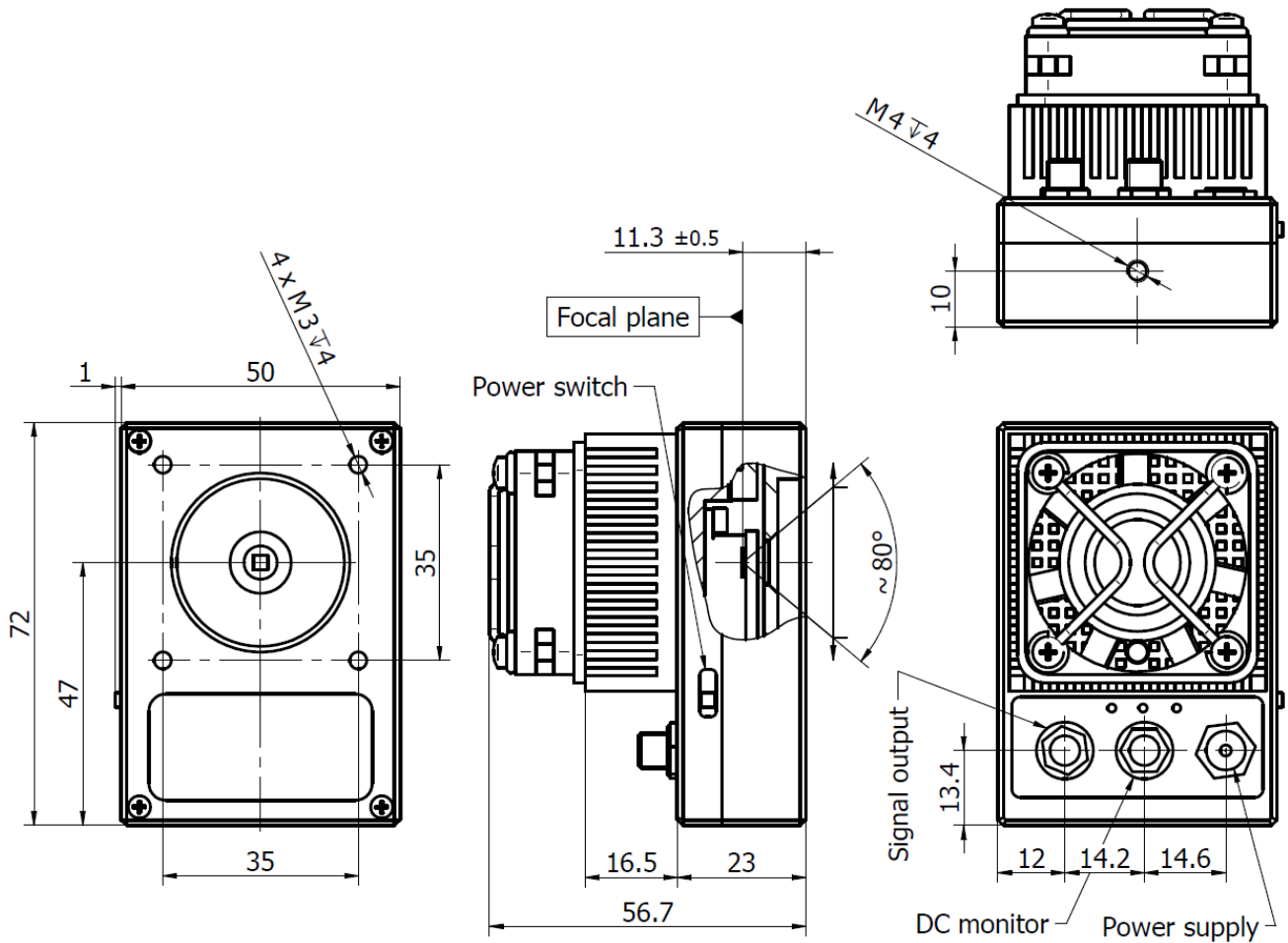
#### Features

- Wide frequency bandwidth over 1 GHz
- Integrated TEC controller and fan
- Single power supply
- DC monitor
- Optimised for effective heat dissipation
- Compatible with optical accessories
- Fast delivery

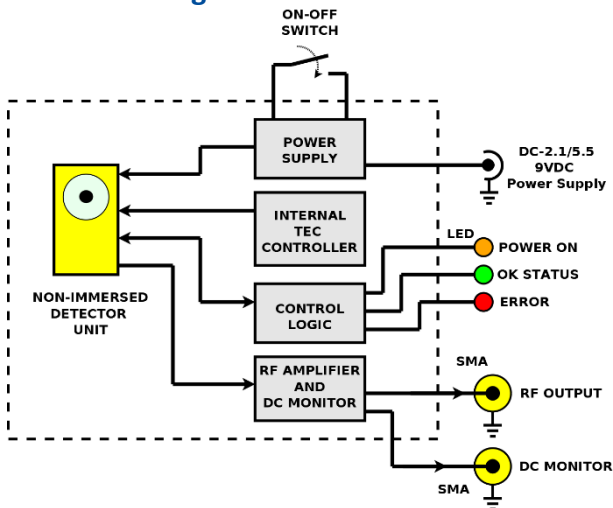
#### Applications

- Dual-comb spectroscopy
- Heterodyne detection
- Characterization of pulsed laser sources
- LIDAR
- Object scanners
- Time-resolved fluorescence spectroscopy systems
- Free-space optical communication

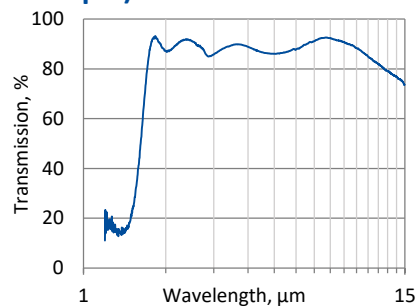
**Mechanical layout, mm**



**Schematic diagram**



**Spectral transmission of wZnSeAR window (typical example)**



**Included accessories**

- 2xSMA-BNC cables + AC adaptor

**Dedicated accessories**

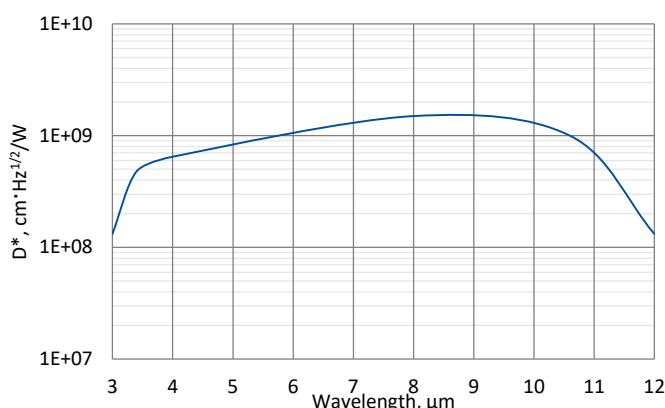
- [OTA](#) optical threaded adapter
- [DRB-2](#) base mounting system

## UHSM-I-10.6

### 3 – 12 $\mu\text{m}$ and over 700 MHz HgCdTe ultra high speed IR detection module with optically immersed photovoltaic detector

**UHSM-I-10.6** is ultra high speed „all-on-one“ IR detection module. Thermoelectrically cooled, optically immersed photovoltaic detector, based on HgCdTe heterostructure, is integrated with transimpedance, AC coupled preamplifier, a fan and a thermoelectric cooler controller in a compact housing.  $3^\circ$  wedged zinc selenide anti-reflection coated (wZnSeAR) window prevents unwanted interference effects. UHSM-I-10.6 detection module is very convenient and user-friendly device, thus can be easily used in a variety of LWIR applications requiring wide frequency bandwidth.

#### Spectral response ( $T_a = 20^\circ\text{C}$ )



Exemplary spectral detectivity, the spectral response of delivered devices may differ.



#### Specification ( $T_a = 20^\circ\text{C}$ )

Parameter	Typical value
<b>Optical parameters</b>	
Cut-on wavelength $\lambda_{\text{cut-on}}$ (10%), $\mu\text{m}$	$\leq 3.0$
Peak wavelength $\lambda_{\text{peak}}$ , $\mu\text{m}$	$8.5 \pm 0.5$
Optimum wavelength $\lambda_{\text{opt}}$ , $\mu\text{m}$	10.6
Cut-off wavelength $\lambda_{\text{cut-off}}$ (10%), $\mu\text{m}$	$12.5 \pm 0.3$
Detectivity $D^*(\lambda_{\text{peak}}, 100 \text{ MHz})$ , $\text{cm}\cdot\text{Hz}^{1/2}/\text{W}$	$\geq 1.5 \times 10^9$
Detectivity $D^*(\lambda_{\text{opt}}, 100 \text{ MHz})$ , $\text{cm}\cdot\text{Hz}^{1/2}/\text{W}$	$\geq 1.0 \times 10^9$
Output noise density $v_n(100 \text{ MHz})$ , $\text{nV}/\text{Hz}^{1/2}$	$\leq 90$
<b>Electrical parameters (<math>R_L = 50 \Omega</math>)</b>	
Voltage responsivity $R_v(\lambda_{\text{peak}})$ , $\text{V}/\text{W}$	$\geq 1.0 \times 10^3$
Voltage responsivity $R_v(\lambda_{\text{opt}})$ , $\text{V}/\text{W}$	$\geq 7.0 \times 10^2$
Low cut-off frequency $f_{\text{lo}}$ , $\text{Hz}$	300
High cut-off frequency $f_{\text{hi}}$ , $\text{Hz}$	$\geq 700\text{M}$
1/f noise corner frequency $f_c$ , $\text{Hz}$	$\leq 10\text{M}$
Power supply voltage $V_{\text{SUP}}$ , $\text{V}$	+9
<b>DC monitor (approx. 1 V offset, <math>R_L = 1 \text{ M}\Omega</math>)</b>	
Voltage responsivity $R_v(\lambda_{\text{peak}})$ , $\text{V}/\text{W}$	$\geq 3.8 \times 10^3$
Voltage responsivity $R_v(\lambda_{\text{opt}})$ , $\text{V}/\text{W}$	$\geq 2.7 \times 10^2$
Low cut-off frequency $f_{\text{lo}}$ , $\text{Hz}$	DC
High cut-off frequency $f_{\text{hi}}$ , $\text{Hz}$	260
<b>Other information</b>	
Active element material	epitaxial HgCdTe heterostructure
Optical area $A_o$ , $\text{mm}\times\text{mm}$	1x1
Window	wZnSeAR
Acceptance angle $\Phi$	$\sim 36^\circ$
Ambient operating temperature $T_a$ , $^\circ\text{C}$	10 to 30
Signal output socket (RF output)	SMA
DC monitor socket	SMA
Power supply socket	DC 2.1/5.5
Mounting hole	M4
Fan	yes

<sup>\*)</sup>  $R_L$  – load resistance

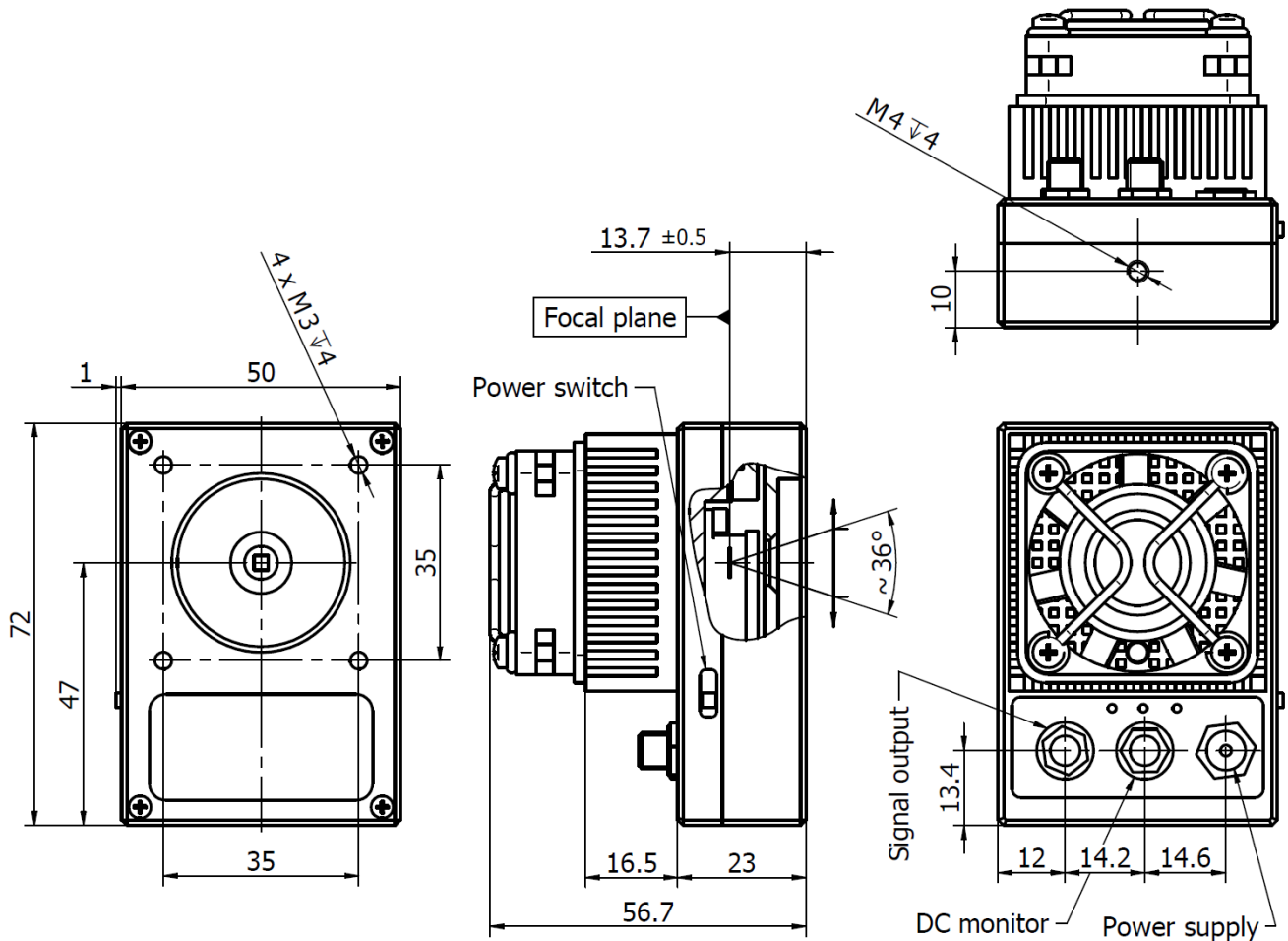
#### Features

- High S/N ratio
- Wide frequency bandwidth over 700 MHz
- Integrated TEC controller and fan
- Single power supply
- DC monitor
- Optimised for effective heat dissipation
- Compatible with optical accessories
- Fast delivery

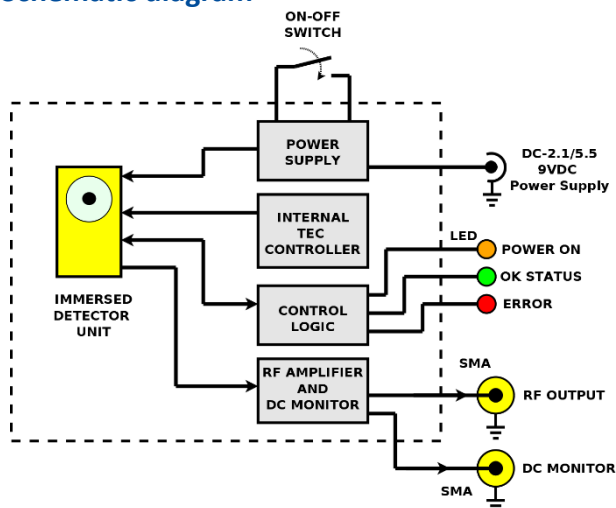
#### Applications

- Dual-comb spectroscopy
- Heterodyne detection
- Characterization of pulsed laser sources
- LIDAR
- Object scanners
- Time-resolved fluorescence spectroscopy systems
- Free-space optical communication
- Telemetry

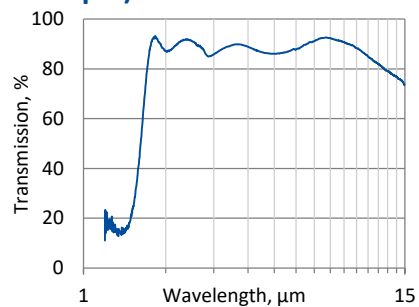
**Mechanical layout, mm**



**Schematic diagram**



**Spectral transmission of wZnSeAR window (typical example)**



**Included accessories**

- 2x SMA-BNC cables + AC adaptor

**Dedicated accessories**

- [OTA](#) optical threaded adapter
- [DRB-2](#) base mounting system

---

# INFRARED DETECTORS AND DETECTION MODULES – OPTIONAL

VIGO offers various types of infrared detectors based on Mercury Cadmium Telluride, Indium Arsenide and Indium Arsenide Antimonide featuring different parameters.

## Main features

- Optimized at any wavelength from 2 – 14  $\mu\text{m}$  spectral range
- With or without immersion technology
- Uncooled or thermoelectrically cooled
- Different sizes of active/optical area
- Different packages
- Different infrared windows
- Different acceptance angle
- Wide range of dedicated preamplifiers and accessories

## How to choose and infrared detector?

For making a detector selection, following points should be taken into consideration:

- wavelength or wavelength range,
- detectivity,
- speed of response.

VIGO detectors are optimized for various wavelengths. Depending on the required parameters a proper detector type should be selected.

Detector series	Spectral response range, $\mu\text{m}$															Features
	2	3	4	5	6	7	8	9	10	11	12	13	14	15	16	
<a href="#">HgCdTe (MCT) photoconductive detectors</a>																<ul style="list-style-type: none"> <li>▪ Broad 1 – 16 <math>\mu\text{m}</math> spectral range</li> <li>▪ Active area from <math>25 \times 25 \mu\text{m}^2</math> to <math>4 \times 4 \text{mm}^2</math></li> <li>▪ High detectivity</li> <li>▪ Low speed</li> <li>▪ Long lifetime and MTBF</li> <li>▪ Stability and reliability</li> <li>▪ 1/f noise</li> <li>▪ Uncooled and TE cooled</li> <li>▪ Immersion microlens technology available</li> </ul>
<a href="#">HgCdTe (MCT) photovoltaic detectors</a>																<ul style="list-style-type: none"> <li>▪ Near BLIP detection in 3 – 6 <math>\mu\text{m}</math> range</li> <li>▪ &lt; 10x gap to BLIP for <math>\lambda &gt; 7 \mu\text{m}</math></li> <li>▪ No bias required</li> <li>▪ No 1/f noise</li> <li>▪ Bandwidth: <ul style="list-style-type: none"> <li>tens of MHz (without reverse bias)</li> <li><math>\geq 1\text{GHz}</math> (with reverse bias)</li> </ul> </li> <li>▪ LWIR devices limited to small areas</li> <li>▪ Uncooled and TE cooled</li> <li>▪ Immersion microlens technology available</li> </ul>
<a href="#">HgCdTe (MCT) photovoltaic multiple junction detectors</a>																<ul style="list-style-type: none"> <li>▪ Wide 2 – 12 <math>\mu\text{m}</math> spectral range</li> <li>▪ Large active areas up to <math>4 \times 4 \text{mm}^2</math></li> <li>▪ No bias required</li> <li>▪ No 1/f noise</li> <li>▪ Short time constant <math>\leq 1.5 \text{ns}</math></li> <li>▪ Operation from DC to high frequency</li> <li>▪ Sensitive to IR radiation polarisation</li> <li>▪ Uncooled and TE cooled</li> <li>▪ Immersion microlens technology available</li> </ul>
<a href="#">HgCdTe (MCT) photoelectromagnetic detectors</a>																<ul style="list-style-type: none"> <li>▪ Wide 2 – 12 <math>\mu\text{m}</math> spectral range</li> <li>▪ Room temperature operation</li> <li>▪ No bias required</li> <li>▪ No 1/f noise</li> <li>▪ Large active area up to <math>2 \times 2 \text{mm}^2</math></li> <li>▪ Short time constant <math>\leq 1.2 \text{ns}</math></li> <li>▪ Sensitive to IR radiation polarisation</li> <li>▪ Immersion microlens technology available</li> </ul>
<a href="#">InAs and InAsSb photovoltaic detectors</a>																<ul style="list-style-type: none"> <li>▪ Spectral range 2 – 5.5 <math>\mu\text{m}</math></li> <li>▪ Temperature stable up to <math>300^\circ\text{C}</math></li> <li>▪ Mechanically durable</li> <li>▪ Complying with the RoHS Directive</li> <li>▪ No bias required</li> <li>▪ No 1/f noise</li> <li>▪ Sensitive to IR radiation polarisation</li> <li>▪ Uncooled and TE cooled</li> <li>▪ Immersion microlens technology available</li> </ul>

### Detector code

Different information such as detector type, optical immersion, number of stages thermoelectric cooler, the wavelength a detector is optimized for, size of active/optical area, package type, window type and acceptance angle combine to create VIGO System's detector code.

Detector type	Immersion	–	Cooling	–	Optimal wavelength	–	Active/optical area	–	Package	–	Window	–	Acceptance angle
---------------	-----------	---	---------	---	--------------------	---	---------------------	---	---------	---	--------	---	------------------

Please see particular detector series datasheets to get available options of each detector type.

## How to choose a preamplifier?



Infrared detection module integrates infrared photodetector and preamplifier in a common package.

The integration makes detectors less vulnerable to:

- over-bias,
- electrostatic discharges,
- electromagnetic interferences,
- other environmental exposures.

Additional advantages of integration are: improved high-frequency performance, output signal standardization, miniaturization and cost reduction.

The broad line of transimpedance preamplifiers is especially designed for integration with VIGO IR detectors.

Main feature	Photo	Preamplifier type	Detector type	Low cut-on frequency $f_{lo}$ , Hz	High cut-off frequency $f_{hi}$ , Hz	Transimpedance $K_i$ , V/A	Radiator / fan	TEC controller	Mounting hole
all-in-one		<a href="#">AIP</a>	TE cooled PC/ PCI TE cooled PV/PVI TE cooled PVA/PVIA TE cooled PVM/PVMI	DC, 10, 100, 1k, 10k	100k, 1M, 10M, 100M, 250M	up to 200k (fixed)	on board	on board	M4
programmable		<a href="#">PIP</a>	TE cooled PC/ PC TE cooled PV/PVI TE cooled PVA/PVIA TE cooled PVM/PVMI	DC/10 (digitally adjustable)	150k/1.5M/20M 1.5M/15M/200M (digitally adjustable)	2.5k – 150k 0.5k – 30k (digitally adjustable)	on board	PTCC-01 obligatory	M4
standard		<a href="#">MIP</a>	TE cooled PC/ PC TE cooled PV/PVI TE cooled PVA/PVIA TE cooled PVM/PVMI	DC, 10, 100, 1k, 10k	100k, 1M, 10M, 100M, 250M	up to 200k (fixed)	on board	PTCC-01 necessary	M4
fast		<a href="#">FIP</a>	TE cooled PV/PVI	1k, 10k	1G	up to 8.5k (fixed)	on board	PTCC-01 necessary	M4
small		<a href="#">SIP-TO8</a>	TE cooled PC/ PC TE cooled PV/PVI TE cooled PVA/PVIA TE cooled PVM/PVMI	DC, 10, 100, 1k, 10k	100k, 1M, 10M, 100M, 250M	up to 100k (tunable)	external heatsink necessary	PTCC-01 necessary	none
small		<a href="#">SIP-TO39</a>	uncooled PC/ PCI uncooled PV/PVI uncooled PVA/PVIA uncooled PVM/PVMI	DC, 10, 100, 1k, 10k	100k, 1M, 10M, 100M, 250M	up to 100k (tunable)	not necessary	not necessary	none

To obtain the most optimal parameters of integrated module each preamplifier is individually matched to the selected detector. The parameters of integrated set will be known after final evaluation (matching, adjustment and final tests).

If you need any assistance in selecting VIGO product appropriate for your application, please contact **VIGO Technical Support Team:** [techsupport@vigo.com.pl](mailto:techsupport@vigo.com.pl)

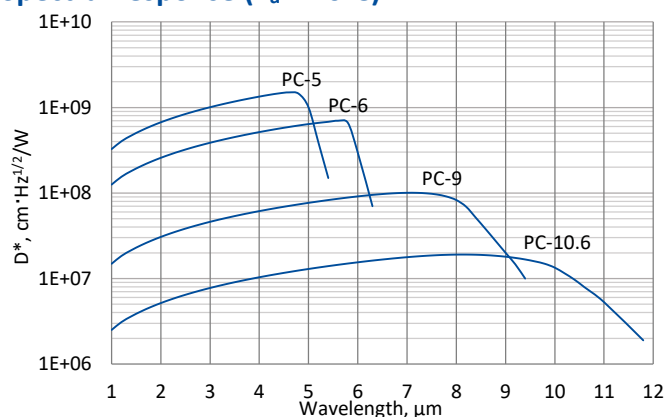


## PC series

### 1 – 12 $\mu\text{m}$ HgCdTe ambient temperature photoconductive detectors

**PC series** features uncooled IR photoconductive detectors based on sophisticated HgCdTe heterostructures for the best performance and stability. The devices are optimized for the maximum performance at  $\lambda_{\text{opt}}$ . The devices should operate in optimum bias voltage and current readout mode. Performance at low frequencies is reduced due to 1/f noise. The 1/f noise corner frequency increases with the cut-off wavelength.

#### Spectral response ( $T_a = 20^\circ\text{C}$ )



Exemplary spectral detectivity, the spectral response of delivered devices may differ.

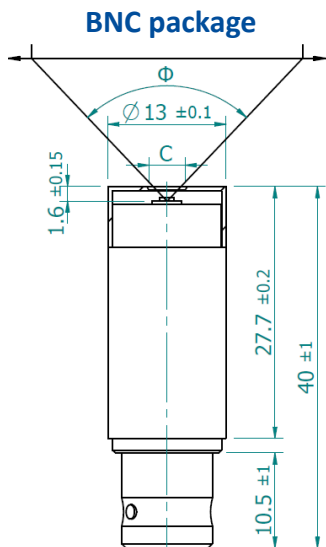
#### Specification ( $T_a = 20^\circ\text{C}$ )

Parameter	Detector type			
	PC-5	PC-6	PC-9	PC-10.6
Active element material	epitaxial HgCdTe heterostructure			
Optimal wavelength $\lambda_{\text{opt}}$ , $\mu\text{m}$	5.0	6.0	9.0	10.6
Detectivity $D^*(\lambda_{\text{peak}}, 20\text{kHz})$ , $\text{cm}\cdot\text{Hz}^{1/2}/\text{W}$	$\geq 1.5 \times 10^9$	$\geq 7.0 \times 10^8$	$\geq 1.0 \times 10^8$	$\geq 1.9 \times 10^7$
Detectivity $D^*(\lambda_{\text{opt}}, 20\text{kHz})$ , $\text{cm}\cdot\text{Hz}^{1/2}/\text{W}$	$\geq 1.0 \times 10^9$	$\geq 3.0 \times 10^8$	$\geq 2.0 \times 10^7$	$\geq 9.0 \times 10^6$
Current responsivity-active area length product $R_i(\lambda_{\text{opt}}) \cdot L$ , $\text{A}\cdot\text{mm}/\text{W}$	$\geq 0.07$	$\geq 0.02$	$\geq 0.003$	$\geq 0.001$
Time constant $\tau$ , ns	$\leq 5000$	$\leq 500$	$\leq 10$	$\leq 3$
1/f noise corner frequency $f_c$ , Hz		$\leq 10\text{k}$		$\leq 20\text{k}$
Bias voltage-active area length ratio $V_b/L$ , V/mm	$\leq 4.5$	$\leq 4.0$	$\leq 3.6$	$\leq 3.0$
Resistance $R$ , $\Omega$	$\leq 1200$	$\leq 600$	$\leq 300$	$\leq 120$
Active area $A$ , $\text{mm}\times\text{mm}$	0.05×0.05, 0.1×0.1, 0.25×0.25, 0.5×0.5, 1×1, 2×2, 3×3, 4×4			
Package	TO39 BNC	TO39 BNC	TO39 BNC	TO39 BNC
Acceptance angle $\Phi$	$\sim 90^\circ$	$\sim 90^\circ$	$\sim 90^\circ$	$\sim 90^\circ$
Window	none			

\*) Aperture C =  $\varnothing 4$  mm.

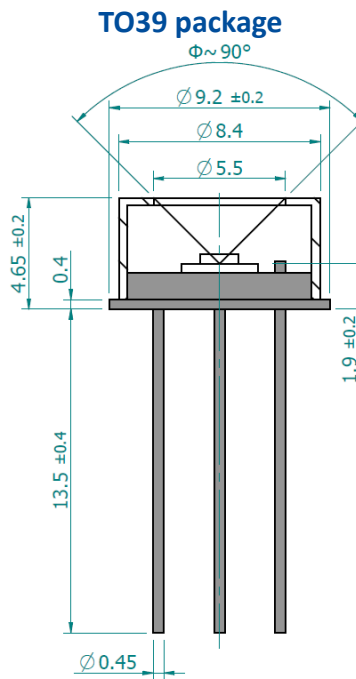
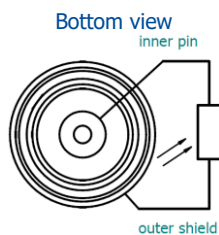
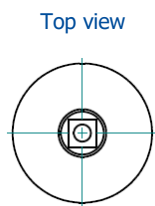
\*\*) Aperture C =  $\varnothing 6$  mm.

**Mechanical layout, mm**

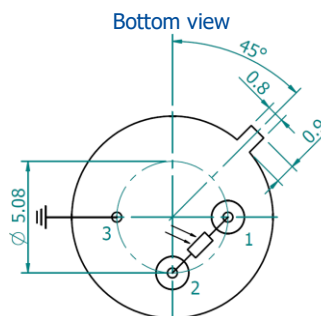


Parameter	Value
Active area, mm×mm	0.05×0.05 – 2×2 3×3 – 4×4
C, mm	Ø4 Ø6
Acceptance angle $\Phi$	~102° ~124°

C – aperture



$\Phi$  – acceptance angle



Function	Pin number
Detector	1, 2
Chassis ground	3

**Dedicated preamplifier**



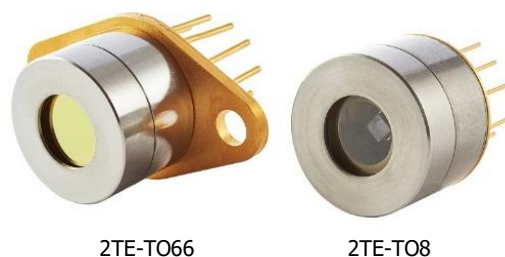
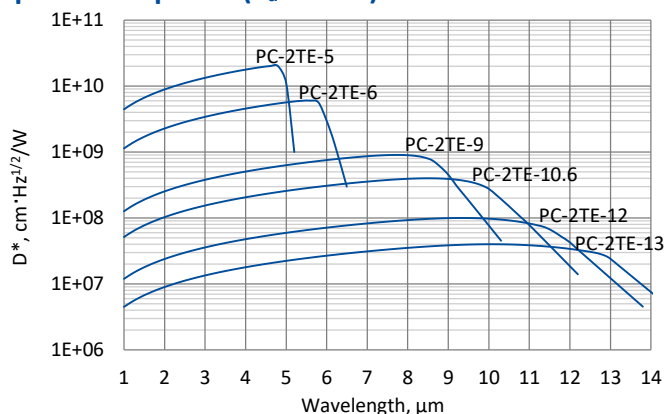
small SIP-TO39

## PC-2TE series

### 1 – 14 $\mu\text{m}$ HgCdTe two-stage thermoelectrically cooled photoconductive detectors

**PC-2TE series** features two-stage thermoelectrically cooled IR photoconductive detectors based on sophisticated HgCdTe heterostructures for the best performance and stability. The devices are optimized for the maximum performance at  $\lambda_{\text{opt}}$ . The devices should operate in optimum bias voltage and current readout mode. Performance at low frequencies is reduced due to 1/f noise. The 1/f noise corner frequency increases with the cut-off wavelength. 3° wedged sapphire (wAl<sub>2</sub>O<sub>3</sub>) or zinc selenide anti-reflection coated (wZnSeAR) window prevents unwanted interference effects.

#### Spectral response ( $T_a = 20^\circ\text{C}$ )



Exemplary spectral detectivity, the spectral response of delivered devices may differ.

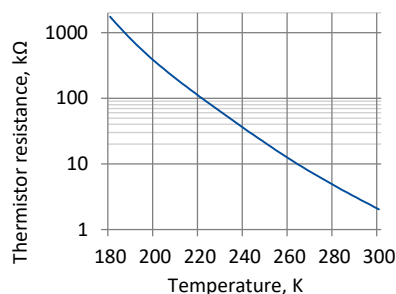
#### Specification ( $T_a = 20^\circ\text{C}$ )

Parameter	Detector type					
	PC-2TE-5	PC-2TE-6	PC-2TE-9	PC-2TE-10.6	PC-2TE-12	PC-2TE-13
Active element material	epitaxial HgCdTe heterostructure					
Optimal wavelength $\lambda_{\text{opt}}$ , $\mu\text{m}$	5.0	6.0	9.0	10.6	12.0	13.0
Detectivity $D^*(\lambda_{\text{opt}}, 20\text{kHz})$ , $\text{cm}\cdot\text{Hz}^{1/2}/\text{W}$	$\geq 1.0 \times 10^{10}$	$\geq 3.0 \times 10^9$	$\geq 4.5 \times 10^8$	$\geq 1.4 \times 10^8$	$\geq 4.5 \times 10^7$	$\geq 2.3 \times 10^7$
Detectivity $D^*(\lambda_{\text{peak}}, 20\text{kHz})$ , $\text{cm}\cdot\text{Hz}^{1/2}/\text{W}$	$\geq 2.0 \times 10^{10}$	$\geq 6.0 \times 10^9$	$\geq 9.0 \times 10^8$	$\geq 4.0 \times 10^8$	$\geq 1.0 \times 10^8$	$\geq 4.0 \times 10^7$
Current responsivity-active area length product $R_i(\lambda_{\text{opt}}) \cdot L$ , $\text{A}\cdot\text{mm}/\text{W}$	$\geq 0.5$	$\geq 0.18$	$\geq 0.025$	$\geq 0.01$	$\geq 0.005$	$\geq 0.002$
Time constant $\tau$ , ns	$\leq 20000$	$\leq 4000$	$\leq 40$	$\leq 10$	$\leq 3$	$\leq 2$
1/f noise corner frequency $f_c$ , Hz		$\leq 10\text{k}$			$\leq 20\text{k}$	
Bias voltage-active area length ratio $V_b/L$ , V/mm	$\leq 2.0$	$\leq 3.2$	$\leq 2.0$	$\leq 2.25$	$\leq 1.5$	$\leq 1.8$
Resistance $R$ , $\Omega$	$\leq 1200$	$\leq 800$	$\leq 400$	$\leq 300$	$\leq 200$	$\leq 150$
Active element temperature $T_{\text{det}}$ , K	$\sim 230$					
Active area $A$ , $\text{mm}\times\text{mm}$	0.05 $\times$ 0.05, 0.1 $\times$ 0.1, 0.25 $\times$ 0.25, 0.5 $\times$ 0.5, 1 $\times$ 1, 2 $\times$ 2					
Package	TO8, TO66					
Acceptance angle $\Phi$	$\sim 70^\circ$					
Window	wAl <sub>2</sub> O <sub>3</sub>			wZnSeAR		

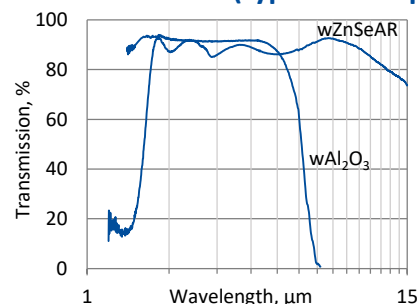
#### Two-stage thermoelectric cooler parameters

Parameter	Value
$T_{\text{det}}$ , K	$\sim 230$
$V_{\text{max}}$ , V	1.3
$I_{\text{max}}$ , A	1.2
$Q_{\text{max}}$ , W	0.36

#### Thermistor characteristics

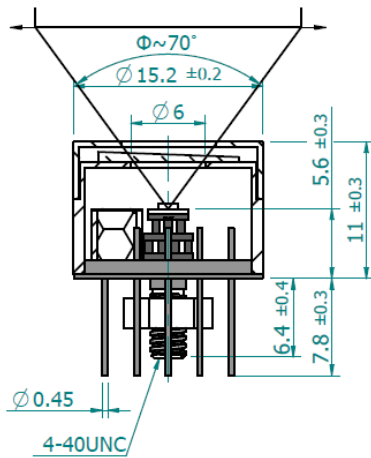


#### Spectral transmission of wAl<sub>2</sub>O<sub>3</sub> and wZnSeAR windows (typical example)



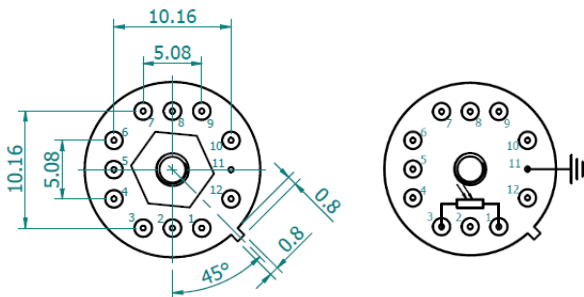
**Mechanical layout, mm**

**2TE-T08 package**



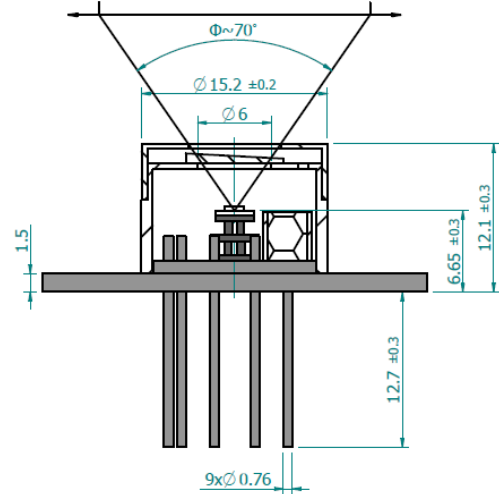
Φ – acceptance angle

Bottom view



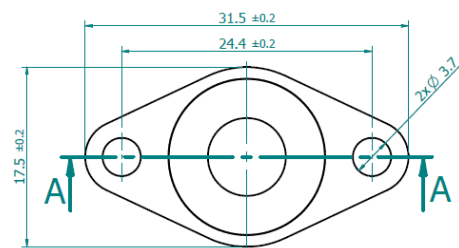
Function	Pin number
Detector	1, 3
Thermistor	7, 9
TE cooler supply	2(+), 8(-)
Chassis ground	11
Not used	4, 5, 6, 10, 12

**2TE-T066 package**

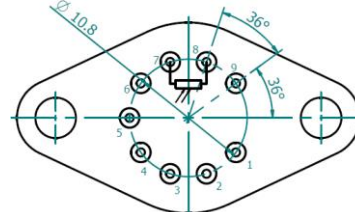


Φ – acceptance angle

Top view



Bottom view



Function	Pin number
Detector	7, 8
Thermistor	5, 6
TE cooler supply	1(+), 9(-)
Not used	2, 3, 4

**Dedicated preamplifiers**



„all-in-one“ AIP



programmable PIP



standard MIP



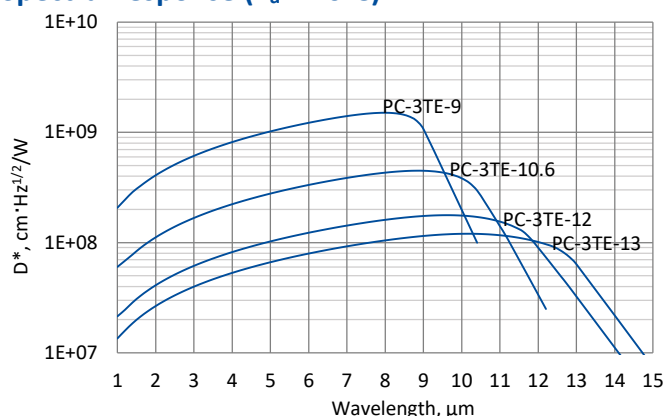
small SIP-T08

## PC-3TE series

### 1 – 15 μm HgCdTe three-stage thermoelectrically cooled photoconductive detectors

**PC-3TE series** features three-stage thermoelectrically cooled IR photoconductive detectors based on sophisticated HgCdTe heterostructures for the best performance and stability. The devices are optimized for the maximum performance at  $\lambda_{opt}$ . The devices should operate in optimum bias voltage and current readout mode. Performance at low frequencies is reduced due to 1/f noise. The 1/f noise corner frequency increases with the cut-off wavelength. 3° wedged zinc selenide anti-reflection coated (wZnSeAR) window prevents unwanted interference effects.

#### Spectral response ( $T_a = 20^\circ\text{C}$ )



Exemplary spectral detectivity, the spectral response of delivered devices may differ.

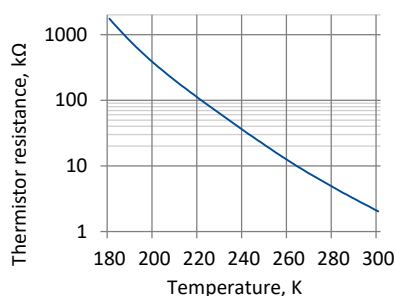
#### Specification ( $T_a = 20^\circ\text{C}$ )

Parameter	Detector type			
	PC-3TE-9	PC-3TE-10.6	PC-3TE-12	PC-3TE-13
Active element material	epitaxial HgCdTe heterostructure			
Optimal wavelength $\lambda_{opt}$ , μm	9.0	10.6	12.0	13.0
Detectivity $D^*(\lambda_{opt}, 20\text{kHz})$ , $\text{cm}^2 \cdot \text{Hz}^{1/2} / \text{W}$	$\geq 1.0 \times 10^9$	$\geq 2.5 \times 10^8$	$\geq 9.0 \times 10^7$	$\geq 6.0 \times 10^7$
Detectivity $D^*(\lambda_{peak}, 20\text{kHz})$ , $\text{cm}^2 \cdot \text{Hz}^{1/2} / \text{W}$	$\geq 1.5 \times 10^9$	$\geq 4.5 \times 10^8$	$\geq 1.8 \times 10^8$	$\geq 1.2 \times 10^8$
Current responsivity-active area length product $R_i(\lambda_{opt}) \cdot L$ , $\text{A} \cdot \text{mm} / \text{W}$	$\geq 0.075$	$\geq 0.02$	$\geq 0.01$	$\geq 0.007$
Time constant $\tau$ , ns	$\leq 60$	$\leq 20$	$\leq 5$	$\leq 4$
1/f noise corner frequency $f_c$ , Hz	$\leq 10\text{k}$		$\leq 20\text{k}$	
Bias voltage-active area length ratio $V_b/L$ , V/mm	$\leq 2.0$		$\leq 1.5$	
Resistance R, $\Omega$	$\leq 400$		$\leq 300$	
Active element temperature $T_{det}$ , K	$\sim 210$			
Active area A, mm×mm	0.05×0.05, 0.1×0.1, 0.25×0.25, 0.5×0.5, 1×1, 2×2			
Package	TO8, TO66			
Acceptance angle $\Phi$	$\sim 70^\circ$			
Window	wZnSeAR			

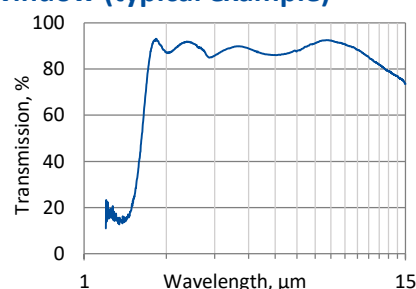
#### Three-stage thermoelectric cooler parameters

Parameter	Value
$T_{det}$ , K	$\sim 210$
$V_{max}$ , V	3.6
$I_{max}$ , A	0.45
$Q_{max}$ , W	0.27

#### Thermistor characteristics

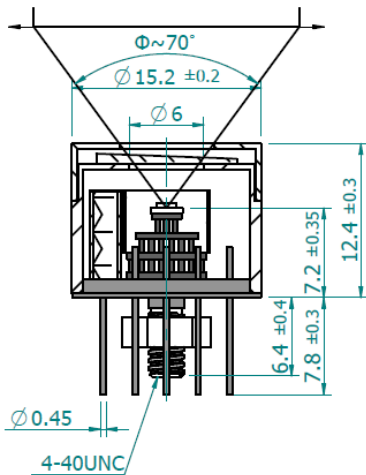


#### Spectral transmission of wZnSeAR window (typical example)



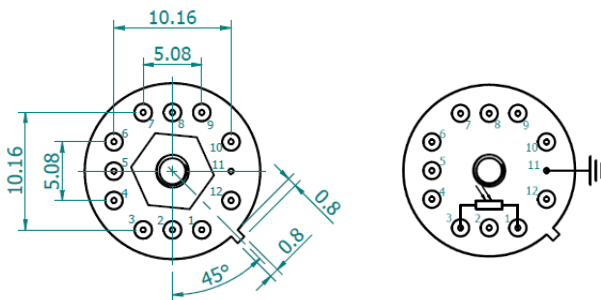
**Mechanical layout, mm**

**3TE-T08 package**



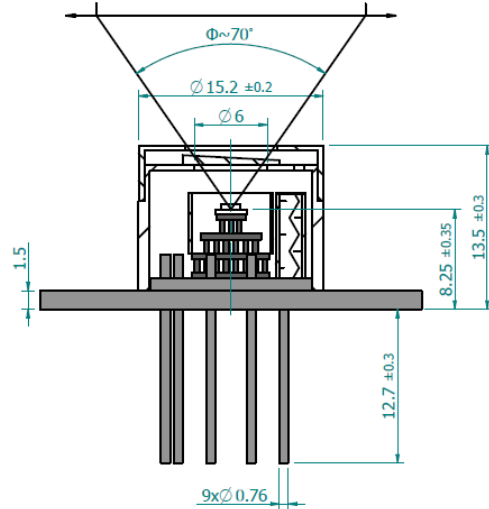
Φ – acceptance angle

**Bottom view**



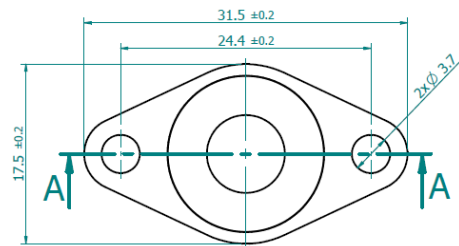
Function	Pin number
Detector	1, 3
Thermistor	7, 9
TE cooler supply	2(+), 8(-)
Chassis ground	11
Not used	4, 5, 6, 10, 12

**3TE-T066 package**

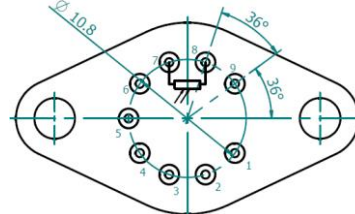


Φ – acceptance angle

**Top view**



**Bottom view**



Function	Pin number
Detector	7, 8
Thermistor	5, 6
TE cooler supply	1(+), 9(-)
Not used	2, 3, 4

**Dedicated preamplifiers**



„all-in-one“ AIP



programmable PIP



standard MIP



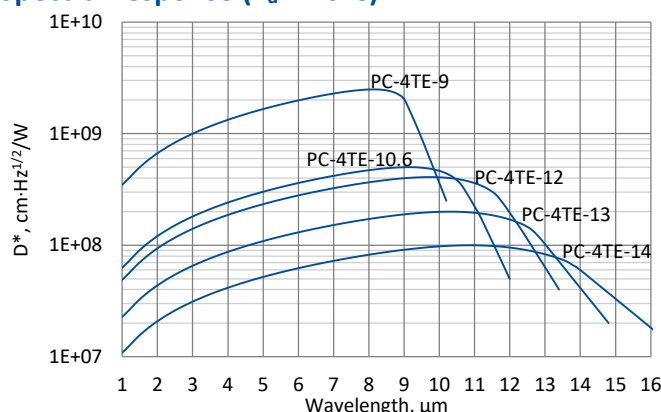
small SIP-T08

## PC-4TE series

### 1 – 16 μm HgCdTe four-stage thermoelectrically cooled photoconductive detectors

**PC-4TE series** features four-stage thermoelectrically cooled IR photoconductive detectors based on sophisticated HgCdTe heterostructures for the best performance and stability. The devices are optimized for the maximum performance at  $\lambda_{opt}$ . The devices should operate in optimum bias voltage and current readout mode. Performance at low frequencies is reduced due to 1/f noise. The 1/f noise corner frequency increases with the cut-off wavelength. 3° wedged zinc selenide anti-reflection coated (wZnSeAR) window prevents unwanted interference effects.

#### Spectral response ( $T_a = 20^\circ\text{C}$ )



Exemplary spectral detectivity, the spectral response of delivered devices may differ.

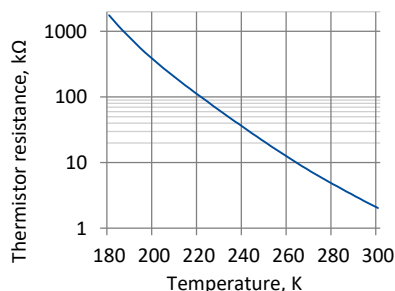
#### Specification ( $T_a = 20^\circ\text{C}$ )

Parameter	Detector type				
	PC-4TE-9	PC-4TE-10.6	PC-4TE-12	PC-4TE-13	PC-4TE-14
Active element material	epitaxial HgCdTe heterostructure				
Optimal wavelength $\lambda_{opt}$ , μm	9.0	10.6	12.0	13.0	14.0
Detectivity $D^*(\lambda_{peak}, 20\text{kHz})$ , $\text{cm}\cdot\text{Hz}^{1/2}/\text{W}$	$\geq 2.5 \times 10^9$	$\geq 5.0 \times 10^8$	$\geq 4.0 \times 10^8$	$\geq 2.0 \times 10^8$	$\geq 1.0 \times 10^8$
Detectivity $D^*(\lambda_{opt}, 20\text{kHz})$ , $\text{cm}\cdot\text{Hz}^{1/2}/\text{W}$	$\geq 2.0 \times 10^9$	$\geq 3.5 \times 10^8$	$\geq 2.0 \times 10^8$	$\geq 1.0 \times 10^8$	$\geq 6.0 \times 10^7$
Current responsivity-active area length product $R_i(\lambda_{opt}) \cdot L$ , $\text{A}\cdot\text{mm}/\text{W}$	$\geq 0.1$	$\geq 0.03$	$\geq 0.015$	$\geq 0.01$	$\geq 0.007$
Time constant $\tau$ , ns	$\leq 80$	$\leq 30$	$\leq 7$	$\leq 6$	$\leq 5$
1/f noise corner frequency $f_c$ , Hz	$\leq 10\text{k}$		$\leq 20\text{k}$		
Bias voltage-active area length ratio $V_b/L$ , V/mm	$\leq 3.8$		$\leq 3.0$		$\leq 2.25$
Resistance R, $\Omega$	$\leq 500$		$\leq 400$		$\leq 300$
Active element temperature $T_{det}$ , K	$\sim 195$				
Active area A, mm $\times$ mm	0.05 $\times$ 0.05, 0.1 $\times$ 0.1, 0.25 $\times$ 0.25, 0.5 $\times$ 0.5, 1 $\times$ 1, 2 $\times$ 2				
Package	TO8, TO66				
Acceptance angle $\Phi$	$\sim 70^\circ$				
Window	wZnSeAR				

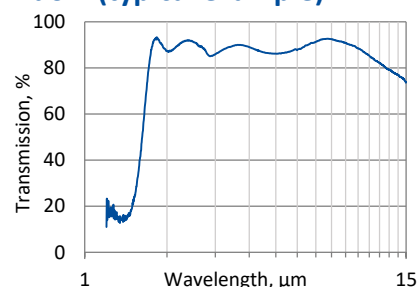
#### Four-stage thermoelectric cooler parameters

Parameter	Value
$T_{det}$ , K	$\sim 195$
$V_{max}$ , V	8.3
$I_{max}$ , A	0.4
$Q_{max}$ , W	0.28

#### Thermistor characteristics

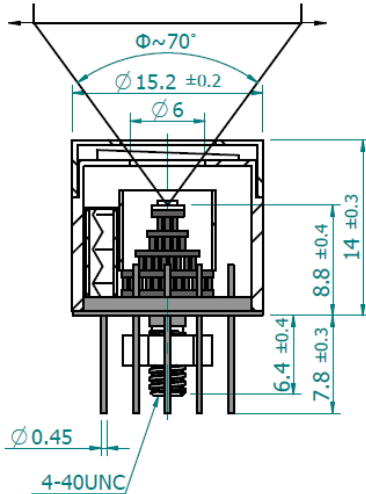


#### Spectral transmission of wZnSeAR window (typical example)



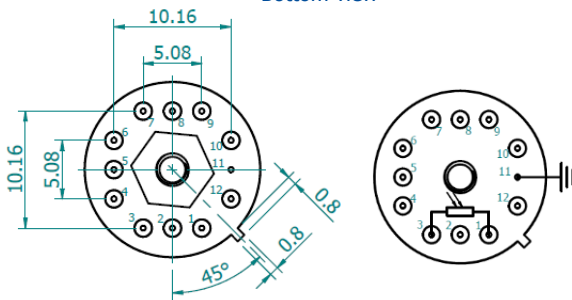
**Mechanical layout, mm**

**4TE-TO8 package**



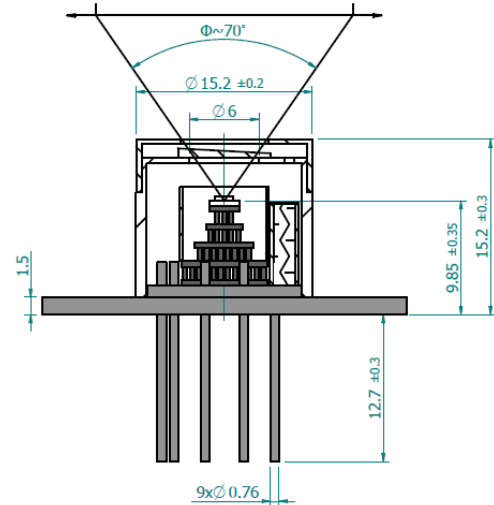
Φ – acceptance angle

**Bottom view**



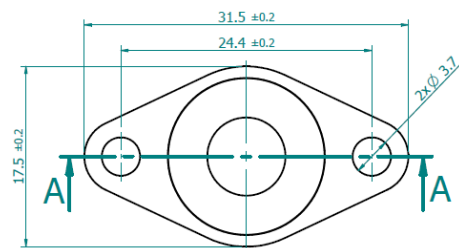
Function	Pin number
Detector	1, 3
Thermistor	7, 9
TE cooler supply	2(+), 8(-)
Chassis ground	11
Not used	4, 5, 6, 10, 12

**4TE-TO66 package**

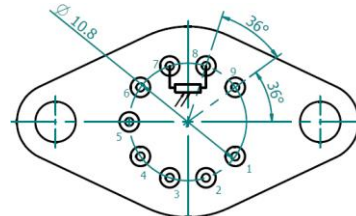


Φ – acceptance angle

**Top view**



**Bottom view**



Function	Pin number
Detector	7, 8
Thermistor	5, 6
TE cooler supply	1(+), 9(-)
Not used	2, 3, 4

**Dedicated preamplifiers**



„all-in-one“ AIP



programmable PIP



standard MIP



small SIP-TO8

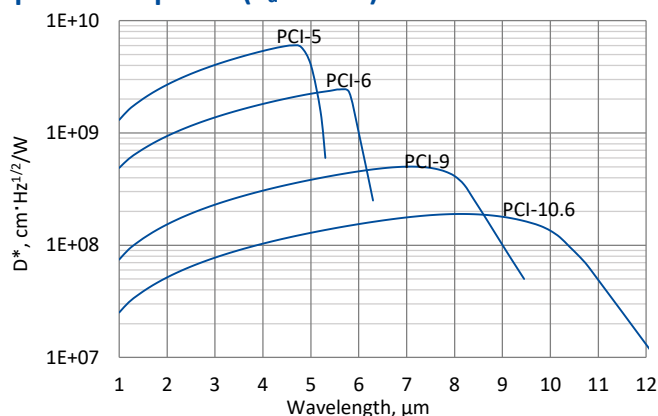


## PCI series

### 1 – 12 $\mu\text{m}$ HgCdTe ambient temperature, optically immersed photoconductive detectors

**PCI series** features uncooled IR photoconductive detectors based on sophisticated HgCdTe heterostructures for the best performance and stability, optically immersed in order to improve parameters of the devices. The detectors are optimized for the maximum performance at  $\lambda_{\text{opt}}$ . Cut-on wavelength is limited by GaAs transmittance ( $\sim 0.9 \mu\text{m}$ ). The devices should operate in optimum bias voltage and current readout mode. Performance at low frequencies is reduced due to  $1/f$  noise. The  $1/f$  noise corner frequency increases with the cut-off wavelength.

#### Spectral response ( $T_a = 20^\circ\text{C}$ )

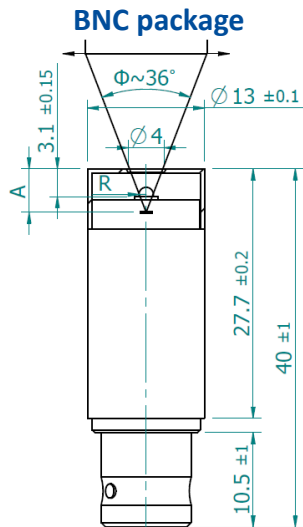


Exemplary spectral detectivity, the spectral response of delivered devices may differ.

#### Specification ( $T_a = 20^\circ\text{C}$ )

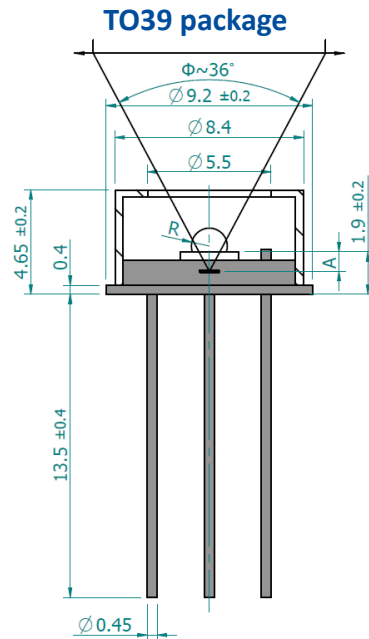
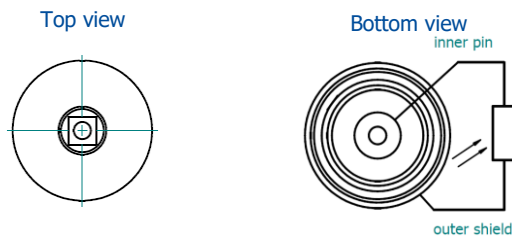
Parameter	Detector type			
	PCI-5	PCI-6	PCI-9	PCI-10.6
Active element material	epitaxial HgCdTe heterostructure			
Optimal wavelength $\lambda_{\text{opt}}$ , $\mu\text{m}$	5.0	6.0	9.0	10.6
Detectivity $D^*(\lambda_{\text{peak}}, 20\text{kHz})$ , $\text{cm}\cdot\text{Hz}^{1/2}/\text{W}$	$\geq 6.0 \times 10^9$	$\geq 2.5 \times 10^9$	$\geq 5.0 \times 10^8$	$\geq 1.0 \times 10^8$
Detectivity $D^*(\lambda_{\text{opt}}, 20\text{kHz})$ , $\text{cm}\cdot\text{Hz}^{1/2}/\text{W}$	$\geq 4.0 \times 10^9$	$\geq 1.0 \times 10^9$	$\geq 1.0 \times 10^8$	$\geq 8.0 \times 10^7$
Current responsivity-optical area length product $R_i(\lambda_{\text{opt}}) \cdot L_0$ , $\text{A}\cdot\text{mm}/\text{W}$	$\geq 0.5$	$\geq 0.2$	$\geq 0.02$	$\geq 0.008$
Time constant $\tau$ , ns	$\leq 5000$	$\leq 500$	$\leq 10$	$\leq 3$
$1/f$ noise corner frequency $f_c$ , Hz		$\leq 10\text{k}$		$\leq 20\text{k}$
Bias voltage-optical area length ratio $V_b/L_0$ , V/mm	$\leq 0.45$	$\leq 0.4$	$\leq 0.36$	$\leq 0.3$
Resistance $R$ , $\Omega$	$\leq 1200$	$\leq 600$	$\leq 300$	$\leq 120$
Optical area $A_0$ , $\text{mm}\times\text{mm}$	0.5 $\times$ 0.5, 1 $\times$ 1, 2 $\times$ 2			
Package	TO39, BNC			
Acceptance angle $\Phi$	$\sim 36^\circ$			
Window	none			

**Mechanical layout, mm**



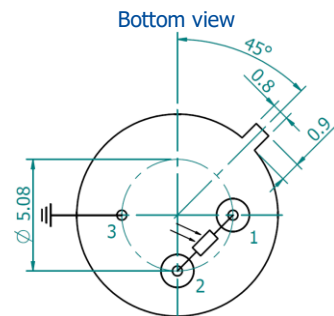
Parameter	Value		
Immersion microlens shape	hyperhemisphere		
Optical area A <sub>0</sub> , mm×mm	0.5×0.5	1×1	2×2
R, mm	0.5	0.8	1.25
A, mm	4.6±0.3	5.5±0.3	6.85±0.30

Φ – acceptance angle  
R – hyperhemisphere microlens radius  
A – distance from the top of BNC package to the focal plane



Parameter	Value		
Immersion microlens shape	hyperhemisphere		
Optical area A <sub>0</sub> , mm×mm	0.5×0.5	1×1	2×2
R, mm	0.5	0.8	1.25
A, mm	1.5±0.2	2.4±0.2	3.75±0.20

Φ – acceptance angle  
R – hyperhemisphere microlens radius  
A – distance from the bottom of hyperhemisphere microlens to the focal plane



Function	Pin number
Detector	1, 2
Chassis ground	3

**Dedicated preamplifier**



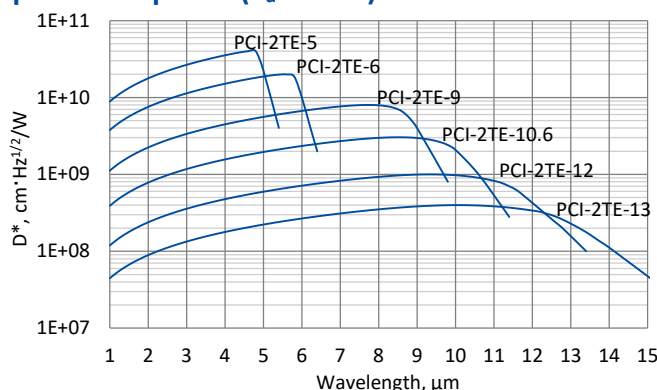
small SIP-TO39

## PCI-2TE series

### 1 – 15 $\mu\text{m}$ HgCdTe two-stage thermoelectrically cooled, optically immersed photoconductive detectors

**PCI-2TE series** features two-stage thermoelectrically cooled IR photoconductive detectors based on sophisticated HgCdTe heterostructures for the best performance and stability, optically immersed in order to improve parameters of the devices. The detectors are optimized for the maximum performance at  $\lambda_{\text{opt}}$ . Cut-on wavelength is limited by GaAs transmittance ( $\sim 0.9 \mu\text{m}$ ). The devices should operate in optimum bias voltage and current readout mode. Performance at low frequencies is reduced due to  $1/f$  noise. The  $1/f$  noise corner frequency increases with the cut-off wavelength.  $3^\circ$  wedged sapphire ( $\text{wAl}_2\text{O}_3$ ) or zinc selenide anti-reflection coated ( $\text{wZnSeAR}$ ) window prevents unwanted interference effects.

#### Spectral response ( $T_a = 20^\circ\text{C}$ )



Exemplary spectral detectivity, the spectral response of delivered devices may differ.

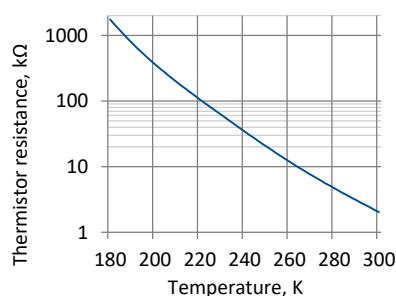
#### Specification ( $T_a = 20^\circ\text{C}$ )

Parameter	Detector type					
	PCI-2TE-5	PCI-2TE-6	PCI-2TE-9	PCI-2TE-10.6	PCI-2TE-12	PCI-2TE-13
Active element material	epitaxial HgCdTe heterostructure					
Optimum wavelength $\lambda_{\text{opt}}$ , $\mu\text{m}$	5.0	6.0	9.0	10.6	12.0	13.0
Detectivity $D^*(\lambda_{\text{peak}}, 20\text{kHz})$ , $\text{cm}^2 \cdot \text{Hz}^{1/2} / \text{W}$	$\geq 4.0 \times 10^{10}$	$\geq 2.0 \times 10^{10}$	$\geq 8.0 \times 10^9$	$\geq 2.8 \times 10^9$	$\geq 1.0 \times 10^9$	$\geq 4.0 \times 10^8$
Detectivity $D^*(\lambda_{\text{opt}}, 20\text{kHz})$ , $\text{cm}^2 \cdot \text{Hz}^{1/2} / \text{W}$	$\geq 2.0 \times 10^{10}$	$\geq 1.0 \times 10^{10}$	$\geq 4.0 \times 10^9$	$\geq 1.0 \times 10^9$	$\geq 4.5 \times 10^8$	$\geq 2.3 \times 10^8$
Current responsivity-optical area length product $R_i(\lambda_{\text{opt}}) \cdot L_o$ , $\text{A} \cdot \text{mm} / \text{W}$	$\geq 3.0$	$\geq 1.5$	$\geq 0.225$	$\geq 0.1$	$\geq 0.05$	$\geq 0.03$
Time constant $\tau$ , ns	$\leq 20000$	$\leq 4000$	$\leq 40$	$\leq 10$	$\leq 3$	$\leq 2$
$1/f$ noise corner frequency $f_c$ , Hz		$\leq 10\text{k}$			$\leq 20\text{k}$	
Bias voltage-optical area length ratio $V_b/L_o$ , V/mm	$\leq 0.2$	$\leq 0.32$	$\leq 0.2$	$\leq 0.225$	$\leq 0.15$	$\leq 0.18$
Resistance $R$ , $\Omega$	$\leq 1200$	$\leq 800$	$\leq 400$	$\leq 300$	$\leq 200$	$\leq 150$
Active element temperature $T_{\text{det}}$ , K	$\sim 230$					
Optical area $A_o$ , mm $\times$ mm	0.5 $\times$ 0.5, 1 $\times$ 1, 2 $\times$ 2					
Package	TO8, TO66					
Acceptance angle $\Phi$	$\sim 36^\circ$					
Window	$\text{wAl}_2\text{O}_3$			$\text{wZnSeAR}$		

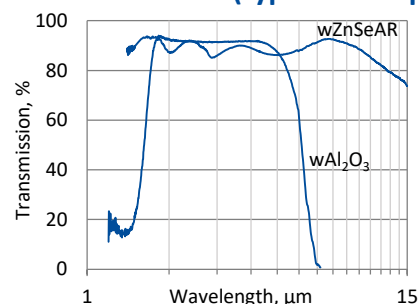
#### Two-stage thermoelectric cooler parameters

Parameter	Value
$T_{\text{det}}$ , K	$\sim 230$
$V_{\text{max}}$ , V	1.3
$I_{\text{max}}$ , A	1.2
$Q_{\text{max}}$ , W	0.36

#### Thermistor characteristics

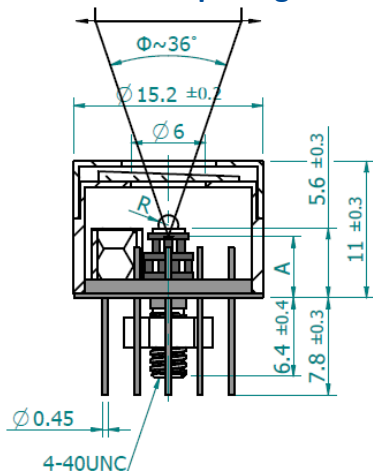


#### Spectral transmission of $\text{wAl}_2\text{O}_3$ and $\text{wZnSeAR}$ windows (typical example)



**Mechanical layout, mm**

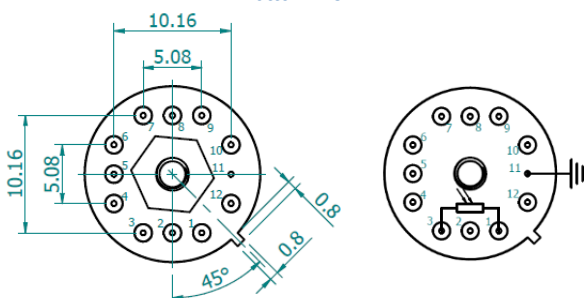
**2TE-T08 package**



Parameter	Value		
Immersion microlens shape	hyperhemisphere		
Optical area A <sub>0</sub> , mm×mm	0.5×0.5	1×1	2×2
R, mm	0.5	0.8	1.25
A, mm	4.1±0.3	3.2±0.3	1.85±0.30

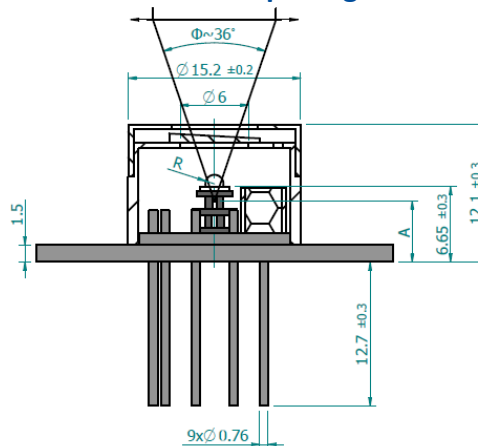
Φ – acceptance angle  
R – hyperhemisphere microlens radius  
A – distance from the bottom of 2TE-T08 header to the focal plane

**Bottom view**



Function	Pin number
Detector	1, 3
Thermistor	7, 9
TE cooler supply	2(+), 8(-)
Chassis ground	11
Not used	4, 5, 6, 10, 12

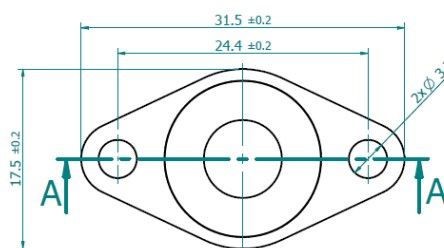
**2TE-T066 package**



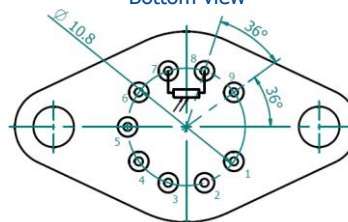
Parameter	Value		
Immersion microlens shape	hyperhemisphere		
Optical area A <sub>0</sub> , mm×mm	0.5×0.5	1×1	2×2
R, mm	0.5	0.8	1.25
A, mm	5.15±0.30	3.2±0.3	1.85±0.30

Φ – acceptance angle  
R – hyperhemisphere microlens radius  
A – distance from the bottom of 2TE-T066 header to the focal plane

**Top view**



**Bottom view**



Function	Pin number
Detector	7, 8
Thermistor	5, 6
TE cooler supply	1(+), 9(-)
Not used	2, 3, 4

**Dedicated preamplifiers**



„all-in-one“ AIP



programmable PIP



standard MIP



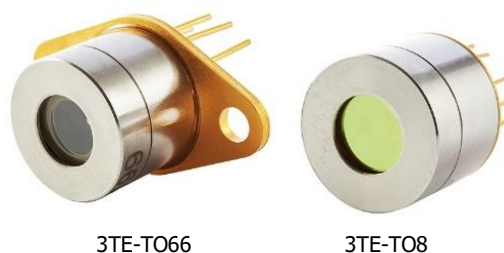
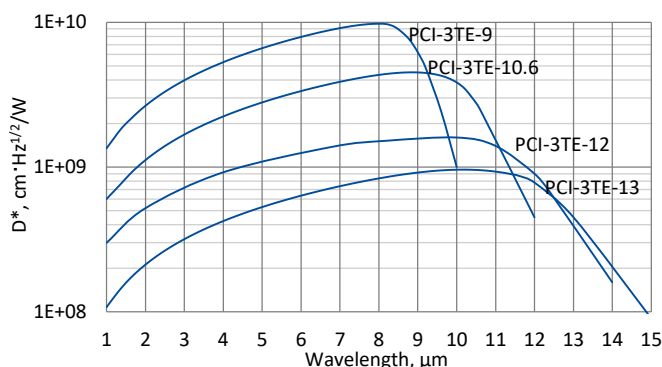
small SIP-T08

## PCI-3TE series

### 1 – 15 μm HgCdTe three-stage thermoelectrically cooled, optically immersed photoconductive detectors

**PCI-3TE series** features three-stage thermoelectrically cooled IR photoconductive detectors based on sophisticated HgCdTe heterostructures for the best performance and stability, optically immersed in order to improve parameters of the devices. The detectors are optimized for the maximum performance at  $\lambda_{opt}$ . Cut-on wavelength is limited by GaAs transmittance ( $\sim 0.9 \mu\text{m}$ ). The devices should operate in optimum bias voltage and current readout mode. Performance at low frequencies is reduced due to  $1/f$  noise. The  $1/f$  noise corner frequency increases with the cut-off wavelength.  $3^\circ$  wedged zinc selenide anti-reflection coated (wZnSeAR) window prevents unwanted interference effects.

#### Spectral response ( $T_a = 20^\circ\text{C}$ )



Exemplary spectral detectivity, the spectral response of delivered devices may differ.

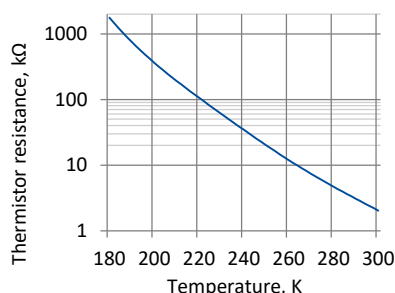
#### Specification ( $T_a = 20^\circ\text{C}$ )

Parameter	Detector type			
	PCI-3TE-9	PCI-3TE-10.6	PCI-3TE-12	PCI-3TE-13
Active element material	epitaxial HgCdTe heterostructure			
Optimal wavelength $\lambda_{opt}$ , $\mu\text{m}$	9.0	10.6	12.0	13.0
Detectivity $D^*(\lambda_{peak}, 20\text{kHz})$ , $\text{cm}\cdot\text{Hz}^{1/2}/\text{W}$	$\geq 1.0 \times 10^{10}$	$\geq 4.5 \times 10^9$	$\geq 1.6 \times 10^9$	$\geq 9.0 \times 10^8$
Detectivity $D^*(\lambda_{opt}, 20\text{kHz})$ , $\text{cm}\cdot\text{Hz}^{1/2}/\text{W}$	$\geq 6.2 \times 10^9$	$\geq 2.5 \times 10^9$	$\geq 9.0 \times 10^8$	$\geq 4.5 \times 10^8$
Current responsivity-optical area length product $R_i(\lambda_{opt}) \cdot L_o$ , $\text{A}\cdot\text{mm}/\text{W}$	$\geq 0.7$	$\geq 0.17$	$\geq 0.07$	$\geq 0.03$
Time constant $\tau$ , ns	$\leq 60$	$\leq 20$	$\leq 5$	$\leq 4$
$1/f$ noise corner frequency $f_c$ , Hz	$\leq 10\text{k}$		$\leq 20\text{k}$	
Bias voltage-optical area length ratio $V_b/L_o$ , V/mm	$\leq 0.2$		$\leq 0.15$	
Resistance $R$ , $\Omega$	$\leq 400$		$\leq 300$	
Active element temperature $T_{det}$ , K		$\sim 210$		
Optical area $A_o$ , mm $\times$ mm		0.5 $\times$ 0.5, 1 $\times$ 1, 2 $\times$ 2		
Package		TO8, TO66		
Acceptance angle $\Phi$		$\sim 36^\circ$		
Window		wZnSeAR		

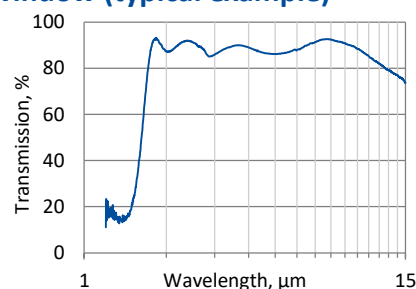
#### Three-stage thermoelectric cooler parameters

Parameter	Value
$T_{det}$ , K	$\sim 210$
$V_{max}$ , V	3.6
$I_{max}$ , A	0.45
$Q_{max}$ , W	0.27

#### Thermistor characteristics

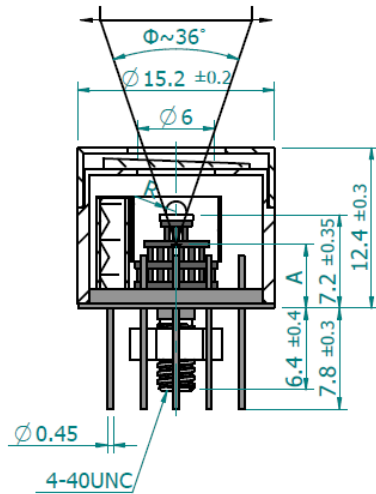


#### Spectral transmission of wZnSeAR window (typical example)



**Mechanical layout, mm**

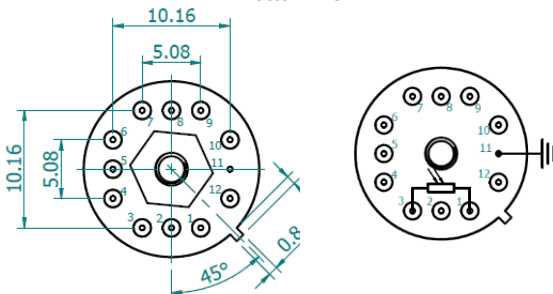
**3TE-TO8 package**



Parameter	Value		
Immersion microlens shape	hyperhemisphere		
Optical area A <sub>0</sub> , mm×mm	0.5×0.5	1×1	2×2
R, mm	0.5	0.8	1.25
A, mm	5.7±0.35	4.8±0.35	3.45±0.35

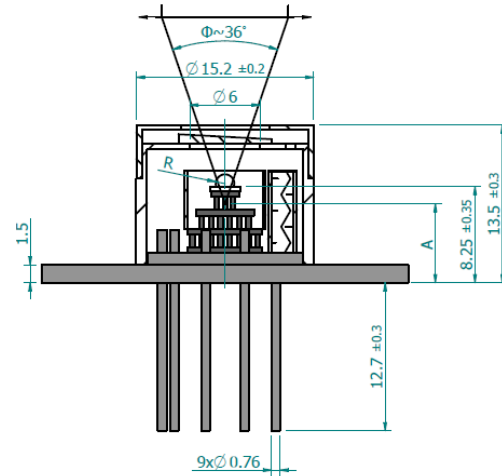
Φ – acceptance angle  
R – hyperhemisphere microlens radius  
A – distance from the bottom of 3TE-TO8 header to the focal plane

**Bottom view**



Function	Pin number
Detector	1, 3
Thermistor	7, 9
TE cooler supply	2(+), 8(-)
Chassis ground	11
Not used	4, 5, 6, 10, 12

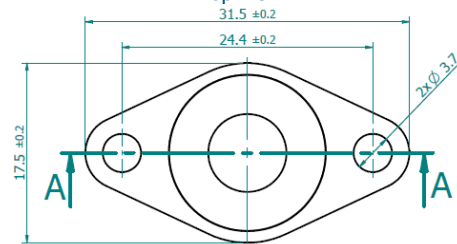
**3TE-TO66 package**



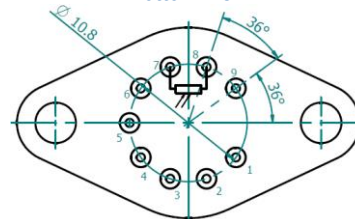
Parameter	Value		
Immersion microlens shape	hyperhemisphere		
Optical area A <sub>0</sub> , mm×mm	0.5×0.5	1×1	2×2
R, mm	0.5	0.8	1.25
A, mm	6.75±0.35	5.85±0.35	4.50±0.35

Φ – acceptance angle  
R – hyperhemisphere microlens radius  
A – distance from the bottom of 3TE-TO66 header to the focal plane

**Top view**



**Bottom view**



Function	Pin number
Detector	7, 8
Thermistor	5, 6
TE cooler supply	1(+), 9(-)
Not used	2, 3, 4

**Dedicated preamplifiers**



„all-in-one“ AIP



programmable PIP



standard MIP



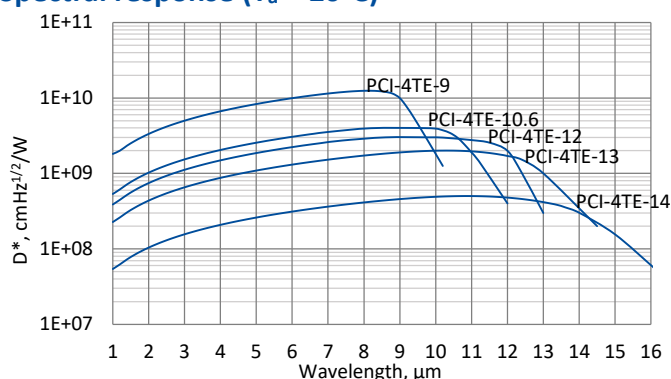
small SIP-TO8

## PCI-4TE series

### 1 – 16 μm HgCdTe four-stage thermoelectrically cooled, optically immersed photoconductive detectors

**PCI-4TE series** features four-stage thermoelectrically cooled IR photoconductive detectors based on sophisticated HgCdTe heterostructures for the best performance and stability, optically immersed in order to improve parameters of the devices. The detectors are optimized for the maximum performance at  $\lambda_{opt}$ . Cut-on wavelength is limited by GaAs transmittance ( $\sim 0.9 \mu\text{m}$ ). The devices should operate in optimum bias voltage and current readout mode. Performance at low frequencies is reduced due to  $1/f$  noise. The  $1/f$  noise corner frequency increases with the cut-off wavelength.  $3^\circ$  wedged zinc selenide anti-reflection coated (wZnSeAR) window prevents unwanted interference effects.

#### Spectral response ( $T_a = 20^\circ\text{C}$ )



Exemplary spectral detectivity, the spectral response of delivered devices may differ.

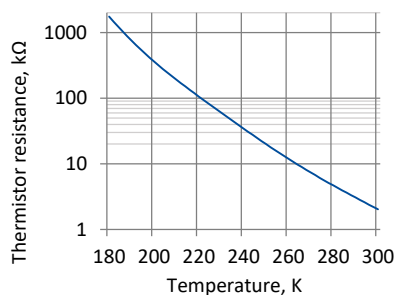
#### Specification ( $T_a = 20^\circ\text{C}$ )

Parameter	Detector type				
	PCI-4TE-9	PCI-4TE-10.6	PCI-4TE-12	PCI-4TE-13	PCI-4TE-14
Active element material	epitaxial HgCdTe heterostructure				
Optimal wavelength $\lambda_{opt}$ , $\mu\text{m}$	9.0	10.6	12.0	13.0	14.0
Detectivity $D^*(\lambda_{peak}, 20\text{kHz})$ , $\text{cm}\cdot\text{Hz}^{1/2}/\text{W}$	$\geq 1.25 \times 10^{10}$	$\geq 4.0 \times 10^9$	$\geq 3.0 \times 10^9$	$\geq 2.0 \times 10^9$	$\geq 5.0 \times 10^8$
Detectivity $D^*(\lambda_{opt}, 20\text{kHz})$ , $\text{cm}\cdot\text{Hz}^{1/2}/\text{W}$	$\geq 1.0 \times 10^{10}$	$\geq 3.0 \times 10^9$	$\geq 2.0 \times 10^9$	$\geq 1.0 \times 10^9$	$\geq 3.0 \times 10^8$
Current responsivity-optical area length product $R_i(\lambda_{opt}) \cdot L_o$ , $\text{A}\cdot\text{mm}/\text{W}$	$\geq 0.9$	$\geq 0.2$	$\geq 0.09$	$\geq 0.05$	$\geq 0.03$
Time constant $\tau$ , ns	$\leq 80$	$\leq 30$	$\leq 7$	$\leq 6$	$\leq 5$
$1/f$ noise corner frequency $f_c$ , Hz	$\leq 10\text{k}$		$\leq 20\text{k}$		
Bias voltage-optical area length ratio $V_b/L_o$ , V/mm	$\leq 0.3$		$\leq 0.24$		$\leq 0.18$
Resistance $R$ , $\Omega$	$\leq 500$		$\leq 400$		$\leq 300$
Active element temperature $T_{det}$ , K			$\sim 195$		
Optical area $A_o$ , $\text{mm}\times\text{mm}$		0.5×0.5, 1×1, 2×2			
Package		TO8, TO66			
Acceptance angle $\Phi$		$\sim 36^\circ$			
Window		wZnSeAR			

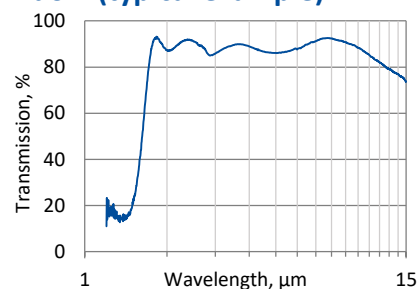
#### Four-stage thermoelectric cooler parameters

Parameter	Value
$T_{det}$ , K	$\sim 195$
$V_{max}$ , V	8.3
$I_{max}$ , A	0.4
$Q_{max}$ , W	0.28

#### Thermistor characteristics

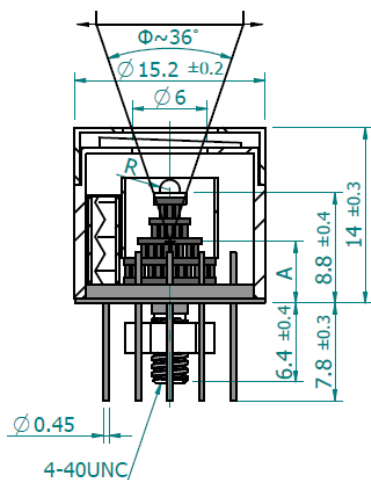


#### Spectral transmission of wZnSeAR window (typical example)



**Mechanical layout, mm**

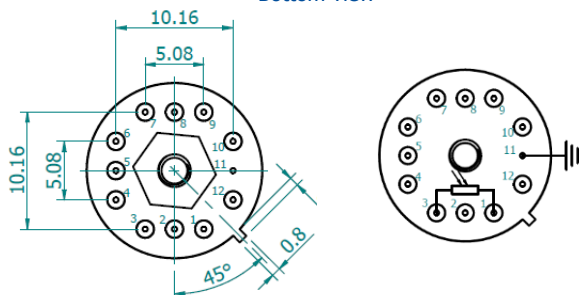
**4TE-TO8 package**



Parameter	Value
Immersion microlens shape	hyperhemisphere
Optical area $A_0$ , mm×mm	0.5×0.5    1×1    2×2
R, mm	0.5    0.8    1.25
A, mm	7.3±0.4    6.4±0.4    5.0±0.4

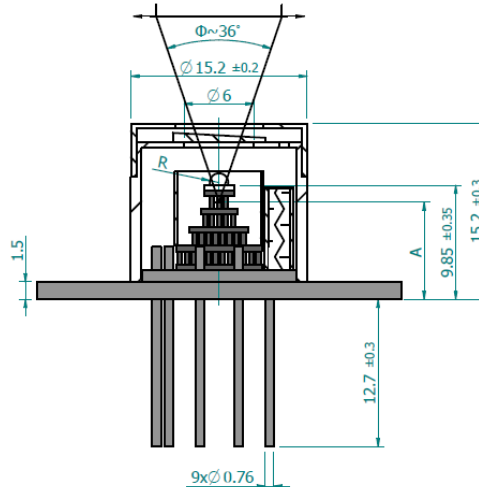
Φ – acceptance angle  
R – hyperhemisphere microlens radius  
A – distance from the bottom of 4TE-TO8 header to the focal plane

**Bottom view**



Function	Pin number
Detector	1, 3
Thermistor	7, 9
TE cooler supply	2(+), 8(-)
Chassis ground	11
Not used	4, 5, 6, 10, 12

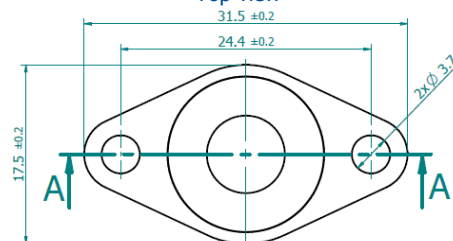
**4TE-TO66 package**



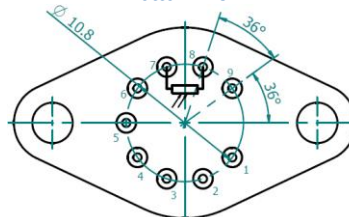
Parameter	Value
Immersion microlens shape	hyperhemisphere
Optical area $A_0$ , mm×mm	0.5×0.5    1×1    2×2
R, mm	0.5    0.8    1.25
A, mm	8.35±0.40    7.45±0.40    6.1±0.4

Φ – acceptance angle  
R – hyperhemisphere microlens radius  
A – distance from the bottom of 4TE-TO66 header to the focal plane

**Top view**



**Bottom view**



Function	Pin number
Detector	7, 8
Thermistor	5, 6
TE cooler supply	1(+), 9(-)
Not used	2, 3, 4

**Dedicated preamplifiers**



„all-in-one“ AIP



programmable PIP



standard MIP



small SIP-TO8

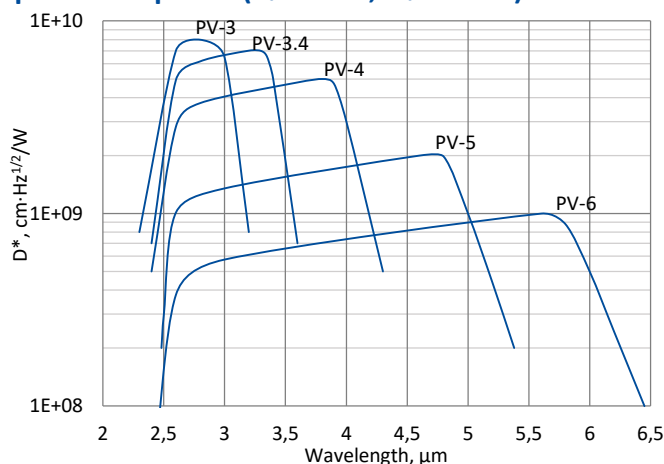


## PV series

### 2.5 – 6.5 $\mu\text{m}$ HgCdTe ambient temperature photovoltaic detectors

**PV series** features uncooled IR photovoltaic detectors based on sophisticated HgCdTe heterostructures for the best performance and stability. The devices are optimized for the maximum performance at  $\lambda_{\text{opt}}$ . Cut-on wavelength can be optimized upon request. Reverse bias may significantly increase response speed and dynamic range. It also results in improved performance at high frequencies, but 1/f noise that appears in biased devices may reduce performance at low frequencies.

#### Spectral response ( $T_a = 20^\circ\text{C}$ , $V_b = 0\text{ mV}$ )

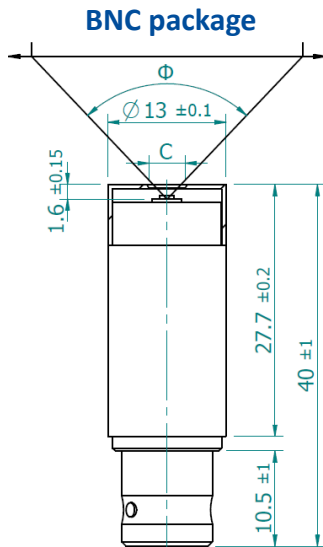


Exemplary spectral detectivity, the spectral response of delivered devices may differ.

#### Specification ( $T_a = 20^\circ\text{C}$ , $V_b = 0\text{ mV}$ )

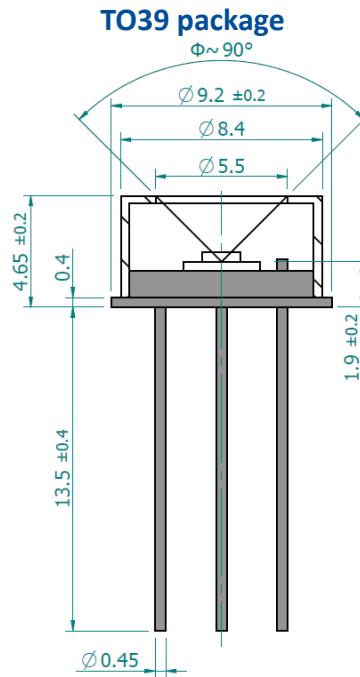
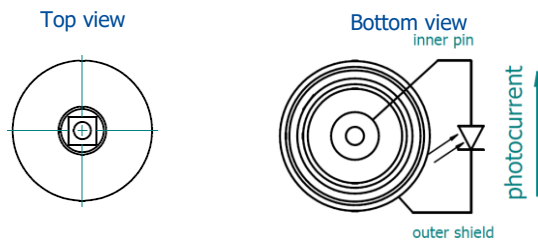
Parameter	Detector type									
	PV-3		PV-3.4		PV-4		PV-5		PV-6	
Active element material	epitaxial HgCdTe heterostructure									
Optimal wavelength $\lambda_{\text{opt}}$ , $\mu\text{m}$	3.0		3.4		4.0		5.0		6.0	
Detectivity $D^*(\lambda_{\text{peak}})$ , $\text{cm}\cdot\text{Hz}^{1/2}/\text{W}$	$\geq 8.0 \times 10^9$		$\geq 7.0 \times 10^9$		$\geq 5.0 \times 10^9$		$\geq 2.0 \times 10^9$		$\geq 1.0 \times 10^9$	
Detectivity $D^*(\lambda_{\text{opt}})$ , $\text{cm}\cdot\text{Hz}^{1/2}/\text{W}$	$\geq 6.5 \times 10^9$		$\geq 5.0 \times 10^9$		$\geq 3.0 \times 10^9$		$\geq 1.0 \times 10^9$		$\geq 5.0 \times 10^8$	
Current responsivity $R_i(\lambda_{\text{opt}})$ , $\text{A}/\text{W}$	$\geq 0.5$		$\geq 0.8$		$\geq 1.0$		$\geq 1.0$		$\geq 1.0$	
Time constant $\tau$ , ns	$\leq 350$		$\leq 260$		$\leq 150$		$\leq 120$		$\leq 80$	
Resistance-active area product $R \cdot A$ , $\Omega \cdot \text{cm}^2$	$\geq 1$		$\geq 0.5$		$\geq 0.1$		$\geq 0.01$		$\geq 0.002$	
Active area $A$ , $\text{mm} \times \text{mm}$	0.05×0.05, 0.1×0.1									
Package	TO39	BNC	TO39	BNC	TO39	BNC	TO39	BNC	TO39	BNC
Acceptance angle $\Phi$	$\sim 90^\circ$	$\sim 102^\circ$	$\sim 90^\circ$	$\sim 102^\circ$	$\sim 90^\circ$	$\sim 102^\circ$	$\sim 90^\circ$	$\sim 102^\circ$	$\sim 90^\circ$	$\sim 102^\circ$
Window	none									

**Mechanical layout, mm**

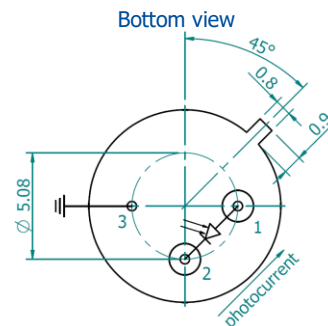


Parameter	Value
Active area, mm×mm	0.05×0.05 – 0.1×0.1
C, mm	Ø4
Acceptance angle Φ	~102°

C – aperture



Φ – acceptance angle



Function	Pin number
Detector	1, 2
Chassis ground	3

**Dedicated preamplifier**



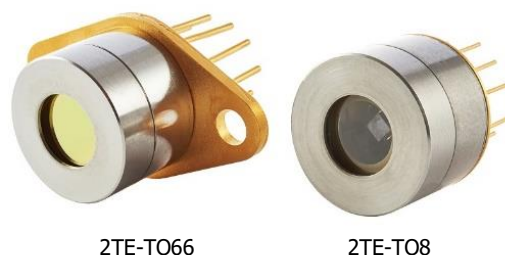
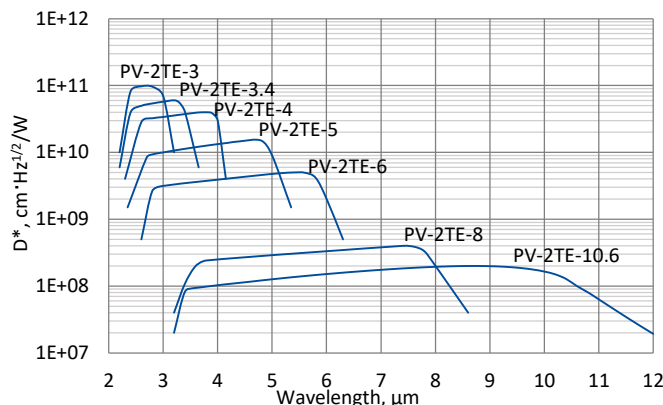
small SIP-TO39

## PV-2TE series

### 2 – 12 μm HgCdTe two-stage thermoelectrically cooled photovoltaic detectors

**PV-2TE series** features two-stage thermoelectrically cooled IR photovoltaic detectors based on sophisticated HgCdTe heterostructures for the best performance and stability. The devices are optimized for the maximum performance at  $\lambda_{opt}$ . Cut-on wavelength can be optimized upon request. Reverse bias may significantly increase response speed and dynamic range. It also results in improved performance at high frequencies, but 1/f noise that appears in biased devices may reduce performance at low frequencies. 3° wedged sapphire (wAl<sub>2</sub>O<sub>3</sub>) or zinc selenide anti-reflection coated (wZnSeAR) window prevents unwanted interference effects.

#### Spectral response ( $T_a = 20^\circ\text{C}$ , $V_b = 0\text{ mV}$ )



Exemplary spectral detectivity, the spectral response of delivered devices may differ.

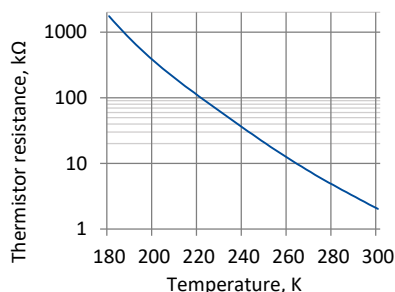
#### Specification ( $T_a = 20^\circ\text{C}$ , $V_b = 0\text{V}$ )

Parameter	Detector type						
	PV-2TE-3	PV-2TE-3.4	PV-2TE-4	PV-2TE-5	PV-2TE-6	PV-2TE-8	PV-2TE-10.6
Active element material	epitaxial HgCdTe heterostructure						
Optimum wavelength $\lambda_{opt}$ , μm	3.0	3.4	4.0	5.0	6.0	8.0	10.6
Detectivity $D^*(\lambda_{peak})$ , cm·Hz <sup>1/2</sup> /W	$\geq 1.0 \times 10^{11}$	$\geq 6.0 \times 10^{10}$	$\geq 4.0 \times 10^{10}$	$\geq 1.5 \times 10^{10}$	$\geq 5.0 \times 10^9$	$\geq 4.0 \times 10^8$	$\geq 2.0 \times 10^8$
Detectivity $D^*(\lambda_{opt})$ , cm·Hz <sup>1/2</sup> /W	$\geq 7.0 \times 10^{10}$	$\geq 4.0 \times 10^{10}$	$\geq 3.0 \times 10^{10}$	$\geq 9.0 \times 10^9$	$\geq 2.0 \times 10^9$	$\geq 2.0 \times 10^8$	$\geq 1.0 \times 10^8$
Current responsivity $R_i(\lambda_{opt})$ , A/W	$\geq 0.5$	$\geq 0.8$	$\geq 1.0$	$\geq 1.3$	$\geq 1.5$	$\geq 0.8$	$\geq 0.4$
Time constant $\tau$ , ns	$\leq 280$	$\leq 200$	$\leq 100$	$\leq 80$	$\leq 50$	$\leq 45$	$\leq 10$
Resistance-active area product $R \cdot A$ , $\Omega \cdot \text{cm}^2$	$\geq 150$	$\geq 3$	$\geq 2$	$\geq 0.1$	$\geq 0.02$	$\geq 0.0002$	$\geq 0.0001$
Active element temperature $T_{det}$ , K	~230						
Active area $A$ , mm×mm	0.05×0.05, 0.1×0.1					0.05×0.05	
Package	TO8, TO66						
Acceptance angle $\Phi$	~70°						
Window	wAl <sub>2</sub> O <sub>3</sub>				wZnSeAR		

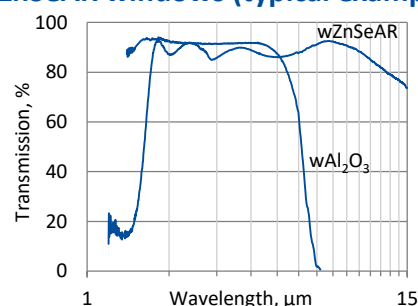
#### Two-stage thermoelectric cooler parameters

Parameter	Value
$T_{det}$ , K	~230
$V_{max}$ , V	1.3
$I_{max}$ , A	1.2
$Q_{max}$ , W	0.36

#### Thermistor characteristics

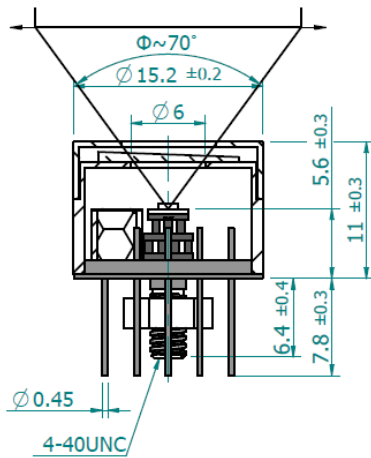


#### Spectral transmission of wAl<sub>2</sub>O<sub>3</sub> and wZnSeAR windows (typical example)



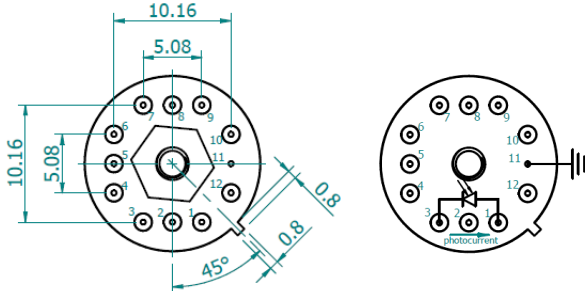
### Mechanical layout, mm

#### 2TE-T08 package



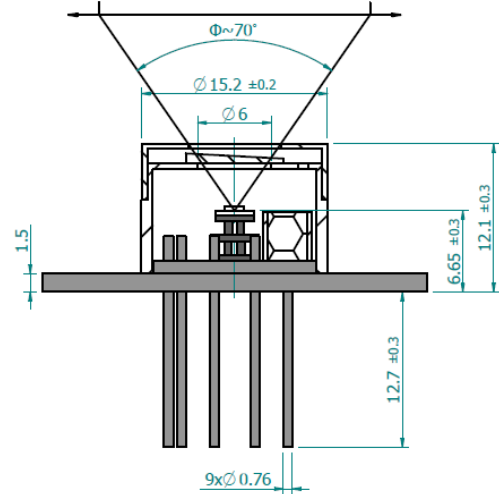
Φ – acceptance angle

Bottom view



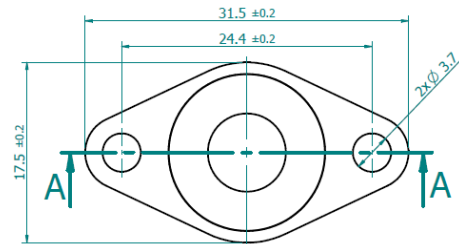
Function	Pin number
Detector	1, 3
Reverse bias (optional)	1(-), 3(+)
Thermistor	7, 9
TE cooler supply	2(+), 8(-)
Chassis ground	11
Not used	4, 5, 6, 10, 12

#### 2TE-T066 package

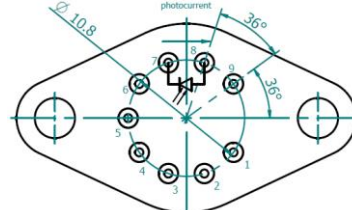


Φ – acceptance angle

Top view



Bottom view



Function	Pin number
Detector	7, 8
Reverse bias (optional)	7(+), 8(-)
Thermistor	5, 6
TE cooler supply	1(+), 9(-)
Not used	2, 3, 4

### Dedicated preamplifiers



„all-in-one“ AIP



programmable PIP



standard MIP



small SIP-T08



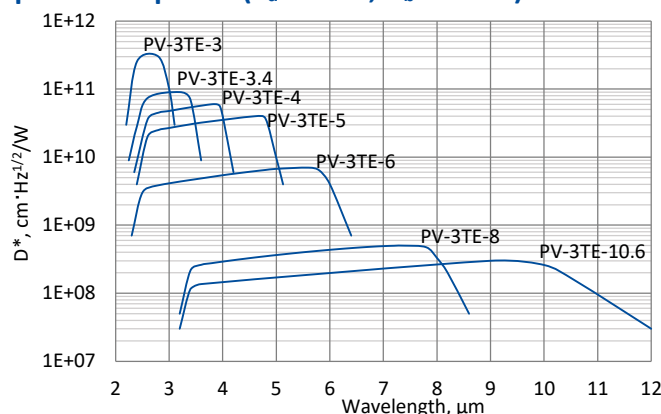
fast FIP

## PV-3TE series

### 2 – 12 μm HgCdTe three-stage thermoelectrically cooled photovoltaic detectors

**PV-3TE series** features three-stage thermoelectrically cooled IR photovoltaic detectors based on sophisticated HgCdTe heterostructures for the best performance and stability. The devices are optimized for the maximum performance at  $\lambda_{opt}$ . Cut-on wavelength can be optimized upon request. Reverse bias may significantly increase response speed and dynamic range. It also results in improved performance at high frequencies, but 1/f noise that appears in biased devices may reduce performance at low frequencies. 3° wedged sapphire (wAl<sub>2</sub>O<sub>3</sub>) or zinc selenide anti-reflection coated (wZnSeAR) window prevents unwanted interference effects.

#### Spectral response ( $T_a = 20^\circ\text{C}$ , $V_b = 0\text{ mV}$ )



Exemplary spectral detectivity, the spectral response of delivered devices may differ.

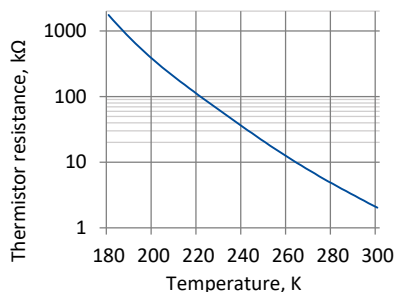
#### Specification ( $T_a = 20^\circ\text{C}$ , $V_b = 0\text{V}$ )

Parameter	Detector type						
	PV-3TE-3	PV-3TE-3.4	PV-3TE-4	PV-3TE-5	PV-3TE-6	PV-3TE-8	PV-3TE-10.6
Active element material	epitaxial HgCdTe heterostructure						
Optimum wavelength $\lambda_{opt}$ , μm	3.0	3.4	4.0	5.0	6.0	8.0	10.6
Detectivity $D^*(\lambda_{peak})$ , cm·Hz <sup>1/2</sup> /W	$\geq 3.0 \times 10^{11}$	$\geq 9.0 \times 10^{10}$	$\geq 6.0 \times 10^{10}$	$\geq 4.0 \times 10^{10}$	$\geq 7.0 \times 10^9$	$\geq 5.0 \times 10^8$	$\geq 3.0 \times 10^8$
Detectivity $D^*(\lambda_{opt})$ , cm·Hz <sup>1/2</sup> /W	$\geq 1.0 \times 10^{11}$	$\geq 7.0 \times 10^{10}$	$\geq 4.0 \times 10^{10}$	$\geq 1.0 \times 10^{10}$	$\geq 4.0 \times 10^9$	$\geq 3.0 \times 10^8$	$\geq 1.5 \times 10^8$
Current responsivity $R_i(\lambda_{opt})$ , A/W	$\geq 0.5$	$\geq 0.8$	$\geq 1.0$	$\geq 1.3$	$\geq 1.5$	$\geq 1.0$	$\geq 0.7$
Time constant $\tau$ , ns	$\leq 280$	$\leq 200$	$\leq 100$	$\leq 80$	$\leq 50$	$\leq 45$	$\leq 10$
Resistance-active area product $R \cdot A$ , $\Omega \cdot \text{cm}^2$	$\geq 240$	$\geq 15$	$\geq 6$	$\geq 0.3$	$\geq 0.025$	$\geq 0.0004$	$\geq 0.0002$
Active element temperature $T_{det}$ , K	~210						
Active area $A$ , mm×mm	0.05×0.05, 0.1×0.1					0.05×0.05	
Package	TO8, TO66						
Acceptance angle $\Phi$	~70°						
Window	wAl <sub>2</sub> O <sub>3</sub>				wZnSeAR		

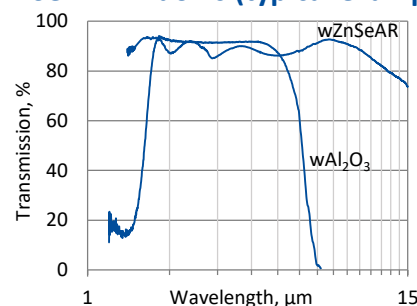
#### Three-stage thermoelectric cooler parameters

Parameter	Value
$T_{det}$ , K	~210
$V_{max}$ , V	3.6
$I_{max}$ , A	0.45
$Q_{max}$ , W	0.27

#### Thermistor characteristics

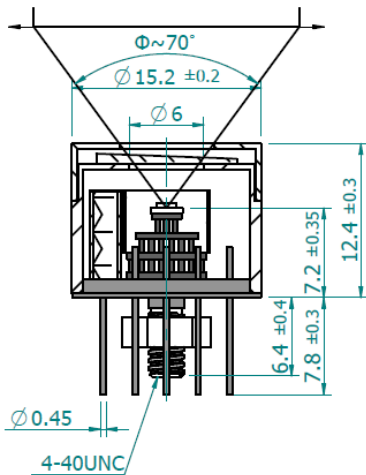


#### Spectral transmission of wAl<sub>2</sub>O<sub>3</sub> and wZnSeAR windows (typical example)



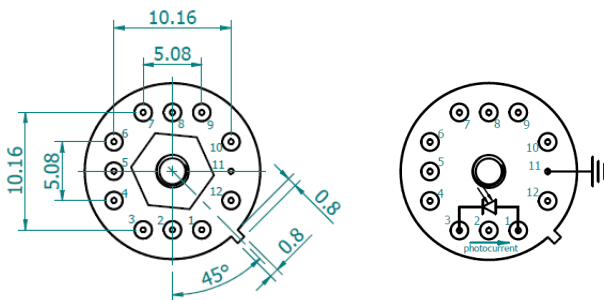
### Mechanical layout, mm

#### 3TE-T08 package



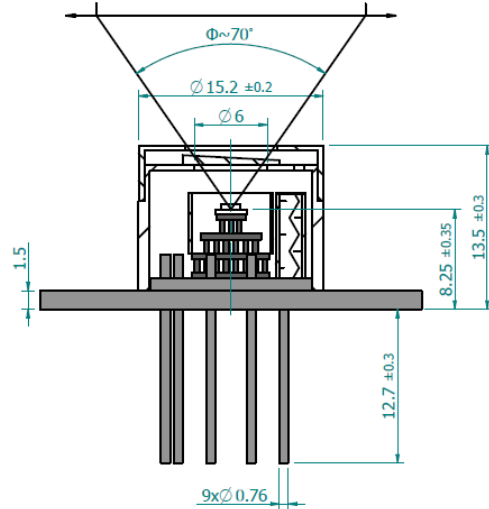
Φ – acceptance angle

#### Bottom view



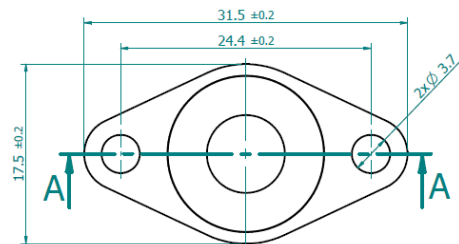
Function	Pin number
Detector	1, 3
Reverse bias (optional)	1(-), 3(+)
Thermistor	7, 9
TE cooler supply	2(+), 8(-)
Chassis ground	11
Not used	4, 5, 6, 10, 12

#### 3TE-T066 package

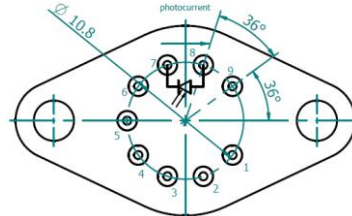


Φ – acceptance angle

#### Top view



#### Bottom view



Function	Pin number
Detector	7, 8
Reverse bias (optional)	7(+), 8(-)
Thermistor	5, 6
TE cooler supply	1(+), 9(-)
Not used	2, 3, 4

### Dedicated preamplifiers



„all-in-one“ AIP



programmable PIP



standard MIP



small SIP-T08



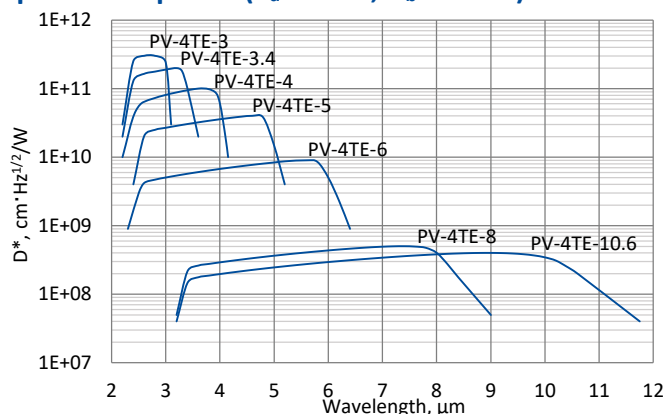
fast FIP

## PV-4TE series

### 2 – 12 μm HgCdTe four-stage thermoelectrically cooled photovoltaic detectors

**PV-4TE series** features four-stage thermoelectrically cooled IR photovoltaic detectors based on sophisticated HgCdTe heterostructures for the best performance and stability. The devices are optimized for the maximum performance at  $\lambda_{opt}$ . Cut-on wavelength can be optimized upon request. Reverse bias may significantly increase response speed and dynamic range. It also results in improved performance at high frequencies, but 1/f noise that appears in biased devices may reduce performance at low frequencies. 3° wedged sapphire (wAl<sub>2</sub>O<sub>3</sub>) or zinc selenide anti-reflection coated (wZnSeAR) window prevents unwanted interference effects.

#### Spectral response ( $T_a = 20^\circ\text{C}$ , $V_b = 0\text{ mV}$ )



Exemplary spectral detectivity, the spectral response of delivered devices may differ.

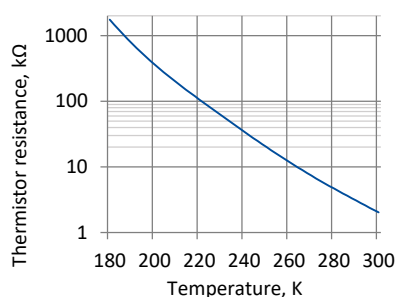
#### Specification ( $T_a = 20^\circ\text{C}$ , $V_b = 0\text{V}$ )

Parameter	Detector type						
	PV-4TE-3	PV-4TE-3.4	PV-4TE-4	PV-4TE-5	PV-4TE-6	PV-4TE-8	PV-4TE-10.6
Active element material	epitaxial HgCdTe heterostructure						
Optimum wavelength $\lambda_{opt}$ , μm	3.0	3.4	4.0	5.0	6.0	8.0	10.6
Detectivity $D^*(\lambda_{peak})$ , cm·Hz <sup>1/2</sup> /W	≥3.0×10 <sup>11</sup>	≥2.0×10 <sup>11</sup>	≥1.0×10 <sup>11</sup>	≥4.0×10 <sup>10</sup>	≥9.0×10 <sup>9</sup>	≥5.0×10 <sup>8</sup>	≥4.0×10 <sup>8</sup>
Detectivity $D^*(\lambda_{opt})$ , cm·Hz <sup>1/2</sup> /W	≥1.5×10 <sup>11</sup>	≥1.0×10 <sup>11</sup>	≥6.0×10 <sup>10</sup>	≥1.5×10 <sup>10</sup>	≥5.0×10 <sup>9</sup>	≥4.0×10 <sup>8</sup>	≥2.0×10 <sup>8</sup>
Current responsivity $R_i(\lambda_{opt})$ , A/W	≥0.5	≥0.8	≥1.0	≥1.3	≥1.5	≥1.5	≥0.5
Time constant $\tau$ , ns	≤280	≤200	≤100	≤80	≤50	≤45	≤25
Resistance-active area product $R \cdot A$ , Ω·cm <sup>2</sup>	≥300	≥20	≥8	≥0.4	≥0.03	≥0.0006	≥0.0005
Active element temperature $T_{det}$ , K	~195						
Active area $A$ , mm×mm	0.05×0.05, 0.1×0.1						
Package	TO8, TO66						
Acceptance angle $\Phi$	~70°						
Window	wAl <sub>2</sub> O <sub>3</sub>				wZnSeAR		

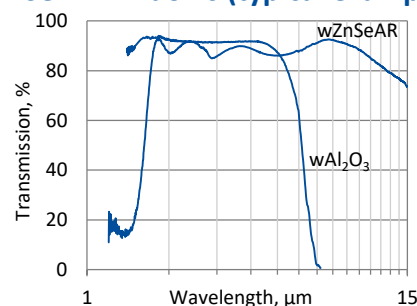
#### Four-stage thermoelectric cooler parameters

Parameter	Value
$T_{det}$ , K	~195
$V_{max}$ , V	8.3
$I_{max}$ , A	0.4
$Q_{max}$ , W	0.28

#### Thermistor characteristics

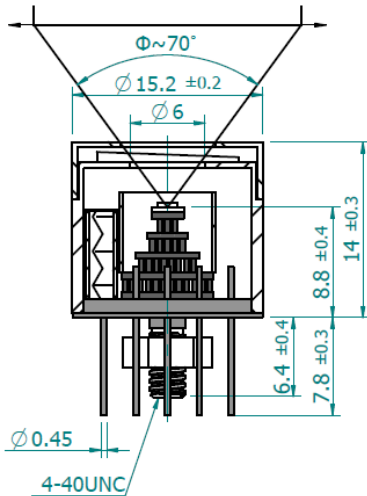


#### Spectral transmission of wAl<sub>2</sub>O<sub>3</sub> and wZnSeAR windows (typical example)



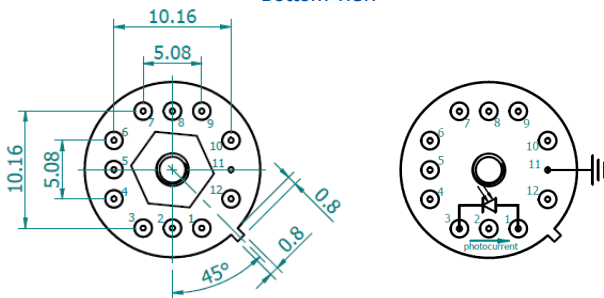
### Mechanical layout, mm

#### 4TE-TO8 package



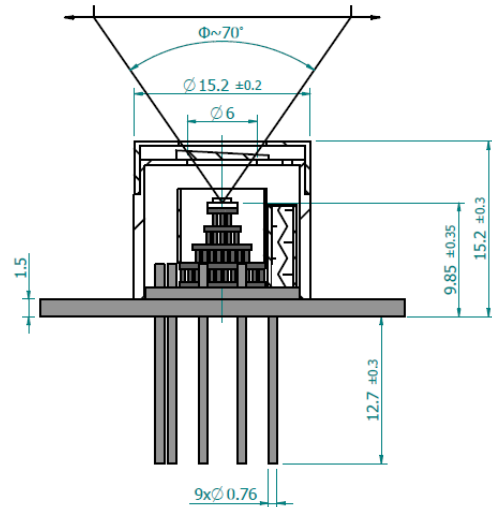
Φ – acceptance angle

#### Bottom view



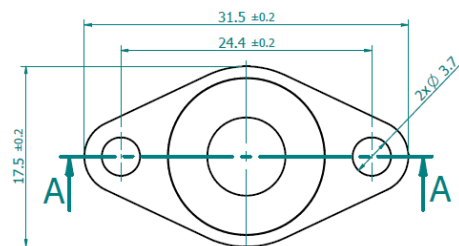
Function	Pin number
Detector	1, 3
Reverse bias (optional)	1(-), 3(+)
Thermistor	7, 9
TE cooler supply	2(+), 8(-)
Chassis ground	11
Not used	4, 5, 6, 10, 12

#### 4TE-TO66 package

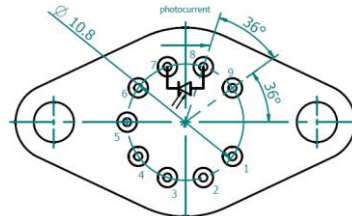


Φ – acceptance angle

#### Top view



#### Bottom view



Function	Pin number
Detector	7, 8
Reverse bias (optional)	7(+), 8(-)
Thermistor	5, 6
TE cooler supply	1(+), 9(-)
Not used	2, 3, 4

### Dedicated preamplifiers



„all-in-one“ AIP



programmable PIP



standard MIP



small SIP-TO8



fast FIP

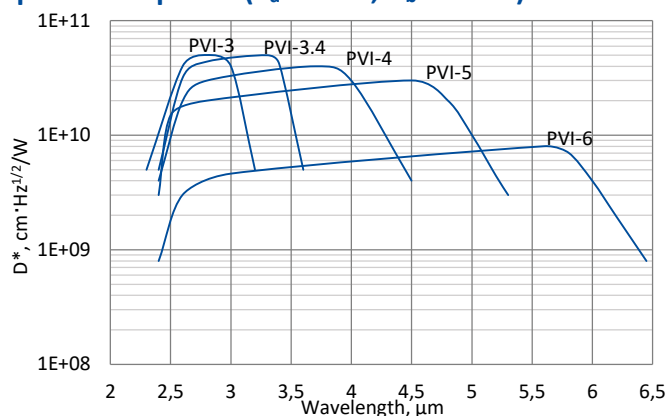


## PVI series

### 2.5 – 6.5 $\mu\text{m}$ HgCdTe ambient temperature, optically immersed photovoltaic detectors

**PVI series** features uncooled IR photovoltaic detectors based on sophisticated HgCdTe heterostructures for the best performance and stability, optically immersed in order to improve parameters of the devices. The detectors are optimized for the maximum performance at  $\lambda_{\text{opt}}$ . Cut-on wavelength can be optimized upon request. Reverse bias may significantly increase speed of response and dynamic range. It results also in improved performance at high frequencies, but  $1/f$  noise that appears in biased devices may reduce performance at low frequencies.

#### Spectral response ( $T_a = 20^\circ\text{C}$ , $V_b = 0\text{ mV}$ )

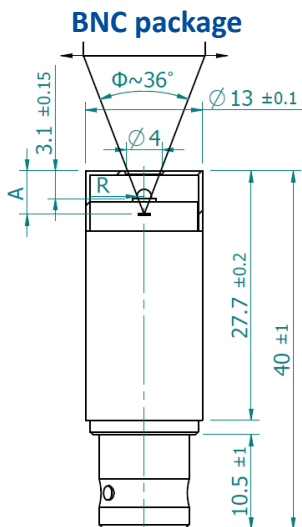


Exemplary spectral detectivity, the spectral response of delivered devices may differ.

#### Specification ( $T_a = 20^\circ\text{C}$ , $V_b = 0\text{ mV}$ )

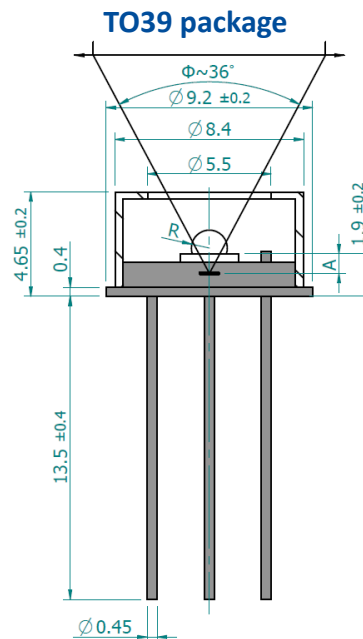
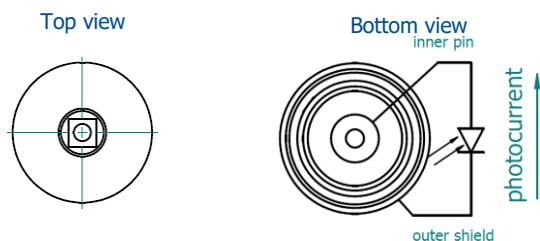
Parameter	Detector type				
	PVI-3	PVI-3.4	PVI-4	PVI-5	PVI-6
Active element material	epitaxial HgCdTe heterostructure				
Optimum wavelength $\lambda_{\text{opt}}$ , $\mu\text{m}$	3.0	3.4	4.0	5.0	6.0
Detectivity $D^*(\lambda_{\text{peak}})$ , $\text{cm}\cdot\text{Hz}^{1/2}/\text{W}$	$\geq 5.0 \times 10^{10}$	$\geq 5.0 \times 10^{10}$	$\geq 3.0 \times 10^{10}$	$\geq 1.5 \times 10^{10}$	$\geq 8.0 \times 10^9$
Detectivity $D^*(\lambda_{\text{opt}})$ , $\text{cm}\cdot\text{Hz}^{1/2}/\text{W}$	$\geq 5.0 \times 10^{10}$	$\geq 4.5 \times 10^{10}$	$\geq 2.0 \times 10^{10}$	$\geq 9.0 \times 10^9$	$\geq 4.0 \times 10^9$
Current responsivity $R_i(\lambda_{\text{opt}})$ , $\text{A}/\text{W}$	$\geq 0.5$	$\geq 0.8$		$\geq 1.0$	
Time constant $\tau$ , ns	$\leq 350$	$\leq 260$	$\leq 150$	$\leq 120$	$\leq 80$
Resistance-optical area product $R \cdot A_o$ , $\Omega \cdot \text{cm}^2$	$\geq 100$	$\geq 50$	$\geq 6$	$\geq 1$	$\geq 0.2$
Optical area $A_o$ , $\text{mm} \times \text{mm}$	0.5×0.5, 1×1				
Package	TO39, BNC				
Acceptance angle $\Phi$	$\sim 36^\circ$				
Window	none				

**Mechanical layout, mm**



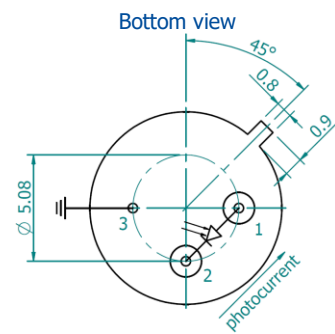
Parameter	Value	
Immersion microlens shape	hyperhemisphere	
Optical area $A_o$ , mm×mm	0.5×0.5	1×1
R, mm	0.5	0.8
A, mm	4.6±0.3	5.5±0.3

$\Phi$  – acceptance angle  
R – hyperhemisphere microlens radius  
A – distance from the top of BNC package to the focal plane



Parameter	Value	
Immersion microlens shape	hyperhemisphere	
Optical area $A_o$ , mm×mm	0.5×0.5	1×1
R, mm	0.5	0.8
A, mm	1.5±0.2	2.4±0.2

$\Phi$  – acceptance angle  
R – hyperhemisphere microlens radius  
A – distance from the bottom of hyperhemisphere microlens to the focal plane



Function	Pin number
Detector	1, 2
Reverse bias (optional)	1(-), 2(+)
Chassis ground	3

**Dedicated preamplifier**



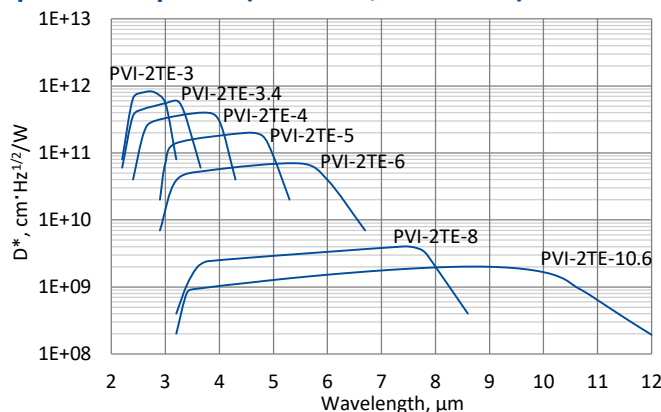
small SIP-TO39

## PVI-2TE series

### 2 – 12 $\mu\text{m}$ HgCdTe two-stage thermoelectrically cooled, optically immersed photovoltaic detectors

**PVI-2TE series** features two-stage thermoelectrically cooled IR photovoltaic detectors based on sophisticated HgCdTe heterostructures for the best performance and stability, optically immersed in order to improve parameters of the devices. The detectors are optimized for the maximum performance at  $\lambda_{\text{opt}}$ . Cut-on wavelength can be optimized upon request. Reverse bias may significantly increase speed of response and dynamic range. It results also in improved performance at high frequencies, but  $1/f$  noise that appears in biased devices may reduce performance at low frequencies.  $3^\circ$  wedged sapphire ( $\text{wAl}_2\text{O}_3$ ) or zinc selenide anti-reflection coated ( $\text{wZnSeAR}$ ) window prevents unwanted interference effects.

#### Spectral response ( $T_a = 20^\circ\text{C}$ , $V_b = 0\text{ mV}$ )



Exemplary spectral detectivity, the spectral response of delivered devices may differ.

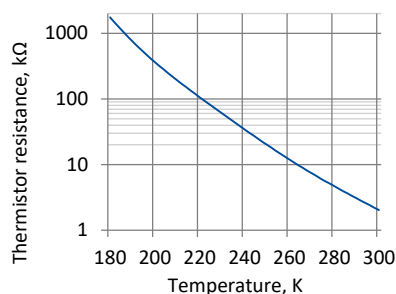
#### Specification ( $T_a = 20^\circ\text{C}$ , $V_b = 0\text{ V}$ )

Parameter	Detector type						
	PVI-2TE-3	PVI-2TE-3.4	PVI-2TE-4	PVI-2TE-5	PVI-2TE-6	PVI-2TE-8	PVI-2TE-10.6
Active element material	epitaxial HgCdTe heterostructure						
Optimum wavelength $\lambda_{\text{opt}}$ , $\mu\text{m}$	3.0	3.4	4.0	5.0	6.0	8.0	10.6
Detectivity $D^*(\lambda_{\text{peak}})$ , $\text{cm}^2\cdot\text{Hz}^{1/2}/\text{W}$	$\geq 8.0 \times 10^{11}$	$\geq 6.0 \times 10^{11}$	$\geq 4.0 \times 10^{11}$	$\geq 2.0 \times 10^{11}$	$\geq 7.0 \times 10^{10}$	$\geq 4.0 \times 10^9$	$\geq 2.0 \times 10^9$
Detectivity $D^*(\lambda_{\text{opt}})$ , $\text{cm}^2\cdot\text{Hz}^{1/2}/\text{W}$	$\geq 5.5 \times 10^{11}$	$\geq 3.0 \times 10^{11}$	$\geq 3.0 \times 10^{11}$	$\geq 9.0 \times 10^{10}$	$\geq 4.0 \times 10^{10}$	$\geq 2.0 \times 10^9$	$\geq 1.0 \times 10^9$
Current responsivity $R_i(\lambda_{\text{opt}})$ , $\text{A}/\text{W}$	$\geq 0.5$	$\geq 0.8$	$\geq 1.3$	$\geq 1.3$	$\geq 1.5$	$\geq 0.8$	$\geq 0.4$
Time constant $\tau$ , ns	$\leq 280$	$\leq 200$	$\leq 100$	$\leq 80$	$\leq 50$	$\leq 45$	$\leq 10$
Resistance-optical area product $R \cdot A_o$ , $\Omega \cdot \text{cm}^2$	$\geq 15000$	$\geq 300$	$\geq 200$	$\geq 10$	$\geq 2$	$\geq 0.02$	$\geq 0.01$
Active element temperature $T_{\text{det}}$ , K	$\sim 230$						
Optical area $A_o$ , $\text{mm} \times \text{mm}$	$0.5 \times 0.5, 1 \times 1$						$0.5 \times 0.5$
Package	TO8, TO66						
Acceptance angle $\Phi$	$\sim 36^\circ$						
Window	$\text{wAl}_2\text{O}_3$				$\text{wZnSeAR}$		

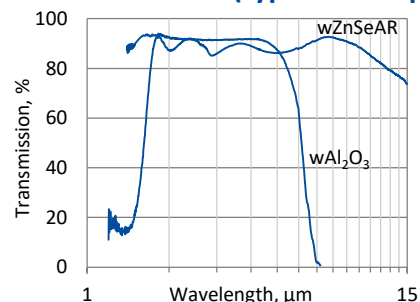
#### Two-stage thermoelectric cooler parameters

Parameter	Value
$T_{\text{det}}$ , K	$\sim 230$
$V_{\text{max}}$ , V	1.3
$I_{\text{max}}$ , A	1.2
$Q_{\text{max}}$ , W	0.36

#### Thermistor characteristics

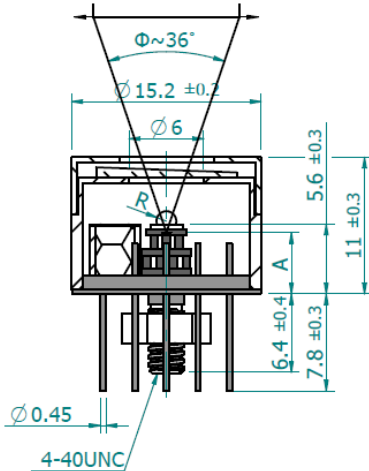


#### Spectral transmission of $\text{wAl}_2\text{O}_3$ and $\text{wZnSeAR}$ windows (typical example)



**Mechanical layout, mm**

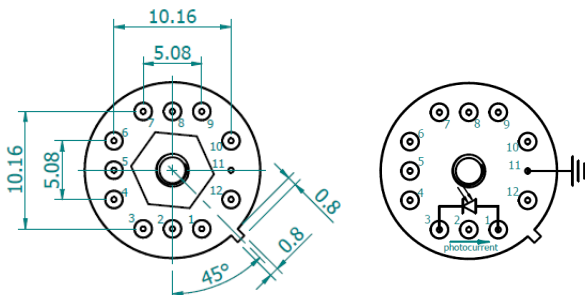
**2TE-T08 package**



Parameter	Value
Immersion microlens shape	hyperhemisphere
Optical area $A_0$ , mm×mm	0.5×0.5 1×1
R, mm	0.5 0.8
A, mm	4.1±0.3 3.2±0.3

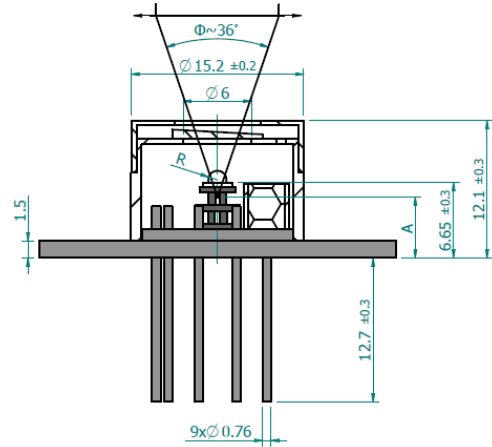
Φ – acceptance angle  
R – hyperhemisphere microlens radius  
A – distance from the bottom of 2TE-T08 header to the focal plane

**Bottom view**



Function	Pin number
Detector	1, 3
Reverse bias (optional)	1(-), 3(+)
Thermistor	7, 9
TE cooler supply	2(+), 8(-)
Chassis ground	11
Not used	4, 5, 6, 10, 12

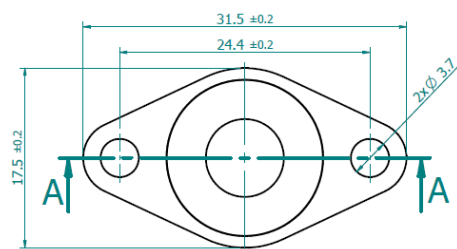
**2TE-T066 package**



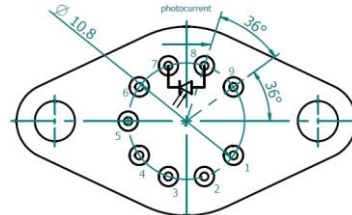
Parameter	Value
Immersion microlens shape	hyperhemisphere
Optical area $A_0$ , mm×mm	0.5×0.5 1×1
R, mm	0.5 0.8
A, mm	5.15±0.30 3.2±0.3

Φ – acceptance angle  
R – hyperhemisphere microlens radius  
A – distance from the bottom of 2TE-T066 header to the focal plane

**Top view**



**Bottom view**



Function	Pin number
Detector	7, 8
Reverse bias (optional)	7(+), 8(-)
Thermistor	5, 6
TE cooler supply	1(+), 9(-)
Not used	2, 3, 4

**Dedicated preamplifiers**



„all-in-one“ AIP



programmable PIP



standard MIP



small SIP-T08



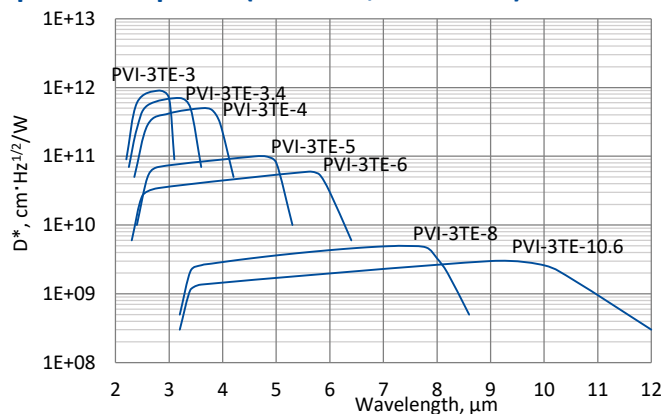
fast FIP

## PVI-3TE series

### 2 – 12 $\mu\text{m}$ HgCdTe three-stage thermoelectrically cooled, optically immersed photovoltaic detectors

**PVI-3TE series** features three-stage thermoelectrically cooled IR photovoltaic detectors based on sophisticated HgCdTe heterostructures for the best performance and stability, optically immersed in order to improve parameters of the devices. The detectors are optimized for the maximum performance at  $\lambda_{\text{opt}}$ . Cut-on wavelength can be optimized upon request. Reverse bias may significantly increase speed of response and dynamic range. It results also in improved performance at high frequencies, but 1/f noise that appears in biased devices may reduce performance at low frequencies. 3° wedged sapphire ( $\text{wAl}_2\text{O}_3$ ) or zinc selenide anti-reflection coated ( $\text{wZnSeAR}$ ) window prevents unwanted interference effects.

#### Spectral response ( $T_a = 20^\circ\text{C}$ , $V_b = 0 \text{ mV}$ )



Exemplary spectral detectivity, the spectral response of delivered devices may differ.

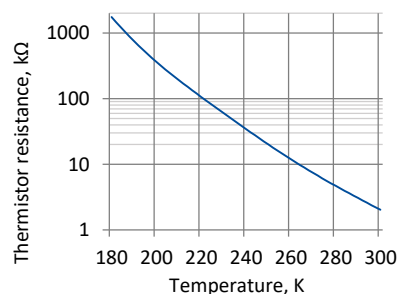
#### Specification ( $T_a = 20^\circ\text{C}$ , $V_b = 0 \text{ mV}$ )

Parameter	Detector type						
	PVI-3TE-3	PVI-3TE-3.4	PVI-3TE-4	PVI-3TE-5	PVI-3TE-6	PVI-3TE-8	PVI-3TE-10.6
Active element material	epitaxial HgCdTe heterostructure						
Optimum wavelength $\lambda_{\text{opt}}$ , $\mu\text{m}$	3.0	3.4	4.0	5.0	6.0	8.0	10.6
Detectivity $D^*(\lambda_{\text{peak}})$ , $\text{cm}\cdot\text{Hz}^{1/2}/\text{W}$	$\geq 9.0 \times 10^{11}$	$\geq 7.0 \times 10^{11}$	$\geq 5.0 \times 10^{11}$	$\geq 1.0 \times 10^{11}$	$\geq 6.0 \times 10^{10}$	$\geq 5.0 \times 10^9$	$\geq 3.0 \times 10^9$
Detectivity $D^*(\lambda_{\text{opt}})$ , $\text{cm}\cdot\text{Hz}^{1/2}/\text{W}$	$\geq 7.0 \times 10^{11}$	$\geq 5.0 \times 10^{11}$	$\geq 3.0 \times 10^{11}$	$\geq 8.0 \times 10^{10}$	$\geq 3.0 \times 10^{10}$	$\geq 3.0 \times 10^9$	$\geq 1.5 \times 10^9$
Current responsivity $R_i(\lambda_{\text{opt}})$ , $\text{A}/\text{W}$	$\geq 0.5$	$\geq 0.8$	$\geq 1.0$	$\geq 1.3$	$\geq 1.5$	$\geq 1.0$	$\geq 0.7$
Time constant $\tau$ , ns	$\leq 280$	$\leq 200$	$\leq 100$	$\leq 80$	$\leq 50$	$\leq 45$	$\leq 10$
Resistance-optical area product $R \cdot A_o$ , $\Omega \cdot \text{cm}^2$	$\geq 24000$	$\geq 1500$	$\geq 600$	$\geq 30$	$\geq 2.5$	$\geq 0.04$	$\geq 0.02$
Active element temperature $T_{\text{det}}$ , K	$\sim 210$						
Optical area $A_o$ , $\text{mm} \times \text{mm}$	$0.5 \times 0.5$ , $1 \times 1$						$0.5 \times 0.5$
Package	TO8, TO66						
Acceptance angle $\Phi$	$\sim 36^\circ$						
Window	$\text{wAl}_2\text{O}_3$				$\text{wZnSeAR}$		

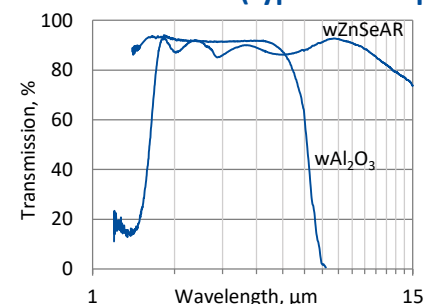
#### Three-stage thermoelectric cooler parameters

Parameter	Value
$T_{\text{det}}$ , K	$\sim 210$
$V_{\text{max}}$ , V	3.6
$I_{\text{max}}$ , A	0.45
$Q_{\text{max}}$ , W	0.27

#### Thermistor characteristics

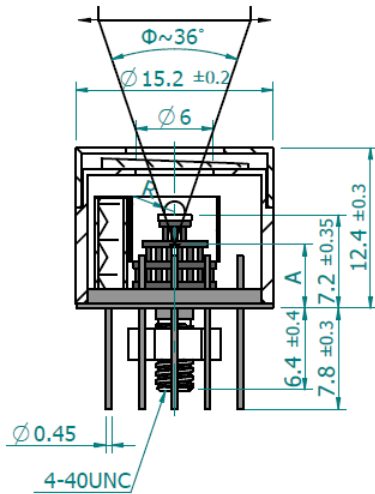


#### Spectral transmission of $\text{wAl}_2\text{O}_3$ and $\text{wZnSeAR}$ windows (typical example)



### Mechanical layout, mm

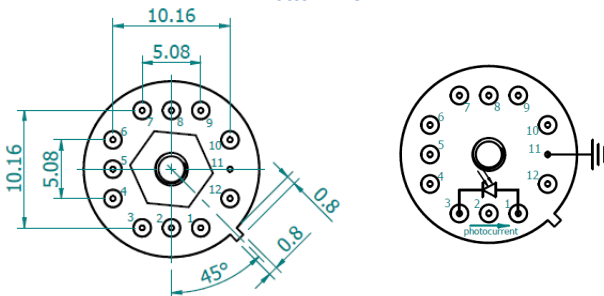
#### 3TE-T08 package



Parameter	Value	
Immersion microlens shape	hyperhemisphere	
Optical area $A_o$ , mm×mm	0.5×0.5	1×1
R, mm	0.5	0.8
A, mm	5.7±0.35	4.8±0.35

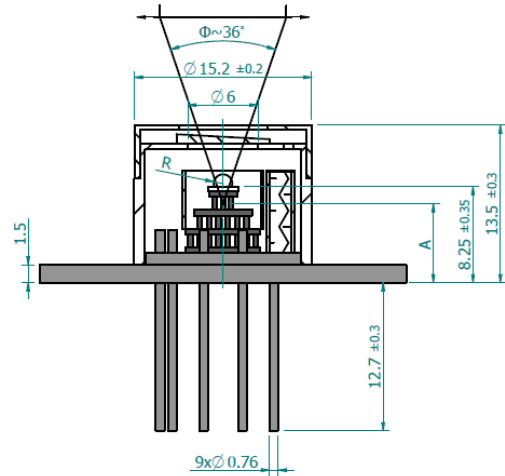
Φ – acceptance angle  
 R – hyperhemisphere microlens radius  
 A – distance from the bottom of 3TE-T08 header to the focal plane

Bottom view



Function	Pin number
Detector	1, 3
Reverse bias (optional)	1(-), 3(+)
Thermistor	7, 9
TE cooler supply	2(+), 8(-)
Chassis ground	11
Not used	4, 5, 6, 10, 12

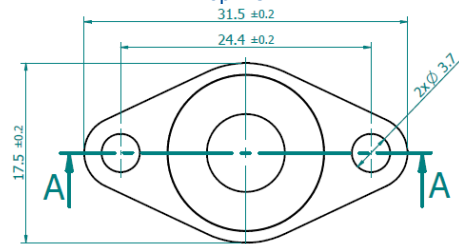
#### 3TE-T066 package



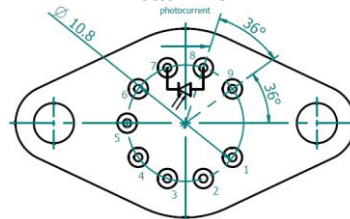
Parameter	Value	
Immersion microlens shape	hyperhemisphere	
Optical area $A_o$ , mm×mm	0.5×0.5	1×1
R, mm	0.5	0.8
A, mm	6.75±0.35	5.85±0.35

Φ – acceptance angle  
 R – hyperhemisphere microlens radius  
 A – distance from the bottom of 3TE-T066 header to the focal plane

Top view



Bottom view



Function	Pin number
Detector	7, 8
Reverse bias (optional)	7(+), 8(-)
Thermistor	5, 6
TE cooler supply	1(+), 9(-)
Not used	2, 3, 4

### Dedicated preamplifiers



„all-in-one“ AIP



programmable PIP



standard MIP



small SIP-T08



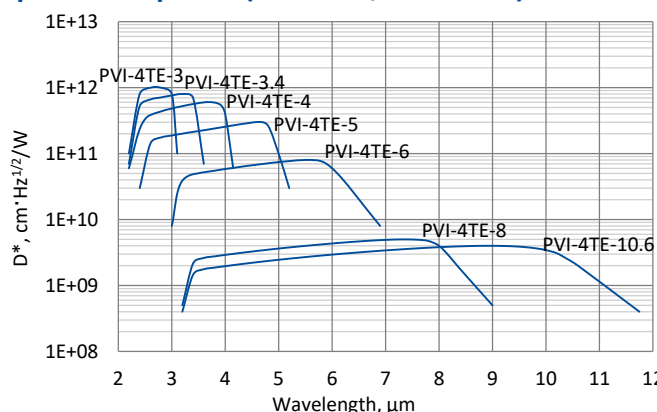
fast FIP

## PVI-4TE series

### 2 – 12 $\mu\text{m}$ HgCdTe four-stage thermoelectrically cooled, optically immersed photovoltaic detectors

**PVI-4TE series** features four-stage thermoelectrically cooled IR photovoltaic detectors based on sophisticated HgCdTe heterostructures for the best performance and stability, optically immersed in order to improve parameters of the devices. The detectors are optimized for the maximum performance at  $\lambda_{\text{opt}}$ . Cut-on wavelength can be optimized upon request. Reverse bias may significantly increase speed of response and dynamic range. It results also in improved performance at high frequencies, but  $1/f$  noise that appears in biased devices may reduce performance at low frequencies.  $3^\circ$  wedged sapphire ( $\text{wAl}_2\text{O}_3$ ) or zinc selenide anti-reflection coated ( $\text{wZnSeAR}$ ) window prevents unwanted interference effects.

#### Spectral response ( $T_a = 20^\circ\text{C}$ , $V_b = 0 \text{ mV}$ )



Exemplary spectral detectivity, the spectral response of delivered devices may differ.

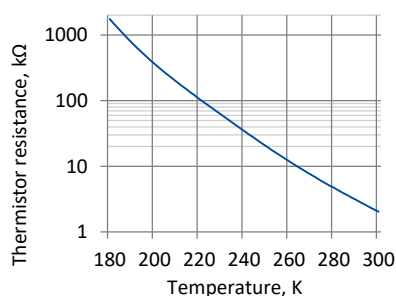
#### Specification ( $T_a = 20^\circ\text{C}$ , $V_b = 0 \text{ V}$ )

Parameter	Detector type						
	PVI-4TE-3	PVI-4TE-3.4	PVI-4TE-4	PVI-4TE-5	PVI-4TE-6	PVI-4TE-8	PVI-4TE-10.6
Active element material	epitaxial HgCdTe heterostructure						
Optimum wavelength $\lambda_{\text{opt}}$ , $\mu\text{m}$	3.0	3.4	4.0	5.0	6.0	8.0	10.6
Detectivity $D^*(\lambda_{\text{peak}})$ , $\text{cm}\cdot\text{Hz}^{1/2}/\text{W}$	$\geq 1.0 \times 10^{12}$	$\geq 8.0 \times 10^{11}$	$\geq 6.0 \times 10^{11}$	$\geq 3.0 \times 10^{11}$	$\geq 8.0 \times 10^{10}$	$\geq 5.0 \times 10^9$	$\geq 4.0 \times 10^9$
Detectivity $D^*(\lambda_{\text{opt}})$ , $\text{cm}\cdot\text{Hz}^{1/2}/\text{W}$	$\geq 8.0 \times 10^{11}$	$\geq 7.0 \times 10^{11}$	$\geq 4.0 \times 10^{11}$	$\geq 1.0 \times 10^{11}$	$\geq 6.0 \times 10^{10}$	$\geq 4.0 \times 10^9$	$\geq 2.0 \times 10^9$
Current responsivity $R_i(\lambda_{\text{opt}})$ , $\text{A}/\text{W}$	$\geq 0.5$	$\geq 0.8$	$\geq 1.0$	$\geq 1.3$	$\geq 1.5$	$\geq 0.5$	$\geq 0.5$
Time constant $\tau$ , ns	$\leq 280$	$\leq 200$	$\leq 100$	$\leq 80$	$\leq 50$	$\leq 45$	$\leq 25$
Resistance-optical area product $R \cdot A_o$ , $\Omega \cdot \text{cm}^2$	$\geq 30000$	$\geq 2000$	$\geq 800$	$\geq 40$	$\geq 3$	$\geq 0.06$	$\geq 0.05$
Active element temperature $T_{\text{det}}$ , K	~195						
Optical area $A_o$ , $\text{mm} \times \text{mm}$	0.5×0.5, 1×1						
Package	TO8, TO66						
Acceptance angle $\Phi$	~36°						
Window	$\text{wAl}_2\text{O}_3$				$\text{wZnSeAR}$		

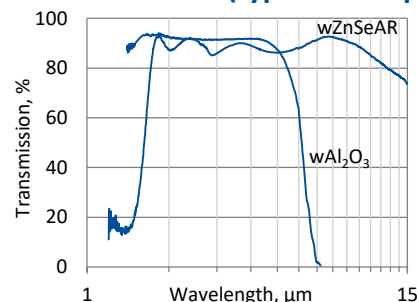
#### Four-stage thermoelectric cooler parameters

Parameter	Value
$T_{\text{det}}$ , K	~195
$V_{\text{max}}$ , V	8.3
$I_{\text{max}}$ , A	0.4
$Q_{\text{max}}$ , W	0.28

#### Thermistor characteristics

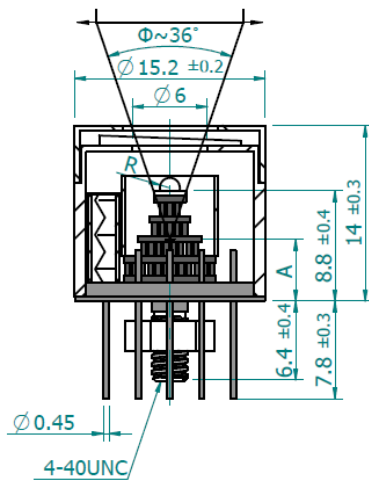


#### Spectral transmission of $\text{wAl}_2\text{O}_3$ and $\text{wZnSeAR}$ windows (typical example)



### Mechanical layout, mm

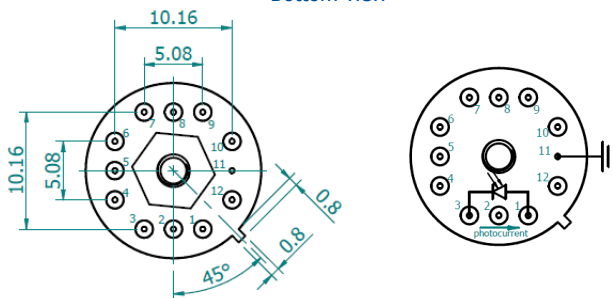
#### 4TE-T08 package



Parameter	Value
Immersion microlens shape	hyperhemisphere
Optical area $A_0$ , mm×mm	0.5×0.5 1×1
R, mm	0.5 0.8
A, mm	7.3±0.4 6.4±0.4

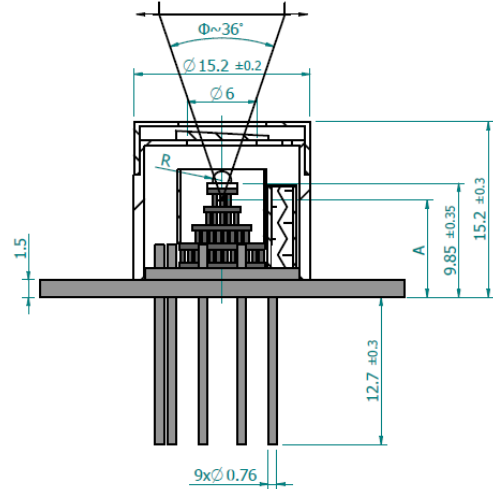
Φ – acceptance angle  
 R – hyperhemisphere microlens radius  
 A – distance from the bottom of 4TE-T08 header to the focal plane

#### Bottom view



Function	Pin number
Detector	1, 3
Reverse bias (optional)	1(-), 3(+)
Thermistor	7, 9
TE cooler supply	2(+), 8(-)
Chassis ground	11
Not used	4, 5, 6, 10, 12

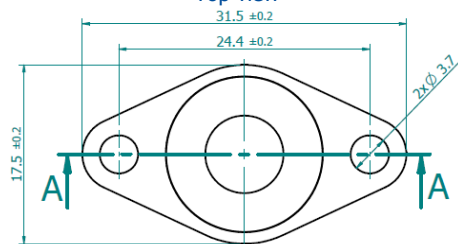
#### 4TE-T066 package



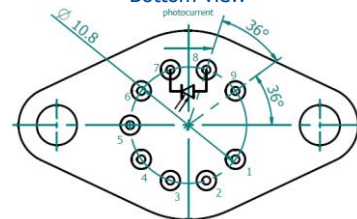
Parameter	Value
Immersion microlens shape	hyperhemisphere
Optical area $A_0$ , mm×mm	0.5×0.5 1×1
R, mm	0.5 0.8
A, mm	8.35±0.40 7.45±0.40

Φ – acceptance angle  
 R – hyperhemisphere microlens radius  
 A – distance from the bottom of 4TE-T066 header to the focal plane

#### Top view



#### Bottom view



Function	Pin number
Detector	7, 8
Reverse bias (optional)	7(+), 8(-)
Thermistor	5, 6
TE cooler supply	1(+), 9(-)
Not used	2, 3, 4

### Dedicated preamplifiers



„all-in-one“ AIP



programmable PIP



standard MIP



small SIP-T08



fast FIP

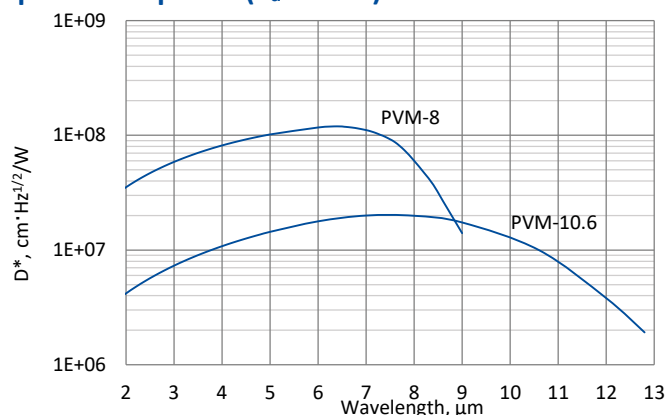


## PVM series

### 2 – 13 $\mu\text{m}$ HgCdTe ambient temperature photovoltaic multiple junction detectors

**PVM series** features uncooled IR photovoltaic multiple junction detectors based on sophisticated HgCdTe heterostructures for the best performance and stability. The detectors are optimized for the maximum performance at  $\lambda_{\text{opt}}$ . They are especially useful as large active area detectors operating within 2 to 13  $\mu\text{m}$  spectral range.

#### Spectral response ( $T_a = 20^\circ\text{C}$ )



Exemplary spectral detectivity, the spectral response of delivered devices may differ.

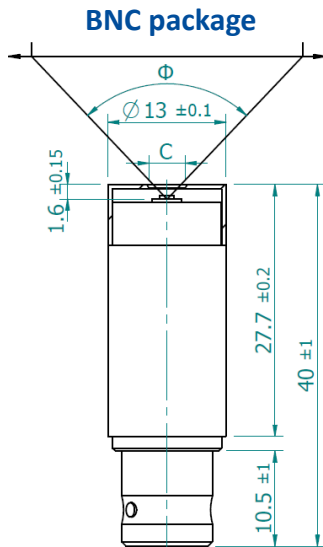
#### Specification ( $T_a = 20^\circ\text{C}$ )

Parameter	Detector type			
	PVM-8		PVM-10.6	
Active element material	epitaxial HgCdTe heterostructure			
Optimal wavelength $\lambda_{\text{opt}}$ , $\mu\text{m}$	8.0		10.6	
Detectivity $D^*(\lambda_{\text{peak}})$ , $\text{cm}\cdot\text{Hz}^{1/2}/\text{W}$	$\geq 1.2 \times 10^8$		$\geq 2.0 \times 10^7$	
Detectivity $D^*(\lambda_{\text{opt}})$ , $\text{cm}\cdot\text{Hz}^{1/2}/\text{W}$	$\geq 6.0 \times 10^7$		$\geq 1.0 \times 10^7$	
Current responsivity-active area length product $R(\lambda_{\text{opt}}) \cdot L$ , $\text{A}\cdot\text{mm}/\text{W}$	$\geq 0.008$		$\geq 0.002$	
Time constant $\tau$ , ns	$\leq 4$		$\leq 1.5$	
Resistance $R$ , $\Omega$	50 to 300		20 to 150	
Active area $A$ , $\text{mm}\times\text{mm}$	1 $\times$ 1, 2 $\times$ 2, 3 $\times$ 3, 4 $\times$ 4			
Package	TO39	BNC	TO39	BNC
Acceptance angle $\Phi$	$\sim 90^\circ$	$\sim 102^\circ$ *) , $\sim 124^\circ$ **) )	$\sim 90^\circ$	$\sim 102^\circ$ *) , $\sim 124^\circ$ **) )
Window	none			

\*) Aperture  $C = \varnothing 4$  mm.

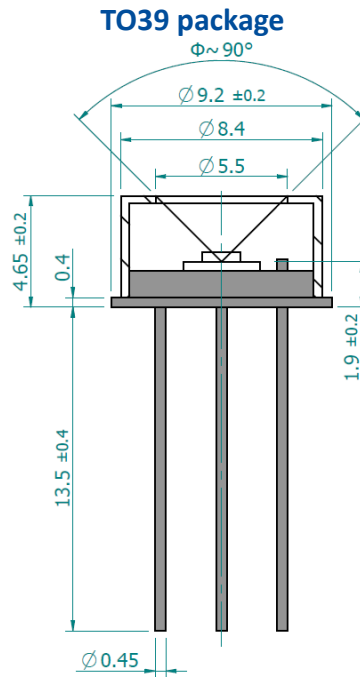
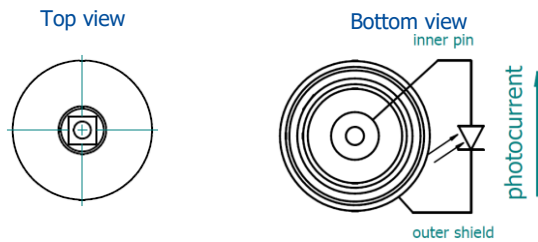
\*\*) Aperture  $C = \varnothing 6$  mm.

**Mechanical layout, mm**

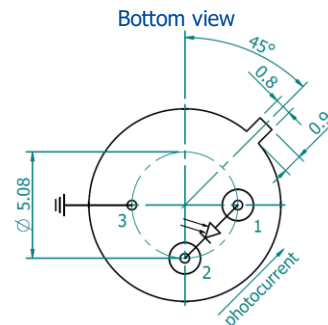


Parameter	Value
Active area, mm×mm	1×1, 2×2 3×3, 4×4
C, mm	Ø4 Ø6
Acceptance angle $\Phi$	~102° ~124°

C - aperture



$\Phi$  - acceptance angle



Function	Pin number
Detector	1, 2
Chassis ground	3

**Dedicated preamplifier**



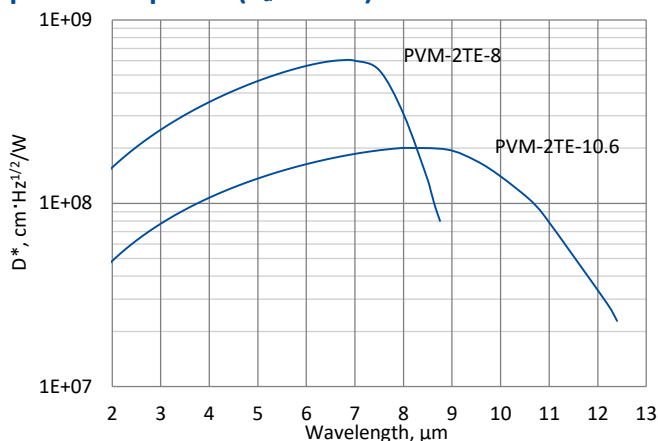
small SIP-TO39

## PVM-2TE series

### 2 – 12 $\mu\text{m}$ HgCdTe two-stage thermoelectrically cooled photovoltaic multiple junction detectors

**PVM-2TE series** features two-stage thermoelectrically cooled IR photovoltaic multiple junction detectors based on sophisticated HgCdTe heterostructures for the best performance and stability. The detectors are optimized for the maximum performance at  $\lambda_{\text{opt}}$ . They are especially useful as large active area detectors operating within 2 to 12  $\mu\text{m}$  spectral range.  $3^\circ$  wedged zinc selenide anti-reflection coated (wZnSeAR) window prevents unwanted interference effects.

#### Spectral response ( $T_a = 20^\circ\text{C}$ )



Exemplary spectral detectivity, the spectral response of delivered devices may differ.

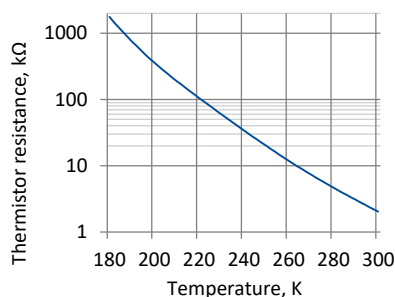
#### Specification ( $T_a = 20^\circ\text{C}$ )

Parameter	Detector type	
	PVM-2TE-8	PVM-2TE-10.6
Active element material	epitaxial HgCdTe heterostructure	
Optimal wavelength $\lambda_{\text{opt}}$ , $\mu\text{m}$	8.0	10.6
Detectivity $D^*(\lambda_{\text{peak}})$ , $\text{cm}\cdot\text{Hz}^{1/2}/\text{W}$	$\geq 6.0 \times 10^8$	$\geq 2.0 \times 10^8$
Detectivity $D^*(\lambda_{\text{opt}})$ , $\text{cm}\cdot\text{Hz}^{1/2}/\text{W}$	$\geq 3.0 \times 10^8$	$\geq 1.0 \times 10^8$
Current responsivity-active area length product $R_i(\lambda_{\text{opt}}) \cdot L$ , $\text{A}\cdot\text{mm}/\text{W}$	$\geq 0.015$	$\geq 0.01$
Time constant $\tau$ , ns	$\leq 4$	$\leq 4$
Resistance $R$ , $\Omega$	150 to 1200	90 to 350
Active element temperature $T_{\text{det}}$ , K	$\sim 230$	
Active area $A$ , $\text{mm}\times\text{mm}$	1×1, 2×2, 3×3	
Package	TO8, TO66	
Acceptance angle $\Phi$	$\sim 70^\circ$	
Window	wZnSeAR	

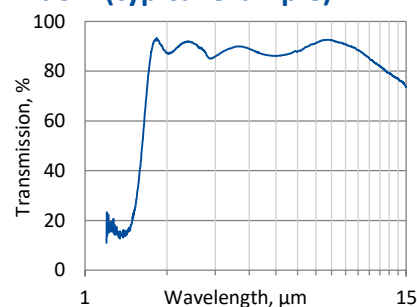
#### Two-stage thermoelectric cooler parameters

Parameter	Value
$T_{\text{det}}$ , K	$\sim 230$
$V_{\text{max}}$ , V	1.3
$I_{\text{max}}$ , A	1.2
$Q_{\text{max}}$ , W	0.36

#### Thermistor characteristics

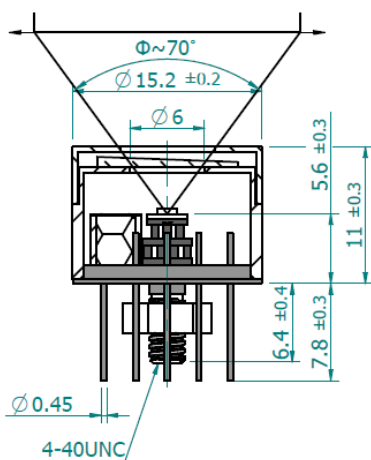


#### Spectral transmission of wZnSeAR window (typical example)



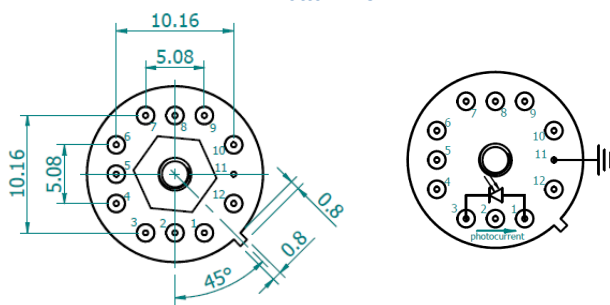
**Mechanical layout, mm**

**2TE-T08 package**



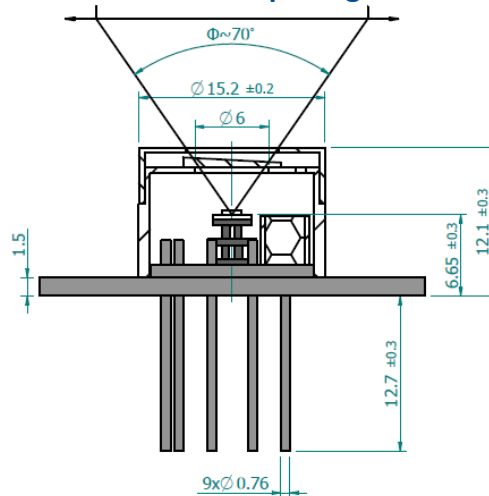
Φ – acceptance angle

Bottom view



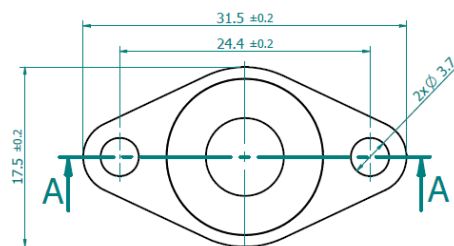
Function	Pin number
Detector	1, 3
Thermistor	7, 9
TE cooler supply	2(+), 8(-)
Chassis ground	11
Not used	4, 5, 6, 10, 12

**2TE-T066 package**

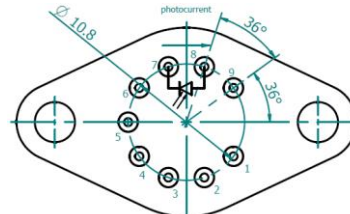


Φ – acceptance angle

Top view



Bottom view



Function	Pin number
Detector	7, 8
Thermistor	5, 6
TE cooler supply	1(+), 9(-)
Not used	2, 3, 4

**Dedicated preamplifiers**



„all-in-one“ AIP



programmable PIP



standard MIP



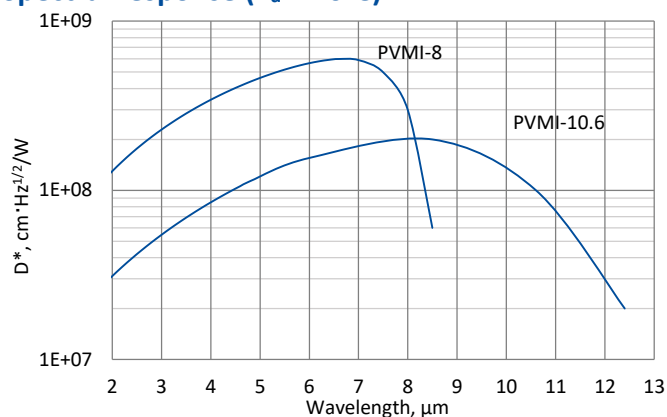
small SIP-T08

## PVMI series

### 2 – 12 $\mu\text{m}$ HgCdTe ambient temperature, optically immersed photovoltaic multiple junction detectors

**PVMI series** features uncooled IR photovoltaic multiple junction detectors based on sophisticated HgCdTe heterostructures for the best performance and stability, optically immersed in order to improve parameters of the devices. The detectors are optimized for the maximum performance at  $\lambda_{\text{opt}}$ . They are especially useful as large optical area detectors operating within 2 to 12  $\mu\text{m}$  spectral range.

#### Spectral response ( $T_a = 20^\circ\text{C}$ )

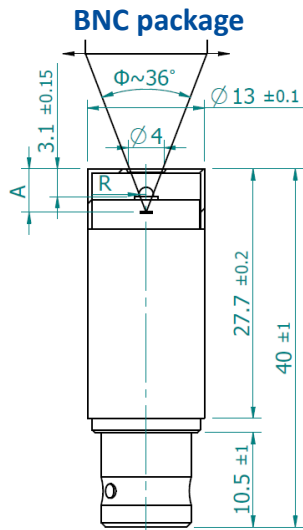


Exemplary spectral detectivity, the spectral response of delivered devices may differ.

#### Specification ( $T_a = 20^\circ\text{C}$ )

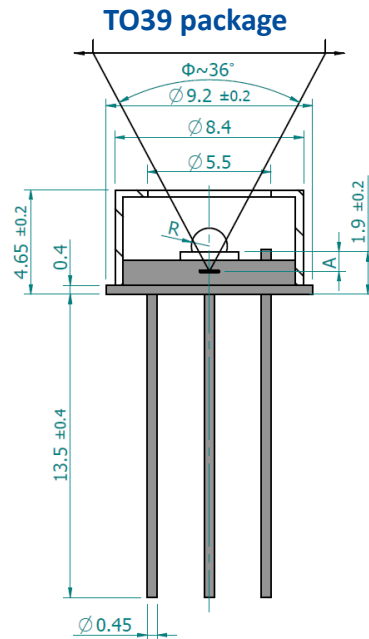
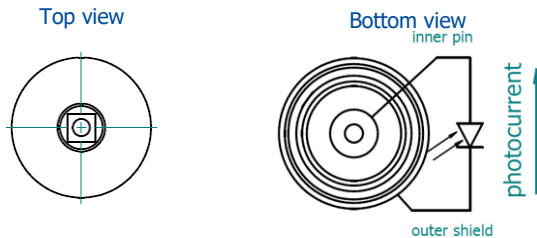
Parameter	Detector type	
	PVMI-8	PVMI-10.6
Active element material	epitaxial HgCdTe heterostructure	
Optimal wavelength $\lambda_{\text{opt}}$ , $\mu\text{m}$	8.0	10.6
Detectivity $D^*(\lambda_{\text{peak}})$ , $\text{cm}\cdot\text{Hz}^{1/2}/\text{W}$	$\geq 6.0 \times 10^8$	$\geq 2.0 \times 10^8$
Detectivity $D^*(\lambda_{\text{opt}})$ , $\text{cm}\cdot\text{Hz}^{1/2}/\text{W}$	$\geq 3.0 \times 10^8$	$\geq 1.0 \times 10^8$
Current responsivity-optical area length product $R_i(\lambda_{\text{opt}}) \cdot L_O$ , $\text{A}\cdot\text{mm}/\text{W}$	$\geq 0.04$	$\geq 0.01$
Time constant $\tau$ , ns	$\leq 4$	$\leq 1.5$
Resistance $R$ , $\Omega$	50 to 300	20 to 150
Optical area $A_O$ , $\text{mm}\times\text{mm}$	1×1	1×1, 2×2
Package	TO39, BNC	
Acceptance angle $\Phi$	$\sim 36^\circ$	
Window	none	

**Mechanical layout, mm**



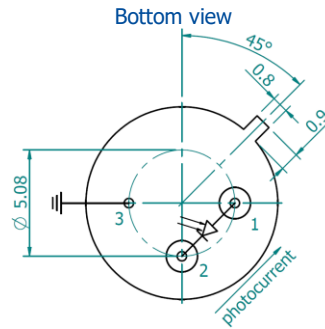
Parameter	Value	
Immersion microlens shape	hyperhemisphere	
Optical area $A_o$ , mm×mm	1×1	2×2
R, mm	0.8	1.25
A, mm	5.5±0.3	6.85±0.30

Φ – acceptance angle  
R – hyperhemisphere microlens radius  
A – distance from the top of BNC package to the focal plane



Parameter	Value	
Immersion microlens shape	hyperhemisphere	
Optical area $A_o$ , mm×mm	1×1	2×2
R, mm	0.8	1.25
A, mm	2.4±0.2	3.75±0.20

Φ – acceptance angle  
R – hyperhemisphere microlens radius  
A – distance from the bottom of hyperhemisphere microlens to the focal plane



Function	Pin number
Detector	1, 2
Chassis ground	3

**Dedicated preamplifier**



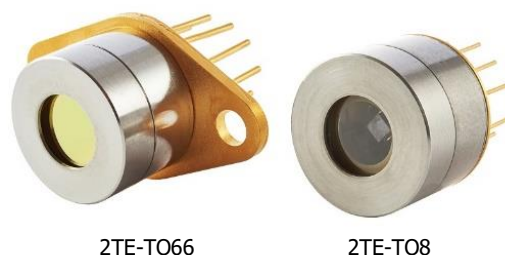
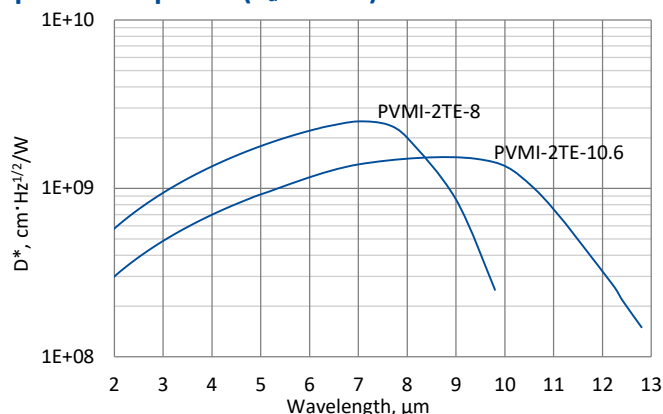
small SIP-TO39

## PVMI-2TE series

### 2 – 13 μm HgCdTe two-stage thermoelectrically cooled, optically immersed photovoltaic multiple junction detectors

**PVMI-2TE series** features two-stage thermoelectrically cooled IR photovoltaic multiple junction detectors based on sophisticated HgCdTe heterostructures for the best performance and stability, optically immersed in order to improve parameters of the devices. The detectors are optimized for the maximum performance at  $\lambda_{opt}$ . They are especially useful as large optical area detectors operating within 2 to 12 μm spectral range. 3° wedged zinc selenide anti-reflection coated (wZnSeAR) window prevents unwanted interference effects.

#### Spectral response ( $T_a = 20^\circ\text{C}$ )



Exemplary spectral detectivity, the spectral response of delivered devices may differ.

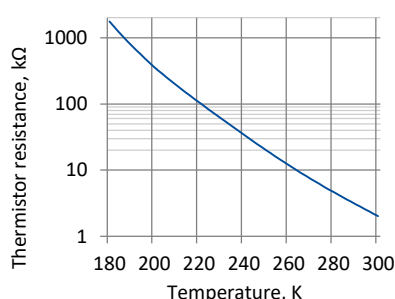
#### Specification ( $T_a = 20^\circ\text{C}$ )

Parameter	Detector type	
	PVMI-2TE-8	PVMI-2TE-10.6
Active element material	epitaxial HgCdTe heterostructure	
Optimal wavelength $\lambda_{opt}$ , μm	8.0	10.6
Detectivity $D^*(\lambda_{peak})$ , $\text{cm}^2 \cdot \text{Hz}^{1/2} / \text{W}$	$\geq 2.5 \times 10^9$	$\geq 1.5 \times 10^9$
Detectivity $D^*(\lambda_{opt})$ , $\text{cm}^2 \cdot \text{Hz}^{1/2} / \text{W}$	$\geq 2.0 \times 10^9$	$\geq 1.0 \times 10^9$
Current responsivity $R_i(\lambda_{opt})$ , A/W	$\geq 0.1$	
Time constant $\tau$ , ns	$\leq 4$	$\leq 3$
Resistance R, $\Omega$	150 to 1000	90 to 350
Active element temperature $T_{det}$ , K	$\sim 230$	
Optical area $A_o$ , mm×mm	1×1	
Package	TO8, TO66	
Acceptance angle $\Phi$	$\sim 36^\circ$	
Window	wZnSeAR	

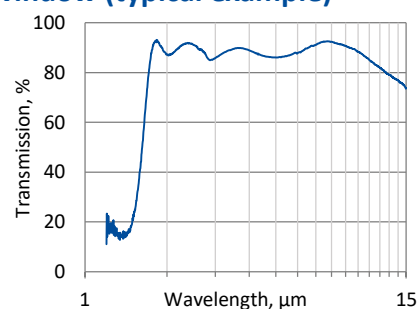
#### Two-stage thermoelectric cooler parameters

Parameter	Value
$T_{det}$ , K	$\sim 230$
$V_{max}$ , V	1.3
$I_{max}$ , A	1.2
$Q_{max}$ , W	0.36

#### Thermistor characteristics

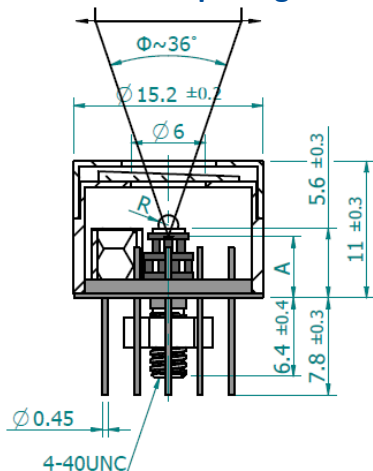


#### Spectral transmission of wZnSeAR window (typical example)



**Mechanical layout, mm**

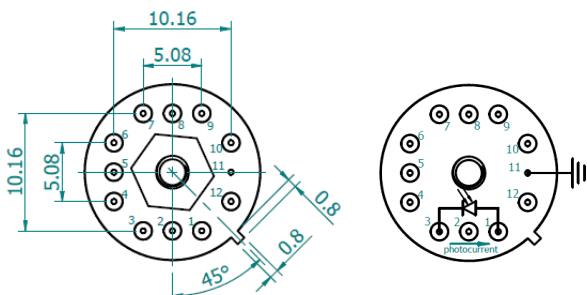
**2TE-T08 package**



Parameter	Value
Immersion microlens shape	hyperhemisphere
Optical area $A_0$ , mm×mm	1×1
R, mm	0.8
A, mm	3.2±0.3

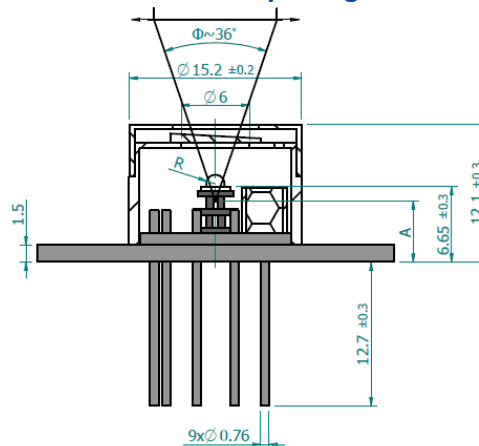
Φ – acceptance angle  
R – hyperhemisphere microlens radius  
A – distance from the bottom of 2TE-T08 header to the focal plane

**Bottom view**



Function	Pin number
Detector	1, 3
Thermistor	7, 9
TE cooler supply	2(+), 8(-)
Chassis ground	11
Not used	4, 5, 6, 10, 12

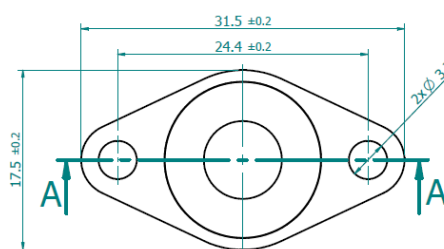
**2TE-T066 package**



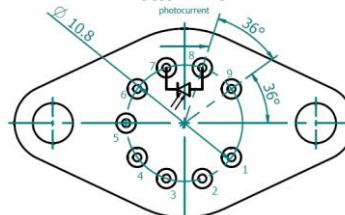
Parameter	Value
Immersion microlens shape	hyperhemisphere
Optical area $A_0$ , mm×mm	1×1
R, mm	0.8
A, mm	3.2±0.3

Φ – acceptance angle  
R – hyperhemisphere microlens radius  
A – distance from the bottom of 2TE-T066 header to the focal plane

**Top view**



**Bottom view**



Function	Pin number
Detector	7, 8
Thermistor	5, 6
TE cooler supply	1(+), 9(-)
Not used	2, 3, 4

**Dedicated preamplifiers**



„all-in-one” AIP



programmable PIP



standard MIP



small SIP-T08

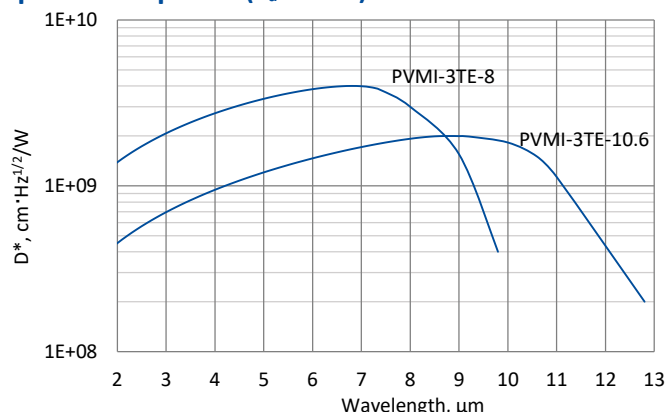


## PVMI-3TE series

### 2 – 13 $\mu\text{m}$ HgCdTe three-stage thermoelectrically cooled, optically immersed photovoltaic multiple junction detectors

**PVMI-3TE series** features three-stage thermoelectrically cooled IR photovoltaic multiple junction detectors based on sophisticated HgCdTe heterostructures for the best performance and stability, optically immersed in order to improve parameters of the devices. The detectors are optimized for the maximum performance at  $\lambda_{\text{opt}}$ . They are especially useful as large optical area detectors operating within 2 to 12  $\mu\text{m}$  spectral range. 3° wedged zinc selenide anti-reflection coated (wZnSeAR) window prevents unwanted interference effects.

#### Spectral response ( $T_a = 20^\circ\text{C}$ )



Exemplary spectral detectivity, the spectral response of delivered devices may differ.

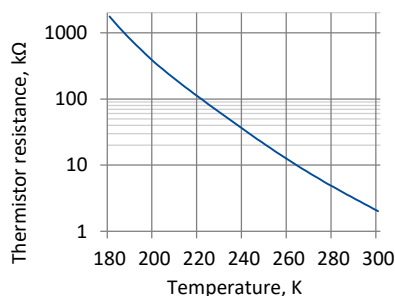
#### Specification ( $T_a = 20^\circ\text{C}$ )

Parameter	Detector type	
	PVMI-3TE-8	PVMI-3TE-10.6
Active element material	epitaxial HgCdTe heterostructure	
Optimal wavelength $\lambda_{\text{opt}}$ , $\mu\text{m}$	8.0	10.6
Detectivity $D^*(\lambda_{\text{peak}})$ , $\text{cm}\cdot\text{Hz}^{1/2}/\text{W}$	$\geq 4.0 \times 10^9$	$\geq 2.0 \times 10^9$
Detectivity $D^*(\lambda_{\text{opt}})$ , $\text{cm}\cdot\text{Hz}^{1/2}/\text{W}$	$\geq 3.0 \times 10^9$	$\geq 1.5 \times 10^9$
Current responsivity $R_i(\lambda_{\text{opt}})$ , A/W	$\geq 0.15$	$\geq 0.10$
Time constant $\tau$ , ns	$\leq 4$	$\leq 3$
Resistance R, $\Omega$	200 to 1500	100 to 400
Active element temperature $T_{\text{det}}$ , K	$\sim 210$	
Optical area $A_0$ , mm $\times$ mm	1 $\times$ 1	
Package	TO8, TO66	
Acceptance angle $\Phi$	$\sim 36^\circ$	
Window	wZnSeAR	

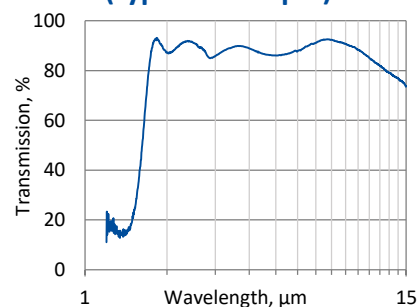
#### Three-stage thermoelectric cooler parameters

Parameter	Value
$T_{\text{det}}$ , K	$\sim 210$
$V_{\text{max}}$ , V	3.6
$I_{\text{max}}$ , A	0.45
$Q_{\text{max}}$ , W	0.27

#### Thermistor characteristics

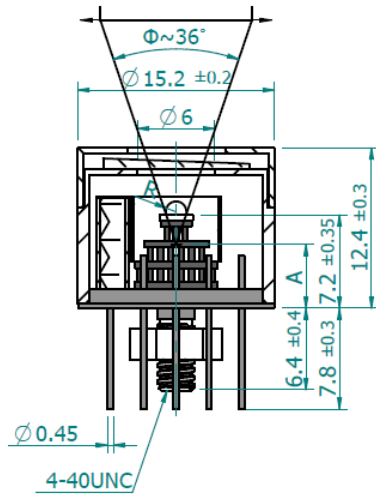


#### Spectral transmission of wZnSeAR window (typical example)



**Mechanical layout, mm**

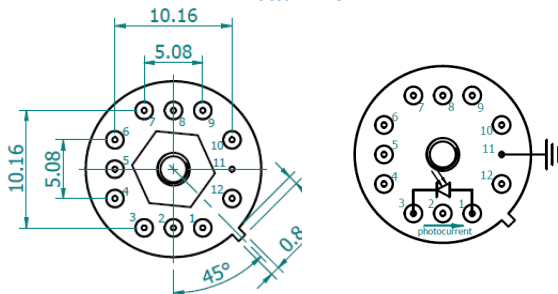
**3TE-T08 package**



Parameter	Value
Immersion microlens shape	hyperhemisphere
Optical area $A_0$ , mm×mm	1×1
R, mm	0.8
A, mm	4.8±0.35

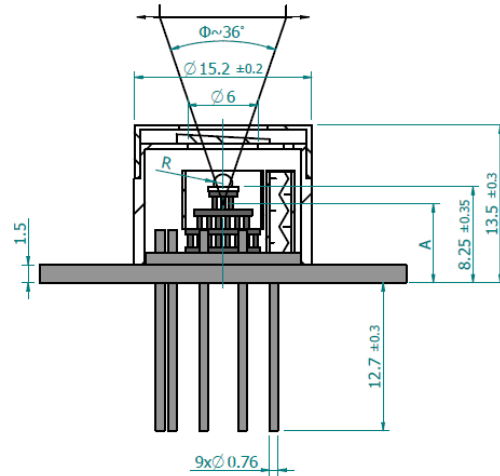
Φ – acceptance angle  
R – hyperhemisphere microlens radius  
A – distance from the bottom of 3TE-T08 header to the focal plane

**Bottom view**



Function	Pin number
Detector	1, 3
Thermistor	7, 9
TE cooler supply	2(+), 8(-)
Chassis ground	11
Not used	4, 5, 6, 10, 12

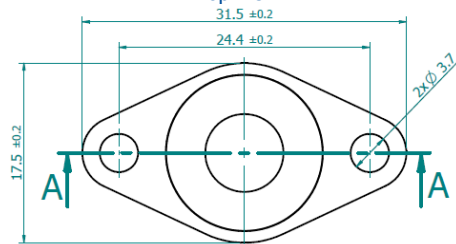
**3TE-T066 package**



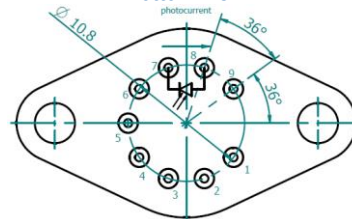
Parameter	Value
Immersion microlens shape	hyperhemisphere
Optical area $A_0$ , mm×mm	1×1
R, mm	0.8
A, mm	5.85±0.35

Φ – acceptance angle  
R – hyperhemisphere microlens radius  
A – distance from the bottom of 3TE-T066 header to the focal plane

**Top view**



**Bottom view**



Function	Pin number
Detector	7, 8
Thermistor	5, 6
TE cooler supply	1(+), 9(-)
Not used	2, 3, 4

**Dedicated preamplifiers**



„all-in-one“ AIP



programmable PIP



standard MIP



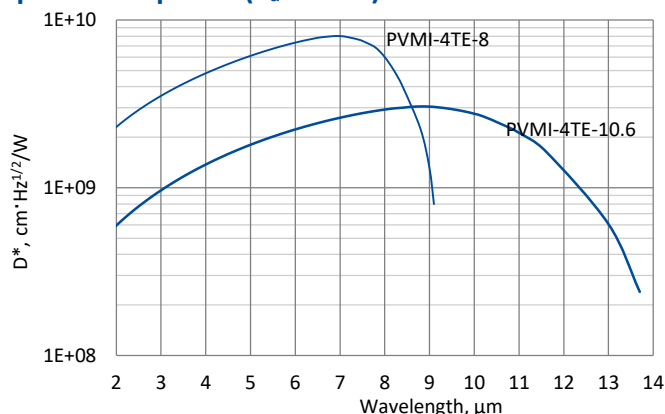
small SIP-T08

## PVMI-4TE series

### 2 – 13 $\mu\text{m}$ HgCdTe four-stage thermoelectrically cooled, optically immersed photovoltaic multiple junction detectors

**PVMI-3TE series** features four-stage thermoelectrically cooled IR photovoltaic multiple junction detectors based on sophisticated HgCdTe heterostructures for the best performance and stability, optically immersed in order to improve parameters of the devices. The detectors are optimized for the maximum performance at  $\lambda_{\text{opt}}$ . They are especially useful as large optical area detectors operating within 2 to 13  $\mu\text{m}$  spectral range. 3° wedged zinc selenide anti-reflection coated (wZnSeAR) window prevents unwanted interference effects.

#### Spectral response ( $T_a = 20^\circ\text{C}$ )



Exemplary spectral detectivity, the spectral response of delivered devices may differ.

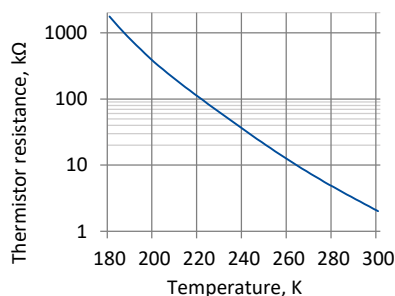
#### Specification ( $T_a = 20^\circ\text{C}$ )

Parameter	Detector type	
	PVMI-4TE-8	PVMI-4TE-10.6
Active element material	epitaxial HgCdTe heterostructure	
Optimal wavelength $\lambda_{\text{opt}}$ , $\mu\text{m}$	8.0	10.6
Detectivity $D^*(\lambda_{\text{peak}})$ , $\text{cm}\cdot\text{Hz}^{1/2}/\text{W}$	$\geq 8.0 \times 10^9$	$\geq 3.0 \times 10^9$
Detectivity $D^*(\lambda_{\text{opt}})$ , $\text{cm}\cdot\text{Hz}^{1/2}/\text{W}$	$\geq 6.0 \times 10^9$	$\geq 2.5 \times 10^9$
Current responsivity $R_i(\lambda_{\text{opt}})$ , A/W	$\geq 0.20$	$\geq 0.18$
Time constant $\tau$ , ns	$\leq 4$	$\leq 3$
Resistance R, $\Omega$	500 to 2500	120 to 500
Active element temperature $T_{\text{det}}$ , K	$\sim 195$	
Optical area $A_0$ , mm $\times$ mm	1 $\times$ 1	
Package	TO8, TO66	
Acceptance angle $\Phi$	$\sim 36^\circ$	
Window	wZnSeAR	

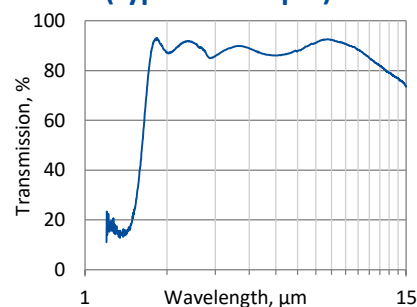
#### Four-stage thermoelectric cooler parameters

Parameter	Value
$T_{\text{det}}$ , K	$\sim 195$
$V_{\text{max}}$ , V	8.3
$I_{\text{max}}$ , A	0.4
$Q_{\text{max}}$ , W	0.28

#### Thermistor characteristics

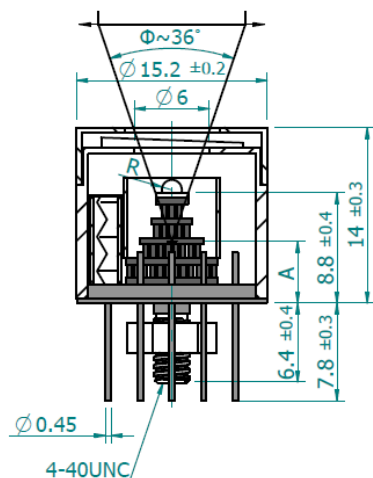


#### Spectral transmission of wZnSeAR window (typical example)



### Mechanical layout, mm

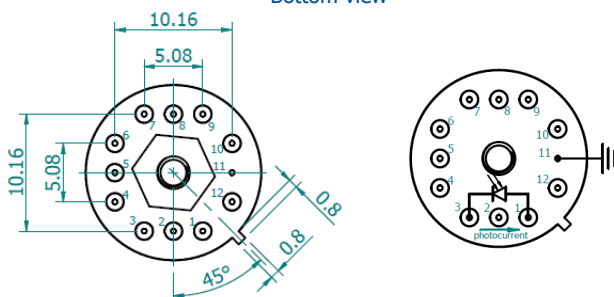
#### 4TE-T08 package



Parameter	Value
Immersion microlens shape	hyperhemisphere
Optical area $A_0$ , mm×mm	1×1
R, mm	0.8
A, mm	6.4±0.4

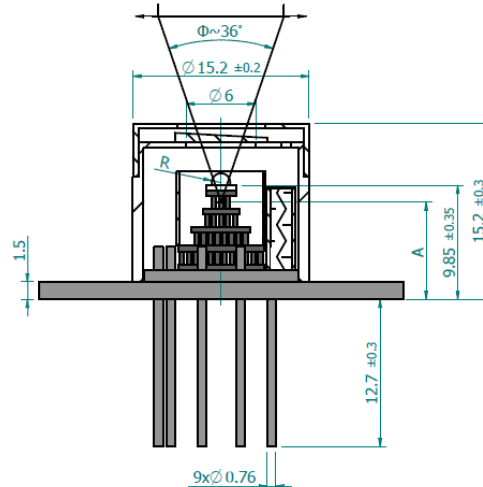
Φ – acceptance angle  
 R – hyperhemisphere microlens radius  
 A – distance from the bottom of 4TE-T08 header to the focal plane

#### Bottom view



Function	Pin number
Detector	1, 3
Thermistor	7, 9
TE cooler supply	2(+), 8(-)
Chassis ground	11
Not used	4, 5, 6, 10, 12

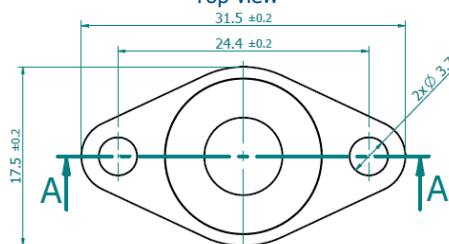
#### 4TE-T066 package



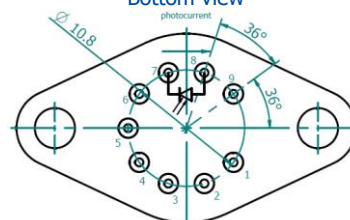
Parameter	Value
Immersion microlens shape	hyperhemisphere
Optical area $A_0$ , mm×mm	1×1
R, mm	0.8
A, mm	7.45±0.40

Φ – acceptance angle  
 R – hyperhemisphere microlens radius  
 A – distance from the bottom of 4TE-T066 header to the focal plane

#### Top view



#### Bottom view



Function	Pin number
Detector	7, 8
Thermistor	5, 6
TE cooler supply	1(+), 9(-)
Not used	2, 3, 4

### Dedicated preamplifiers



„all-in-one“ AIP



programmable PIP



standard MIP



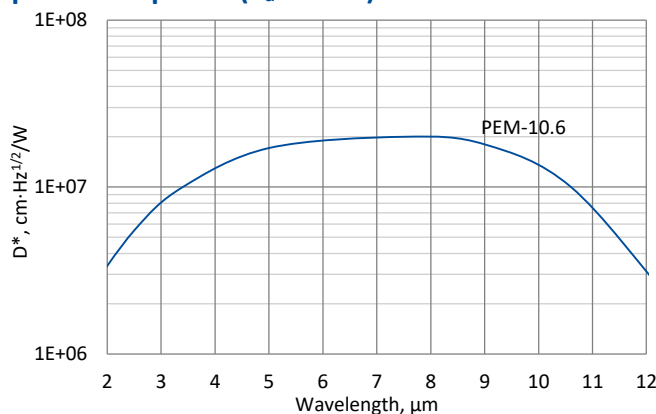
small SIP-T08

## PEM series

### 2 – 12 μm HgCdTe ambient temperature photoelectromagnetic detectors

**PEM series** features uncooled HgCdTe photovoltaic IR detectors based on photoelectromagnetic effect in the semiconductor – spatial separation of optically generated electrons and holes in the magnetic field. The devices are designed for the maximum performance at 10.6 μm and especially useful as a large active area detectors to detect CW and low frequency modulated radiation. These devices are mounted in specialized packages with incorporated magnetic circuit inside. 3° wedged zinc selenide anti-reflection coated (wZnSeAR) window prevents unwanted interference effects and protects against pollution.

#### Spectral response ( $T_a = 20^\circ\text{C}$ )



PEM-TO8

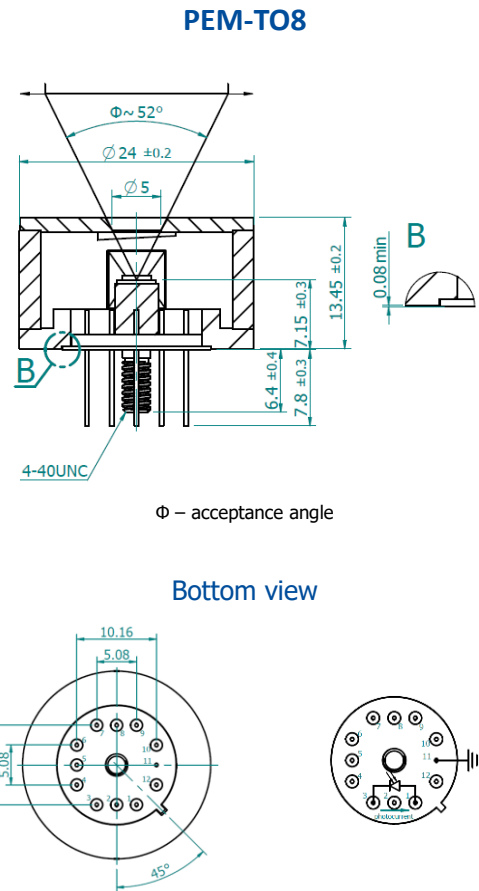
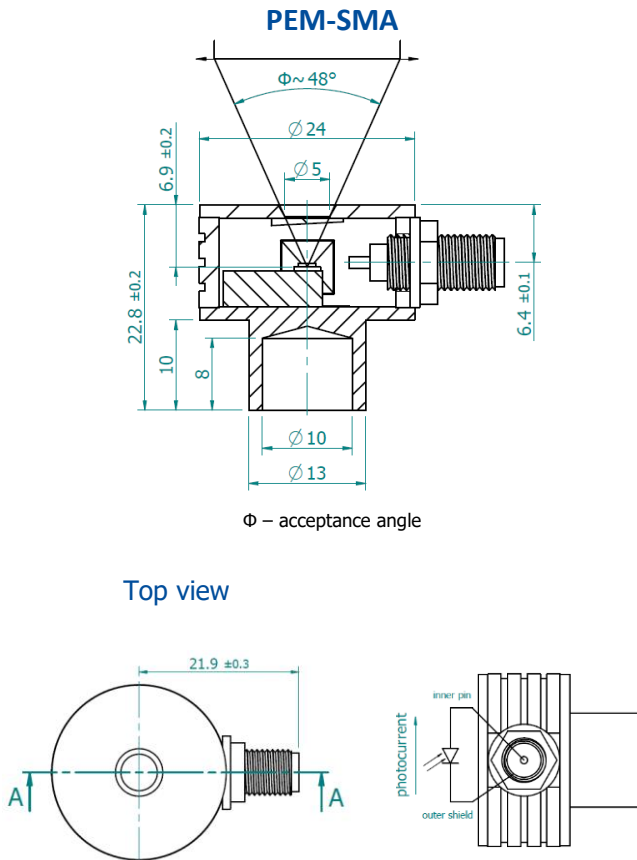
PEM-SMA

Exemplary spectral detectivity, the spectral response of delivered devices may differ.

#### Specification ( $T_a = 20^\circ\text{C}$ )

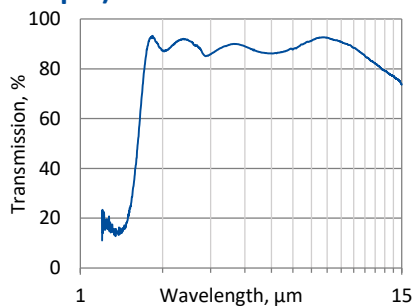
Parameter	Detector type	
	PEM-10.6	
Active element material	epitaxial HgCdTe heterostructure	
Optimal wavelength $\lambda_{opt}$ , μm	10.6	
Detectivity $D^*(\lambda_{peak})$ , $\text{cm}\cdot\text{Hz}^{1/2}/\text{W}$	$\geq 2.0 \times 10^7$	
Detectivity $D^*(\lambda_{opt})$ , $\text{cm}\cdot\text{Hz}^{1/2}/\text{W}$	$\geq 1.0 \times 10^7$	
Current responsivity-active area length product $R_i(\lambda_{opt}) \cdot L$ , $\text{A}\cdot\text{mm}/\text{W}$	$\geq 0.002$	
Time constant $\tau$ , ns	$\leq 1.2$	
Resistance $R$ , $\Omega$	$\geq 40$	
Active area $A$ , $\text{mm}\times\text{mm}$	1×1, 2×2	
Package	PEM-SMA	PEM-TO8
Acceptance angle $\Phi$	~48°	~52°
Window	wZnSeAR	

**Mechanical layout, mm**



Function	Pin number
Detector	1, 3
Chassis ground	11
Not used	2, 4, 5, 6, 7, 8, 9, 10, 12

**Spectral transmission of wZnSeAR window (typical example)**



**Dedicated preamplifier**



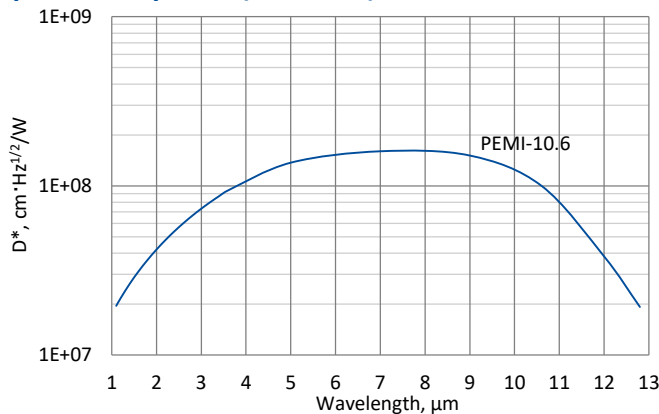
standard MIP

## PEMI series

### 2 – 12 $\mu\text{m}$ HgCdTe ambient temperature, optically immersed photoelectromagnetic detectors

**PEMI series** features uncooled HgCdTe photovoltaic optically immersed IR detectors based on photoelectromagnetic effect in the semiconductor – spatial separation of optically generated electrons and holes in the magnetic field. The devices are designed for the maximum performance at 10.6  $\mu\text{m}$  and especially useful as large optical area detectors to detect CW and low frequency modulated radiation. These devices are mounted in specialized packages with incorporated magnetic circuit inside. 3° wedged zinc selenide anti-reflection coating (wZnSeAR) window prevents unwanted interference effects and protects against pollution.

#### Spectral response ( $T_a = 20^\circ\text{C}$ )

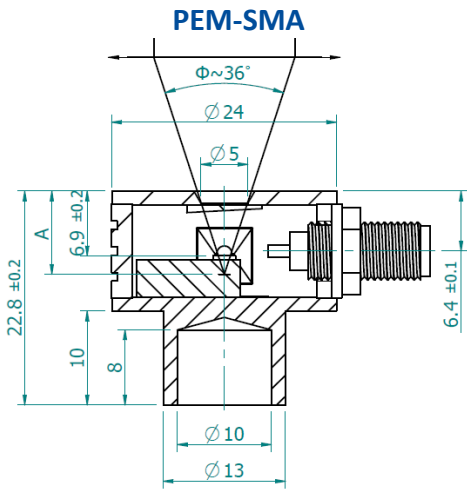


Exemplary spectral detectivity, the spectral response of delivered devices may differ.

#### Specification ( $T_a = 20^\circ\text{C}$ )

Parameter	Detector type
	PEMI-10.6
Active element material	epitaxial HgCdTe heterostructure
Optimal wavelength $\lambda_{\text{opt}}$ , $\mu\text{m}$	10.6
Detectivity $D^*(\lambda_{\text{peak}})$ , $\text{cm}\cdot\text{Hz}^{1/2}/\text{W}$	$\geq 1.6 \times 10^8$
Detectivity $D^*(\lambda_{\text{opt}})$ , $\text{cm}\cdot\text{Hz}^{1/2}/\text{W}$	$\geq 1.0 \times 10^8$
Current responsivity-optical area length product $R(\lambda_{\text{opt}}) \cdot L$ , $\text{A}\cdot\text{mm}/\text{W}$	$\geq 0.01$
Time constant $\tau$ , ns	$\leq 1.2$
Resistance $R$ , $\Omega$	40 to 100
Optical area $A_o$ , $\text{mm}\times\text{mm}$	1×1, 2×2
Package	PEM-SMA, PEM-TO8
Acceptance angle $\Phi$	$\sim 36^\circ$
Window	wZnSeAR

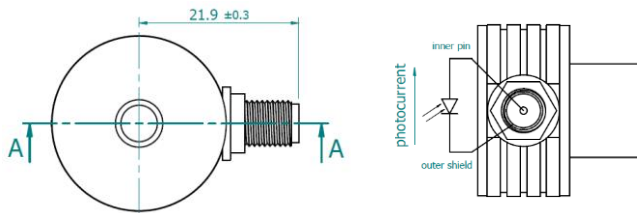
**Mechanical layout, mm**



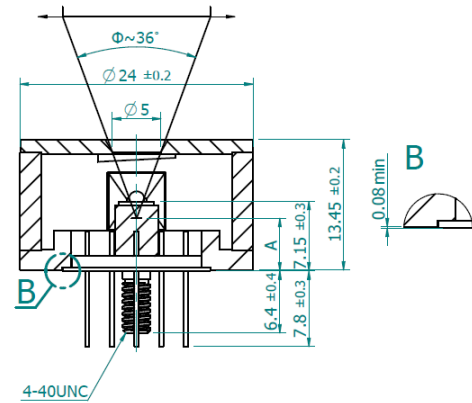
Parameter	Value
Immersion microlens shape	hyperhemisphere
Optical area $A_0$ , mm×mm	1×1    2×2
R, mm	0.8    1.25
A, mm	9.3±0.4    10.65±0.40

Φ – acceptance angle  
R – hyperhemisphere microlens radius  
A – distance from the top of PEM-SMA lid to the focal plane

Top view



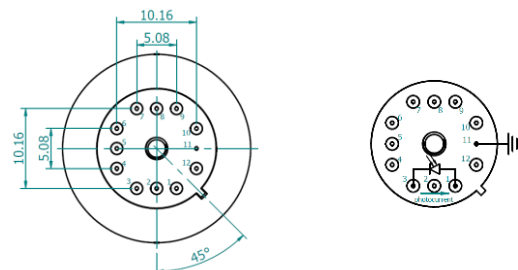
**PEM-TO8**



Parameter	Value
Immersion microlens shape	hyperhemisphere
Optical area $A_0$ , mm×mm	1×1    2×2
R, mm	0.8    1.25
A, mm	4.75±0.30    3.4±0.4

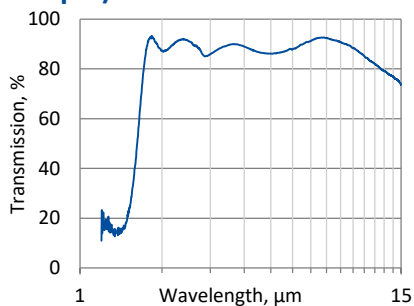
Φ – acceptance angle  
R – hyperhemisphere microlens radius  
A – distance from the bottom of PEM-TO8 header to the focal plane

Bottom view



Function	Pin number
Detector	1, 3
Chassis ground	11
Not used	2, 4, 5, 6, 7, 8, 9, 10, 12

**Spectral transmission of wZnSeAR window (typical example)**



**Dedicated preamplifier**



standard MIP

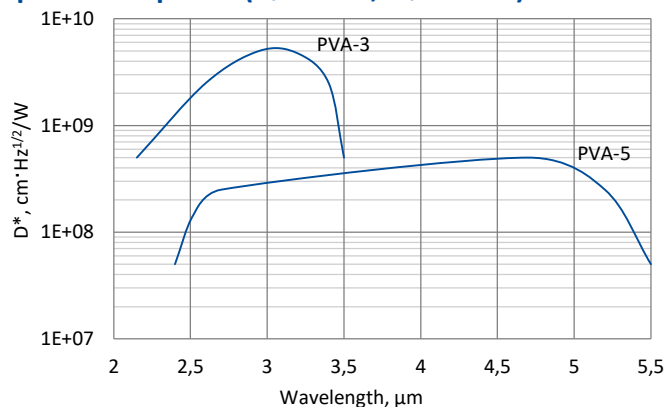


## PVA series

### 2.0 – 5.5 $\mu\text{m}$ InAs and InAsSb ambient temperature photovoltaic detectors

**PVA series** features uncooled IR photovoltaic detectors based on  $\text{InAs}_{1-x}\text{Sb}_x$  alloys. The devices are temperature stable up to  $300^\circ\text{C}$  and mechanically durable. They do not contain mercury or cadmium and are complying with the RoHS Directive.

#### Spectral response ( $T_a = 20^\circ\text{C}$ , $V_b = 0\text{ mV}$ )

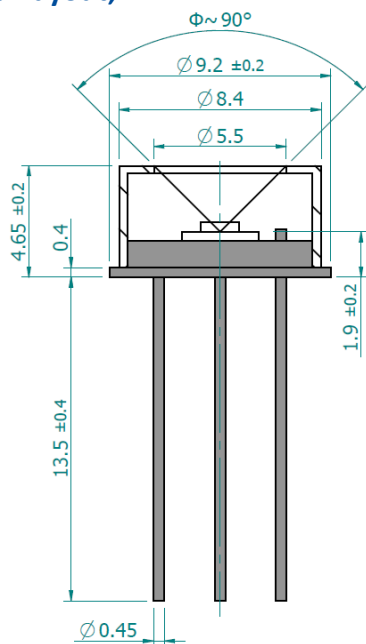


Exemplary spectral detectivity, the spectral response of delivered devices may differ.

#### Specification ( $T_a = 20^\circ\text{C}$ , $V_b = 0\text{ mV}$ )

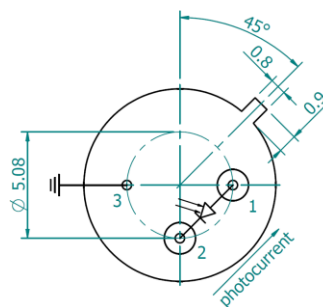
Parameter	Detector type	
	PVA-3	PVA-5
Active element material	epitaxial InAs heterostructure	epitaxial InAsSb heterostructure
Cut-on wavelength $\lambda_{\text{cut-on}}$ (10%), $\mu\text{m}$	$2.15 \pm 0.20$	$2.3 \pm 0.2$
Peak wavelength $\lambda_{\text{peak}}$ , $\mu\text{m}$	$2.95 \pm 0.30$	$4.7 \pm 0.3$
Cut-off wavelength $\lambda_{\text{cut-off}}$ (10%), $\mu\text{m}$	$3.5 \pm 0.2$	$5.5 \pm 0.2$
Detectivity $D^*(\lambda_{\text{peak}})$ , $\text{cm}\cdot\text{Hz}^{1/2}/\text{W}$	$\geq 5.0 \times 10^9$	$\geq 5.0 \times 10^8$
Current responsivity $R_i(\lambda_{\text{peak}})$ , A/W	$\geq 1.3$	$\geq 1.3$
Time constant $\tau$ , ns	$\leq 20$	$\leq 60$
Resistance R, $\Omega$	$\geq 2\text{k}$	$\geq 70$
Active area A, mm $\times$ mm	0.1 $\times$ 0.1	
Package	TO39	
Acceptance angle $\Phi$	$\sim 90^\circ$	
Window	none	

**Mechanical layout, mm**



Φ – acceptance angle

Bottom view



Function	Pin number
Detector	1, 2
Chassis ground	3

**Dedicated preamplifier**



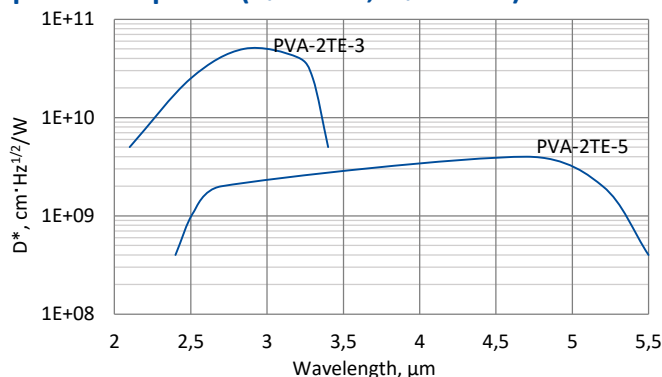
small SIP-T039

## PVA-2TE series

### 2.0 – 5.5 $\mu\text{m}$ InAs and InAsSb two-stage thermoelectrically cooled photovoltaic detectors

**PVA-2TE series** features two-stage thermoelectrically cooled IR photovoltaic detectors based on InAsSb alloys. The devices are temperature stable up to 300°C and mechanically durable. They do not contain mercury or cadmium and are complying with the RoHS Directive. 3° wedged sapphire ( $\text{wAl}_2\text{O}_3$ ) window prevents unwanted interference effects.

#### Spectral response ( $T_a = 20^\circ\text{C}$ , $V_b = 0\text{ mV}$ )



Exemplary spectral detectivity, the spectral response of delivered devices may differ.

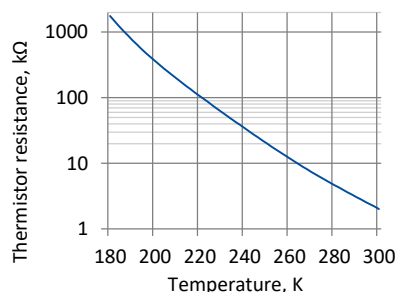
#### Specification ( $T_a = 20^\circ\text{C}$ , $V_b = 0\text{ mV}$ )

Parameter	Detector type	
	PVA-2TE-3	PVA-2TE-5
Active element material	epitaxial InAs heterostructure	epitaxial InAsSb heterostructure
Cut-on wavelength $\lambda_{\text{cut-on}}$ (10%), $\mu\text{m}$	$2.1 \pm 0.2$	$2.4 \pm 0.2$
Peak wavelength $\lambda_{\text{peak}}$ , $\mu\text{m}$	$2.9 \pm 0.3$	$4.7 \pm 0.3$
Cut-off wavelength $\lambda_{\text{cut-off}}$ (10%), $\mu\text{m}$	$3.4 \pm 0.2$	$5.5 \pm 0.2$
Detectivity $D^*(\lambda_{\text{peak}})$ , $\text{cm}\cdot\text{Hz}^{1/2}/\text{W}$	$\geq 5.0 \times 10^{10}$	$\geq 4.0 \times 10^9$
Current responsivity $R_i(\lambda_{\text{peak}})$ , A/W	$\geq 1.3$	$\geq 1.5$
Time constant $\tau$ , ns	$\leq 15$	$\leq 20$
Resistance R, $\Omega$	$\geq 200\text{k}$	$\geq 1.0\text{k}$
Active element temperature $T_{\text{det}}$ , K	~230	
Active area A, mm $\times$ mm	0.1 $\times$ 0.1	
Package	TO8	
Acceptance angle $\Phi$	~70°	
Window	$\text{wAl}_2\text{O}_3$	

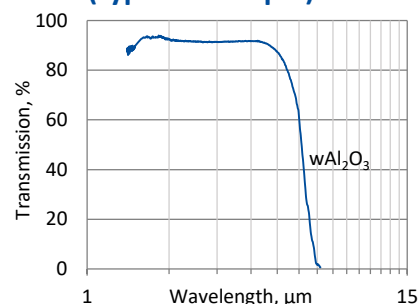
#### Two-stage thermoelectric cooler parameters

Parameter	Value
$T_{\text{det}}$ , K	~230
$V_{\text{max}}$ , V	1.3
$I_{\text{max}}$ , A	1.2
$Q_{\text{max}}$ , W	0.36

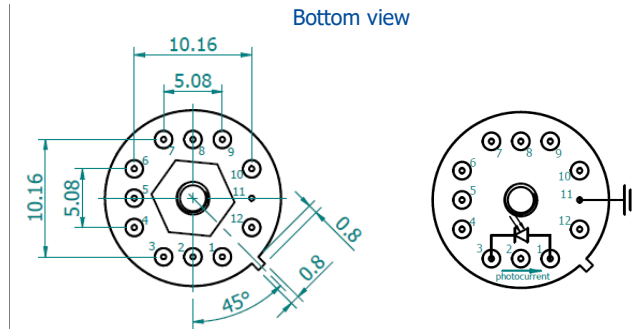
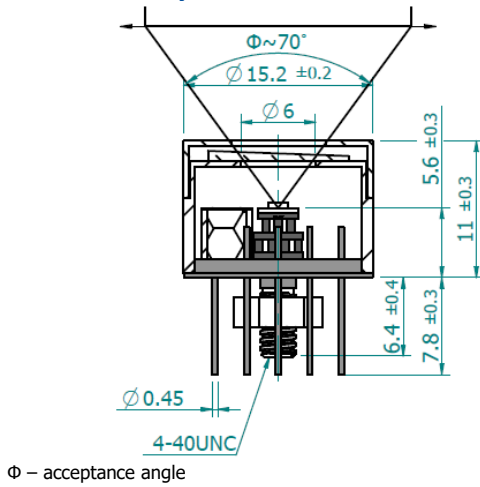
#### Thermistor characteristics



#### Spectral transmission of $\text{wAl}_2\text{O}_3$ window (typical example)



**Mechanical layout, mm**



Function	Pin number
Detector	1, 3
Thermistor	7, 9
TE cooler supply	2(+), 8(-)
Chassis ground	11
Not used	4, 5, 6, 10, 12

**Dedicated preamplifiers**



„all-in-one“ AIP



programmable PIP



standard MIP



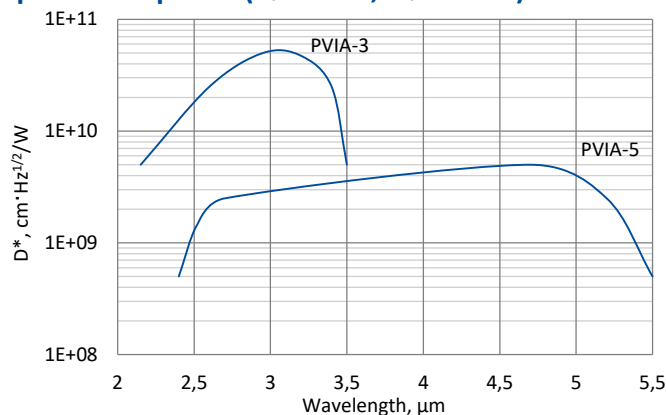
small SIP-T08

## PVIA series

### 2.0 – 5.5 $\mu\text{m}$ InAs and InAsSb ambient temperature, optically immersed photovoltaic detectors

**PVIA series** features uncooled IR photovoltaic detectors based on InAsSb alloys, optically immersed in order to improve performance of the devices. The detectors are temperature stable up to 300°C and mechanically durable. They do not contain mercury or cadmium and are complying with the RoHS Directive.

#### Spectral response ( $T_a = 20^\circ\text{C}$ , $V_b = 0\text{ mV}$ )

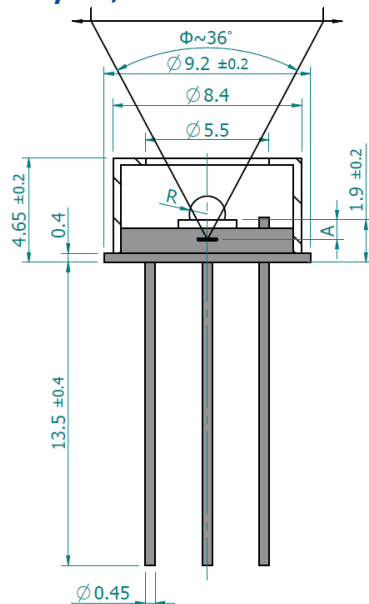


Exemplary spectral detectivity, the spectral response of delivered devices may differ.

#### Specification ( $T_a = 20^\circ\text{C}$ , $V_b = 0\text{ mV}$ )

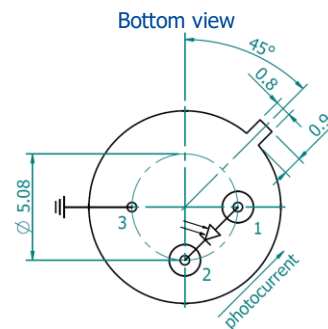
Parameter	Detector type	
	PVIA-3	PVIA-5
Active element material	epitaxial InAs heterostructure	epitaxial InAsSb heterostructure
Cut-on wavelength $\lambda_{\text{cut-on}}$ (10 %), $\mu\text{m}$	$2.15 \pm 0.20$	$2.3 \pm 0.2$
Peak wavelength $\lambda_{\text{peak}}$ , $\mu\text{m}$	$2.95 \pm 0.30$	$4.7 \pm 0.3$
Cut-off wavelength $\lambda_{\text{cut-off}}$ (10 %), $\mu\text{m}$	$3.5 \pm 0.2$	$5.5 \pm 0.2$
Current responsivity $R_i(\lambda_{\text{peak}})$ , A/W	$\geq 1.3$	$\geq 1.3$
Detectivity $D^*(\lambda_{\text{peak}})$ , $\text{cm}\cdot\text{Hz}^{1/2}/\text{W}$	$\geq 5.0 \times 10^{10}$	$\geq 5.0 \times 10^9$
Time constant $\tau$ , ns	$\leq 20$	$\leq 15$
Resistance $R$ , $\Omega$	$\geq 2\text{k}$	$\geq 70$
Optical area $A_o$ , $\text{mm} \times \text{mm}$	1×1	
Package	TO39	
Acceptance angle $\Phi$	$\sim 36^\circ$	
Window	none	

### Mechanical layout, mm



Parameter	Value
Immersion microlens shape	hyperhemisphere
Optical area $A_0$ , mm×mm	1×1
R, mm	0.8
A, mm	2.4±0.2

Φ – acceptance angle  
 R – hyperhemisphere microlens radius  
 A – distance from the bottom of hyperhemisphere microlens to the focal plane



Function	Pin number
Detector	1, 2
Chassis ground	3

### Dedicated preamplifier



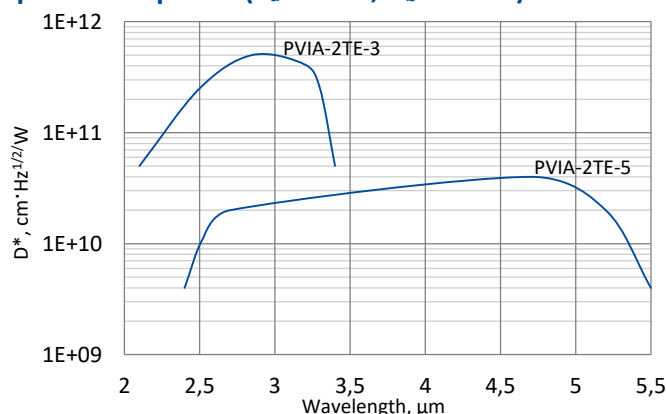
small SIP-T039

## PVIA-2TE series

### 2.0 – 5.5 $\mu\text{m}$ InAs and InAsSb two-stage thermoelectrically cooled, optically immersed photovoltaic detectors

**PVIA-2TE series** features two-stage thermoelectrically cooled IR photovoltaic detectors based on InAsSb alloys, optically immersed in order to improve performance of the devices. The detectors are temperature stable up to 300°C and mechanically durable. They do not contain mercury or cadmium and are complying with the RoHS Directive. 3° wedged sapphire ( $\text{wAl}_2\text{O}_3$ ) window prevents unwanted interference effects.

#### Spectral response ( $T_a = 20^\circ\text{C}$ , $V_b = 0\text{ mV}$ )



Exemplary spectral detectivity, the spectral response of delivered devices may differ.

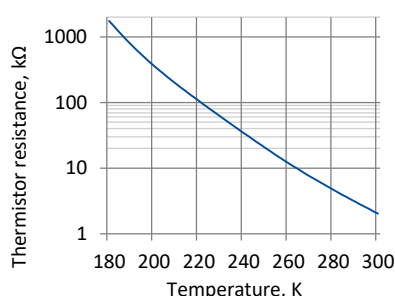
#### Specification ( $T_a = 20^\circ\text{C}$ , $V_b = 0\text{ mV}$ )

Parameter	Detector type	
	PVIA-2TE-3	PVIA-2TE-5
Active element material	epitaxial InAs heterostructure	epitaxial InAsSb heterostructure
Cut-on wavelength $\lambda_{\text{cut-on}}$ (10 %), $\mu\text{m}$	2.1±0.2	2.4±0.2
Peak wavelength $\lambda_{\text{peak}}$ , $\mu\text{m}$	2.9±0.3	4.7±0.3
Cut-off wavelength $\lambda_{\text{cut-off}}$ (10 %), $\mu\text{m}$	3.4±0.2	5.5±0.2
Detectivity $D^*(\lambda_{\text{peak}})$ , $\text{cm}\cdot\text{Hz}^{1/2}/\text{W}$	$\geq 5.0 \times 10^{11}$	$\geq 4.0 \times 10^{10}$
Current responsivity $R_i(\lambda_{\text{peak}})$ , A/W	$\geq 1.3$	$\geq 1.5$
Time constant $\tau$ , ns	$\leq 15$	$\leq 5$
Resistance R, $\Omega$	$\geq 200\text{k}$	$\geq 1.0\text{k}$
Active element temperature $T_{\text{det}}$ , K	~230	
Optical area $A_o$ , mm×mm	1×1	
Package	TO8	
Acceptance angle $\Phi$	~36°	
Window	$\text{wAl}_2\text{O}_3$	

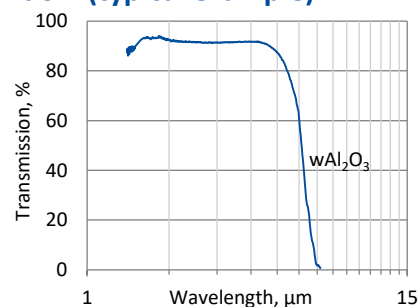
#### Two-stage thermoelectric cooler parameters

Parameter	Value
$T_{\text{det}}$ , K	~230
$V_{\text{max}}$ , V	1.3
$I_{\text{max}}$ , A	1.2
$Q_{\text{max}}$ , W	0.36

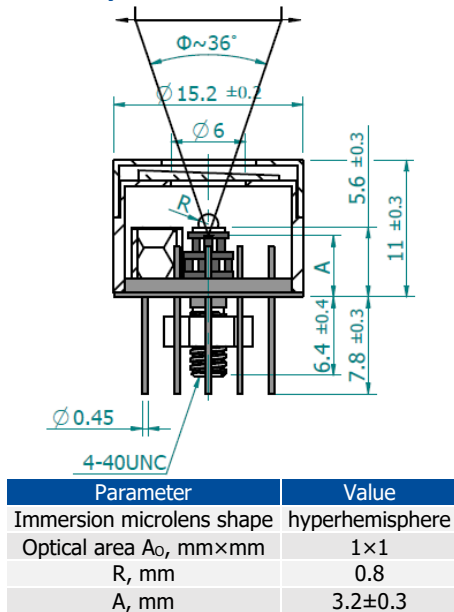
#### Thermistor characteristics



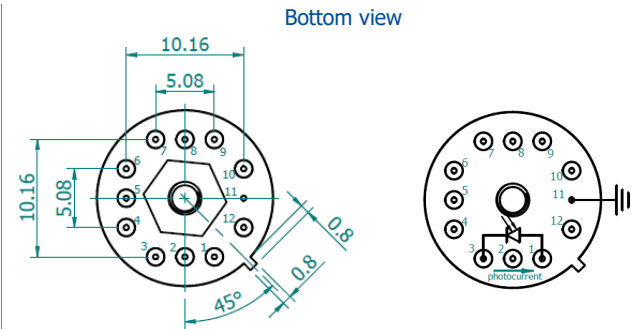
#### Spectral transmission of $\text{wAl}_2\text{O}_3$ window (typical example)



**Mechanical layout, mm**



Φ – acceptance angle  
R – hyperhemisphere microlens radius  
A – distance from the bottom of the 2TE-T08 header to the focal plane



Function	Pin number
Detector	1, 3
Reverse bias (optional)	1(-), 3(+)
Thermistor	7, 9
TE cooler supply	2(+), 8(-)
Chassis ground	11
Not used	4, 5, 6, 10, 12

**Dedicated preamplifiers**



„all-in-one“ AIP



programmable PIP



standard MIP



small SIP-T08

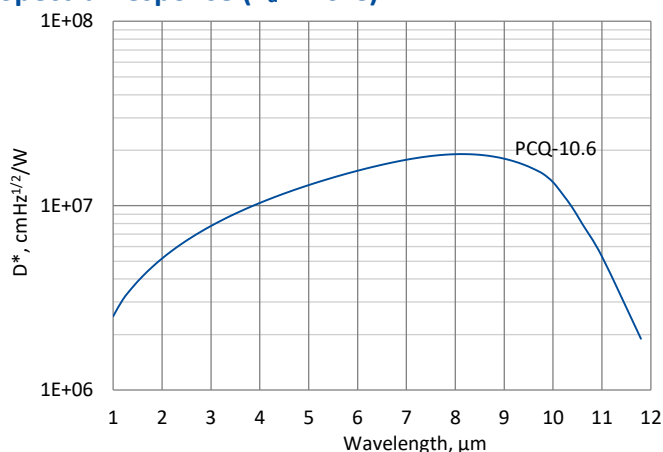


## PCQ

### 2 – 11 $\mu\text{m}$ HgCdTe ambient temperature photoconductive quadrant detector

**PCQ** is uncooled IR photoconductive quadrant detector based on sophisticated HgCdTe heterostructures for the best performance and stability. Quadrant detector consists of four separate active elements arranged in a quadrant geometry. The device is optimized for the maximum performance at 10.6  $\mu\text{m}$ . The detector should operate in optimum bias voltage and current readout mode. Performance at low frequencies is reduced due to 1/f noise. The main application of PCQ detectors is laser beam profiling and positioning.

#### Spectral response ( $T_a = 20^\circ\text{C}$ )

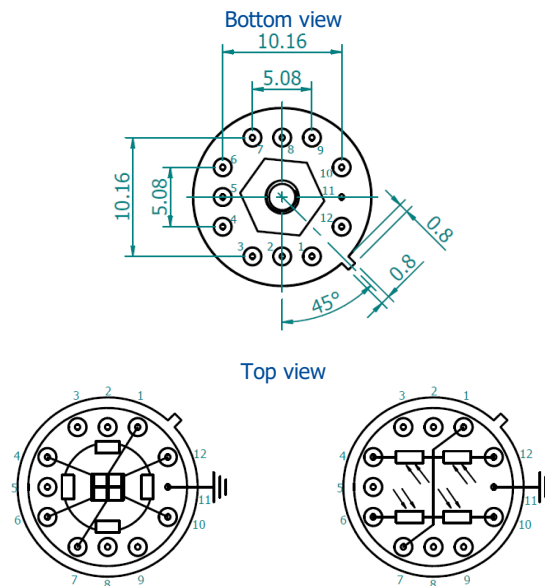
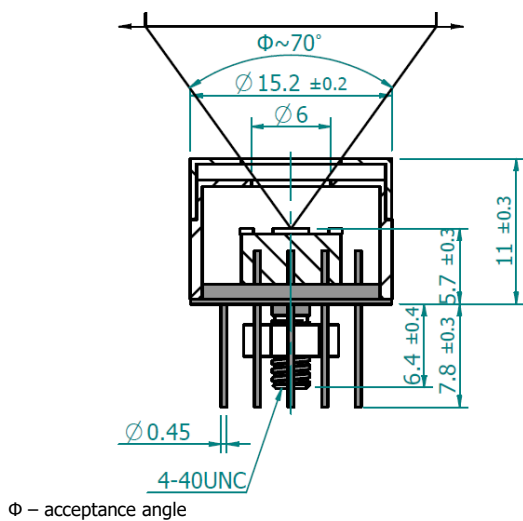


Exemplary spectral detectivity, the spectral response of delivered devices may differ.

#### Specification ( $T_a = 20^\circ\text{C}$ )

Parameter	Detector type
	PCQ-10.6
Active elements material	epitaxial HgCdTe heterostructure
Optimal wavelength $\lambda_{\text{opt}}$ , $\mu\text{m}$	10.6
Detectivity $D^*(\lambda_{\text{peak}}, 20\text{kHz})$ , $\text{cm}\cdot\text{Hz}^{1/2}/\text{W}$	$\geq 1.9 \times 10^7$
Detectivity $D^*(\lambda_{\text{opt}}, 20\text{kHz})$ , $\text{cm}\cdot\text{Hz}^{1/2}/\text{W}$	$\geq 9.0 \times 10^6$
Current responsivity-active area length product $R(\lambda_{\text{opt}}) \cdot L$ , $\text{A}\cdot\text{mm}/\text{W}$	$\geq 0.001$
Time constant $\tau$ , ns	$\leq 5$
1/f noise corner frequency $f_c$ , Hz	$\leq 20\text{k}$
Bias voltage-active area length ratio $V_b/L$ , V/mm	$\leq 6.0$
Resistance $R$ , $\Omega$	$\leq 240$
Active area of single element $A$ , $\text{mm}\times\text{mm}$	1×1
Distance between elements, $\mu\text{m}$	20
Package	TO8
Acceptance angle $\Phi$	$\sim 70^\circ$
Window	none

**Mechanical layout, mm**



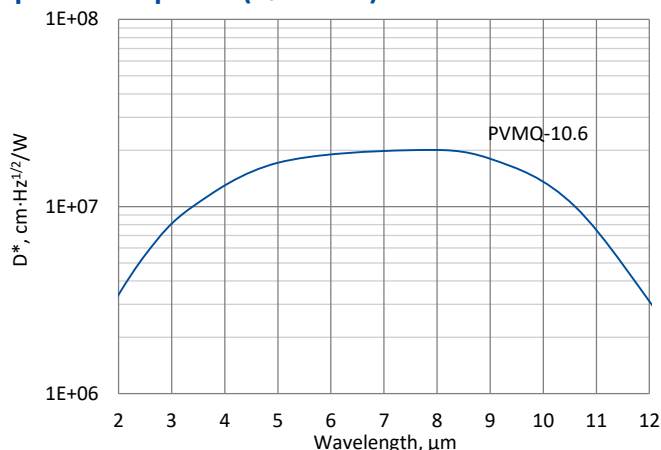
Function	Pin number
Detector 1	12
Detector 2	10
Detector 3	6
Detector 4	4
Common	1, 7
Chassis ground	11
Not used	2, 3, 5, 8, 9

## PVMQ

### 2 – 11 $\mu\text{m}$ HgCdTe ambient temperature photovoltaic multiple junction quadrant detector

**PVMQ** is uncooled IR photovoltaic multiple junction quadrant detector based on sophisticated HgCdTe heterostructures for the best performance and stability. Quadrant detector consists of four separate active elements arranged in a quadrant geometry. The device is optimized for the maximum performance at 10.6  $\mu\text{m}$ . The main application of PVMQ detector is laser beam profiling and positioning.

#### Spectral response ( $T_a = 20^\circ\text{C}$ )

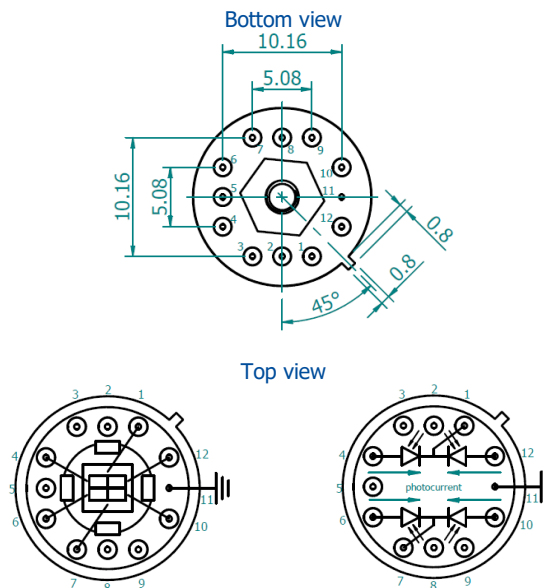
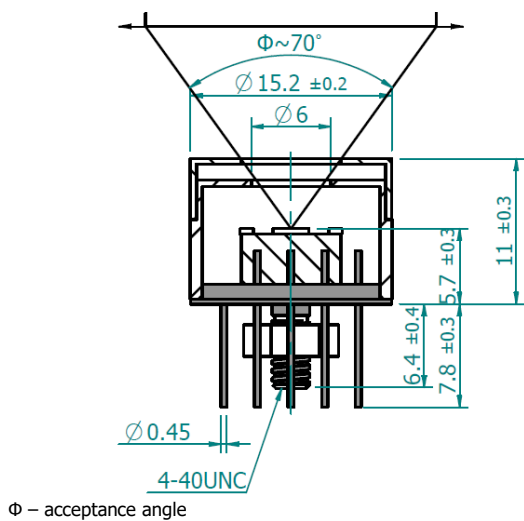


Exemplary spectral detectivity, the spectral response of delivered devices may differ.

#### Specification ( $T_a = 20^\circ\text{C}$ )

Parameter	Detector type
	PVMQ-10.6
Active elements material	epitaxial HgCdTe heterostructure
Optimal wavelength $\lambda_{\text{opt}}$ , $\mu\text{m}$	10.6
Detectivity $D^*(\lambda_{\text{peak}})$ , $\text{cm}\cdot\text{Hz}^{1/2}/\text{W}$	$\geq 2.0 \times 10^7$
Detectivity $D^*(\lambda_{\text{opt}})$ , $\text{cm}\cdot\text{Hz}^{1/2}/\text{W}$	$\geq 1.0 \times 10^7$
Current responsivity $R_i(\lambda_{\text{opt}})$ , A/W	$\geq 0.002$
Time constant $\tau$ , ns	$\leq 1.5$
Resistance R, $\Omega$	30 to 150
Active area of single element A, mm $\times$ mm	1 $\times$ 1
Distance between elements, $\mu\text{m}$	200
Package	TO8
Acceptance angle $\Phi$	$\sim 70^\circ$
Window	none

**Mechanical layout, mm**



Function	Pin number
Detector 1	12
Detector 2	10
Detector 3	6
Detector 4	4
Common	1, 7
Chassis ground	11
Not used	2, 3, 5, 8, 9

## AIP series

**AIP** is a new generation of transimpedance, AC or DC coupled preamplifiers. It is designed to operate with either biased or non-biased VIGO detectors. AIP is „all-in-one“ device – a preamplifier is integrated with a fan and a thermoelectric cooler controller in a compact housing. It is very convenient and user-friendly device, thus can be easily used in a variety of applications.

### Features

- Integrated TEC controller and fan
- Frequency bandwidth up to 250 MHz
- Single power supply
- DC monitor
- Optimised for effective heat dissipation
- Compatible with optical accessories
- Cost effective OEM version available
- Universal and flexible



### Specification ( $T_a = 20^\circ\text{C}$ )

Parameter	Typical value	Conditions, remarks
Low cut-off frequency $f_{lo}$ , Hz	DC, 10, 100, 1k, 10k	
High cut-off frequency $f_{hi}$ , Hz	100k, 1M, 10M, 100M, 250M	
Transimpedance $K_i$ , V/A	up to 200k	fixed
Output impedance $R_{out}$ , $\Omega$	50	
Output voltage swing $V_{out}$ , V	$\pm 2$ $\pm 1$	$f_{hi} \leq 1 \text{ MHz}, R_L = 1 \text{ M}\Omega^*)$ $f_{hi} > 1 \text{ MHz}, R_L = 50 \Omega^*)$
Output voltage offset $V_{off}$ , mV	max $\pm 20^{**})$	
Power supply voltage $V_{sup}$ , V	+5 +12	with 2TE and 3TE cooled detectors with 4TE cooled detectors
Power supply current $I_{sup}$ , mA	max $\pm 50$	
Ambient operating temperature $T_a$ , $^\circ\text{C}$	10 to 30	
Signal output socket	SMA	RF output
DC output socket	SMA	DC monitor
Supply socket	DC 2.1/5.5 DC 2.5/5.5	$V_{sup} = +12 \text{ V}$ $V_{sup} = +5 \text{ V}$
Mounting hole	M4	
Fan	yes	

<sup>\*)</sup>  $R_L$  – load resistance

<sup>\*\*)</sup> Measured with equivalent resistor at the input instead of the detector, it is to avoid the environmental thermal radiation impact.

### Types of VIGO detectors that can be integrated with AIP preamplifier

- **Photoconductive**  
PC-2TE, PC-3TE, PC-4TE
- **Photoconductive optically immersed**  
PCI-2TE, PCI-3TE, PCI-4TE
- **Photovoltaic**  
PV-2TE, PVA-2TE, PV-3TE, PV-4TE
- **Photovoltaic optically immersed**  
PVI-2TE, PVIA-2TE, PVI-3TE, PVI-4TE
- **Photovoltaic multiple junction**  
PVM-2TE
- **Photovoltaic multiple junction optically immersed**  
PVMI-2TE, PVMI-3TE, PVMI-4TE

### Code description

Type	$f_{lo}$ , Hz	$f_{hi}$ , Hz	Version
AIP	DC	100	S <sup>*)</sup> (with package)
	10	1M	
	100	10M	
	1k	100M	
	10k	250M	

<sup>\*)</sup> OEM version available upon request.

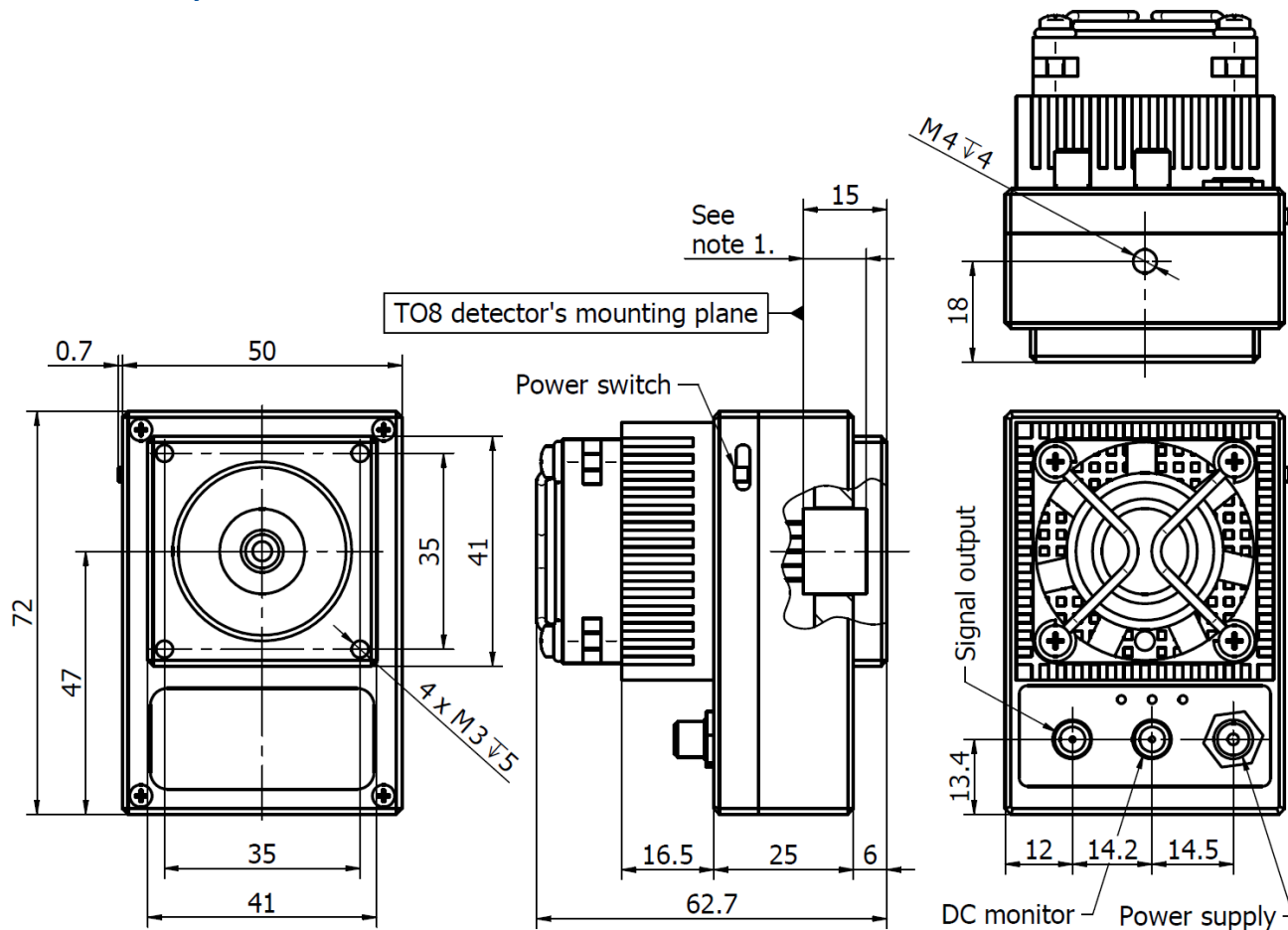
### Included accessories

- 2x **SMA-BNC** cables + **AC adaptor**

### Dedicated accessories

- **OTA** optical threaded adapter
- **DRB-2** base mounting system

**Mechanical layout, mm**



Notes:

1. TO8 detector dimensions in the "TO8 technical drawing".

## PIP series

**PIP** is a series of programmable “smart” preamplifiers. Due to the modern internal configuration, it offers extreme flexibility combined with superior signal parameters and high reliability. Built-in voltage monitor allows to check and optimize the working conditions (supply voltages, detector bias voltage, first and last stage output voltage offset etc.).

There is also possible to change the gain, coupling (AC/DC), optimize the first stage transimpedance and manually or automatically suppress the voltage offset.

Optimized parameters are stored into the internal EEPROM memory and automatically loaded after the power is on. Reset to default settings is available at any time. For detection module safety detector bias adjusting is blocked by default. User can request to enable this option while ordering.

For proper operation PTCC-01 TEC controller is required.



### Specification ( $T_a = 20^\circ\text{C}$ )

Parameter	Typical value	Conditions, remarks
Low cut-off frequency $f_{lo}$ , Hz	DC/10	user configurable by software
High cut-off frequency $f_{hi}$ , Hz	150k/1.5M/20M 1.5M/15M/200M	user configurable by software
Transimpedance $K_i$ , V/A	2.5k – 150k 0.5k – 30k	digitally adjustable first stage transimpedance = 1 k $\Omega$ first stage transimpedance = 5 k $\Omega$
Output impedance $R_{out}$ , $\Omega$	50	
Output voltage swing $V_{out}$ , V	$\pm 1$	$R_L = 50 \Omega^*)$
Output voltage offset $V_{off}$ , mV	max $\pm 20^{**})$	
Ambient operating temperature $T_a$ , $^\circ\text{C}$	10 to 30	
Signal output socket	SMA	
Power supply and TEC control socket	LEMO (female)	ECG.0B.309.CLN
Mounting hole	M4	
Fan	yes	

<sup>\*)</sup>  $R_L$  – load resistance

<sup>\*\*)</sup> Measured with equivalent resistor at the input instead of the detector, it is to avoid the environmental thermal radiation impact.

### Parameters configurable by the user

- Output voltage offset
- Gain (in 40 dB range)
- Bandwidth  
150 kHz/1.5 MHz/20 MHz  
1.5 MHz/15 MHz/100 MHz
- Coupling AC/DC
- Detector's parameters (temperature, reverse bias etc.)

### Types of VIGO detectors that can be integrated with PIP preamplifier

- Photoconductive**  
PC-2TE, PC-3TE, PC-4TE
- Photoconductive optically immersed**  
PCI-2TE, PCI-3TE, PCI-4TE
- Photovoltaic**  
PV-2TE, PVA-2TE, PV-3TE, PV-4TE
- Photovoltaic optically immersed**  
PVI-2TE, PVIA-2TE, PVI-3TE, PVI-4TE
- Photovoltaic multiple junction**  
PVM-2TE
- Photovoltaic multiple junction optically immersed**  
PVMI-2TE, PVMI-3TE, PVMI-4TE

### Included accessories

- SMA-BNC, LEMO-DB9** cables

### Dedicated accessories

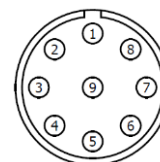
- PTCC-01-BAS** TEC controller + **USB: TypeA-MicroB** cable + **AC adaptor**
- PTCC-01-ADV** TEC controller + **USB: TypeA-MicroB** cable + **AC adaptor**
- PTCC-01-OEM** TEC controller + **USB: TypeA-MicroB**, **KK2-POWER** cables
- OTA** optical threaded adapter
- DRB-2** base mounting system

### Code description

Type	$f_{lo}$	$f_{hi}$
PIP	UC <sup>*)</sup> (DC/10 Hz)	LS <sup>*)</sup> (150 kHz/1.5 MHz/20 MHz)
		HS <sup>*)</sup> (1.5 MHz/15 MHz/200 MHz)

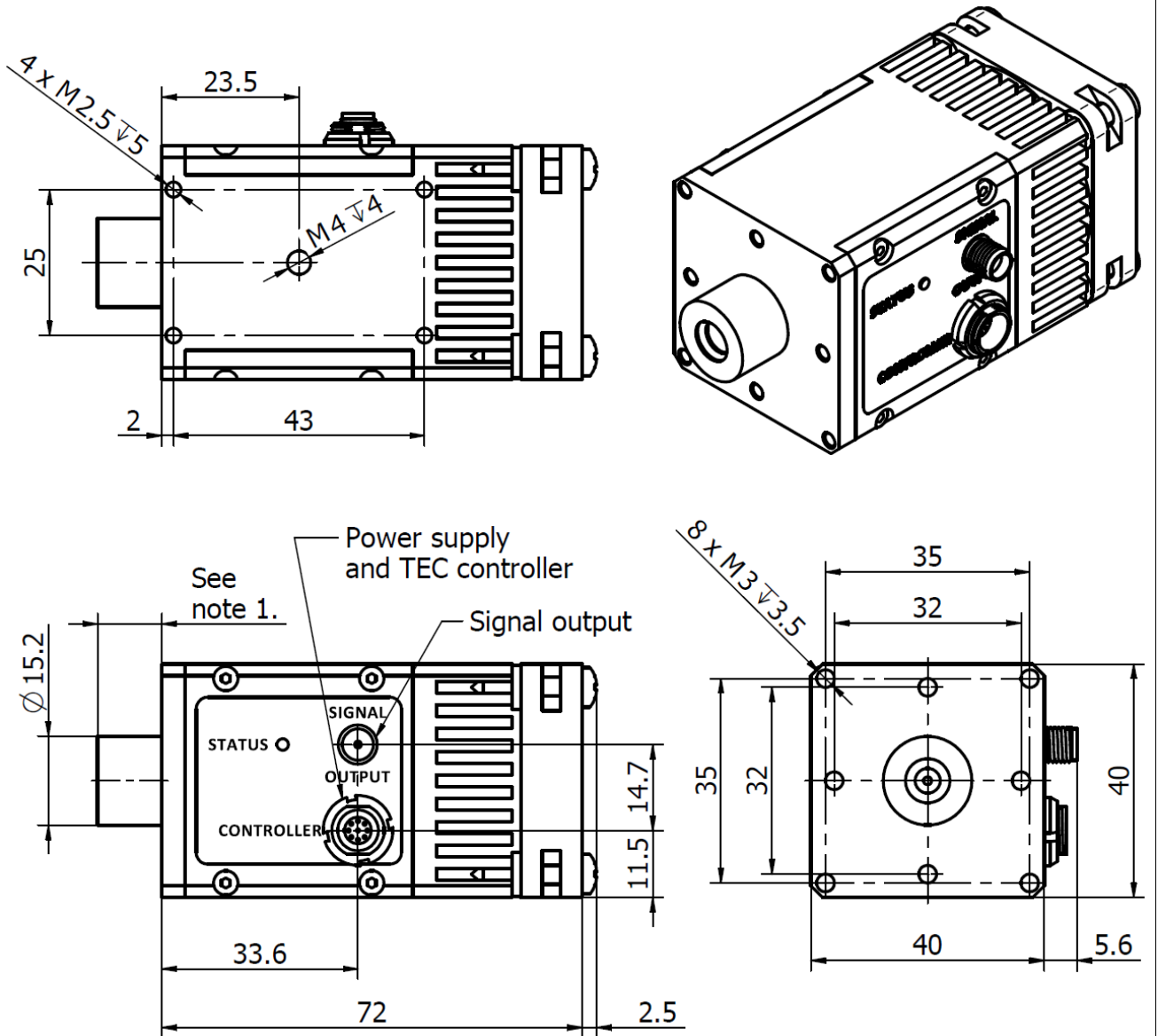
<sup>\*)</sup> User configurable by software.

### Power supply and TEC control socket LEMO (female) ECG.0B.309.CLN



Function	Symbol	Pin number
Fan and programmable preamp internal logic auxiliary supply	FAN+	1
Thermistor output (2)	TH2	2
TEC supply input (-)	TEC-	3
Power supply input (-)	$-V_{sup}$	4
Ground	GND	5
Power supply input (+)	$+V_{sup}$	6
TEC supply input (+)	TEC+	7
Thermistor output (1)	TH1	8
Bidirectional data pin	DATA	9

**Mechanical layout, mm**



- Notes:
2. TO8 detector dimensions in the "TO8 technical drawing".



## MIP series

**MIP** is a series of medium-size transimpedance, DC or AC coupled preamplifiers, intended to operate with either biased or non-biased VIGO detectors. MIP is equipped with a fan and does not require any additional external heatsink. It is one of the most user-friendly preamplifier which surely facilitate work.

### Features

- Frequency bandwidth up to 250 MHz
- Integrated fan
- Compatible with optical accessories



### Specification ( $T_a = 20^\circ\text{C}$ )

Parameter	Typical value	Conditions, remarks
Low cut-off frequency $f_{lo}$ , Hz	DC, 10, 100, 1k, 10k	
High cut-off frequency $f_{hi}$ , Hz	100k, 1M, 10M, 100M, 250M	
Transimpedance $K_i$ , V/A	up to 200k	fixed
Output impedance $R_{out}$ , $\Omega$	50	
Output voltage swing $V_{out}$ , V	$\pm 10$ $\pm 1$	$f_{hi} \leq 1 \text{ MHz}, R_L = 1 \text{ M}\Omega^*)$ $f_{hi} > 1 \text{ MHz}, R_L = 50 \Omega^*)$
Output voltage offset $V_{off}$ , mV	max $\pm 20^{**})$	
Power supply voltage $V_{sup}$ , V	$\pm 15$ $\pm 9$	$f_{hi} \leq 1 \text{ MHz}$ $f_{hi} > 1 \text{ MHz}$
Power supply current $I_{sup}$ , mA	max $\pm 50$	
Ambient operating temperature $T_a$ , $^\circ\text{C}$	10 to 30	
Signal output socket	SMA	
Power supply and TEC control socket	LEMO (female)	ECG.0B.309.CLN
Mounting hole	M4	
Fan	yes	

<sup>\*)</sup>  $R_L$  – load resistance

<sup>\*\*)</sup> Measured with equivalent resistor at the input instead of the detector, it is to avoid the environmental thermal radiation impact.

### Types of VIGO detectors that can be integrated with MIP preamplifier

- **Photoconductive**  
PC-2TE, PC-3TE, PC-4TE
- **Photoconductive optically immersed**  
PCI-2TE, PCI-3TE, PCI-4TE
- **Photovoltaic**  
PV-2TE, PVA-2TE, PV-3TE, PV-4TE
- **Photovoltaic optically immersed**  
PVI-2TE, PVIA-2TE, PVI-3TE, PVI-4TE
- **Photovoltaic multiple junction**  
PVM-2TE
- **Photovoltaic multiple junction optically immersed**  
PVMI-2TE, PVMI-3TE, PVMI-4TE

### Included accessories

- **SMA-BNC, LEMO-DB9** cables

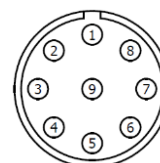
### Dedicated accessories

- **PTCC-01-BAS** TEC controller + **USB: TypeA-MicroB** cable + **AC adaptor**
- **PTCC-01-ADV** TEC controller + **USB: TypeA-MicroB** cable + **AC adaptor**
- **PTCC-01-OEM** TEC controller + **USB: TypeA-MicroB**, **KK2-POWER** cables
- **OTA** optical threaded adapter
- **DRB-2** base mounting system

### Code description

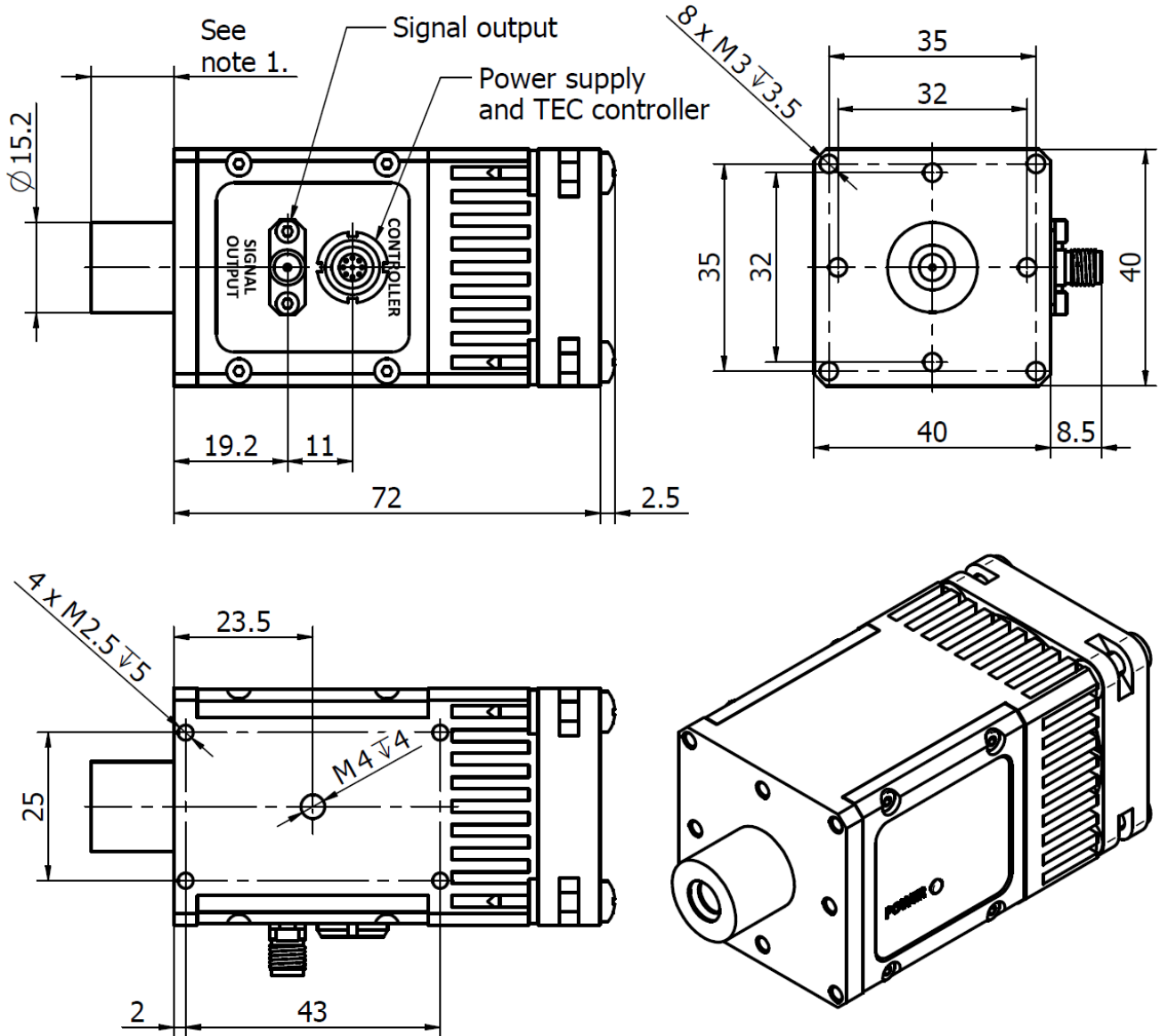
Type	$f_{lo}$ , Hz	$f_{hi}$ , Hz
MIP	DC	100
	10	1M
	100	10M
	1k	100M
	10k	250M

### Power supply and TEC control socket LEMO (female) ECG.0B.309.CLN



Function	Symbol	Pin number
Fan (+)	FAN+	1
Thermistor output (2)	TH2	2
TEC supply input (-)	TEC-	3
Power supply input (-)	$-V_{sup}$	4
Ground	GND	5
Power supply input (+)	$+V_{sup}$	6
TEC supply input (+)	TEC+	7
Thermistor output (1)	TH1	8
Data pin	DATA	9

**Mechanical layout, mm**



Notes:

1. TO8 detector dimensions in the "TO8 technical drawing".

## FIP series

**FIP** is a series of high speed, transimpedance, AC coupled preamplifiers, intended to operate with biased TE cooled VIGO detectors. Fast preamplifier enables precise I-V conversion, detector biasing up to 800 mV and simultaneously maintains compact size and keeps current noise low. FIP is equipped with a fan and does not require additional heat dissipation. It is suitable for applications requiring wide frequency bandwidth. Additional DC output is available as an option.

### Features

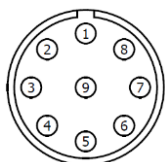
- Wide frequency bandwidth up to 1 GHz
- Integrated fan
- DC monitor as an option

### Specification ( $T_a = 20^\circ\text{C}$ )

Parameter	Typical value	Conditions, remarks
Low cut-off frequency $f_{lo}$ , Hz	1k, 10k	
High cut-off frequency $f_{hi}$ , Hz	1G	
Transimpedance $K_i$ , V/A	up to 8.5k	fixed
Output impedance $R_{out}$ , $\Omega$	50	
Output voltage swing $V_{out}$ , V	$\pm 1$	$R_L = 50 \Omega^*)$
Power supply voltage $V_{sup}$ , V	+12 / -5	
Power supply current $I_{sup}$ , mA	+100 -50	
Ambient operating temperature $T_a$ , $^\circ\text{C}$	10 to 30	
Signal output socket	SMA	RF output
DC monitor socket	SMA	option
Power supply and TEC control socket	LEMO (female)	ECG.0B.309.CLN
Mounting hole	M4	
Fan	yes	

<sup>\*)</sup>  $R_L$  – load resistance

### Power supply and TEC control socket LEMO (female) ECG.0B.309.CLN



Function	Symbol	Pin number
Fan (+)	FAN+	1
Thermistor output (2)	TH2	2
TEC supply input (-)	TEC-	3
Power supply input (-)	$-V_{sup}$	4
Ground	GND	5
Power supply input (+)	$+V_{sup}$	6
TEC supply input (+)	TEC+	7
Thermistor output (1)	TH1	8
Data pin	DATA	9



### Types of VIGO detectors that can be integrated with FIP preamplifier

- Photovoltaic**  
PV-2TE, PV-3TE, PV-4TE
- Photovoltaic optically immersed**  
PVI-2TE, PVI-3TE, PVI-4TE

### Code description

Type	$f_{lo}$ , Hz	$f_{hi}$ , Hz	Version
FIP	1k 10k	1G	D (with DC monitor) ND (without DC monitor)

### Included accessories

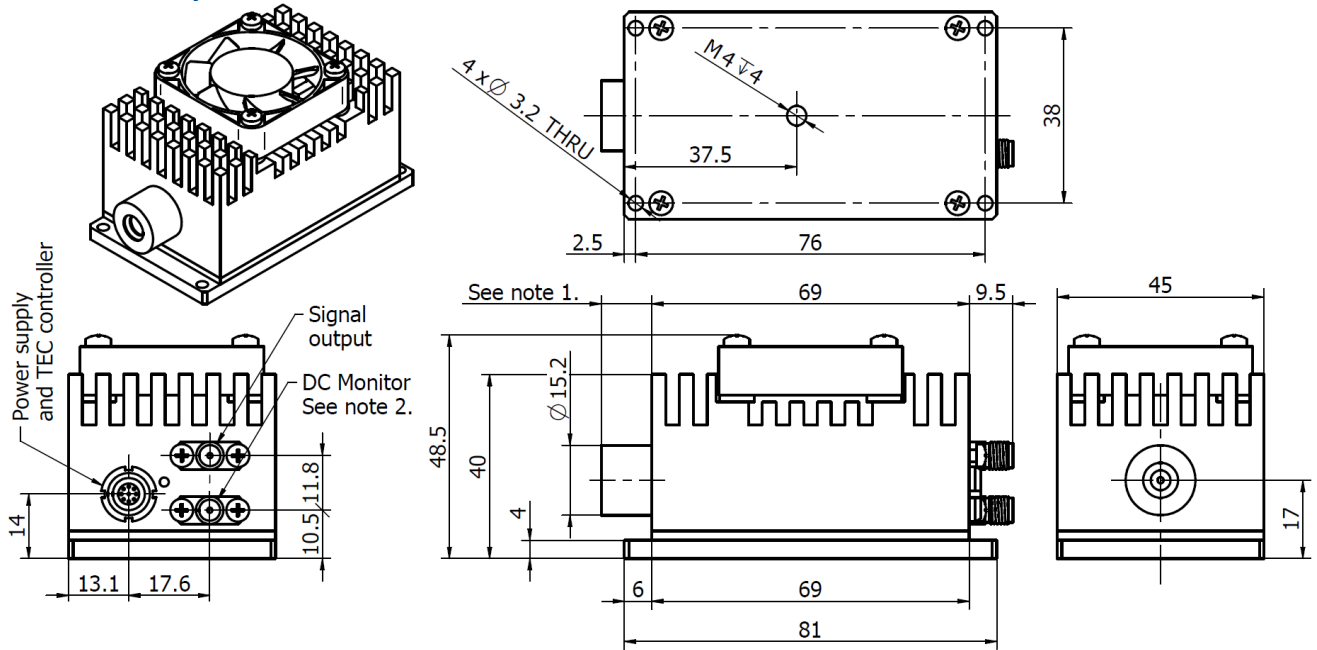
- SMA-BNC<sup>\*)</sup>, LEMO-DB9** cables

<sup>\*)</sup> Additional SMA-BNC cable for FIP-xx-xx-D version.

### Dedicated accessories

- PTCC-01-BAS** TEC controller + **USB: TypeA-MicroB** cable + **AC adaptor**
- PTCC-01-ADV** TEC controller + **USB: TypeA-MicroB** cable + **AC adaptor**
- PTCC-01-OEM** TEC controller + **USB: TypeA-MicroB, KK2-POWER** cables
- DRB-2** base mounting system

**Mechanical layout, mm**



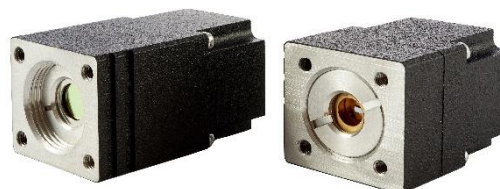
- Notes:
1. TO8 detector dimensions in the "TO8 technical drawing".
  2. Only for FIP-xx-xx-D version.

## SIP series

**SIP** is a series of ultra-small transimpedance, AC or DC coupled preamplifiers. It is designed to operate with either biased or non-biased detectors. It is compatible with uncooled detectors in TO39 package (SIP-TO39) or thermoelectrically cooled detectors in TO8 package (SIP-TO8). SIP is dedicated for OEM applications and requires external heatsink (MHS-2). There is a possibility to adjust gain (devices with a frequency bandwidth up to 100 MHz).

### Features

- Very small size
- Frequency bandwidth up to 250 MHz
- Adjustable gain as an option



SIP-TO8

SIP-TO39

### Specification ( $T_a = 20^\circ\text{C}$ )

Parameter	Typical value	Conditions, remarks
Low cut-off frequency $f_{lo}$ , Hz	DC, 10, 100, 1k, 10k	
High cut-off frequency $f_{hi}$ , Hz	100k, 1M, 10M, 100M, 250M	
Transimpedance $K_i$ , V/A	up to 100k	tunable
Transimpedance range $K_{i\max}/K_{i\min}$	up to 5	dependent on $f_{hi}$
Output impedance $R_{out}$ , $\Omega$	50	
Output voltage swing $V_{out}$ , V	$\pm 10$ $\pm 1$	$f_{hi} \leq 1\text{ MHz}$ , $R_L = 1\text{ M}\Omega^{*)}$ $f_{hi} > 1\text{ MHz}$ , $R_L = 50\ \Omega^{*)}$
Output voltage offset $V_{off}$ , mV	max $\pm 20^{**)}$	
Power supply voltage $V_{sup}$ , V	$\pm 15$ $\pm 9$	$f_{hi} \leq 1\text{ MHz}$ $f_{hi} > 1\text{ MHz}$
Power supply current $I_{sup}$ , mA	max $\pm 50$	no detector biasing
Ambient operating temperature $T_a$ , $^\circ\text{C}$	10 to 30	
Signal output socket	MMCX	
Power supply and TEC control socket	AMP2x4 (male)	AMPMODU 2x4
Mounting hole	none	
Fan	no	external heatsink necessary

<sup>\*)</sup>  $R_L$  – load resistance

<sup>\*\*)</sup> Measured with equivalent resistor at the input instead of the detector, it is to avoid the environmental thermal radiation impact.

### Types of VIGO detectors that can be integrated with SIP-TO8 preamplifier

- **Photoconductive**  
PC-2TE, PC-3TE, PC-4TE
- **Photoconductive optically immersed**  
PCI-2TE, PCI-3TE, PCI-4TE
- **Photovoltaic**  
PV-2TE, PVA-2TE, PV-3TE, PV-4TE
- **Photovoltaic optically immersed**  
PVI-2TE, PVIA-2TE, PVI-3TE, PVI-4TE
- **Photovoltaic multiple junction**  
PVM-2TE
- **Photovoltaic multiple junction optically immersed**  
PVMI-2TE, PVMI-3TE, PVMI-4TE

### Types of VIGO detectors that can be integrated with SIP-TO39 preamplifier

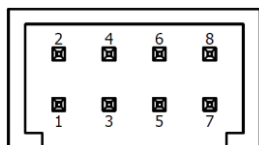
- **Photoconductive**  
PC
- **Photoconductive optically immersed**  
PCI
- **Photovoltaic**  
PV, PVA
- **Photovoltaic optically immersed**  
PVI, PVIA
- **Photovoltaic multiple junction**  
PVM
- **Photovoltaic multiple junction optically immersed**  
PVMI

### Code description

Type	$f_{lo}$ , Hz	$f_{hi}$ , Hz	Detector package	Gain adjustment
SIP	DC	100k	TO8 TO39	G <sup>*)</sup> (with gain adjustment) NG (without gain adjustment)
	10	1M		
	100	10M		
	1k	100M		
	10k	250M		

<sup>\*)</sup> Only for SIP preamplifier with  $f_{hi} \leq 100\text{ MHz}$ .

### Power supply and TEC control socket AMPMODU 2x4 (male)



Function	Symbol	Pin number
Power supply input (-)	$-V_{sup}$	1
Thermistor output/Not connected	TH2/N.C.	2 <sup>*)</sup>
Data pin/Ground	DATA/GND	3 <sup>**)</sup>
TEC supply input (-)/Not connected	TEC-/N.C.	4 <sup>*)</sup>
Ground	GND	5
Thermistor output/Not connected	TH1/N.C.	6 <sup>*)</sup>
Power supply input (+)	$+V_{sup}$	7
TEC supply input (+)/Not connected	TEC+/N.C.	8 <sup>*)</sup>

<sup>\*)</sup> N.C. – only for SIP-TO39 version.

<sup>\*\*)</sup> GND – only for SIP-TO39 version.

### Included accessories

- **MMCX-BNC, AMP2x4-DB9** cables

### Dedicated accessories for SIP-TO8

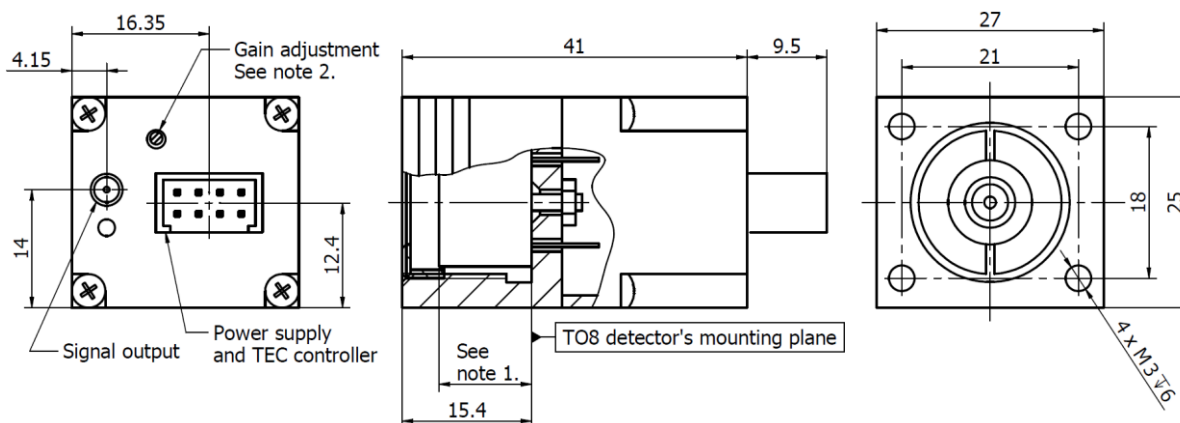
- **PTCC-01-BAS** TEC controller + **USB: TypeA-MicroB** cable + **AC adaptor**
- **PTCC-01-ADV** TEC controller + **USB: TypeA-MicroB** cable + **AC adaptor**
- **PTCC-01-OEM** TEC controller + **USB: TypeA-MicroB, KK2-POWER** cables
- **MHS-2** heatsink

### Dedicated accessories for SIP-TO39

- **PPS-03** preamplifier power supply + **AC adaptor**

### Mechanical layout, mm

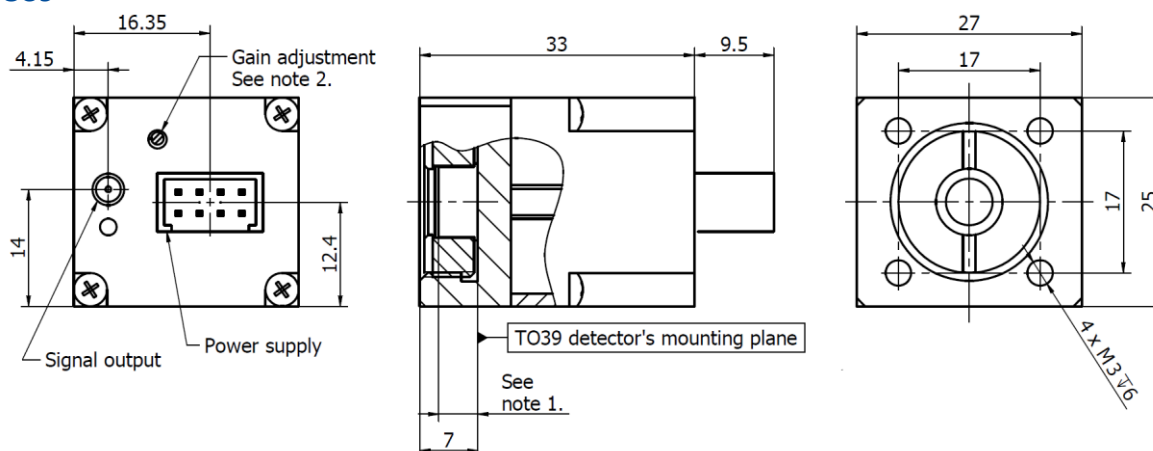
#### SIP-TO8



Notes:

1. TO8 detector dimensions in the "TO8 technical drawing".
3. Only for SIP-xx-xx-TO8-G version.

#### SIP-TO39



Notes:

1. TO8 detector dimensions in the "TO39 technical drawing".
2. Only for SIP-xx-xx-TO39-G version.

## ACCESSORIES

- [PTCC-01 series](#) thermoelectric cooler controllers
- [PPS-03 series](#) preamplifier power supplies
- [AC adaptor and cables](#)
- [DRB-2](#) base mounting system
- [MHS-2](#) heatsink
- [DH-2](#) detector holder
- [MH-1](#) module holder
- [OTA](#) optical threaded adapter

## PTCC-01 series

**PTCC-01** is a series of programmable, precision low-noise thermoelectric cooler controllers. They are designed to operate with VIGO IR detection modules: LabM-6, LabM-I-16.6 and containing TE cooled detectors and preamplifiers: PIP, MIP, FIP, SIP-TO8.



PTCC-01-ADV

PTCC-01-BAS

PTCC-01-OEM

### Available options

#### PTCC-01-ADV (advanced)

- TEC controller and preamplifier power supply encapsulated in a small size package.
- Configurable by built-in function keys or PC software available on VIGO website.
- Status LCD indicator.

#### PTCC-01-BAS (basic)

- TEC controller and preamplifier power supply encapsulated in a small size package.
- Configurable by PC software available on VIGO website.
- Status LED indicator.

#### PTCC-01-OEM (oem)

- TEC controller and preamplifier power supply without package.
- Configurable by PC software available on VIGO website.
- Status LED indicator and status/data connector.

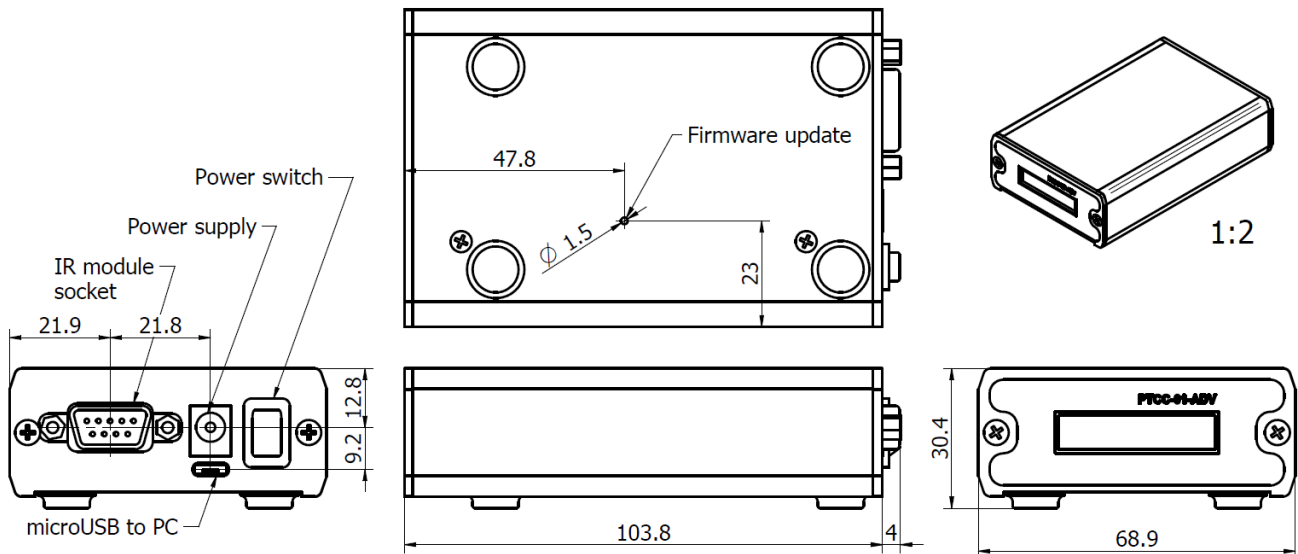
### Specification ( $T_a = 20^\circ\text{C}$ )

Parameter	Typical value	Conditions, remarks
Temperature stability, K	$\pm 0.01$	
Temperature readout stability, mK	max 1.0	
Detector temperature settling time, s	25	2TE
	45	3TE
	60	4TE
Maximum TEC output current, A	1.20	2TE
	0.45	3TE
	0.40	4TE
Output voltage range, V	min 3.0	
	max 14.5	
Power supply voltage $V_{sup}$ , $V_{DC}$	min 9.0	
	max 16.0	
Power supply current $I_{sup}$ , mA	500	$I_{TEC} = 0.45 \text{ A}$ , $U_{TEC} = 7.5 \text{ V}$
Series resistance of the connecting cable, $\Omega$	1	total resistance of the wires supplying TEC element
Ambient operating temperature, $^\circ\text{C}$	5 to 45	
Storage temperature, $^\circ\text{C}$	-20 to 70	
IR module socket	DB9 (female) DUBOX2x5 (male)	D-sub 9 pin (PTCC-01-ADV, PTCC-01-BAS) PTCC-01-OEM
Power supply socket	DC 2.1/5.5	PTCC-01-ADV, PTCC-01-BAS
	KK2	PTCC-01-OEM
Weight, g	51 $\pm$ 5	PTCC-01-OEM
	155 $\pm$ 5	PTCC-01-BAS
	190 $\pm$ 5	PTCC-01-ADV

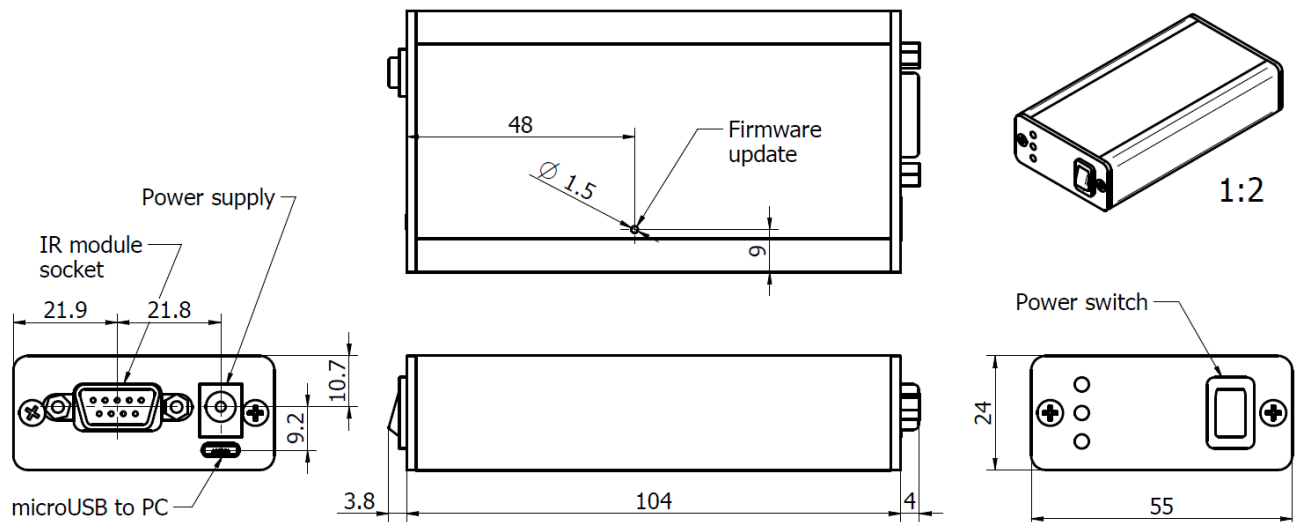


## Mechanical layout, mm

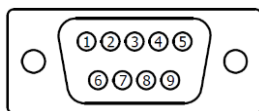
### PTCC-01-ADV



### PTCC-01-BAS



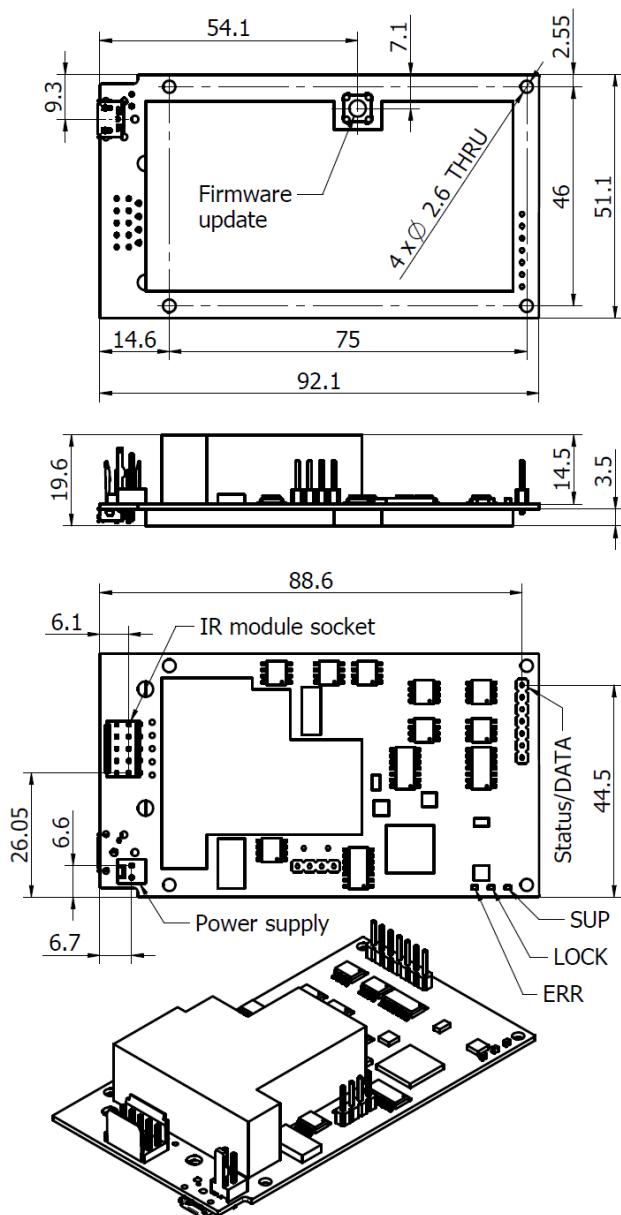
### IR module socket D-sub 9 pin (male)



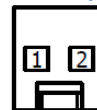
Function	Symbol	Pin number
TEC supply output (+)	TEC+	1
TEC supply output (-)	TEC-	2
Ground	GND	3
Thermistor input (1)	TH1	4
Thermistor input (2)	TH2	5
Power supply output (-)	-V <sub>sup</sub>	6
FAN and programmable preamp internal logic auxiliary supply	+5V	7
Bidirectional data port	DATA	8
Power supply output (+)	+V <sub>sup</sub>	9
Shield	GND-SH	metal cover

## Mechanical layout, mm

### PTCC-01-OEM

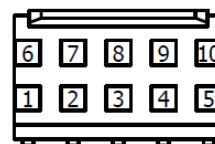


### Power supply socket KK2 (male)



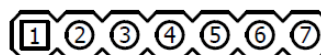
Function	Symbol	Pin number
TEC controller supply input (+)	TECC+	1
TEC controller ground	TEC GND	2

### IR module socket DUBOX2x5 (male)



Function	Symbol	Pin number
TEC supply output (+)	TEC+	1
TEC supply output (-)	TEC-	2
Ground	GND	3
Thermistor input (1)	TH1	4
Thermistor input (2)	TH2	5
Power supply output (-)	-V <sub>sup</sub>	6
FAN and programmable preamp internal logic auxiliary supply	+5V	7
Bidirectional data port	DATA	8
Power supply output (+)	+V <sub>sup</sub>	9
Shield	GND-SH	10

### Status/DATA socket Pin-header 1x7



Function	Symbol	Pin number
Error indicator	ERR – LED	1
Temperature control loop lock indicator	LOCK – LED	2
Module power supply on indicator	SUP – LED	3
Auxiliary supply	3.3 V	4
Transmitted data (RS-232)	TXD	5
Common (signal) ground (RS-232)	GND	6
Received data (RS-232)	RXD	7

### Included accessories for PTCC-01-ADV and PTCC-01-BAS

- **USB: TypeA-MicroB** cable + **AC adaptor**
- **Smart Manager** software

### Included accessories for PTCC-01-OEM

- **USB: TypeA-MicroB, KK2-POWER** cables + **AC adaptor**
- **Smart Manager** software

## PPS-03 series

**PPS-03** is a small-size, easy to use and universal preamplifier power supply, designed to operate with VIGO detection module microM-10.6 and other devices containing uncooled detectors in TO39 packages and preamplifiers SIP-TO39.



### Specification (T<sub>a</sub> = 20°C)

Parameter	Value	Conditions, remarks
Power supply voltage V <sub>sup</sub> , V <sub>DC</sub>	min 9.0 max 16.0	
Output voltage, V <sub>DC</sub>	±15 ±9	PPS-03-15 PPS-03-09
Output current, mA	±100	
IR module socket	DB9 (female)	D-sub 9 pin
Power supply socket	DC 2.1/5.5	
Weight, g	100±5	

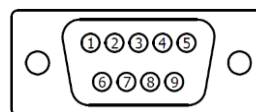
### Code description

Type	Output voltage, V <sub>DC</sub>
PPS-03	09 15

### Included accessories

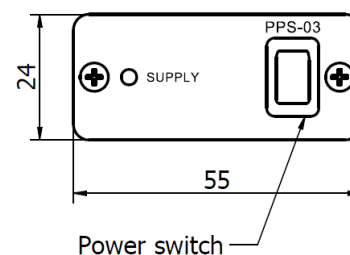
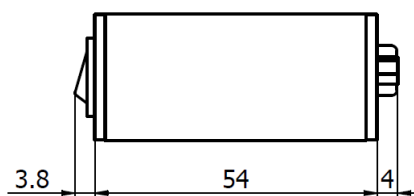
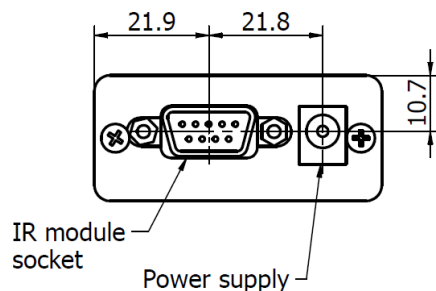
- AC adaptor

### IR module socket D-sub 9 pin (male)



Function	Symbol	Pin number
Not connected	N.C.	1
Not connected	N.C.	2
Ground	GND	3
Not connected	N.C.	4
Not connected	N.C.	5
Power supply output (-)	-V <sub>sup</sub>	6
Not connected	N.C.	7
Not connected	N.C.	8
Power supply output (+)	+V <sub>sup</sub>	9

### Mechanical layout, mm



## AC adaptor and cables

### AC adaptor



GE18 05-P1J  
GE18 09-P1J  
GE18 12-P1J  
Sockets: EU, UK, AU ,US

### Cable for PC connection



USB: TypeA-MicroB

### Signal output cables



SMA-SMA



SMA-BNC



BNC-BNC



MMCX-SMA



MMCX-BNC

### Power supply and TEC control cables



LEMO-DB9



AMP2x4-DB9



AMP2x4-DUBOX2x5



LEMO-DBOX2x5

### Power supply cables



KK2-POWER



JWPF-DB9

## DRB-2 base mounting system

**DRB-2** is a stable base mounting system dedicated for VIGO detection modules with M4 mounting hole and VIGO uncooled detectors in BNC and PEM-SMA packages. DRB-2 has adjustable height and is compatible with M6 optical breadboards.

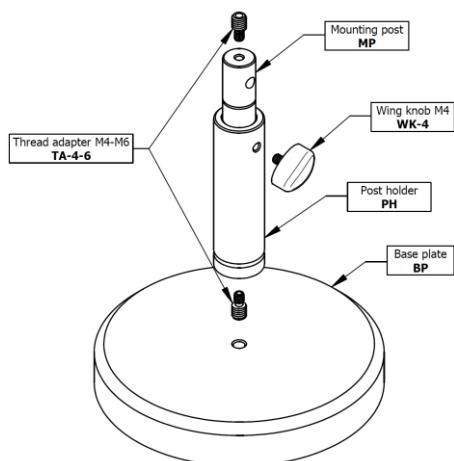
### DRB-2 consists of:

- base plate BP
- mounting post MP
- post holder PH

**BP** is a base plate made of black, lacquered steel. It provides mechanical stable conditions for mounting system. Weight: 1756 g.

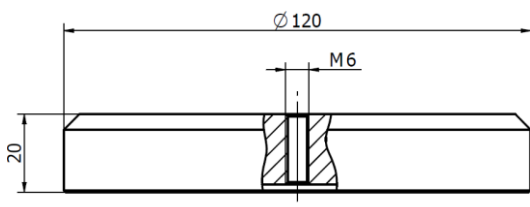
**MP** is a mounting post made of stainless steel. It is equipped with two thread adapters TA-4-6. Weight: 115 g.

**PH** is a post holder made of black anodized aluminium. It is equipped with wink knob WK-4. Weight: 60 g.

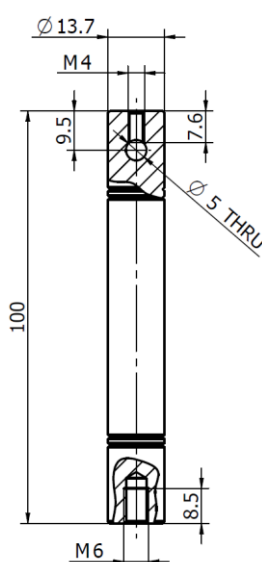


### Mechanical layout, mm

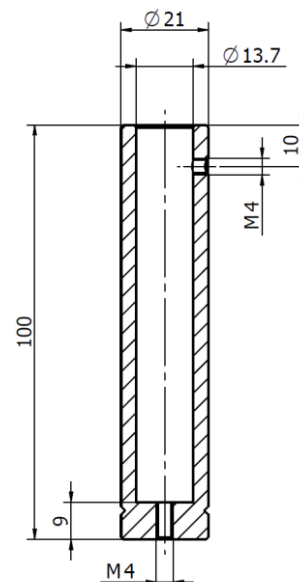
#### Base plate BP



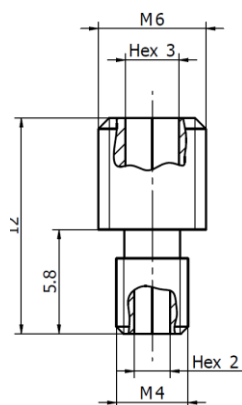
#### Mounting post MP



#### Post holder PH



#### Thread adapter M4-M6

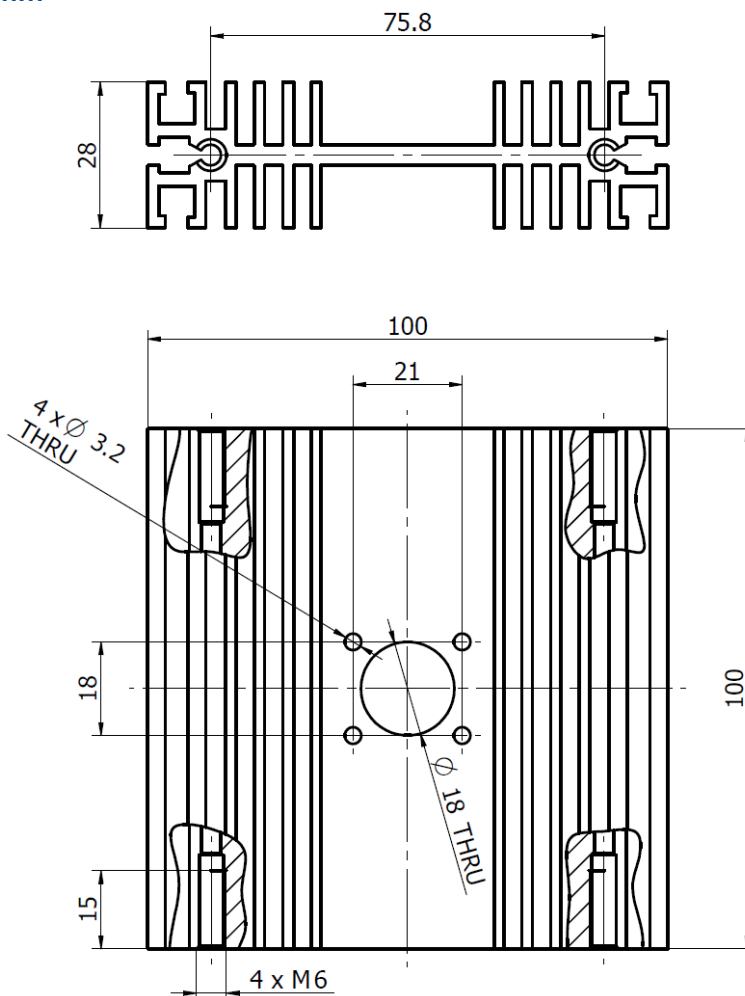


## MHS-2 heatsink

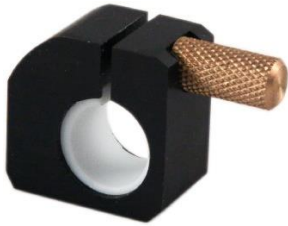
**MHS-2** is an external heatsink made of black anodized aluminium, dedicated for OEM VIGO detection modules integrated with TE cooled detectors and preamplifier SIP-TO8. It provides suitable dissipation of heat generated by the Peltier cooler. Its thermal resistance is  $\sim 1.5$  K/W.



### Mechanical layout, mm

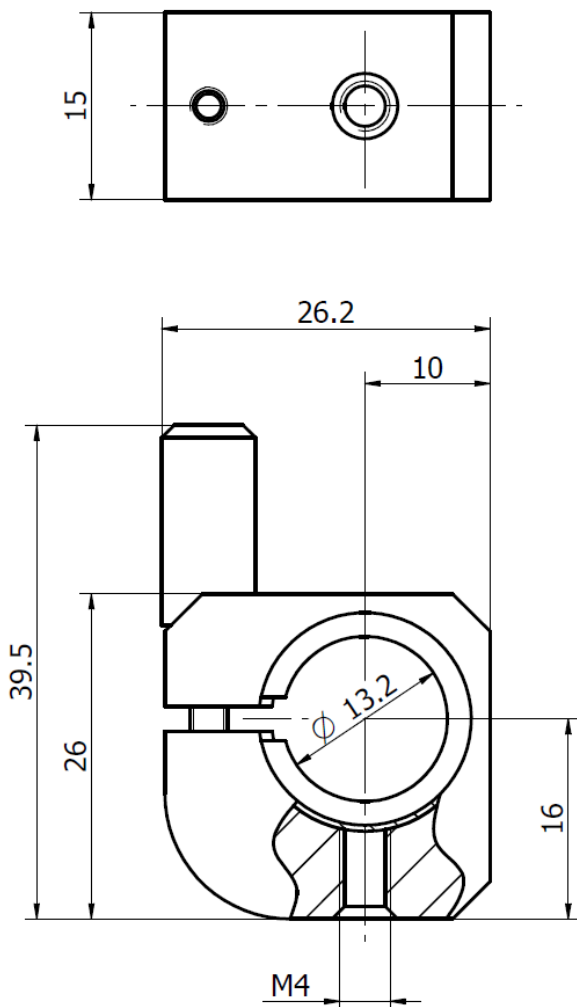


## DH-2 detector holder

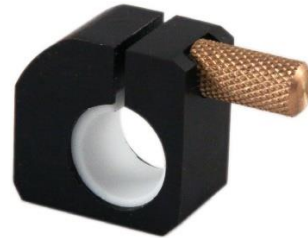


**DH-2** is a detector holder with M4 mounting hole, dedicated for assembly VIGO uncooled detectors in BNC and PEM-SMA packages. It is compatible with DRB-2 mounting system.

### Mechanical layout, mm

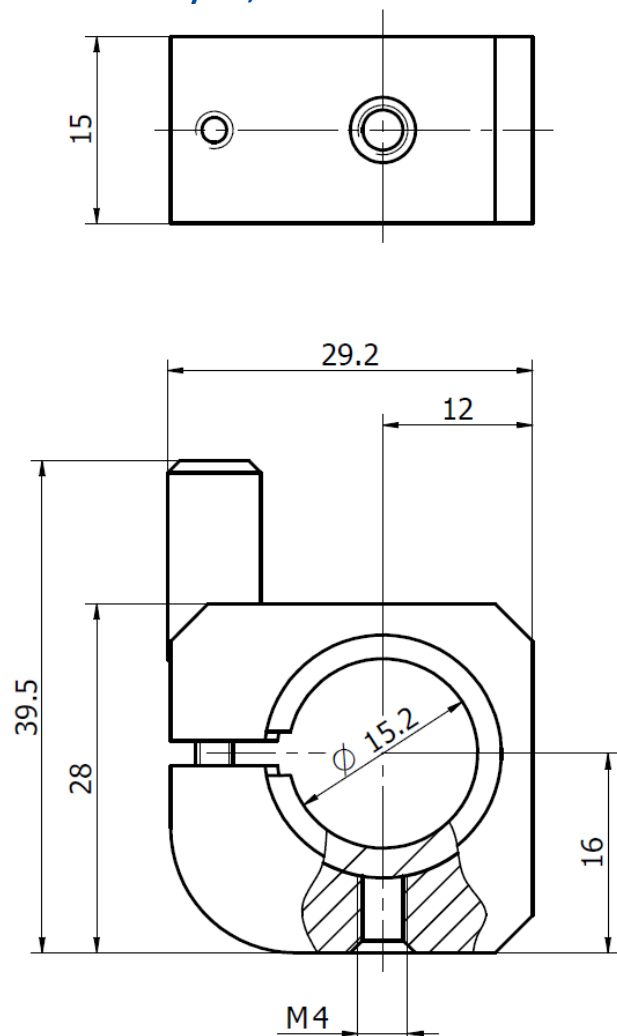


## MH-1 module holder



**MH-1** is a module holder with M4 mounting hole, dedicated for assembly VIGO microM-10.6 detection modules. It is compatible with DRB-2 mounting system.

### Mechanical layout, mm



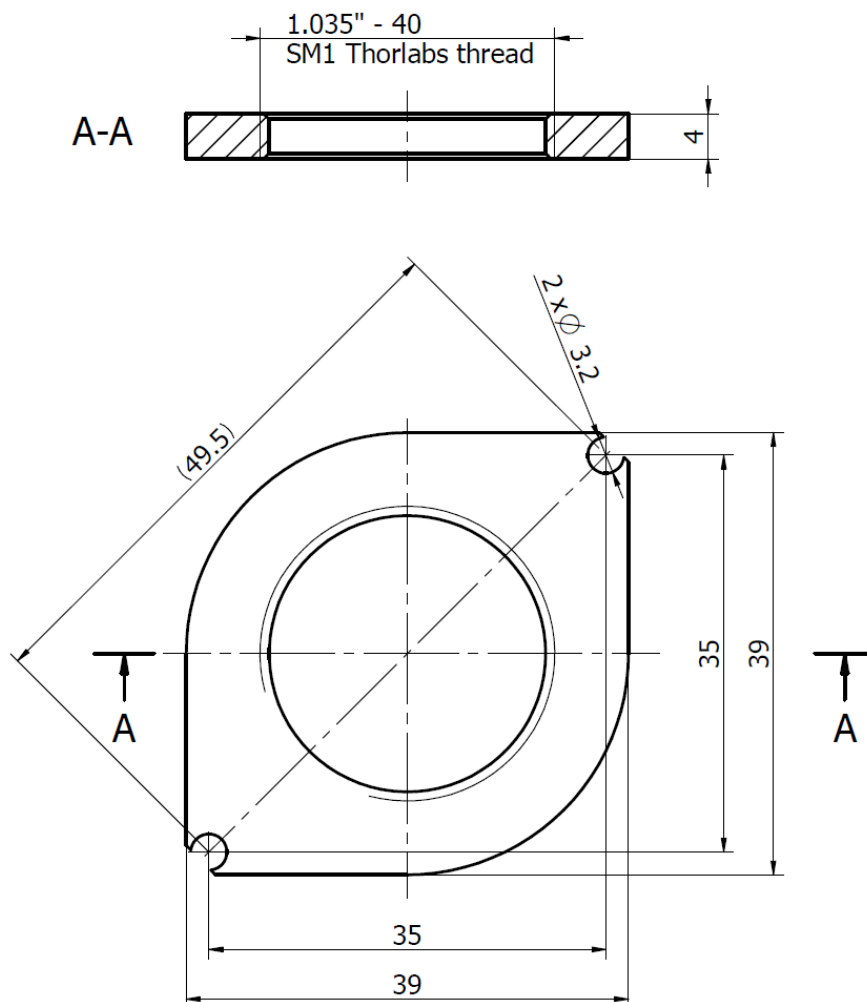
## OTA optical threaded adapter

**OTA** is an optical threaded adapter made of black anodized aluminium. It is an accessory which allows to build complex systems containing VIGO detection modules (AIP, MIP, PIP) and optical components.

OTA is compatible with all types Thorlabs SM1 threaded lens tubes.



### Mechanical layout, mm





# GLOSSARY AND TECHNICAL INFORMATION

## Glossary

### Infrared detectors

Infrared photodetectors are semiconductor electro-optical devices that convert infrared radiation into an electrical signal.

### Photoconductive detectors PC

Photoconductive detectors based on the photoconductive effect. Infrared radiation generates charge carriers in the semiconductor active region decreasing its resistance. The resistance change is sensed as a current change by applying a constant voltage bias. The devices are characterized by near linear current-voltage characteristics. The electric field  $E$  in photoconductors is constant across the device. It equals ratio of bias voltage  $V_b$  and distance between contacts  $L$ :

$$E = \frac{V_b}{L}$$

The optimum bias voltage is specified in the Final test report (supplied with each VIGO device) and depends on detector size, operating temperature and spectral response.

### Photovoltaic detectors PV, PVM

Photovoltaic detectors (photodiodes) are semiconductor structures with one (PV) or multiple (PVM), homo- or heterojunctions. Absorbed photons produce charge carriers that are collected at the contacts, resulting in external photocurrent. Photodiodes have complex current voltage characteristics. The devices can operate either at flicker-free zero bias or with reverse voltage. Reverse bias voltage is frequently applied to increase responsivity, differential resistance, improve high frequency performance and increase the dynamic range. Unfortunately, at the expense of flicker noise  $1/f$  in most cases.

Photovoltaic detectors are more vulnerable to electrostatic discharges than photoconductors.

### Photoelectromagnetic detectors PEM

Photovoltaic detectors are based on the photoelectromagnetic effect based on spatial separation of optically generated electrons and holes in the magnetic field. The devices do not require electrical bias and show no flicker noise  $1/f$ . The PEM devices are typically used as fast, uncooled detectors of the long wavelength radiation.

### Active element material $Hg_{1-x}Cd_xTe$

$Hg_{1-x}Cd_xTe$  also known as Mercury Cadmium Telluride, MCT, HgCdTe, (Cd, Hg)Te or MerCardTel. It is a variable band gap alloy, commonly used for fabrication of photodetectors with tunable spectral response.

### Active element material $InAs_{1-x}Sb_x$

$InAs_{1-x}Sb_x$  also known as Indium Arsenide Antimonide or InAsSb is another variable band gap alloy used for fabrication of photodetectors with tunable spectral response.

### Active area $A$ , mm $\times$ mm

The physical area of a photosensitive element, the active region that converts incoming optical radiation into electric output signal.

$$A = W \text{ (width)} \times L \text{ (length)}.$$

In photoconductors  $L$  is a distance between contacts.

### Optical area $A_o$ , mm $\times$ mm

The apparent optical area of the detector which is "seen". It is equal to physical area of the detector active element unless an optical concentrator is used. The optical detector area can be significantly magnified in detectors supplied with optical concentrators, i.e. immersion microlenses. For more information please see chapter [Optical immersion technology](#).

$$A_o = W_o \text{ (width)} \times L_o \text{ (length)}.$$

### Cut-on wavelength $\lambda_{cut-on}$ (10%), $\mu m$

The shorter wavelength at which a detector responsivity reaches 10% of the peak value.

### Peak wavelength $\lambda_{peak}$ , $\mu m$

The wavelength of detector maximum responsivity.

### Cut-off wavelength $\lambda_{cut-off}$ (10%), $\mu m$

The longer wavelength at which a detector responsivity reaches 10% of the peak value.

### Normalized detectivity $D^*$ , cm $\cdot$ Hz $^{1/2}$ /W

The signal-to-noise ratio (SNR) at a detector output normalized to 1 W radiant power, a 1 cm $^2$  detector optical area and a 1 Hz noise bandwidth.

### Noise equivalent power NEP, nW/Hz $^{1/2}$

The incident power on the detector generating a signal output equal to the 1 Hz bandwidth noise output. Stated another way, the NEP is the signal level that produces a signal-to-noise ratio (SNR) of 1.

### Photocurrent $I_{ph}$

Photocurrent is the current generated by infrared radiation, which is not in thermal equilibrium with detector. For small irradiation, the photocurrent is proportional to incident radiation power  $P$ .

$$I_{ph} = R_i \cdot P$$

$R_i$  is the current responsivity.

### Current responsivity $R_i$ , A/W

Current responsivity is the ratio of photocurrent and power of radiation. The current responsivity is typically measured for monochromatic radiation (the spectral current responsivity) and blackbody radiation (the blackbody current responsivity). The responsivity typically remains constant for weak radiation and tends to decrease with more strong radiation.

### Current responsivity-active area length product $R_i \cdot L$ and current responsivity-optical area length product $R_i \cdot L_o$ , A $\cdot$ mm/W

The current responsivity of unbiased PEM, PVM and biased (with constant electric field  $E$ ) PC detectors is proportional to the reciprocal active area length  $L$  (optical area length  $L_o$ ). Therefore, the current responsivity  $R_i \cdot L$  ( $R_i \cdot L_o$ ) is used to compare devices of various formats.

Another normalized current responsivity,  $R_i \cdot L/E$  ( $R_i \cdot L_o/E$ ), is used to compare responsivity of photoconductive detectors of various format, and operating with different electric fields.

### Time constant $\tau$ , ns

Typically, detector time response can be described by the one pole filter characteristics. Time constant is the time it takes detector to reach  $1/e \approx 37\%$  of the initial signal value. The time constant is related to the 3dB high cut-off frequency  $f_{hi}$ :

$$\tau = 1/(2\pi \cdot f_{hi})$$

Time constant for one pole filter is related to 10-90% rise time  $t_r$ :

$$t_r = 2.2 \cdot \tau$$

### Bias voltage-active area length ratio $V_b/L$ , V/mm

Normalized photoconductive bias voltage for nonimmersed detectors.

### Bias voltage-optical area length ratio $V_b/L_o$ , V/mm

Normalized photoconductive bias voltage for immersed detectors.

### Flicker noise $1/f$

It is a frequency dependent noise. It occurs in any biased devices.

### 1/f noise corner frequency $f_c$ , Hz

Frequency, at which the low frequency noise equals to the white noise (e.g. the Johnson or shot noise), the flicker noise dominates at  $f < f_c$ .

### Resistance-active area product $R \cdot A$ , $\Omega \cdot \text{cm}^2$

Normalized detector resistance for nonimmersed photovoltaic detectors. It is used to compare photodiodes with different sizes of active areas, in which dynamic resistance decreases proportionally to the detector active area.

### Resistance-optical area product $R \cdot A_o$ , $\Omega \cdot \text{cm}^2$

Normalized detector resistance for immersed photovoltaic detectors. It is used to compare photodiodes with different sizes of optical areas, in which dynamic resistance decreases proportionally to the detector optical area.

### Active element temperature $T_{det}$ , K

The detector active element temperature.

### Acceptance angle $\Phi$ , deg

Acceptance angle is the maximum cone angle at which incoming radiation can be captured by a detector. Radiation coming from a larger angle will not reach the detector. In systems without external objectives, acceptance angle and field of view (FOV) are identical.

### Infrared detection modules

Detection module integrates detector, preamplifier, thermoelectric cooler, and other components (detector biasing circuit, heat dissipation system, optics etc.) in a common package. The operation of detection modules can be described in similar way as for detectors, by specifying their spectral and frequency characteristics of responsivity and detectivity.

### Voltage responsivity $R_v$ , V/W

The output voltage divided by optical power incident on the detector. For spectra measurements it can be expressed as:

$$R_v(\lambda) = R_i(\lambda) \cdot K_i$$

### Low cut-off frequency $f_{lo}$ , Hz

The minimum frequency at which a detection module gain reaches -3dB of the peak value or 0 for DC coupling devices.

### High cut-off frequency $f_{hi}$ , Hz

The maximum frequency at which a detection module gain reaches -3dB of the peak value.  $f_{hi}$  of the preamplifier may differ from  $f_{hi}$  of the detection module.

### Noise measurement frequency $f_0$ , Hz

Frequency at which output voltage noise density is measured selectively.

### Transimpedance $K_i$ , V/A

Current to voltage conversion ratio:

$$K_i = \frac{V_{out}}{I_{in}}$$

### Current signal $I_{in}$ , A

Current signal from photodetector when exposed to incident radiant power.

### Output noise voltage density $v_n$ , nV/Hz<sup>1/2</sup>

Noise voltage density measured at preamplifier output.

### Output impedance $R_{out}$ , $\Omega$

Impedance that appears in series with the output from an ideal amplifier.

### Load resistance $R_L$ , $\Omega$

Resistance of the detection module's load.

### Output voltage $V_{out}$ , V

Output signal of the detection module.

### Output voltage offset $V_{off}$ , mV

Output DC voltage of the detection module without input signal.

### Power supply input $+V_{sup}$ and $-V_{sup}$ , V

Supply voltage required for correct detection module operation.

### Power supply current $I_{sup}$ , mA

Supply current consumption during correct detection module operation.

### GND

Point of zero potential. It is common power supply ground and signal ground.

### Ambient operating temperature $T_a$ , °C

Ambient temperature during test measurements.

### Thermoelectric coolers and thermoelectric cooler controllers

#### Active element temperature $T_{det}$ , K

The detector active element temperature.

#### Maximum thermoelectric cooler current $I_{max}$ , A

Maximum current resulting in greatest  $\Delta T_{max}$ .

#### Maximum thermoelectric cooler voltage $V_{max}$ , V

Maximum voltage drop resulting in greatest  $\Delta T_{max}$ .

**Maximum heat pumping capacity  $Q_{\max}$ , W**

$Q_{\max}$  rated at  $\Delta T = 0$ . At other  $\Delta T$  cooling capacity should be estimated as  $Q = Q_{\max} \cdot (1 - \Delta T/\Delta T_{\max})$ .

**Maximum temperature difference  $\Delta T_{\max}$ , K**

$\Delta T_{\max}$  rated at  $Q = 0$ . At other  $Q$  the temperature difference should be estimated as  $\Delta T = \Delta T_{\max} \cdot (1 - Q/Q_{\max})$ .

**Temperature stability, K**

It indicates the possible error in the temperature on the thermoelectric cooler.

**Temperature readout stability, mK**

It indicates the possible error in readout of the temperature of the thermoelectric cooler provided by controller.

**Detector temperature settling time, s**

The time taken by the cooling system to reach appropriate temperature of the detector active element.

**Maximum TEC output current, A**

Maximum current that is provided by the controller to the thermoelectric cooler.

**Output voltage range, V**

Range of voltage on output of module.

**Power supply voltage  $V_{\text{sup}}$ , V<sub>DC</sub>**

Supply voltage required for correct thermoelectric cooler controller operation.

**Power supply current  $I_{\text{sup}}$ , mA**

Supply current required for correct thermoelectric cooler controller operation.

**Series resistance of the connecting cable,  $\Omega$** 

Material parameter. It is resistance of the supply cable. It depends on the cable length.

## Detector's packages and infrared windows

Photo	Package type	Cooling	Window	Detector type
	BNC	uncooled	no	PC, PCI, PV, PVI, PVM, PVMI
	TO39	uncooled	no	PC, PCI, PV, PVI, PVA, PVIA, PVM, PVMI
	PEM-SMA	uncooled	yes	PEM, PEMI
	PEM-TO8	uncooled	yes	PEM, PEMI
	TO8	uncooled	no	PCQ, PVMQ
	TO8	TE cooled	yes	PC-2TE, PC-3TE, PC-4TE PCI-2TE, PCI-3TE, PCI-4TE PV-2TE, PVA-2TE, PV-3TE, PV-4TE PVI-2TE, PVIA-2TE, PVI-3TE, PVI-4TE PVM-2TE PVMI-2TE, PVMI-3TE, PVMI-4TE
	TO66	TE cooled	yes	PC-2TE, PC-3TE, PC-4TE PCI-2TE, PCI-3TE, PCI-4TE PV-2TE, PVA-2TE, PV-3TE, PV-4TE PVI-2TE, PVIA-2TE, PVI-3TE, PVI-4TE PVM-2TE PVMI-2TE, PVMI-3TE, PVMI-4TE

Uncooled detectors are typically provided in BNC or TO39 packages without the window.

The exception are the specialized PEM packages. Due to magnetic circuit incorporated into the package, 3° wedged zinc selenide anti-reflection coated (wZnSeAR) window is supplied to protect against external pollution. There are two versions of packages dedicated for photoelectromagnetic detectors:

- PEM-SMA with SMA signal output connector which makes it convenient in use,
- PEM-TO8 on TO8 header which enables integration with VIGO preamplifier.

### Encapsulation

Thermoelectrically cooled detectors are mounted in metal packages: TO8 and TO66 sealed with IR windows. The packages are filled with dry, heavy, noble gases (Krypton / Xenone mixture) of low thermal conductivity. Water vapor condensation is prevented by humidity absorber container mounted inside the package and careful polymer sealing. For low temperature fluctuation anti-convection shields is also apply.

### Infrared windows

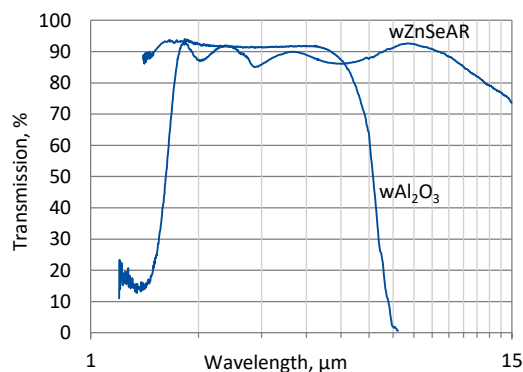
We provide two types windows as a standard:

- 3° wedged sapphire (wAl<sub>2</sub>O<sub>3</sub>)
- 3° wedged zinc selenide anti-reflection coated (wZnSeAR)

3° wedge prevents „fringing” – unwanted interference effects.

Material	Hardness, kg/mm <sup>2</sup>	Wedging	Anti-reflection coating	Symbol
sapphire	1370	3°	no	wAl <sub>2</sub> O <sub>3</sub>
zinc selenide	120	3°	yes	wZnSeAR

### Spectral transmission of wAl<sub>2</sub>O<sub>3</sub> and wZnSeAR windows (typical example)



## Thermoelectric cooling

Some of VIGO devices are provided with thermoelectric cooling. Cooling of infrared detectors reduces noises, increases responsivity, shifts the cut-off wavelength toward longer wavelengths (in HgCdTe detectors) and toward shorter wavelengths (in InAs / InAsSb detectors). Two-, three- and four-stage thermoelectric coolers are available. Operation of TE coolers is based on Peltier effect. Thermoelectric coolers are supplied with DC power supply.

### Thermoelectric coolers parameters<sup>\*)</sup>

Parameter	Cooling		
	2TE	3TE	4TE
Active element temperature $T_{det}$ , K	~230	~210	~195
Maximum TEC voltage $V_{max}$ , V	1.3	3.6	8.3
Maximum TEC current $I_{max}$ , A	1.20	0.45	0.40
Maximum heat pumping capacity $Q_{max}$ , W	0.36	0.27	0.28

<sup>\*)</sup> Depend on temperature of the hot side of the TE cooler. Typically specified for 300 K.

## Temperature control

Thermoelectrically cooled detectors are equipped with built-in thermistor to provide precise control and measurements of detector active element temperature.

The electricity applied to between terminals of thermistors should be under the maximum power dissipation at 25°C (100 mW) not to destroy the thermosensor. For the measurement of resistance, the power should not exceed 1 mW.

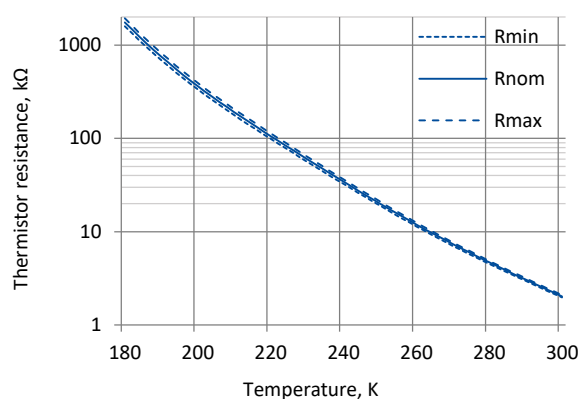
The relation between the resistance and the temperature:

$$R_T = R_{T_0} \exp\left(\beta \cdot \frac{T_0 - T}{T \cdot T_0}\right)$$

$$R_{T_0} = 2.2 \text{ k}\Omega \pm 3\% \text{ at } T_0 = 298 \text{ K}$$

$$\beta = 3500 \text{ K} \pm 1\%$$

### Thermistor characteristics



### Resistance vs. temperature of thermistor

T, K	T, °C	R <sub>min</sub> , kΩ	R <sub>nom</sub> , kΩ	R <sub>max</sub> , kΩ
180	-93	1594.97	1757.95	1935.84
182	-91	1336.02	1469.90	1615.75
184	-89	1124.16	1234.66	1354.81
186	-87	950.46	1042.11	1141.58
188	-85	807.57	883.99	966.78
190	-83	689.57	753.62	822.88
192	-81	591.68	645.64	703.89
194	-79	510.07	555.75	604.98
196	-77	441.68	480.54	522.34
198	-75	384.05	417.25	452.91
200	-73	335.23	363.71	394.26
202	-71	293.65	318.17	344.43
204	-69	258.05	279.23	301.88
206	-67	227.41	245.76	265.36
208	-65	200.91	216.85	233.85
210	-63	177.89	191.77	206.55
212	-61	157.81	169.92	182.79
214	-59	140.22	150.80	162.03
216	-57	124.76	134.02	143.83
218	-55	111.14	119.25	127.83
220	-53	99.10	106.21	113.72
222	-51	88.44	94.67	101.25
224	-49	78.98	84.44	90.21
226	-47	70.57	75.37	80.42
228	-45	63.09	67.30	71.73
230	-43	56.42	60.12	64.01
232	-41	50.49	53.74	57.15
234	-39	45.19	48.05	51.04
236	-37	40.47	42.98	45.61
238	-35	36.26	38.47	40.77

T, K	T, °C	R <sub>min</sub> , kΩ	R <sub>nom</sub> , kΩ	R <sub>max</sub> , kΩ
240	-33	32.51	34.45	36.47
242	-31	29.16	30.87	32.64
244	-29	26.18	27.68	29.24
246	-27	23.51	24.84	26.21
248	-25	21.14	22.30	23.51
250	-23	19.02	20.05	21.11
252	-21	17.13	18.04	18.98
254	-19	15.45	16.25	17.07
256	-17	13.95	14.65	15.38
258	-15	12.61	13.23	13.87
260	-13	11.41	11.96	12.53
262	-11	10.34	10.83	11.33
264	-9	9.38	9.82	10.26
266	-7	8.52	8.91	9.31
268	-5	7.75	8.10	8.45
270	-3	7.07	7.37	7.69
272	-1	6.45	6.72	7.00
274	1	5.89	6.13	6.38
276	3	5.38	5.60	5.83
278	5	4.93	5.13	5.32
280	7	4.52	4.69	4.87
282	9	4.15	4.30	4.46
284	11	3.81	3.95	4.09
286	13	3.50	3.63	3.75
288	15	3.22	3.33	3.45
290	17	2.96	3.06	3.17
292	19	2.73	2.82	2.91
294	21	2.51	2.59	2.68
296	23	2.32	2.39	2.46
298	25	2.13	2.20	2.27

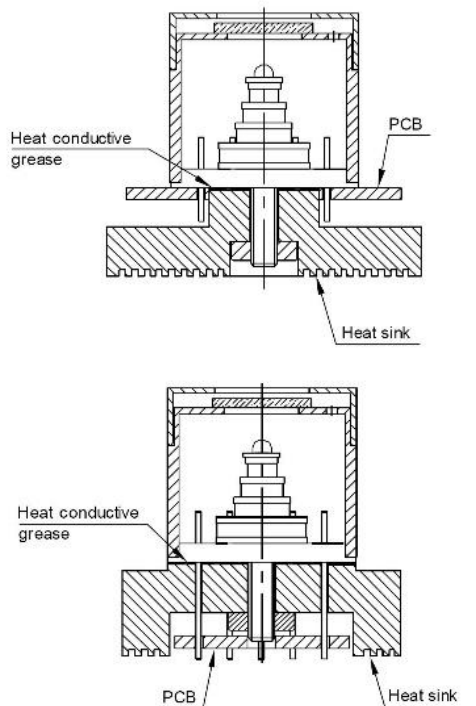
## Heat sinking

Suitable heat sinking is necessary to dissipate heat generated by the Peltier cooler or excessive optical irradiation. Since heat is almost 100% dissipated at the base of the detector header, it must be firmly attached to the heat sink.

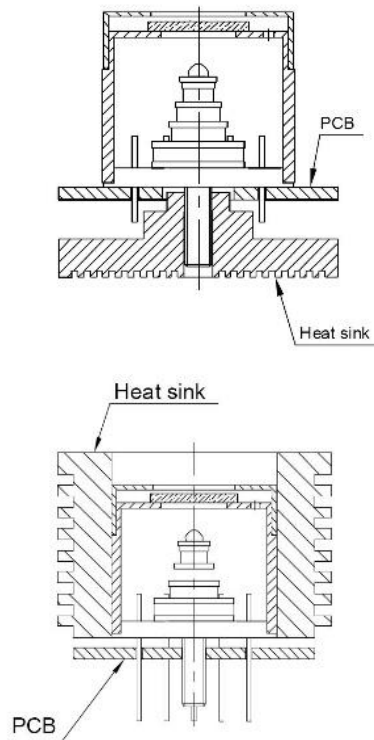
A thin layer of heat conductive epoxy or silicon (thermal) grease should be used to improve thermal contact between the detector header and the heat sink to maximize heat transfer. Heat sinking via the detector cylindrical cap or via the mounting screw is not sufficient.

A heatsink thermal resistance of  $\sim 2$  K/W is typically recommended for the most 2TE and 3TE coolers. For 4TE cooler, heatsink thermal resistance  $\sim 1$  K/W is recommended.

### Correct heatsink placement



### Incorrect heatsink placement



## Optical immersion technology

In order to improve performance and get the best signal-to-noise ratio of the devices, optical immersion technology may be applied. It is successfully used in all types VIGO detectors.

Optical immersion is the monolithic integration of detector active element with hyperhemispherical microlens (default). It makes optical linear size of detector active area 11 times larger compared to its physical size. This results in improvement of detectivity  $D^*$  by one order of magnitude. Also detector electric capacitance  $C_d$  is reduced by a factor of two orders of magnitude compared to conventional detector of the same optical area. Acceptance angle  $\Phi$  is reduced to  $\sim 36^\circ$  – the microlens naturally shields background radiation which is one of the factors of noise. Hemispherical microlens is available as a custom option.

Optical power limitations for optically immersed detectors are more restrictive than for detectors without immersion microlens – for more information please see chapter [Precautions for use](#).

### Optically immersed detectors parameters

Parameter	Microlens shape			
	Hemisphere <sup>*)</sup>		Hyperhemisphere	
	Theory	GaAs	Theory	GaAs
Distance L	R	R	$R \cdot (n+1)$	$4.3 \cdot R$
$d / d'$	n	3.3	$n^2$	10.9
$D^*_{imm} / D^*_{non-imm}$	n	3.3	$n^2$	10.9
Acceptance angle $\Phi$	$180^\circ$	$180^\circ$	$2 \arcsin(1/n)$	$\sim 36^\circ$

<sup>\*)</sup> Custom option

n – refractive index of microlens material (GaAs),  $n = 3.3$

d – optical (apparent) detector size

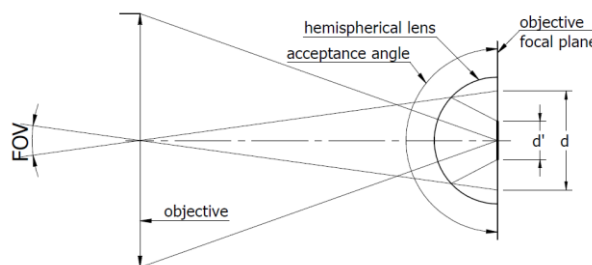
d' – physical detector size

R – lens radius

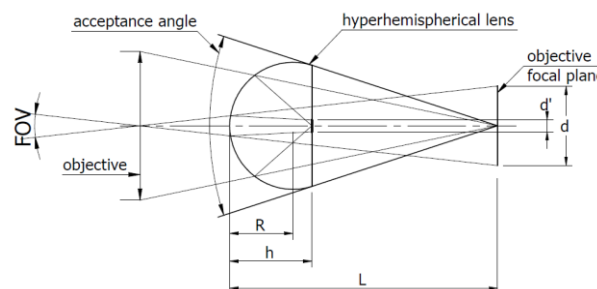
L – lens face to objective focal plane distance

h – lens thickness,  $h = R + R/n$

### Function and properties of hemisphere microlens



### Function and properties of hyperhemisphere microlens





## Precautions for use

### Operating temperature

A detector should be operated at its optimal temperature given in the Final test report (delivered with every device).

### Maximum voltage

Do not operate the photovoltaic detector at higher bias voltages than suggested in the Final test report (delivered with every device).

### Be careful using ohmmeters for photovoltaic detectors!

Standard ohmmeters may overbias and damage the detector. This is especially true for small physical area or SWIR photovoltaic detectors. Bias of 10 mV can be used for resistance measurements of any type of detector. Ask for conditions of I-V plot measurements!

### Usage

Devices can operate in the 10% to 80 % humidity, in the -20°C to +30 °C ambient temperature range. Operation at >30°C ambient may reduce performance for standard Peltier coolers. Ask for devices that can operate in the +30°C to +80°C ambient temperature range.

### Storage

The following conditions should be fulfilled for safe and reliable operation of detector:

- store in dark place, 10% to 90% humidity and -20°C to +50°C temperature,
- avoid exposing to the direct sunlight and strong UV/VIS light as this may result in degradation of the detector performance,
- avoid electrostatic discharges at leads therefore, the devices should be stored having leads shorted.

### Beam power limitations

Damage thresholds, specified as integrated power of incoming radiation:

- For devices without immersion microlens irradiated with continuous wave (CW) or single pulses of more than 1 μs duration, irradiated power on the active area must not exceed 100 W/cm<sup>2</sup>. The irradiance of a pulse shorter than 1 μs must not exceed 1 MW/cm<sup>2</sup>.
- For optically immersed detectors irradiated with CW or single pulse longer than 1 μs irradiance on the apparent optical active area must not exceed 2.5 W/cm<sup>2</sup>. The irradiance of the pulse shorter than 1 μs must not exceed 10 kW/cm<sup>2</sup>.
- For repeated irradiation with pulses shorter than 1 μs, the equivalent CW irradiation, average power over the pulse-to-pulse period should be less than the CW damage threshold according to equation:

$$\text{equivalent CW radiation power density} = \frac{\text{pulse peak power}}{\text{focus area}} \cdot \text{pulse duration} \cdot \text{repetition rate}$$

Saturation thresholds vary by detector type and can be provided upon request.

### Handling

Particular attention should be paid to not scratch a surface of the window. A damaged window may entirely degrade the detector performance. Excessive mechanical stress applied to the package itself or to a device containing the package may result in permanent damage. Peltier element inside thermoelectrically cooled detectors is susceptible to mechanical shocks. Great care should be taken when handling cooled detectors.

### Cleaning window

Keep the window clean. Use a soft cotton cloth damped with isopropyl alcohol and wipe off the surface gently if necessary.

### Mechanical shocks

The Peltier elements may be damaged by excessive mechanical shock or vibration. Care is recommended during manipulations and normal use. Drop impacts against a hard surface are particularly dangerous.

### Shaping leads

Avoid bending the leads at a distance less than 2 mm from a base of the package to prevent glass seal damage. When shaping the leads, maximum two right angle bends and three twists at the distance minimum 6 mm from the base of the package. Keep the leads of the detecting element shorted when shaping!

### Soldering leads

IR detectors can be easily damaged by excessive heat. Special care should be taken when soldering the leads. Usage of heat sinks is highly recommended. Tweezers can be used for this purpose; when soldering, clamp a lead at a place between the soldering iron and the base of the package. To avoid destructive influence of ESD and other accidental voltages (e.g. from a non-grounded soldering iron) rules for handling LSI integrated circuits should be applied to IR detectors too. Leads should be soldered at +370 °C or below within 5 s.

## How to choose an IR Detector & Preamplifier

### Choosing a Detector

There are four issues:

- The wavelength or wavelength region of interest
- The required speed of response
- Required sensitivity
- Other characteristics (e.g., required power consumption, size, hardness, price)

#### **Wavelength or wavelength region of interest.**

Our IR quantum detectors are usually sensitive enough to be useful only at wavelengths shorter than 13 microns or longer. Though some models retain useful sensitivity in visible and near infrared, we suggest they be used there only when such use allows the user to avoid adding complexity to the system by not adding a more suitable detector like silicon or germanium photodiode to a system already having ours for the longer wavelength.

#### **Required speed of response.**

If the system is to monitor rapidly changing input signals, like laser pulses, you need a fast detector. We offer nanosecond response to 11+ microns. If the system is to provide real-time control of a process, you probably only need microsecond or millisecond response. If the system just needs to turn off the room lights after the last person leaves the room, a quite slow response is probably fine. Our photovoltaic detectors typically provide excellent service for all frequencies from DC to tens or even hundreds of megahertz. Our photoconductive types (like all photoconductors), though fast, have excess noise at low frequencies (called 1/f or 'flicker' noise) and must normally be chopped at a suitable frequency and synchronously demodulated to achieve slow response.

#### **Sensitivity**

How much sensitivity do you need? The best objective expression of "sensitivity" is the signal-to-noise-ratio (S/N) that a photodetector and its following electronics produces at the point where the information is to be used.  $S/N > 10$  is often plenty and  $S/N > 100$  is normally more than enough to eliminate perceived noise when viewed as an oscilloscope trace by the human eye. Higher S/N is needed as the required precision of measurement increases. Sensitivity is often costly in both money, system complexity and logistics (such as LN<sub>2</sub> cooling). **D\*** (spoken "D-star") is a figure of merit for IR photodetectors that attempts to allow comparison between types. When it comes to D\*, bigger is better.

For detailed info on how to predict the performance of a photodetector from knowledge of wavelength, frequency, D\*, etc., and thus determine the S/N you can expect in your system, see our application note, "Predicting the Performance of a Photodetector".

#### **Other detector characteristics**

Characteristics that may influence your choice of a detector include power consumption, logistics like LN<sub>2</sub> for cooling if required, size, robustness, and price.

## **Choosing a Preamplifier**

1. Determine the detector you intend to purchase.
2. Determine the highest frequency you expect to see or the system chopping frequency.
3. Multiply the highest frequency or the chopping frequency by 10 if you want to resolve the waveform cleanly.
4. Consult our table of available preamps. Normally select a DC-coupled preamp for use with photovoltaic devices or an AC-coupled preamp for use with photoconductive devices, or consult us.
5. Consult us if you need customized bandwidth or special gain for your preamp. We routinely customize.



# Predicting the performance of a photodetector

by Fred Perry,

Boston Electronics Corporation, 91 Boylston Street, Brookline, MA 02445 USA.

Comments and corrections and questions are welcome.

The performance of a photodetector system can be predicted from the parameters  $D^*$  (detectivity), Responsivity, time constant and saturation level, and from some knowledge about the noise in the system. No photodetector should be purchased until a prediction has been made.

- **Detectivity and NEP**

The principal issue usually facing the system designer is whether the system will have sufficient sensitivity to detect the optical signal which is of interest. Detector manufacturers assist in making this determination by publishing the figure of merit " $D^*$ ".  $D^*$  is defined as follows:

$$D^* \equiv \frac{\sqrt{A \times \Delta f}}{NEP} \quad (\text{equation 1})$$

where  $A$  is the detector area in  $\text{cm}^2$

$\Delta f$  is the signal bandwidth in hertz

and  $NEP$  is an acronym for "Noise Equivalent Power", the optical input power to the detector that produces a signal-to-noise ratio of unity ( $S/N=1$ ).

$D^*$  is a "figure of merit" and is invaluable in comparing one device with another. The fact that  $S/N$  varies in proportion to  $\sqrt{A}$  and  $\sqrt{\Delta f}$  is a fundamental property of infrared photodetectors.

- **Active Area**

Consider a target about which we wish to measure some optical property. If the image of the target is larger than the photodetector, some energy from the target falls outside the area of the detector and is lost. By increasing the detector size we can intercept more energy. Assuming the energy density at the focal plane is constant in watts/cm<sup>2</sup>, doubling the linear dimension of the detector means that the energy intercepted increases by  $2^2 = 4$  times. But NEP increases only as  $\sqrt{4} = 2$ . Conversely, if the image of the target is small compared to the detector size, and if there are no pointing issues related to making the image of the target fall on the photodetector, then halving the linear dimension of the photodetector will similarly double S/N, since the input optical signal S stays constant while the NEP DECREASES by a factor of  $\sqrt{4} = 2$ . The moral of this story is: Neither throw away photons nor detector area. Know your system well enough to decide on an optimized active area.

- **Bandwidth**

Error theory tells us that signal increases in a linear fashion but noise (if it is random) adds 'RMS'. That is, Signal increases in proportion to the time we observe the phenomenon, but Noise according to the square root of the observation time. This means that if we observe for a microsecond and achieve signal-to-noise of  $\beta$ , in an integration time of 100 microseconds we can expect S/N of  $\sqrt{100}\beta = 10\beta$ . Bandwidth is related to integration time by the formula

$$\Delta f = \frac{1}{2\pi\tau} \quad (\text{equation 2})$$

where  $\tau$  is the integration time or "time constant" of the system in seconds. Time constant  $\tau$  is the time it takes for the detector (or the system) output to reach a value of  $\left(1 - \frac{1}{e}\right) \cong 63\%$  of its final, steady state value.

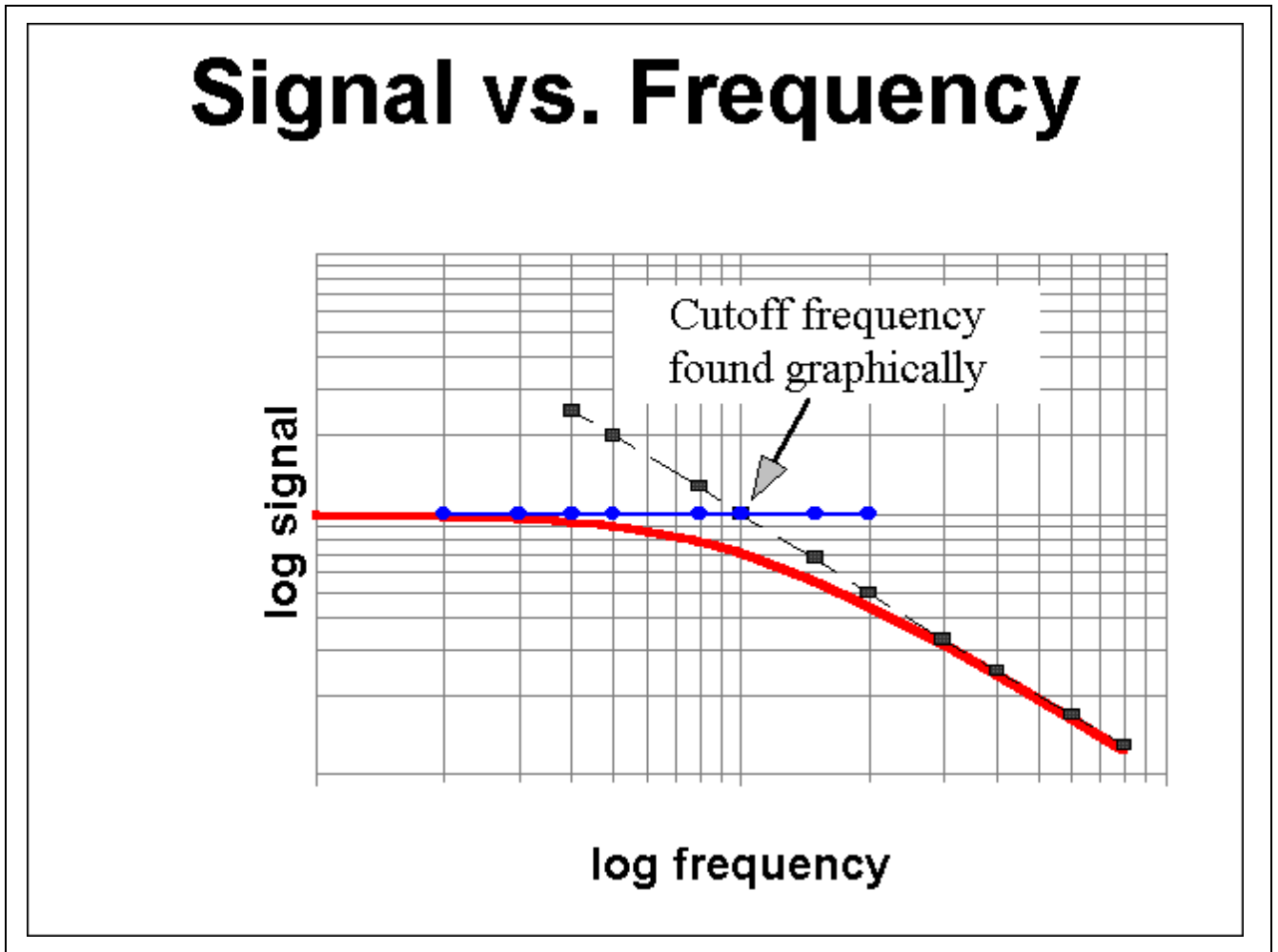
- **Signal**

Signal in all quantum photodetectors is constant versus frequency at low frequencies but begins to decline as the frequency increases. The decline is a

function of the time constant. If  $S_{low}$  is the signal at  $f_{low}$ , a few hertz, the signal at arbitrary frequency  $f \gg f_{low}$  is

$$S_f = \frac{S_{low}}{\sqrt{1 + (2\pi\tau)^2}} \quad (\text{equation 3})$$

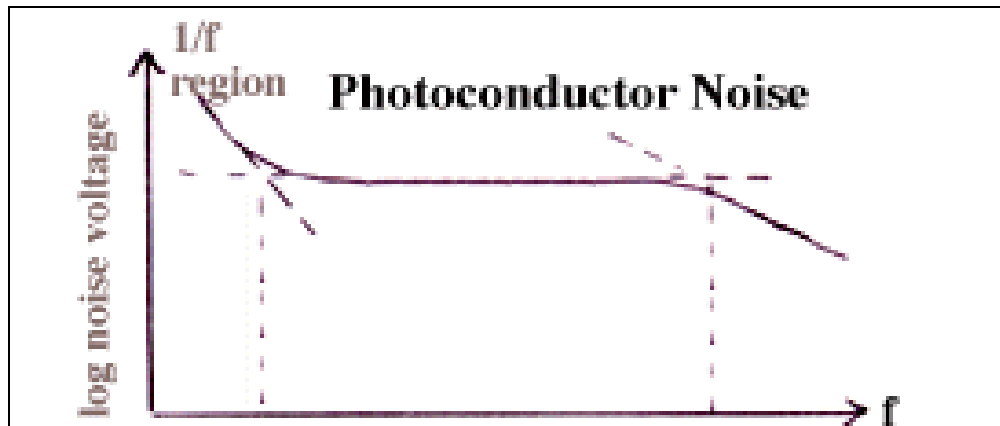
This is graphically illustrated below. Frequency  $f_c$  is the point at which  $S_f = \frac{1}{\sqrt{2}} S_{low}$ .



- **Noise**

Noise is not as simple as signal. Photoconductive devices like PbS, PbSe, and most HgCdTe exhibit “flicker” or 1/f noise, which is excess noise at low frequencies. Consequently, Signal-to-Noise ratio and  $D^*$  are degraded at these

frequencies.  $1/f$  noise actually varies as  $\sqrt{\frac{1}{f}}$  in voltage terms. At high frequencies, the detector noise actually decreases according to the same relationship as signal decreases. However, the difficulty in constructing following amplifier electronics that are significantly lower in noise than the photodetector results in system always having a noise at high frequencies that is no better than noise at low frequencies. The following set of graphs illustrates this.

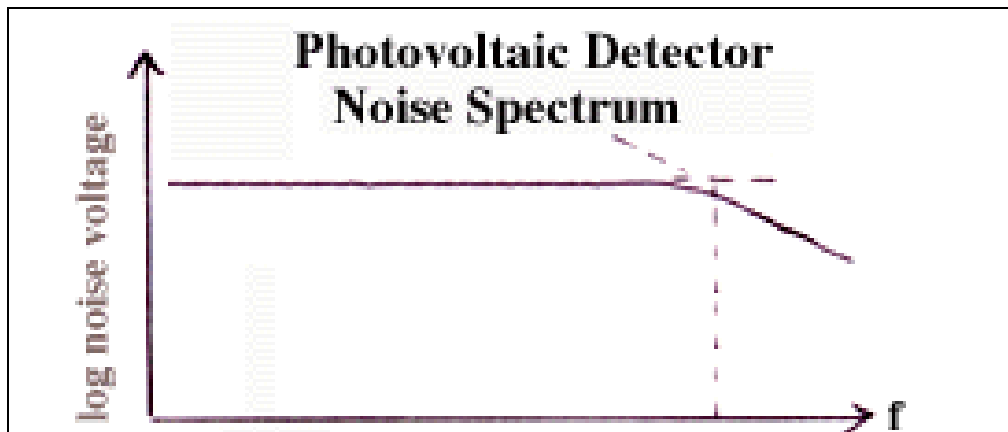


To predict low frequency performance of a photoconductor, the extent to which  $D^*$  is degraded by  $1/f$  noise must be estimated. Either of the following ways is applicable:

1. use the manufacturer's published graphical data of  $D^*$  versus frequency to determine the multiplication factor  $N_{excess}$  to use to convert minimum guaranteed  $D^*$  at its measured frequency to  $D^*$  at the frequency of interest.
2. use the  $1/f$  "corner frequency"  $f_{corner} > f_{low}$  reported by the manufacturer to estimate the degradation factor at  $f_{low}$  as

$$\text{excess noise factor } N_{excess} = \sqrt{\frac{f_{corner}}{f_{low}}} \quad (\text{equation 4})$$

In contrast to photoconductors, photovoltaic detectors normally have no  $1/f$  noise. Signal is flat to or near DC and therefore  $D^*$  is constant below the high frequency roll-off region, so no low frequency correction need be made.



- **Spectral response correction**

The  $D^*$  of a quantum detector varies with wavelength  $\lambda$ . The detector manufacturer typically guarantees  $D^*$  at the wavelength of peak response,  $D^*(peak)$ . When using the device at another wavelength  $\lambda$ , the  $D^*$  should be corrected by an appropriate factor:

$$R_{\lambda} = \frac{(\text{response} - \text{at} - \lambda)}{(\text{response} - \text{at} - \text{peak})}$$

$$D_{\lambda}^* = D_{peak}^* \times R_{\lambda} \quad (\text{equation 5})$$

where the relative response at wavelength  $\lambda$  is estimated by inspection of spectral response curves or other data supplied by the manufacturer.

Therefore, the optical input power required to produce a signal-to-noise ratio of 1:1 for a stated system response time and wavelength becomes:

Case 1: Photoconductor at low frequency:

$$NEP_{\lambda} = \frac{\sqrt{A \times \Delta f}}{D_{\lambda}^*} \times N_{excess} \quad (\text{equation 6})$$

Case 2: Photovoltaic detector at low to moderate frequency:



$$NEP_{\lambda} = \frac{\sqrt{A \times \Delta f}}{D_{\lambda}^*} \quad (\text{equation 7})$$

Case 3: Photoconductor or photovoltaic frequency at higher frequency:

$$NEP_{\lambda} = \frac{\sqrt{A \times \Delta f}}{S_f \times D_{\lambda}^*} \quad (\text{equation 8})$$

This yields an estimate of the input optical power to achieve a voltage output with S/N=1.

- **Upper Limits**

Another important question is the dynamic range of the system, e.g. the ratio of the maximum signal available to the *NEP* of the system. The upper limit of the system is typically set by the electrical gain of the preamp or the vertical gain of the oscilloscope used to display the signal, combined with the maximum output signal of the preamp or the maximum vertical deflection of the oscilloscope. The dynamic range of the system is then expressed in multiples of the system *NEP*.

Let the preamp gain be *G*. Let the responsivity of the detector in volts per watt (or volts per division in the case of an oscilloscope) at low frequency be *R<sub>low</sub>* and at frequency *f* let it be *R<sub>f</sub>* where

$$R_f = R_{low} \times S_f \quad (\text{equation 10})$$

The voltage signal from the detector into the preamp or oscilloscope when S/N=1 corresponding to this responsivity will be

$$V_f = NEP \times R_f \quad (\text{equation 11})$$

Then the output of the preamp at frequency *f* and S/N=1 will be

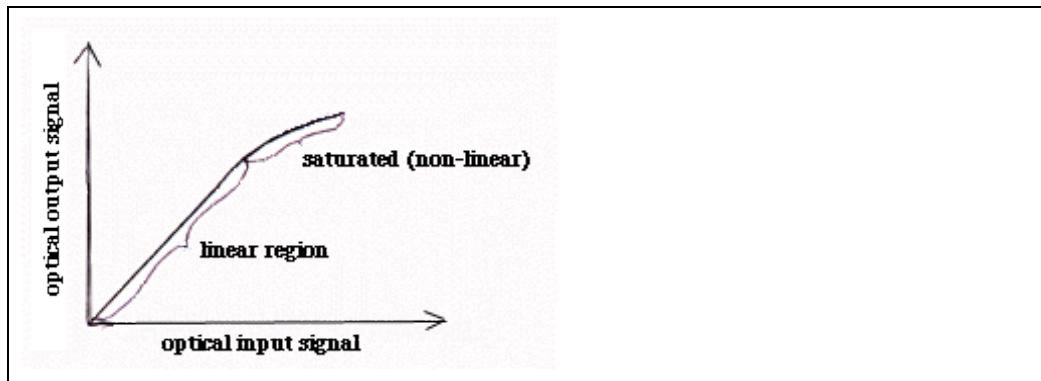
$$V_{preamp} = V_f \times G \quad (\text{equation 12})$$

Let the maximum output of the system be  $\Psi_{preamp}$  volts (or  $\Psi_{vertical}$  vertical divisions in the case of an oscilloscope). The multiple of the NEP that corresponds to the maximum output  $\Psi_{preamp}$  will therefore be

$$\text{Preamp Dynamic Range} \quad D = \frac{\Psi_{preamp}}{V_f \times G} \quad (\text{equation 13})$$

Of course, with an oscilloscope it is usually possible to turn down the gain and thus increase the dynamic range. However, preamps usually have fixed gain. In that case the input optical must be attenuated in order to keep the output from the preamp from saturating.

Sometimes the photodetector itself will saturate before the preamp. Some process, thermal or photonic, intrinsic to the photodetector may limit its output. In this case, the maximum available (saturation) output signal should be specified by the device manufacturer, typically as a not-to-exceed output voltage  $\Psi_{detector}$ . Graphically the situation is illustrated as follows:



Case 1: Dynamic Range limited by the preamp

$$D = \frac{\Psi_{preamp}}{V_f \times G} < \frac{\Psi_{detector}}{V_f} \quad (\text{equation 14})$$

Case 2: Dynamic Range limited by the detector

$$D = \frac{\Psi_{detector}}{V_f} < \frac{\Psi_{preamp}}{V_f \times G} \quad (\text{equation 15})$$

This completes our prediction of system performance. We have calculated the input optical signal that corresponds to  $S/N=1$ , and the maximum output that can be extracted from the system in terms of a multiplier of the minimum input signal. The multiplier is “dynamic range”.

- **System options**

As the designer, you have the following additional degrees of freedom in designing a system:

1. You may increase the size of his optics in order to deliver more optical energy to the photodetector. The key concept to remember is that throughput in any optical system, defined as  $T = A \times \Omega$ , where  $A$  is area in  $\text{cm}^2$  and  $\Omega$  is solid angle field of view in steradians, is a constant in the system. If  $A_D$  is detector area and  $\Omega_D$  is detector FOV, then collector area  $A_C$  and collector FOV  $\Omega_C$  are at best satisfy  $A_C \times \Omega_C = T = A_D \times \Omega_D$ . Increasing the collector aperture decreases the FOV.
2. You may increase the efficiency of his optics (transmittance and reflectance optimization, etc).
3. You may increase the power of his source in a cooperative, active system (though not in a passive one).
4. You may increase the time he observes the signal, that is decrease the bandwidth and increase the time constant.

=====

- **Appendix: Sample Calculations**

See next page.

## Time Constant and High Frequency Cut Off Calculator

Time Constant ( $\tau$ ) (nsec)	Frequency (MHz) $f_h$		Time Constant ( $\tau$ ) (nsec)	Frequency (MHz) $f_h$
0.1	1592.36		10	15.92
0.2	796.18		20	7.96
0.3	530.79		40	3.98
0.4	398.09		80	1.99
0.5	318.47		100	1.59
0.6	265.39		120	1.33
0.7	227.48		140	1.14
0.8	199.04		150	1.06
0.9	176.93		160	1.00
1	159.24		180	0.88
2	79.62		200	0.80
3	53.08		220	0.72
4	39.81		240	0.66
5	31.85		250	0.64
6	26.54		260	0.61
7	22.75		280	0.57
8	19.90		300	0.53
9	17.69		320	0.50

$$f_h = 1/(2*\pi*\tau)$$

$f_h$  = high cutoff frequency

$\tau$  = time constant of detector (unbiased or biased) - see detector data sheet for values

### Calculator

enter tau to calculate for high cutoff frequency

1.5	106.10	MHz
$\tau$	$f_h$	

 **Boston**Electronics

[www.boselec.com](http://www.boselec.com)

[boselec@boselec.com](mailto:boselec@boselec.com)

617-566-3821